

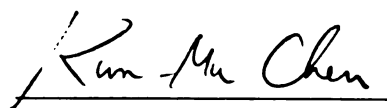


This is to certify that the
thesis entitled
TRAVELING WAVE ANTENNAS
WITH IMPEDANCE LOADING
presented by

Dennis P. Nyquist

has been accepted towards fulfillment
of the requirements for

Ph. D. degree in Elec. Engr.


Major professor

Date November 21, 1966

TRAVELING WAVE ANTENNAS
WITH IMPEDANCE LOADING

By

Dennis P. Nyquist

AN ABSTRACT

Submitted to
Michigan State University
in partial fulfillment of the requirements
for the degree of

DOCTOR OF PHILOSOPHY

Department of Electrical Engineering

1966

The cir
wire traveling
In this thesis,
class of thin-w
circular loop an
in either case
antenna current
be excited on s
impedance load

It is we
an essentially
are highly freq
strong function
this sensitivity
a single frequ

A trave
which is essen
standing wave
antenna is rela
more, the radi
modified as co

ABSTRACT

TRAVELING WAVE ANTENNAS
WITH IMPEDANCE LOADING

by Dennis P. Nyquist

The circuit and radiation characteristics associated with thin-wire traveling wave antennas are desirable for certain applications. In this thesis, specific consideration is given to two members of the class of thin-wire antennas: (1) the linear antenna and (2) the circular loop antenna. An impedance loading technique is utilized in either case to modify the usual standing wave distribution of antenna current. It is indicated that a traveling wave of current may be excited on such thin-wire antennas through the use of an optimum impedance loading.

It is well known that conventional thin-wire antennas support an essentially standing wave distribution of current. Such antennas are highly frequency sensitive, in that their input impedance is a strong function of the excitation frequency. As a consequence of this sensitivity, antennas of this type are ordinarily used only at a single frequency or over a very narrow band of frequencies.

A traveling wave antenna supports a distribution of current which is essentially an outward traveling wave. In contrast to its standing wave counterpart, the input impedance of a traveling wave antenna is relatively broadband as a function of frequency. Furthermore, the radiation fields of such an antenna are considerably modified as compared with those of a corresponding conventional

antenna. These
a wider beamwidth
directivity with

It is the
traveling wave
radiation chara
utilized where re
lumped impeda
loading to yield
determined in
excitation. It
loading may be
the use of such
while maintain
unloaded anten

A theore
and loop anten
(1) determine
a function of
and the frequ
yield an outwa
of utilizing a
corresponding
emphasis is p
since the high
interest.

antenna. These radiation patterns are in general characterized by a wider beamwidth for electrically small antennas, and improved directivity with a notable absence of minor lobes for large antennas.

It is the object of this research to realize a high efficiency traveling wave antenna and to evaluate its corresponding circuit and radiation characteristics. An impedance loading technique is utilized whereby the antenna is doubly loaded with a pair of identical lumped impedances. The position and impedance of an optimum loading to yield an outward traveling wave of antenna current are determined in terms of the antenna dimensions and its frequency of excitation. It is indicated that a purely non-dissipative optimum loading may be utilized if its position is properly chosen. Through the use of such a loading, a traveling wave antenna may be realized while maintaining the high efficiency characteristic of a conventional unloaded antenna.

A theoretical analysis is made of the impedance loaded linear and loop antenna configurations. It is the object of this analysis to: (1) determine approximately the distribution of antenna current as a function of its dimensions, the impedance and position of the loading, and the frequency of excitation; (2) determine the optimum loading to yield an outward traveling wave of current; (3) investigate the possibility of utilizing a purely non-dissipative loading; and (4) calculate the corresponding input impedance and radiation fields. Particular emphasis is placed upon the use of a non-dissipative optimum loading, since the high efficiency associated with such a loading is of fundamental interest.

It is ve
may indeed be
located, pure
of the paramet
compare favor
The frequency
utilizing an opt

Perhaps
conclusion that
use of a purely
reactance and
is indicated th
single frequen
frequencies.
radiation field
its dimensions
are presented
theoretical re

It is verified experimentally that a traveling wave of current may indeed be obtained on a linear antenna through the use of a properly located, purely reactive loading. The experimentally measured values of the parameters for such an optimum loading are demonstrated to compare favorably with those which were determined theoretically. The frequency dependence of the input impedance to a linear antenna utilizing an optimum non-dissipative loading is evaluated experimentally.

Perhaps the most significant result of this research is the conclusion that a traveling wave antenna may be realized through the use of a purely non-dissipative loading. Explicit expressions for the reactance and position of such an optimum loading are presented. It is indicated that a purely reactive loading can be optimum only at a single frequency, a resistive component being required at all other frequencies. Approximate expressions for the input impedance and radiation fields of the traveling wave antenna are given in terms of its dimensions and the frequency of excitation. Numerical examples are presented for antennas of specific dimensions to illustrate these theoretical results.

TRAVELING WAVE ANTENNAS
WITH IMPEDANCE LOADING

By

Dennis P. Nyquist

A THESIS

Submitted to
Michigan State University
in partial fulfillment of the requirements
for the degree of

DOCTOR OF PHILOSOPHY

Department of Electrical Engineering

1966

The au

chairman Dr.

the preparatio

Hoffman of the

form of a gra

The research

Air Force Cas

AF19(c28)-55

9/5/48

ACKNOWLEDGMENT

The author wishes to express his indebtedness to committee chairman Dr. K. M. Chen for his guidance and encouragement in the preparation of this thesis. He also wishes to thank Mr. J. W. Hoffman of the Division of Engineering Research for support in the form of a graduate fellowship during the conduct of this research. The research reported in this thesis was supported in part by the Air Force Cambridge Research Laboratories under contract AF19(628)-5372.

Acknowledgments

List of Figures

PART I. Trajectory
Optimization

1 Introduction

1.1. General

1.2. Problem Statement

1.3. Objectives

1.4. Scope

1.5. Organization

1.6. Summary

2 Approximate
Load

2.1. General

2.2. Problem Statement

2.3. Objectives

2.4. Scope

2.5. Summary

3 Optimization
of A

3.1. General

3.2. Problem Statement

3.3. Objectives

3.4. Scope

3.5. Summary

3.6. Summary

TABLE OF CONTENTS

	Page
Acknowledgment	ii
List of Figures	vi
PART I. Traveling Wave Linear Antenna with Optimum Impedance Loading	
1 Introduction.	1
1.1. Introduction	1
1.2. Definition of a Traveling Wave Linear Antenna. . .	1
1.3. Important Characteristics of a Traveling Wave Dipole	3
1.4. Previous Research on the Traveling Wave Linear Antenna	5
1.5. Object of the Present Research	8
1.6. Outline for Investigation of Traveling Wave Linear Antenna with Optimum Impedance Loading	9
2 Approximate Distribution of Current on a Doubly Loaded Linear Antenna.	11
2.1. Geometry of the Doubly Loaded Linear Antenna. .	11
2.2. Dimensions of Interest for a One-Dimensional Theory.	11
2.3. Formulation of an Inegral Equation for the Distribution of Cylinder Current	14
2.4. Approximate Solution for the Distribution of Current on the Doubly Loaded Cylinder.	20
2.5. Input Impedance of the Doubly Loaded Linear Antenna.	24
3 Optimum Loading for a Traveling Wave Distribution of Antenna Current.	26
3.1. Physical Interpretation of the Distribution of Current on a Doubly Loaded Dipole	26
3.2. Optimum Loading Impedance for a Traveling Wave Distribution of Cylinder Current	28
3.3. Purely Resistive Optimum Loading	30
3.4. Purely Reactive Optimum Loading	36
3.5. The Distribution of Current and Input Impedance Corresponding to an Optimum Loading.	47
3.6. Calculation of the Expansion Parameter $\Psi(z)$	62

4 Radia
Linea

4.1.

4.2.

4.3.

5 Exper
with 2

5.1.

5.2.

5.3.

5.4.

5.5.

PART II. Tr
In

6 Intr

6.1

6.2

6.3

6.4

6.5

6.6

7 D

C

7.

7.

7.

7

7

TABLE OF CONTENTS (continued)

	Page
4 Radiation Characteristics of a Traveling Wave Linear Antenna	72
4.1. Distribution of Cylinder Current for Calculation of Radiation Fields	72
4.2. Radiation Fields of the Traveling Wave Linear Antenna.	75
4.3. Comparison of Radiation Patterns for Traveling Wave and Standing Wave Linear Antennas	81
5 Experimental Study of Traveling Wave Antenna with Non-Dissipative Loading	87
5.1. Object of the Experimental Investigation	87
5.2. Description of the Experimental Arrangement .	90
5.3. Traveling Wave Distribution of Current on Monopole with Purely Non-Dissipative Loading.	99
5.4. Effects of Variations in Loading Parameters and Frequency Upon the Traveling Wave Distribution of Current	103
5.5. Input Impedance of a Traveling Wave Linear Antenna with Non-Dissipative Loading	109
 PART II. Traveling Wave Loop Antenna with Optimum Impedance Loading	
6 Introduction.	114
6.1. Introduction	114
6.2. Definition of a Traveling Wave Loop Antenna. .	114
6.3. Important Characteristics of a Traveling Wave Loop Antenna	116
6.4. Previous Research on the Traveling Wave Loop Antenna.	118
6.5. Object of the Present Research	120
6.6. Outline for Theoretical Investigation of a Traveling Wave Loop Antenna with Optimum Impedance Loading	121
7 Distribution of Current on a Doubly Loaded Circular Loop Antenna	122
7.1. Geometry of the Doubly Loaded Circular Loop Antenna.	122
7.2. Dimensions of Interest for a One- Dimensional Theory	124
7.3. A Rigorous Fourier Series Solution for the Distribution of Current on a Doubly Loaded Loop; Its Failure to Yield the Parameters of an Optimum Loading	125
7.4. Approximate Distribution of Current on a Doubly Loaded Loop Antenna	135
7.5. Input Impedance of a Doubly Loaded Loop Antenna	144

8 Optim
Distr

8.1.

8.2.

8.3.

8.4.

8.5.

9 Radia
Loop

9.1.

9.2.

9.3.

References .

Appendix A.

TABLE OF CONTENTS (continued)

	Page
8 Optimum Loading for a Traveling Wave	
Distribution of Loop Current	145
8.1. Physical Interpretation of the Distribution of Current on a Doubly Loaded Loop Antenna .	145
8.2. Optimum Loading Impedance for a Traveling Wave Distribution of Loop Current	146
8.3. Purely Reactive Optimum Loading.	148
8.4. The Distribution of Current and Input Impedance Corresponding to an Optimum Loading	162
8.5. Calculation of the Expansion Parameters $\Psi_i(\theta)$, $\Psi_q(\theta)$, and $\Psi(\theta)$	169
9 Radiation Characteristics of a Traveling Wave Loop Antenna	182
9.1. Distribution of Loop Current for Calculation of Radiation Fields	182
9.2. Radiation Fields of the Traveling Wave Loop Antenna	184
9.3. Comparison of Radiation Patterns for Traveling Wave and Standing Wave Loop Antennas	194
References	201
Appendix A. Electromagnetic Potentials in Antenna Theory.	203

Figure

- 2.1. Germ
- 3.1. Resist
Load
Length
- 3.2. Optim
of L
Anten
- 3.3. React
Load
Length
- 3.4. React
Load
Length
- 3.5. Optim
Load
Anten
- 3.6. Optim
Load
Anten
- 3.7. Ampl
to an
of P
- 3.8. Ampl
to an
Posit
- 3.9. Input
Load
($h = 1$)
- 3.10. Input
Load
($h = 1$)
- 3.11. Input
Leng
Posit

LIST OF FIGURES

Figure		Page
2.1.	Geometry of Impedance Loaded Dipole	12
3.1.	Resistance and Position of Optimum Dissipative Loading as a Function of the Antenna Electrical Length	32
3.2.	Optimum Impedance (purely resistive at 600 mhz) of Loading with Fixed Position as a Function of the Antenna Electrical Length	35
3.3.	Reactance and Position of Optimum Non-Dissipative Loading as a Function of the Antenna Electrical Length ($h = 50 \text{ cm} = \lambda_0$ at 600 mhz)	38
3.4.	Reactance and Position of Optimum Non-Dissipative Loading as a Function of the Antenna Electrical Length ($h = 100 \text{ cm} = 2\lambda_0$ at 600 mhz)	39
3.5.	Optimum Impedance (purely reactive at 600 mhz) of Loading with Fixed Position as a Function of the Antenna Electric Length ($h = 50 \text{ cm}$)	42
3.6.	Optimum Impedance (purely reactive at 600 mhz) of Loading with Fixed Position as a Function of the Antenna Electrical Length ($h = 100 \text{ cm}$)	43
3.7.	Amplitude and Phase of Antenna Current Corresponding to an Optimum Resistance Loading $[R_L]_0$ as a Function of Position Along Antenna	51
3.8.	Amplitude and Phase of Antenna Current Corresponding to an Optimum Non-Dissipative Loading as a Function Position Along Antenna	52
3.9.	Input Impedance of Antenna with Optimum Resistance Loading as a Function of its Electrical Length ($h = 31.25 \text{ cm}$)	55
3.10.	Input Impedance of Antenna with Optimum Reactance Loading as a Function of its Electrical Length ($h = 100 \text{ cm}$)	56
3.11.	Input Impedance as a Function of Antenna Electrical Length for Constant Resistance Loading of Fixed Position (optimum at 600 mhz)	58

Figure

- 3.12. Input
Anten
Comp
- 3.13. Comp
Expan
Elect
- 3.14. Comp
of Ex
Anten
- 4.1. Geom
Elect
Lines
- 4.2. Radia
Anten
- 4.3. Radia
Anten
- 4.4. Radia
Anten
- 5.1. Expe
- 5.2. Struc
- 5.3. Struc
- 5.4. Expe
 $h = \lambda$
Load
- 5.5. Expe
 $h = 2$
Load
- 5.6. Effect
Len
of Co
- 5.7. Effect
Reac
Mon

LIST OF FIGURES (continued)

Figure	Page
3.12. Input Impedance as a Function of Frequency for Antenna with Loading Consisting of Reactive Component of Optimum Impedance	61
3.13. Comparison of Approximate and Exact Values of Expansions Parameters $\Psi(z)$ as a Function of Electrical Position Along Antenna	67
3.14. Comparison of Approximate and Corrected Values of Expansion Parameter Ψ as a Function of Antenna Electrical Length	70
4.1. Geometry for Calculation of Radiation Zone Electromagnetic Fields of a Traveling Wave Linear Antenna	73
4.2. Radiation Patterns of Traveling and Standing Wave Antennas with $\beta_o h = 2\pi$	82
4.3. Radiation Patterns of Traveling and Standing Wave Antennas with $\beta_o h = 7\pi/2$	83
4.4. Radiation Patterns of Traveling and Standing Wave Antennas with $\beta_o h = 4\pi$	84
5.1. Experimental Arrangement	91
5.2. Structure of Model Monopole Antenna	92
5.3. Structure of Loop Type Current Probe	92
5.4. Experimental Current Distribution of Antenna with $h = \lambda_o$; Unloaded and with Optimum Reactance Loading	101
5.5. Experimental Current Distribution of Antenna with $h = 2\lambda_o$; Unloaded and with Optimum Reactance Loading	102
5.6. Effect (experimental) of Variations in Monopole End Length (h-d) upon its Traveling Wave Distribution of Current	105
5.7. Effect (experimental) of Variation in Loading Reactance on the Traveling Wave Distribution of Monopole Current	106

Figure

- 5.8. Effect
Freq
Mon
- 5.9. Expe
Freq
Ante
- 7.1. Geom
Loop
- 5.1. Real
Wave
Circ
- 5.2. Posi
Funct
- 5.3. Reac
Funct
- 5.4. Imper
3 b
Elect
- 5.5. Ampl
Corre
Load
- 5.6. Input
Funct
- 5.7. Curre
of P
- 5.8. Chara
of P
- 5.9. Curre
the E
- 5.10. Chara
the E
- 5.11. Expan
Elect

LIST OF FIGURES (continued)

Figure		Page
5.8.	Effect (experimental) of Variations in Excitation Frequency on the Traveling Wave Distribution of Monopole Current	108
5.9.	Experimental Input Impedance as a Function of Frequency for Loaded and Unloaded Monopole Antennas	111
7.1.	Geometry of the Doubly Impedance Loaded Loop Antenna	123
8.1.	Real and Imaginary Parts of the Normalized Complex Wave Number as a Function of the Electrical Loop Circumference	151
8.2.	Position of Optimum Non-Dissipative Loading as a Function of the Electrical Loop Circumference. . . .	156
8.3.	Reactance of Optimum Non-Dissipative Loading as a Function of the Electrical Loop Circumference. . . .	157
8.4.	Impedance of Optimum Loading (purely reactive for $\beta_o b = 2.5$) with Fixed Position as a Function of Electrical Loop Circumference $\beta_o b$	159
8.5.	Amplitude and Phase of Current Along Loop Corresponding to an Optimum Non-Dissipative Loading.	166
8.6.	Input Impedance of Loop with Optimum Loading as a Function of the Electric Loop Circumference	168
8.7.	Current Expansion Parameter $\Psi_i(\theta)$ as a Function of Position Along the Loop	175
8.8.	Charge Expansion Parameter $\Psi_q(\theta)$ as a Function of Position Along the Loop	176
8.9.	Current Expansion Parameter Ψ_i as a Function of the Electrical Loop Circumference	179
8.10.	Charge Expansion Parameter Ψ_q as a Function of the Electrical Loop Circumference	180
8.11.	Expansion Parameter Ψ as a Function of the Electrical Loop Circumference	181

Figure

9.1. Loop
Zone

9.2. Radi
Func

9.3. Radi
Func

9.4. Radi
Func

9.5. Radi
Func

LIST OF FIGURES (continued)

Figure		Page
9.1.	Loop Geometry for Calculation of Radiation Zone Fields	186
9.2.	Radiation Pattern in Plane of Loop ($\theta = 90^\circ$) as a Function of ϕ for $\beta_o b = 1$	195
9.3.	Radiation Pattern in Plane of Loop ($\theta = 90^\circ$) as a Function of ϕ for $\beta_o b = 1.5$	196
9.4.	Radiation Pattern in Plane of Loop ($\theta = 90^\circ$) as a Function of ϕ for $\beta_o b = 2.5$	197
9.5.	Radiation Pattern in Plane of Loop ($\theta = 90^\circ$) as a Function of ϕ for $\beta_o b = 4.0$	198

PART I

TRAVELING WAVE LINEAR ANTENNA
WITH OPTIMUM IMPEDANCE LOADING

1.1. Introduction

It is the purpose of this paper to present a high efficiency antenna system corresponding to the loading technique. This is doubly loaded antenna system. Theoretical analysis is determined as a function of the input impedance and the output impedance of the cylinder. The antenna is placed upon a dielectric substrate. The loading, since it is a function of the efficiency of the antenna, is a function of the traveling wave antenna through the input impedance. The input impedance is a function of the dipole having a function of the excitation.

1.2. Definition

A traveling wave antenna which supports

CHAPTER I

INTRODUCTION

1.1. Introduction

It is the object of the first part of this research to realize a high efficiency traveling wave linear antenna and to evaluate its corresponding circuit and radiation characteristics. An impedance loading technique is utilized in which the cylindrical dipole antenna is doubly loaded with a pair of identical lumped impedances. A theoretical investigation of this configuration is carried out to determine approximately the distribution of current on the cylinder as a function of its dimensions, the excitation frequency, and the impedance and position of the double loading. The optimum loading impedance to yield a traveling wave distribution of current over most of the cylinder is determined from this result. Particular emphasis is placed upon the possibility of utilizing a purely non-dissipative loading, since this would provide the means of realizing a high efficiency traveling wave linear antenna. It is verified experimentally that a traveling wave of current can indeed be excited on a linear antenna through the use of a properly positioned purely reactive loading. The input impedance and radiation fields of a traveling wave linear dipole having such a non-dissipative optimum loading are evaluated as a function of the cylinder dimensions and the frequency of excitation.

1.2. Definition of a Traveling Wave Linear Antenna

A traveling wave linear antenna is defined as a linear antenna which supports a traveling wave distribution of current. The traveling

wave of current
linear dipole, and
amplitude of the
excitation point.
phase is essential
this research, a
antennas such that
may be utilized w
omation, the distr
to the axis of the

The chara
have been studied
first mathematical
antenna. The res
axial distribution
enable to find a s
Some time later,
to Hallen's intent
This solution and
linear antenna co
found that these
corresponding ex

Since it is
ordinary linear
some modification
support a travel

wave of current is excited by a voltage generator at the center of the linear dipole, and travels outward toward its ends. While the amplitude of the current wave decays as it advances outward from the excitation point, since it continuously radiates energy into space, its phase is essentially a linear function of position along the antenna. In this research, a restriction is made to the class of long thin-wire antennas such that an expedient but approximate one-dimensional theory may be utilized with good accuracy. In this one-dimensional approximation, the distribution of dipole current is assumed to flow parallel to the axis of the thin cylinder comprising the linear antenna.

The characteristics of thin-wire center fed linear antennas have been studied extensively. Historically, Hallen¹ developed the first mathematical theory describing the circuit properties of a linear antenna. The result of this theory was an integral equation for the axial distribution of current on the linear dipole. Hallen was, however, unable to find a simple closed form solution to this integral equation. Some time later, King² obtained an approximate closed form solution to Hallen's integral equation through the use of an iterative technique. This solution indicated that the distribution of current on a conventional linear antenna consists essentially of a standing current wave. It was found that these approximate theoretical results agreed very well with corresponding experimental measurements of the antenna current.

Since it has been observed that the current distribution on an ordinary linear antenna is essentially a standing wave, then evidently some modification of its structure is necessary in order that it might support a traveling wave of current. In the present research, an

impedance load:

antenna current.

with a pair of id

that is, when its

antenna may be r

bution of current

A linear

of current. The

characteristics.

distribution. Fr

the input impedan

Similarly the ra

forward manner

circuit and radiat

by its current dis

characteristics s

respectively, to s

1.3. Important C

A conven

in that its input

This frequency o

distribution of an

the maxima and

along the dipole.

current at the dr

series strongly

impedance loading technique is utilized to modify the distribution of antenna current. This method consists of doubly loading the dipole with a pair of identical impedances. When the loading is optimum, that is, when its impedance and position are properly chosen, the antenna may be made to support the desired traveling wave distribution of current along the majority of its length.

A linear antenna is completely characterized by its distribution of current. The dipole is fully described by its circuit and radiation characteristics, which are readily determined from its current distribution. From a knowledge of the current at its excitation point, the input impedance of a linear antenna may be immediately calculated. Similarly, the radiation pattern of the dipole is determined in a straightforward manner in terms of its distribution of current. Since the circuit and radiation characteristics of a linear antenna are determined by its current distribution, then it might be expected that these characteristics should differ greatly for distributions corresponding, respectively, to standing and traveling current waves.

1.3. Important Characteristics of a Traveling Wave Dipole

A conventional linear dipole antenna is highly frequency sensitive, in that its input impedance is a strong function of the excitation frequency. This frequency dependence is a direct consequence of the standing wave distribution of antenna current. As the frequency of excitation is varied, the maxima and minima of the standing wave of current shift in position along the dipole. With the excitation potential fixed therefore, the current at the driving point of the dipole, and hence its input impedance, varies strongly with changes in the excitation frequency. As a consequence

of this frequency
used only at a set
frequencies.

In contrast
antenna has an impedance
independent of frequency
of the traveling wave
amplitude of the wave
the antenna, except for
variation in the current
in the current at the
wave dipole is the
is this broadband
a traveling wave

The radiation
characterized by
short. As the frequency
to form a new radiation
The beamwidth
increases, which
(high gain) if it is
These minor lobes
fraction of that of the
characteristics
applications.

of this frequency sensitivity, a conventional linear antenna is ordinarily used only at a single frequency, or over a very narrow band of frequencies.

In contrast to the standing wave dipole, a traveling wave antenna has an input impedance characteristic which is relatively independent of frequency. This broadband character is a consequence of the traveling wave distribution of dipole current. Since the amplitude of the traveling wave of current is essentially constant along the antenna, except for the smooth decay due to radiation, then a variation in the excitation frequency does not result in a rapid change in the current at the driving point. The input impedance of a traveling wave dipole is therefore a relatively weak function of frequency. It is this broadband character which is the most important property of a traveling wave linear antenna.

The radiation pattern of a conventional standing wave dipole is characterized by a single major lobe when the antenna is electrically short. As the electrical length is increased, this single lobe splits to form a new major lobe in conjunction with a minor lobe structure. The beamwidth of the major lobe decreases as the antenna length increases, which would result in increasingly improved directivity (high gain) if it were not for the presence of the minor lobe structure. These minor lobes, however, have an amplitude which is a large fraction of that of the major lobe. Consequently, the directional characteristics of a long linear antenna are not desirable for most applications.

The radiation characteristics of a traveling wave linear antenna are quite different from those of its standing wave counterpart. An electrically short traveling wave dipole is characterized by a radiation pattern having a single major lobe with a very wide beamwidth. As the electrical length of the antenna is increased, the beamwidth of this single lobe continually decreases. A minor lobe does not appear in the pattern until the antenna length is much greater than that of the comparable standing wave antenna. An electrically long traveling wave antenna may thus be utilized to realize an improved directivity, this improvement being a consequence of the relatively narrow major lobe beamwidth which may be obtained without the appearance of a minor lobe structure. When the traveling wave antenna is sufficiently long that minor lobes finally do appear, their amplitude is lower than that of the initial minor lobe structure associated with the standing wave counterpart antenna.

The modified radiation pattern characteristic of a traveling wave linear antenna may be desirable for certain purposes. In particular, the wide beamwidth of a short dipole and the absence of minor lobes associated with an electrically long antenna may be useful for some applications.

1.4. Previous Research on the Traveling Wave Linear Antenna

It has been established that a traveling wave linear antenna may be realized through the use of a resistance loading technique. Research has been reported on methods which utilize both lumped and distributed purely resistive loadings. A traveling wave distribution of current may be excited on a linear antenna having a purely dissipative

loading through

Altshule

obtained on a line

of optimum lump

ends. This tech

standing wave di

standing wave of

having an equal

section of line n

characteristic r

from the open-c

matched line is

length section a

reasoned by ana

loading a quarter

traveling wave o

end quarter wave

technique could

verified experim

wave was found

and the position

It was fo

distribution of c

about that where

optimum. Cons

characteristic w

loading through the application of either of these techniques.

Altshuler³ proposed that a traveling wave of current could be obtained on a linear antenna by doubly loading the dipole with a pair of optimum lumped resistances placed a quarter wavelength from its ends. This technique was motivated by an analogy between the standing wave distribution of current on a linear antenna and the standing wave of current on a section of lossless transmission line having an equal length and terminated in an open-circuit. Such a section of line may be matched by placing a resistance equal to its characteristic resistance in series with the line a quarter wavelength from the open-circuited end. The distribution of current on the matched line is a traveling current wave, except on the quarter wavelength section at the end where the standing wave persists. It was reasoned by analogy therefore, that, by placing an optimum resistance loading a quarter wavelength from the ends of a linear antenna, a traveling wave distribution of current might be excited on all but its end quarter wavelength. That such a lumped resistance loading technique could indeed yield the desired traveling wave of current was verified experimentally, where a slowly decaying traveling current wave was found to exist on the antenna between its excitation point and the position of the loading.

It was found further that an approximately traveling wave distribution of current was maintained for a range of frequencies about that where the resistance and position of the loading were optimum. Consequently, a relatively broadband input impedance characteristic was measured for a dipole having a fixed resistance

loading of fixed
significantly from
of the loading wave
dipole current re
the input impedance
characteristic of
radiation character
experimentally :

It has been shown
wave dipole may
conductor whose
position along the
a rapidly decaying
entire dipole.
that the optimum
of the excitation
consequently be
broadband input
pattern general
demonstrated t

Although
the preceding p
distribution of
disadvantage.
techniques have
dissipated in th

loading of fixed position. When the excitation frequency was varied significantly from its center value, where the resistance and position of the loading were optimum, it was found that the distribution of dipole current reverted back to an essentially standing wave. Further, the input impedance again displayed the strong frequency dependence characteristic of a conventional unloaded antenna. The expected radiation characteristics of a traveling wave antenna were measured experimentally for such a resistance loaded dipole.

It has been demonstrated by Wu and King⁴ that a traveling wave dipole may be realized by constructing it of a dissipative conductor whose resistance varies in a prescribed manner with position along the antenna. Theoretically, such a loading will yield a rapidly decaying traveling wave distribution of current along the entire dipole. This distributed loading technique has the advantage that the optimum resistance of the loading is essentially independent of the excitation frequency, so that the traveling wave of current may consequently be maintained over a wide band of frequencies. The broadband input impedance characteristic and modified radiation pattern generally associated with traveling wave antennas were demonstrated to characterize this particular dipole structure.

Although each of the resistance loading techniques discussed in the preceding paragraphs may be utilized to obtain a traveling wave distribution of current on a linear antenna, they share a common disadvantage. Traveling wave antennas realized through these techniques have a very low efficiency due to the great amount of power dissipated in the resistive loadings. In either case, the efficiency is of

the order of 50%

of both techniques

1.5. Object of

It has been

for obtaining a

antenna are very

applied to yield

of the power sup

dissipative load

gross inefficiency

It is the

high efficiency t

utilizing a lumped

loading is to be

be experienced a

will be effective

linear antenna w

standing wave d

In this in

thin perfectly c

doubly loaded w

about the excitat

choosing a load

The optimum loa

on the cylinder i

utilizing a prope

be investigated.

the order of 50% or less, which severely limits the practical value of both techniques.

1.5. Object of the Present Research

It has been indicated that the resistance loading techniques for obtaining a traveling wave distribution of current on a linear antenna are very inefficient. Although these schemes may be applied to yield the desired traveling wave of current, 50% or more of the power supplied by the source is lost in joule heating of the dissipative loading, rather than being radiated into space. Such a gross inefficiency is intolerable in the majority of applications.

It is the object of the present research therefore to realize a high efficiency traveling wave antenna through a new technique utilizing a lumped non-dissipative impedance loading. Since the loading is to be non-dissipative with this method, no power loss will be experienced and essentially all the power supplied by the source will be effectively radiated. The efficiency of such a traveling wave linear antenna will thus be comparable to that of a conventional standing wave dipole.

In this investigation, the antenna is assumed to consist of a thin perfectly conducting cylinder which is excited at its center and doubly loaded with a pair of identical impedances placed symmetrically about the excitation point. There are two degrees of freedom in choosing a loading with such a configuration; its impedance and position. The optimum loading to yield a traveling wave distribution of current on the cylinder is to be determined. In particular, the possibility of utilizing a properly positioned purely reactive optimum loading is to be investigated.

Through
and radiation ch
distribution of c
dissipative elem
realized while r
wave dipole.

1.6. Outline of
with Optic

The pres
with optimum in
Initially, an app
dipole is under
loading which w
current. At a l
these theoretica
theoretically pr
a traveling wave

It is the
approximately t
as a function of
impedance and
in terms of the
the parameters
distribution of c
utilizing a pr
corresponding c
utilizing such an

Through this reactive loading technique, the desirable circuit and radiation characteristics associated with a traveling wave distribution of current may be obtained without the introduction of dissipative elements. A traveling wave linear antenna is thus realized while retaining the high efficiency of a conventional standing wave dipole.

1.6. Outline for Investigation of Traveling Wave Linear Antenna with Optimum Impedance Loading

The present investigation of a traveling wave linear antenna with optimum impedance loading is broken into two distinct parts. Initially, an approximate theoretical study of the doubly loaded dipole is undertaken to determine the parameters of an optimum loading which will yield a traveling wave distribution of cylinder current. At a later point, an experimental study is made to verify these theoretical results. It is demonstrated in particular that the theoretically predicted optimum impedance loading will indeed yield a traveling wave of current on a linear antenna.

It is the purpose of the theoretical analysis to: (1) determine approximately the distribution of current on the doubly loaded cylinder as a function of its dimensions, the excitation frequency, and the impedance and position of the loading; (2) obtain from this result (in terms of the cylinder dimensions and its frequency of excitation) the parameters of an optimum double loading to yield a traveling wave distribution of current on the cylinder; (3) investigate the possibility of utilizing a purely non-dissipative optimum loading; (4) calculate the corresponding circuit and radiation characteristics of a linear antenna utilizing such an optimum impedance loading.

An exper
verify that, at a
current may in
a purely reacti
of such a travel
effects of varia
upon the distrib
made of the fre
wave antenna w
results are con
standing wave li

An experimental arrangement is to be assembled in order to verify that, at a given frequency, a traveling wave distribution of current may indeed be excited on a linear antenna through the use of a purely reactive optimum loading. Further, the circuit characteristics of such a traveling wave dipole are to be studied experimentally. The effects of variations in the excitation frequency and loading parameters upon the distribution of antenna current are evaluated. A study is also made of the frequency dependence of the input impedance to the traveling wave antenna with purely non-dissipative loading. These experimental results are compared with similar ones for a corresponding conventional standing wave linear antenna.

APPROX

DO

2.1. Geometry

The geom
taken to be as in
circular cylinder
center by a harm
potential V_0 .
identical lumped
its center. With
freedom in choos

In this re
impedances are
cylinder at the e
that point and to
loading impedanc
and to be center
then correspond
mational approx
the linear dimen
negligibly small

2.2. Dimension

It is assu
cylinder whose h
where the latter

CHAPTER 2

APPROXIMATE DISTRIBUTION OF CURRENT ON A DOUBLY LOADED LINEAR ANTENNA

2.1. Geometry of the Doubly Loaded Linear Antenna

The geometry of the doubly impedance loaded linear dipole is taken to be as indicated in Figure 2.1. A thin perfectly conducting circular cylinder of length $2h$ and diameter $2a$ is excited at its center by a harmonic voltage source of angular frequency ω and potential V_0 . The cylinder is symmetrically loaded with a pair of identical lumped impedances Z_L at a distance d on either side of its center. With such a configuration, there are two degrees of freedom in choosing a loading; its impedance and position.

In this research, both the source of excitation and the loading impedances are idealized to be point elements. The gap in the cylinder at the excitation point $z = 0$ is assumed to be centered about that point and to have a length of 2δ . Similarly, the gaps at the loading impedances at $z = \pm d$ are assumed to have a length of 2δ and to be centered about those points. The point element assumption then corresponds to letting δ tend to zero as a limit. This mathematical approximation is equivalent to the physical requirement that the linear dimensions of the excitation and loading elements be negligibly small compared with the length of the cylinder itself.

2.2. Dimensions of Interest for a One-Dimensional Theory

It is assumed that the linear antenna consists of a long thin cylinder whose half-length is very much greater than its radius, where the latter is taken to be a small fraction of the wavelength.

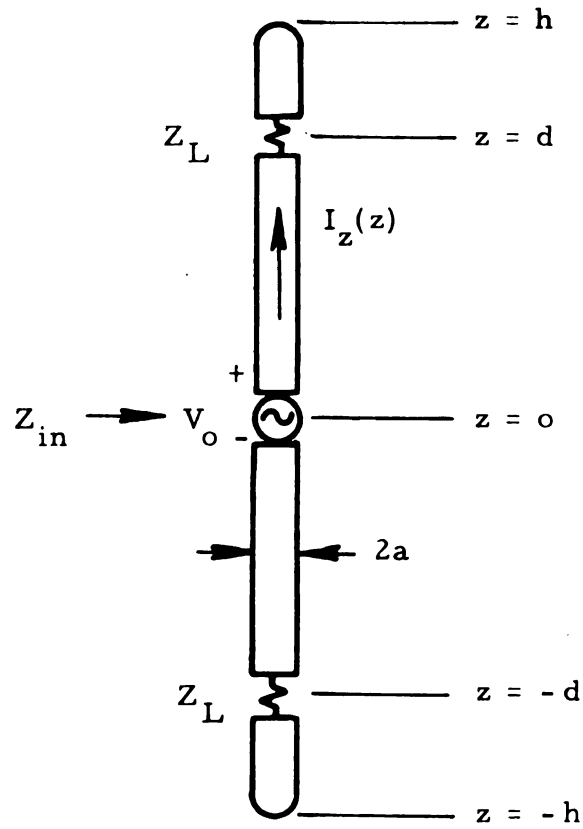


Figure 2.1. Geometry of Impedance Loaded Dipole

Under these conditions
about its axis, and
excited on the cylinder
That is, the current
which flows parallel to
which are impenetrable

where $\beta_0 = 2\pi$
in the free space

Conditions
approximation to
With this technique
calculated as the
is assumed to be
throughout the cylinder
concentrated air
vector potential
be calculated as
cylinder. However
when conditions
mentioned approximation
facilitates the solution
would otherwise be

Under these circumstances, and due to the symmetry of the cylinder about its axis, it may be assumed that the distribution of current excited on the cylinder by the source at its center is one-dimensional. That is, the current is assumed to have only a z-component $I_z(z)$ which flows parallel to the cylinder axis. The dimensional restrictions which are implicit in such a one-dimensional theory are thus

$$\begin{aligned} h &\gg a \\ \beta_0 a &\ll 1 \end{aligned} \tag{2.1}$$

where $\beta_0 = 2\pi/\lambda_0$ is the free space wave number which corresponds to the free space wavelength λ_0 .

Conditions (2.1) are also sufficient to validate the usual approximation technique utilized in the study of thin wire antennas. With this technique, the vector potential at the antenna surface is calculated as the contour integral of the total antenna current, which is assumed to flow along its axis. In reality, the current flows throughout the cross section of the cylinder, and is actually most concentrated along its surface due to the skin effect phenomena. The vector potential at the antenna surface should in general, therefore, be calculated as a volume integral of the current density on the cylinder. However, it has been indicated by Hallen¹ and King² that, when conditions (2.1) are satisfied, the error introduced by the above mentioned approximation is negligible. This approximation technique facilitates the solution for the distribution of antenna current, which would otherwise be very much more complicated.

2.3. Formulation Cylinder (C)

The boundary
surface is

where \hat{n} is a unit
vector the electric field
the tangential component
surface of the cylinder
satisfied, then the
to be one-dimensional
Under these conditions
of the cylinder wall

where $E_z^a(z)$ is
for $z = a$ and $E_z^i(z)$

Since the
be perfectly continuous
vanishing only in
expressed as

$$E_z^a(z) =$$

2.3. Formulation of an Integral Equation for the Distribution of Cylinder Current

The boundary condition on the electric field at the antenna surface is

$$(\hat{n} \times \vec{E}) = 0 \quad (2.2)$$

where \hat{n} is a unit outward normal vector at a point on the surface and \vec{E} the electric field at the same point. This condition requires that the tangential component of electrical field be continuous across the surface of the cylinder. Since conditions (2.1) are assumed to be satisfied, then the distribution of current on the cylinder may be taken to be one-dimensional, i. e., to have only an axial component $I_z(z)$. Under these circumstances, the tangential electrical field at the surface of the cylinder will have only a z -component and condition (2.2) becomes

$$E_z^a(z) = E_z^i(z) \quad (2.3)$$

where $E_z^a(z)$ is the field just within the surface of the cylinder at $r = a^-$ and $E_z^i(z)$ is the field at $r = a^+$ just outside its surface.

Since the cylinder comprising the linear antenna is taken to be perfectly conducting, then the applied field $E_z^a(z)$ may be non-vanishing only in the gaps at $z = 0, \pm d$. Thus $E_z^a(z)$ may be expressed as

$$E_z^a(z) = \begin{cases} \frac{Z_L I_z(d)}{2\delta} & \text{for } -d - \delta < z < -d + \delta \\ -\frac{V_0}{2\delta} & \text{for } -\delta < z < \delta \\ \frac{Z_L I_z(d)}{2\delta} & \text{for } d - \delta < z < d + \delta \end{cases} \quad (2.4)$$

where $I_z(d)$ is
zero in accordance
the symmetry of

The total voltage

A result consists

$$E_z^a(z)$$

where $f(z)$ is

The induced
the antenna, due
calculated from
 \vec{A} , 0 as

Since the time
then it is possible
potentials and
is thus obtained

$$E_z^a(z) = 0 \quad \text{for all other point on } -h \leq z \leq h \quad (2.5)$$

where $I_z(d)$ is the current at the loading impedance and 2δ tends to zero in accordance with the point element assumption. In result (2.4), the symmetry of the distribution of current has been utilized as

$$I_z(-z) = I_z(z) \quad (2.6)$$

The total voltage drop along the cylinder must be given by

$$-\int_{-h}^h E_z^a(z) dz = V_o - 2 Z_L I_z(d) \quad (2.7)$$

A result consistent with equations (2.6) and (2.7) is

$$E_z^a(z) = -V_o \delta(z) + Z_L I_z(d) [\delta(z-d) + \delta(z+d)] \quad (2.8)$$

where $\delta(z)$ is the Diract delta function.

The induced electric field $E_z^i(z)$ just outside the surface of the antenna, due to the current and charge on the cylinder, may be calculated from the vector and scalar potentials⁵ (see Appendix A) \vec{A} , ϕ as

$$E_z^i(z) = -(\nabla \phi)_z - \left(\frac{\partial \vec{A}}{\partial t} \right)_z \quad (2.9)$$

Since the time variation is assumed to be harmonic of the form $e^{j\omega t}$, then it is possible to make the replacement $\frac{\partial}{\partial t} \rightarrow j\omega$, where the potentials and fields are then understood to be complex valued. There is thus obtained

$$E_z^i(z) = -(\nabla \phi)_z - j\omega A_z \quad (2.10)$$

where $A_z(z)$

The vector an

which may be

with which equ

Since the distr

potential will b

(2.12) gives

If resul

to satisfy the b

the cylinder, t

for the vector r

$$\left[\frac{\partial^2}{\partial z^2} - \Delta \right]$$

This differenti

complementar

$$A_z^c(z)$$

where $A_z(z)$ and $\phi(z)$ are the potentials at the surface of the cylinder. The vector and scalar potentials are related by the Lorentz condition, which may be expressed in the form

$$\phi = \frac{j\omega}{\beta_o} \nabla \cdot \vec{A} \quad (2.11)$$

with which equation (2.10) becomes

$$E_z^i(z) = - \frac{j\omega}{\beta_o} [\nabla(\nabla \cdot \vec{A})]_z - j\omega A_z \quad (2.12)$$

Since the distribution of cylinder current is axial, then the vector potential will have only a z -component $A_z(z)$ as well,⁵ and equation (2.12) gives

$$E_z^i(z) = - \frac{j\omega}{\beta_o} \frac{\partial^2 A_z}{\partial z^2} - j\omega A_z \quad (2.13)$$

If results (2.8) and (2.13) are substituted into condition (2.3), to satisfy the boundary condition on the electric field at the surface of the cylinder, then a second order inhomogeneous differential equation for the vector potential at the antenna surface is obtained as

$$\left[\frac{\partial^2}{\partial z^2} + \beta_o^2 \right] A_z(z) = \frac{j\beta_o^2}{\omega} \{ -V_o \delta(z) + Z_L I_z(d) [\delta(z-d) + \delta(z+d)] \} \quad (2.14)$$

This differential equation must be satisfied for $-h \leq z \leq h$. A complementary solution of equation (2.14) is well known to be

$$A_z^c(z) = C_1 e^{j\beta_o z} + C_2 e^{-j\beta_o z} \quad -h \leq z \leq h \quad (2.15)$$

where C_1 and
solution is deter

$$A_z^p(z) = \frac{V}{2\pi}$$

which is readil
(2.14). In this
free space. Th
surface is obta

$$A_z(z) =$$

Since th
about the excit
exhibits a sim

Solution (2.17)
 $C_2 = C_1$, whi

$$A_z(z)$$

where C_1 and C_2 are arbitrary complex constants. The particular solution is determined as

$$A_z^p(z) = \frac{V_o}{2v_o} e^{-j\beta_o |z|} - \frac{Z_L I_z(d)}{2v_o} [e^{-j\beta_o |z-d|} + e^{-j\beta_o |z+d|}]$$

$$-h \leq z \leq h \quad (2.16)$$

which is readily verified by direct substitution into differential equation (2.14). In this last result, $v_o = \omega/\beta_o$ is the velocity of propagation in free space. The complete solution for the vector potential at the antenna surface is obtained by the superposition of results (2.15) and (2.16) as

$$A_z(z) = C_1 e^{j\beta_o z} + C_2 e^{-j\beta_o z} + \frac{V_o}{2v_o} e^{-j\beta_o |z|}$$

$$- \frac{Z_L I_z(d)}{2v_o} [e^{-j\beta_o |z-d|} + e^{-j\beta_o |z+d|}] \quad -h \leq z \leq h$$

$$(2.17)$$

Since the distribution of current on the cylinder is symmetric about the excitation point, then the vector potential at its surface exhibits a similar symmetry² such that

$$A_z(-z) = A_z(z) \quad (2.18)$$

Solution (2.17) may be made to satisfy this boundary condition only if $C_2 = C_1$, which yields the simplified result

$$A_z(z) = C_1 e^{j\beta_o z} + C_1 e^{-j\beta_o z} + \frac{V_o}{2v_o} e^{-j\beta_o |z|}$$

$$- \frac{Z_L I_z(d)}{2v_o} [e^{-j\beta_o |z-d|} + e^{-j\beta_o |z+d|}] \quad -h \leq z \leq h$$

$$(2.19)$$

It should be not

been obtained s

a functional dep

As indic

surface may be

axial distributi

$$A_z(z)$$

where μ_0 is th

is the Green's f

The factor $R =$

the Euclidean d

axis at z' and

If the tw

$A_z(z)$ at the an

h the result

$$\frac{\mu_0}{4\pi} \int_{-h}^h$$

This expressio

It should be noted that a solution in terms of complex exponentials has been obtained since a traveling wave distribution of current having such a functional dependence is to be sought eventually.

As indicated in section 2.2, the vector potential at the cylinder surface may be written as the Helmholtz integral over an assumed axial distribution of current (see Appendix A) as

$$A_z(z) = \frac{\mu_o}{4\pi} \int_{-h}^h I_z(z') K(z, z') dz' \quad -h \leq z \leq h \quad (2.20)$$

where μ_o is the permeability of free space and the kernel $K(z, z')$ is the Green's function

$$K(z, z') = \frac{e^{-j\beta_o \sqrt{(z-z')^2 + a^2}}}{\sqrt{(z-z')^2 + a^2}} \quad (2.21)$$

The factor $R = \sqrt{(z-z')^2 + a^2}$ in the Green's function (2.21) represents the Euclidean distance between an element of current on the cylinder axis at z' and an observation point on its surface at z .

If the two expressions (2.19) and (2.20) for the vector potential $A_z(z)$ at the antenna surface are equated, there is obtained for $-h \leq z \leq h$ the result

$$\begin{aligned} \frac{\mu_o}{4\pi} \int_{-h}^h I_z(z') K(z, z') dz' = & C_1 e^{j\beta_o z} + C_1 e^{-j\beta_o z} + \frac{V_o}{2v_o} e^{-j\beta_o |z|} \\ & - \frac{Z_L I_z(d)}{2v_o} [e^{-j\beta_o |z-d|} + e^{-j\beta_o |z+d|}] \end{aligned} \quad (2.22)$$

This expression is an integral equation for the distribution of current

$I_z(z)$ on the d
 h, a as well a
 appear as para
 C_1 and $I_z(d)$
 and must be ex
 conditions.

Since t
 cylinder curre
 of cylinder cur
 condition $I_z(z)$
 solution $I_z(z)$
 subsidiary c. n.

These conditio
 C_1 and $I_z(d)$.

It is to
 equation (2.22)
 for the distrib
 is to be expect
 loaded cylinde

$I_z(z)$ on the doubly loaded linear antenna. The cylinder dimensions h, a as well as the impedance and position Z_L, d of the double loading appear as parameters in the equation. Two as yet undetermined constants C_1 and $I_z(d)$ appear on the right hand side of the integral equation, and must be evaluated through the application of a pair of subsidiary conditions.

Since the antenna structure terminates at $z = h$, then the cylinder current at that point must vanish. Further, the distribution of cylinder current must be continuous, with the result that the condition $I_z(z=d) = I_z(d)$ must hold at the location of the loading. The solution $I_z(z)$ of integral equation (2.22) must therefore satisfy the subsidiary conditions

$$I_z(z=h) = 0 \quad (2.23)$$

$$I_z(z=d) = I_z(d)$$

These conditions are sufficient to facilitate evaluation of the constants C_1 and $I_z(d)$.

It is to be noted that, in the special case where $Z_L = 0$, equation (2.22) reduces to a variation of Hallen's integral equation² for the distribution of current on a conventional linear dipole. This is to be expected, since when $Z_L = 0$ the structure of the doubly loaded cylinder reduces to that of an ordinary linear antenna.

2.4. Approx Doubly

It has

equation (2.2

of current on

been solved a

expression f

through what

technique. T

equation (2.2

on the right h

undetermined

on the right a

shifted source

becomes very

An int

by Chen⁶ in th

loaded cylindr

solution for th

of simple func

to result (2.2

mitted. The

approximation

A mor

preceding par

Chen⁷ in con

2. 4. Approximate Solution for the Distribution of Current on the Doubly Loaded Cylinder

It has been indicated that, for the special case where $Z_L = 0$, equation (2.22) reduces to Hallen's integral equation for the distribution of current on a conventional linear antenna. Hallen's equation has been solved approximately by King.² A relatively simple closed form expression for the distribution of cylinder current may be obtained through what has become known as the King-Middleton iterative technique. The application of this technique to obtain a solution to equation (2.22) is, however, impractical since: (1) the constant $I_z(d)$ on the right hand side of the integral equation depends upon the as yet undetermined distribution of current; (2) the additional terms occurring on the right in equation (2.22) for $Z_L \neq 0$ are equivalent to a pair of shifted sources, which complicate such a solution to the extent that it becomes very unwieldy.

An integral equation similar to result (2.22) has been encountered by Chen⁶ in the investigation of electromagnetic scattering from a doubly loaded cylinder. Through an approximate technique, a rather complex solution for the distribution of cylinder current was obtained in terms of simple functions. This integral equation was essentially identical to result (2.22), with the term involving the excitation potential V_o omitted. The inclusion of this term in equation (2.22) makes Chen's approximation technique too intractable to provide a useful solution.

A more approximate technique than those mentioned in the preceding paragraphs has been reported by Wu and King⁴ and later by Chen⁷ in conjunction with determining the distribution of current on an

impedance l
with corresp
mation techn
vector potent
same point is

The m
of the peaking
the vector po
given by

where $K(z, z)$

The peaking pr
approximate s
impedance loa

Since
(2.1), then K
as a function of
vector potential
from equation
neighborhood of
 $l_2(z)$ is contin

impedance loaded cylinder. In the latter case, an excellent agreement with corresponding experimental results was observed. This approximation technique consists essentially of assuming that the ratio of vector potential at a point on the antenna surface to the current at the same point is constant along the cylinder.

The motivation for this approximate method is a consequence of the peaking property of the kernel $K(z, z')$. It has been found that the vector potential at a point z on the surface of the cylinder is given by

$$A_z(z) = \frac{\mu_o}{4\pi} \int_{-h}^h I_z(z') K(z, z') dz' \quad -h \leq z \leq h \quad (2.20)$$

where $K(z, z')$ is the Green's function

$$K(z, z') = \frac{e^{-j\beta_o \sqrt{(z-z')^2 + a^2}}}{\sqrt{(z-z')^2 + a^2}} \quad (2.21)$$

The peaking property of this kernel is exploited to formulate an approximate solution for the distribution of current on the doubly impedance loaded cylinder.

Since $a \ll h$ by the thin-wire assumption, i. e., condition (2.1), then $K(z, z')$ has a very sharp peak at $z' = z$ when considered as a function of z' on $-h \leq z' \leq h$. Hence the contribution to the vector potential $A_z(z)$ at each point on $-h \leq z \leq h$, as calculated from equation (2.20), is due primarily to current elements in a small neighborhood about the point $z' = z$. Because the distribution of current $I_z(z)$ is continuous, then the current $I_z(z')$ for $z' = z$ makes the major

contribution

It is expected

should be ess

$-h \leq z \leq h$.

The p

identified app

this replacem

which is equiv

constant dimer

and is designat

by King, 2, 4 in

essentially inde

primarily by th

is indeed a con

validity of this

of the following

Accord

of current on t

as

contribution to the vector potential at a point z on the cylinder surface. It is expected from this argument therefore, that the ratio $A_z(z)/I_z(z)$ should be essentially constant at each point along the cylinder, or for $-h \leq z \leq h$.

The preceding conclusion is obtained directly if $K(z, z')$ is identified approximately with the Dirac delta function $\delta(z-z')$. Making this replacement in equation (2.20), there is obtained

$$\frac{A_z(z)}{I_z(z)} = \frac{\mu_0}{4\pi} \quad -h \leq z \leq h \quad (2.24)$$

which is equivalent to the remarks of the last paragraph. An essentially constant dimensionless quantity $\Psi(z)$ is thus defined by

$$\frac{A_z(z)}{I_z(z)} = \frac{\mu_0}{4\pi} \Psi(z) \quad -h \leq z \leq h \quad (2.25)$$

and is designated as the "expansion parameter." It has been indicated by King,^{2, 4} in agreement with the above arguments, that $\Psi(z)$ is essentially independent of z except near $z = \pm h$, and is determined primarily by the antenna dimensions. It is thus asserted that $\Psi(z) = \Psi$ is indeed a constant depending only upon the antenna dimensions. The validity of this assumption will be discussed more fully in section 3.6 of the following chapter.

According to the approximation discussed above, the distribution of current on the cylinder is related to the vector potential at its surface as

$$I_z(z) = \frac{4\pi}{\mu_0 \Psi} A_z(z)$$

An expression
has been obtained
for the antenna current
from equation

$$I_z(z)$$

where $\xi_0 =$

It is to be noted

$$I_z(z) = I_z(-z)$$

Result:

C_1 and $I_z(d)$

solution (2.27)

The straight line

fields finally

$$-h \leq z \leq h \quad a$$

$$I_z(z) =$$

An expression for the vector potential at the surface of the cylinder has been obtained, however, as equation (2.19). The distribution of antenna current on $-h \leq z \leq h$ is therefore obtained approximately from equations (2.26) and (2.19) as

$$I_z(z) = \frac{4\pi}{\mu_o \Psi} C_1 e^{j\beta_o z} + \frac{4\pi}{\mu_o \Psi} C_1 e^{-j\beta_o z} + \frac{2\pi V_o}{\zeta_o \Psi} e^{-j\beta_o |z|} - \frac{2\pi}{\zeta_o \Psi} Z_L I_z(d) [e^{-\beta_o |z-d|} + e^{-j\beta_o |z+d|}] \quad (2.27)$$

where $\zeta_o = \sqrt{\mu_o / \epsilon_o} = 120\pi$ is the intrinsic impedance of free space. It is to be noted that this expression satisfies the symmetry condition $I_z(z) = I_z(-z)$.

Result (2.27) contains the two as yet undetermined constants C_1 and $I_z(d)$. These constants may be evaluated by applying to solution (2.27) the boundary conditions (2.23), which are given by

$$\begin{aligned} I_z(z=h) &= 0 \\ I_z(z=d) &= I_z(d) \end{aligned} \quad (2.23)$$

The straightforward application of these conditions to expression (2.27) yields finally the approximate distribution of cylinder current on $-h \leq z \leq h$ as

$$I_z(z) = \frac{V_o \pi}{\zeta_o \Psi} \left[\frac{D_1}{D_2} e^{-j\beta_o z} + \frac{D_1}{D_2} e^{j\beta_o z} + 2e^{-j\beta_o |z|} - \frac{Z_L}{30T} \left(\frac{D_1}{D_2} \cos \beta_o d + e^{-j\beta_o d} \right) \left(e^{-j\beta_o |z-d|} + e^{-j\beta_o |z+d|} \right) \right] \quad (2.28)$$

In this result

upon the exc

impedance a

An app

the doubly loa

distribution c

in terms of its

and position o

parameter. T

of current on t

following chap

utilized to calc

2.5. Input Imp

The inp

defined by

This expressi

approximate d

and is found to

In this result, the factors T , D_1 , and D_2 are constants depending upon the excitation frequency, the cylinder dimensions, and the impedance and position of the loading as

$$T = \Psi + \frac{Z_L}{60} (1 + e^{-j2\beta_o d}) \quad (2.29)$$

$$D_1 = \frac{Z_L}{30T} e^{-j\beta_o d} \cos \beta_o d - 1 \quad (2.30)$$

$$D_2 = e^{j\beta_o h} \cos \beta_o h - \frac{Z_L}{30T} \cos^2 \beta_o d \quad (2.31)$$

An approximate expression for the distribution of current on the doubly loaded cylinder has been obtained in equation (2.28). This distribution completely characterizes the linear antenna, and is given in terms of its dimensions, the excitation frequency, the impedance and position of the double loading, and the as yet undetermined expansion parameter. The optimum loading to yield a traveling wave distribution of current on the cylinder will be obtained from this result in the following chapter. This traveling wave current distribution will then be utilized to calculate the value of the expansion parameter Ψ .

2.5. Input Impedance of the Doubly Loaded Linear Antenna

The input impedance to the doubly loaded linear antenna is defined by

$$Z_{in} = \frac{V_o}{I_z(z=0)} \quad (2.32)$$

This expression is readily evaluated by using result (2.28) for the approximate distribution of current on the doubly loaded cylinder, and is found to be

$$Z_{in} =$$

An approximate

linear antenna

of excitation.

$$Z_{\text{in}} = 60 \Psi \left[1 + \frac{D_1}{D_2} - \frac{Z_L}{30T} e^{-j\beta_o d} \left(\frac{D_1}{D_2} \cos \beta_o d + e^{-j\beta_o d} \right) \right]^{-1}$$

(2.33)

An approximate relation for the input impedance to the doubly loaded linear antenna is thus obtained in terms of its dimensions, the frequency of excitation, and the impedance and position of the loading.

3.1. Phys
Doub

An a

the doubly l

This solution

sufficient to

restricted to

terms in exp

which are m

The d

from the gene

$$I_z(z) =$$

while that on

$$I_z(z) =$$

CHAPTER 3

OPTIMUM LOADING FOR A TRAVELING WAVE DISTRIBUTION OF ANTENNA CURRENT

3.1. Physical Interpretation of the Distribution of Current on a Doubly Loaded Dipole

An approximate expression for the distribution of current on the doubly loaded linear antenna has been developed as equation (2.28). This solution is valid on $-h \leq z \leq h$, but since $I_z(-z) = I_z(z)$ it is sufficient to consider only the current on $0 \leq z \leq h$. If attention is restricted to the regions $0 \leq z \leq d$ and $d \leq z \leq h$, then the various terms in expression (2.28) may be combined to yield a pair of results which are more physically meaningful.

The distribution of cylinder current for $0 \leq z \leq d$ is obtained from the general result (2.28) as

$$I_z(z) = \frac{V_o \pi}{\zeta_o \Psi} \left\{ \left[2 + \frac{D_1}{D_2} - \frac{Z_L}{30T} e^{-j\beta_o d} \left(\frac{D_1}{D_2} \cos \beta_o d + e^{-j\beta_o d} \right) \right] e^{-j\beta_o z} + \left[\frac{D_1}{D_2} - \frac{Z_L}{30T} e^{-j\beta_o d} \left(\frac{D_1}{D_2} \cos \beta_o d + e^{-j\beta_o d} \right) \right] e^{j\beta_o z} \right\} \quad (3.1)$$

while that on $d \leq z \leq h$ becomes

$$I_z(z) = \frac{V_o \pi}{\zeta_o \Psi} \left\{ \left[2 + \frac{D_1}{D_2} - \frac{Z_L}{15T} \cos \beta_o d \left(\frac{D_1}{D_2} \cos \beta_o d + e^{-j\beta_o d} \right) \right] e^{-j\beta_o z} + \left[\frac{D_1}{D_2} \right] e^{j\beta_o z} \right\} \quad (3.2)$$

A physical

from expe

It is

current ma

inward trav

an outward

$z = 0$. At z

transmitted

traveling wa

outward tra

Similar

current on $z = 0$

traveling cur

an outward tr

transmitted p

wave is refle

$z = h$. The s

wave of curre

$z = h$.

It is in

traveling wave

$0 \leq z \leq d$ and

traveling wave

either region.

supported alo

A physical interpretation of the current distribution is readily obtained from expressions (3.1) and (3.2).

It is observed from equation (3.1) that on $0 \leq z \leq d$ the total current may be considered as a superposition of a pair of outward and inward traveling current waves. The first term in this result represents an outward traveling wave of current which is excited by the source at $z = 0$. At $z = d$ this current wave is partially reflected and partially transmitted. The second term of equation (3.1) represents an inward traveling wave of current which results from the reflection of the outward traveling wave by the impedance discontinuity at $z = d$.

Similarly, equation (3.2) indicates that the distribution of cylinder current on $d \leq z \leq h$ is composed of a pair of oppositely directed traveling current waves. The first term of this expression represents an outward traveling wave of current which is excited at $z = d$ by the transmitted portion of the outward wave on $0 \leq z \leq d$. This current wave is reflected by the structural discontinuity in the cylinder at $z = h$. The second term of equation (3.2) represents the inward traveling wave of current which results from the reflection of the outward wave at $z = h$.

It is indicated therefore, that in general both outward and inward traveling waves of current are supported on each of the two regions $0 \leq z \leq d$ and $d \leq z \leq h$. The superposition of the oppositely directed traveling waves results in a standing wave distribution of current along either region. Thus in the usual case a standing wave of current is supported along the entire cylinder.

3.2. Optimum Cylindrical

It has

loaded cylinder

current over

might be mod

loading, to y

current over

It is e

a purely outw

inward travel

unalterable st

able to suscep

chosen the in

leaving only t

region. Since

reflected from

that such an

The op

wave distrib

from express

inward travel

of this condit

term in equat

traveling wave

3.2. Optimum Loading Impedance for a Traveling Wave Distribution of Cylinder Current

It has been indicated in the preceding section that the doubly loaded cylinder generally supports a standing wave distribution of current over its entire length. The possibility that this distribution might be modified, through the selection of an optimum impedance loading, to yield a purely outward traveling wave distribution of current over most of the cylinder is now to be investigated.

It is evident physically that no choice of the loading will give a purely outward traveling current wave on $d \leq z \leq h$, since the inward traveling wave on that region is due to a reflection from the unalterable structural discontinuity at $z = h$. However, it is reasonable to suspect on physical grounds that if the loading is properly chosen the inward traveling wave on $0 \leq z \leq d$ might be eliminated, leaving only the desired outward traveling wave of current over that region. Since the inward traveling wave on $0 \leq z \leq d$ is actually reflected from the impedance discontinuity at $z = d$, it is expected that such an optimum loading should exist.

The optimum loading impedance to yield an outward traveling wave distribution of cylinder current on $0 \leq z \leq d$ may be obtained from expression (3.1). This situation evidently requires that the inward traveling current wave on that region should vanish. Realization of this condition is accomplished by equating the coefficient of the second term in equation (3.1), which corresponds to the amplitude of the inward traveling wave, to zero as

$$\frac{D_1}{D_2}$$

Using the c

D_2 , respec

impedance,

After consid

cast into the

[2

When the loa

current on 0

wave, while t

Expre

its position

For a given se

function only c

the loading loc

specified in o

certain presc

It has

depends only

the cylinder d

to suspect tha

$$\frac{D_1}{D_2} - \frac{Z_L}{30T} e^{-j\beta_o d} \left(\frac{D_1}{D_2} \cos \beta_o d + e^{-j\beta_o d} \right) = 0 \quad (3.3)$$

Using the defining relations (2.29), (2.30), and (2.31) for T , D_1 , and D_2 , respectively, this equation may be solved for the optimum loading impedance, designated as $[Z_L]_0$, to yield

$$[Z_L]_0 = 30\Psi \frac{e^{j\beta_o d}}{\cos \beta_o d - e^{j\beta_o(h-d)} \cos \beta_o h} \quad (3.4)$$

After considerable straightforward manipulation, result (3.4) may be cast into the simpler form

$$[Z_L]_0 = 30\Psi [1 + j \cot \beta_o(h-d)] \quad (3.5)$$

When the loading impedance is given by this relation, the cylinder current on $0 \leq z \leq d$ becomes the desired purely outward traveling wave, while that on $d \leq z \leq h$ remains the usual standing wave.

Expression (3.5) gives the optimum loading impedance in terms of its position, the cylinder dimensions, and the frequency of excitation. For a given set of antenna dimensions, this optimum impedance is a function only of its position d and the frequency ω . At this point the loading location is completely arbitrary, and may be freely specified in order that the corresponding impedance may satisfy certain prescribed conditions.

It has been indicated that the optimum loading impedance $[Z_L]_0$ depends only upon its position d and the excitation frequency ω once the cylinder dimensions h and a have been specified. This leads one to suspect that, at least at a single frequency, it should be possible to

choose an op

either purely

will be consi

Since

as $\Psi = u +$

of expression

or, in terms

An explicit e

developed in

3.3. Purely

In or

loading, it is

optimum loa

This result

loading as

while its res

choose an optimum position for the loading such that $[Z_L]_0$ will be either purely resistive or purely reactive. These two special cases will be considered individually in the following two sections.

Since Ψ is in general a complex number, it may be written as $\Psi = u + jv$. With this designation, the optimum loading impedance of expression (3.5) becomes

$$[Z_L]_0 = 30(u + jv)[1 + j \cot \beta_o(h-d)] \quad (3.6)$$

or, in terms of real and imaginary parts

$$[Z_L]_0 = 30 \{ [u - v \cot \beta_o(h-d)] + j[v + u \cot \beta_o(h-d)] \} \quad (3.7)$$

An explicit expression for the expansion parameter Ψ is to be developed in section 3.6.

3.3. Purely Resistive Optimum Loading

In order to obtain the condition for a purely resistive optimum loading, it is only necessary to equate the reactive component of the optimum loading impedance given by expression (3.7) to zero as

$$v + u \cot \beta_o(h-d) = 0 \quad (3.8)$$

This result yields the necessary position of an optimum purely resistive loading as

$$\frac{h-d}{\lambda_o} = \frac{1}{2\pi} \tan^{-1} \left(-\frac{u}{v} \right) \quad (3.9)$$

while its resistance becomes

Theoretic

optimum

d satisfie

wave of cu

It v

weak funct

expression

frequency

The

indicated in

λ_0 for th

and a diam

a half-length

obtaining the

was made of

This equation

dimensions

from the fig

over a wide

of such a loa

function of th

depends dire

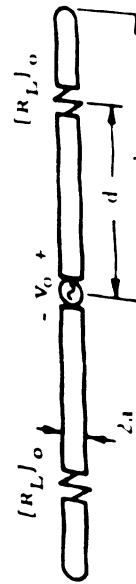
velocity of p

$$\begin{aligned}
[R_L]_0 &= 30 [u - v \cot \beta_0 (h-d)] \\
&= 30 \left(u + \frac{v^2}{u}\right)
\end{aligned} \tag{3.10}$$

Theoretically then, a linear antenna which is doubly loaded with an optimum resistance $[R_L]_0$ as given by result (3.10), whose position d satisfies equation (3.9), will support a purely outward traveling wave of current on $0 \leq z \leq d$.

It will be indicated in section 3.6 that $\Psi = u + jv$ is a relatively weak function of the excitation frequency. Thus it is observed from expressions (3.9) and (3.10) that $(h-d)/\lambda_0$ and $[R_L]_0$ are essentially frequency independent.

The parameters of an optimum purely resistive loading are indicated in Figure (3.1) as a function of the antenna electrical length h/λ_0 for the typical case of an antenna having a half-length of $h = 31.25$ cm and a diameter of $2a = 0.25$ inches. These dimensions correspond to a half-length of $h = 0.625 \lambda_0$ at an excitation frequency of 600 mhz. In obtaining these numerical results from expressions (3.9) and (3.10) use was made of equation (3.37), which will be developed in section 3.6. This equation gives the expansion parameter Ψ in terms of the antenna dimensions h and a , and the excitation frequency ω . It is noted from the figure that both $(h-d)/\lambda_0$ and $[R_L]_0$ are essentially constant over a wide range of frequencies. Thus while the optimum resistance of such a loading is almost constant, its necessary position is a strong function of the frequency of excitation. This is evident since d then depends directly upon $\lambda_0 = v_0/f$, where f is the frequency and v_0 the velocity of propagation in free space.



$h = 31.25 \text{ cm}$
 $z_A = 0.25 \text{ m}$

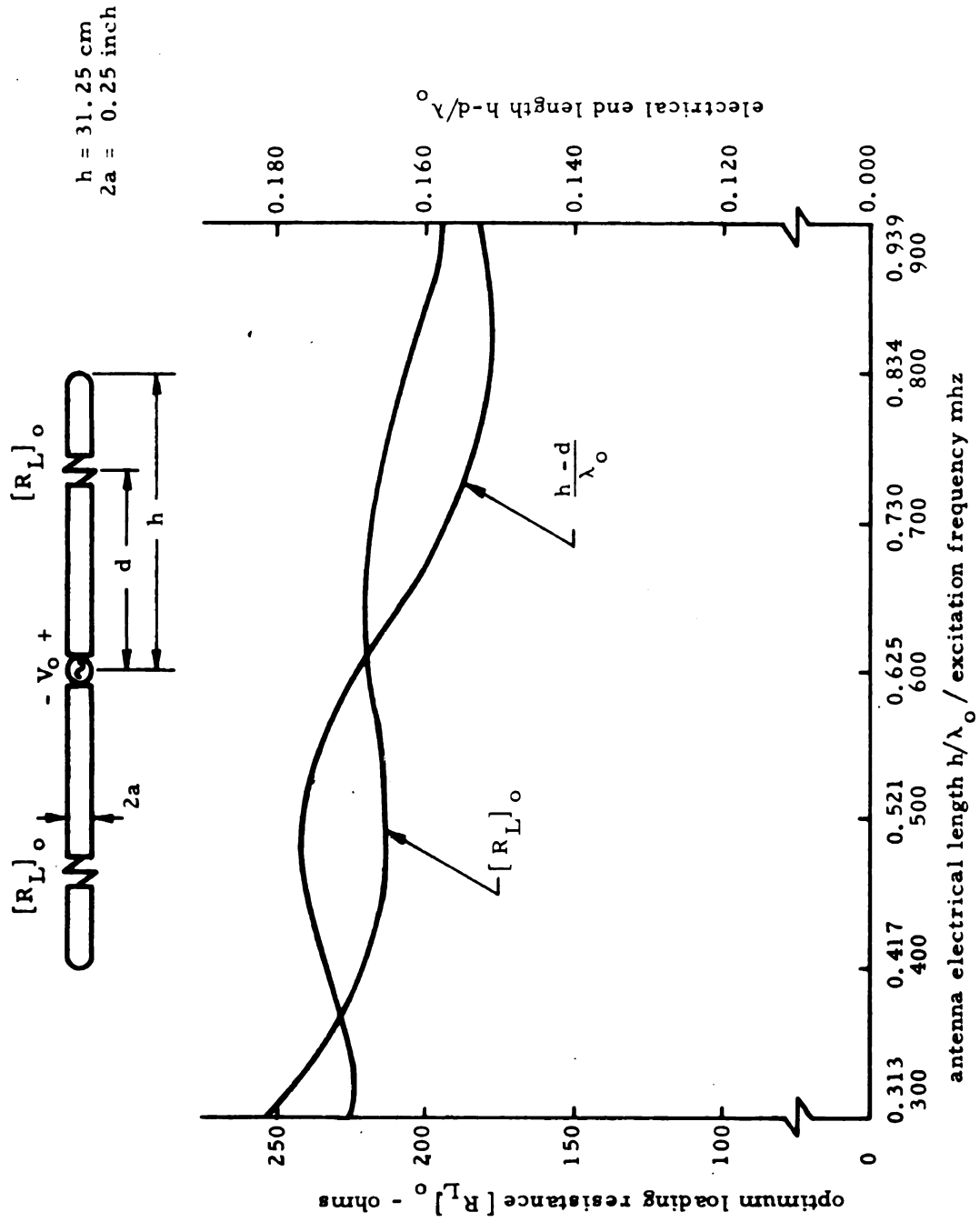


Figure 3.1.1. Resistance and Position of Optimum Dissipative Loading as a Function of the Antenna Electrical Length.

The
reported by
experimental
optimum re
optimum loa
given set of
frequency.
should be pl
ends in orde

For a
 $2a = 0.25$ inc
results indic
of an optimum
240 ohms: (h
experiment w
theoretical va
respectively,
quantitative a
and the avail

It has
resistive opt
frequency. I
of the loadin
an optimum
frequency. I
its impedance

The preceding theoretical results correspond to the research reported by Altshuler.³ As indicated earlier, Altshuler carried out an experimental investigation of a linear antenna doubly loaded with an optimum resistance. This experiment indicated that the value of the optimum loading resistance was essentially constant, i. e., for a given set of antenna dimensions it was a weak function of the excitation frequency. It was found further that such a purely resistive loading should be placed approximately a quarter wavelength from the antenna ends in order to obtain a traveling wave distribution of current.

For an antenna having the same dimensions ($h = 31.25$ cm, $2a = 0.25$ inch) as those which were used in obtaining the theoretical results indicated in Figure 3.1, Altshuler determined the parameters of an optimum purely resistive loading experimentally as: $[R_L]_0 = 240$ ohms; $(h-d) = 0.25 \lambda_0$. The excitation frequency utilized in the experiment was 600 mhz ($\lambda_0 = 50$ cm). A corresponding set of theoretical values are obtained from equations (3.10) and (3.9), respectively, as: $[R_L]_0 = 220$ ohms; $(h-d) = 0.17 \lambda_0$. An excellent quantitative agreement is thus observed between the present theory and the available experimental results.

It has been indicated that the necessary position of a purely resistive optimum loading is a strong function of the excitation frequency. In a practical physical situation, however, the location of the loading must be fixed at some point along the antenna. Hence an optimum purely resistive loading is possible only at a single frequency. If the position of an optimum loading is chosen such that its impedance is purely resistive at a given frequency, then at any

other frequ

reactive com

It is

optimum loa

becomes pur

the dimension

considered.

then its impe

at a frequen

The c

at this locati

electrical len

it is noted tha

for the frequ

optimum imp

a purely outw

It is r

deviations ab

impedance va

essentially c

component of

resistive cor

fixed position

wave distrib

As the frequ

other frequency an optimum impedance must have both resistive and reactive components.

It is interesting to consider the frequency dependence of an optimum loading whose fixed position is so chosen that its impedance becomes purely resistive at a given frequency. An antenna having the dimensions $h = 31.25$ cm and $2a = 0.25$ inch will again be considered. If the optimum loading is placed such that $(h-d) = 0.17\lambda_0$, then its impedance becomes purely resistive with $[R_L]_0 = 220$ ohms at a frequency where $h = 0.625\lambda_0$ (600 mhz).

The optimum impedance of a loading having its position fixed at this location is indicated in Figure 3.2 as a function of the antenna electrical length. This result is obtained from equation (3.5), and it is noted that the reactive component of the impedance vanishes only for the frequency where $h = 0.625\lambda_0$. At any other frequency, the optimum impedance must have a reactive component in order to yield a purely outward traveling wave of current.

It is noted from the figure, however, that for small frequency deviations about the value where the reactive component of the optimum impedance vanishes, the resistive component of this impedance is essentially constant. Furthermore, for such frequencies, the reactive component of the optimum loading impedance is much smaller than its resistive component. Thus a constant purely resistive loading of fixed position may be utilized to realize an approximately traveling wave distribution of antenna current for a band of excitation frequencies. As the frequency deviates further from its value corresponding to an

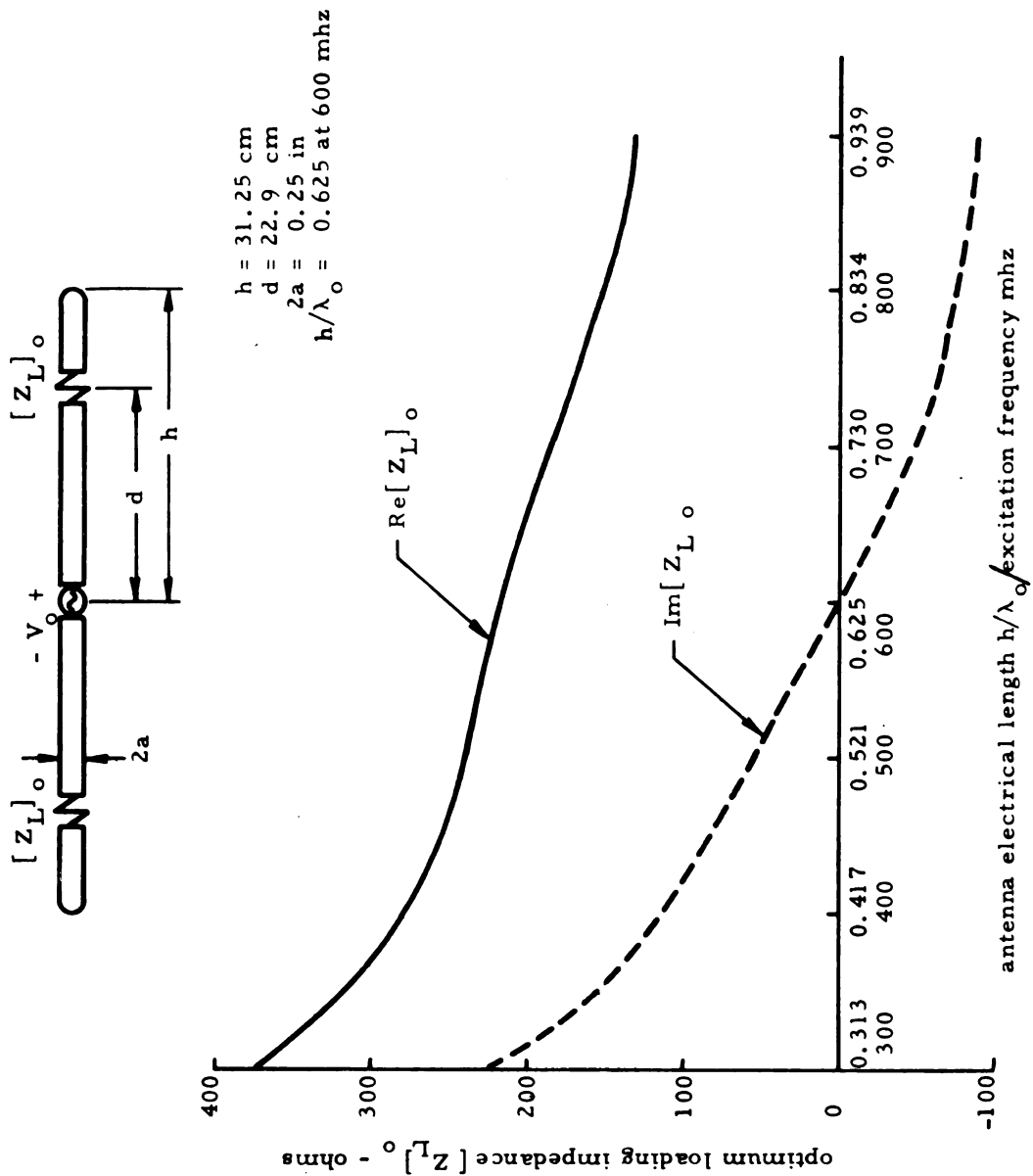


Figure 3.2. Optimum Impedance (purely resistive at 600 mhz) of Loading with Fixed Position as a Function of the Antenna Electrical Length.

optimum

essentia

obtained

3.4. Pu

2

obtained

given by

This res

non-diss

With this

becomes

It is indica

doubly load

reactance

satisfies ec

of current c

In s

independent

optimum loading, the current distribution slowly reverts back to an essentially standing wave. These are exactly the results which were obtained by Altshuler in his experimental study.

3.4. Purely Reactive Optimum Loading

The condition for a purely non-dissipative optimum loading is obtained by equating the resistive component of the optimum impedance given by expression (3.7) to zero as

$$u - v \cot \beta_o(h-d) = 0 \quad (3.11)$$

This result requires that the necessary position of an optimum purely non-dissipative loading be given by

$$\frac{h-d}{\lambda_o} = \frac{1}{2\pi} \tan^{-1} \left(\frac{v}{u} \right) \quad (3.12)$$

With this condition satisfied, the corresponding optimum loading reactance becomes

$$\begin{aligned} [X_L]_0 &= 30 [v + u \cot \beta_o(h-d)] \\ &= 30 \left(v + \frac{u^2}{v} \right) \end{aligned} \quad (3.13)$$

It is indicated theoretically therefore, that a linear antenna which is doubly loaded with an optimum non-dissipative impedance, whose reactance $[X_L]_0$ is given by expression (3.13) and whose position d satisfies equation (3.12), will support a purely outward traveling wave of current on $0 \leq z \leq d$.

In section 3.6 it will be indicated that $\Psi = u + jv$ is relatively independent of the excitation frequency, and depends primarily upon the

antenna d

indicate,

frequency

N

dissipative

following

(1

(2

The optim

$(h-d)/\lambda_0$ a

antenna ele

These num

(3.13). Th

equation (3

dimensions

It is

$(h-d)/\lambda_0$ an

frequencies

dissipative

strong func

resistive

directly up

which the d

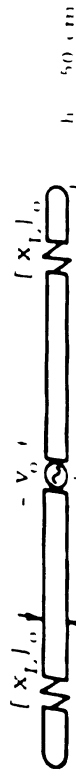
antenna dimensions h and a . Expressions (3.12) and (3.13) therefore indicate, respectively, that $(h-d)/\lambda_0$ and $[X_L]_0$ are essentially frequency independent.

Numerical values for the parameters of an optimum non-dissipative loading will be obtained for a pair of antennas having the following dimensions:

- (1) $h = 50$ cm, $2a = 0.25$ inch; $h = \lambda_0$ at a frequency of $f = 600$ mhz.
- (2) $h = 100$ cm, $2a = 0.25$ inch; $h = 2\lambda_0$ at a frequency of 600 mhz.

The optimum loading reactance $[X_L]_0$ and its necessary location $(h-d)/\lambda_0$ are indicated in Figures 3.3 and 3.4 as a function of the antenna electrical length h/λ_0 for antennas (1) and (2), respectively. These numerical results were obtained from expressions (3.12) and (3.13). The value of the expansion parameter Ψ was calculated from equation (3.37) of section 3.6, which gives Ψ in terms of the antenna dimensions h and a and the excitation frequency ω .

It is observed from the figures that, for either antenna, both $(h-d)/\lambda_0$ and $[X_L]_0$ are essentially constant for a wide band of frequencies. Hence while the optimum reactance of such a non-dissipative loading is rather constant, its necessary position is a strong function of the excitation frequency. As for the case of a purely resistive loading, this is evident since the loading position d depends directly upon the wavelength $\lambda_0 = v_0/f$, where f is the frequency at which the dipole is excited.



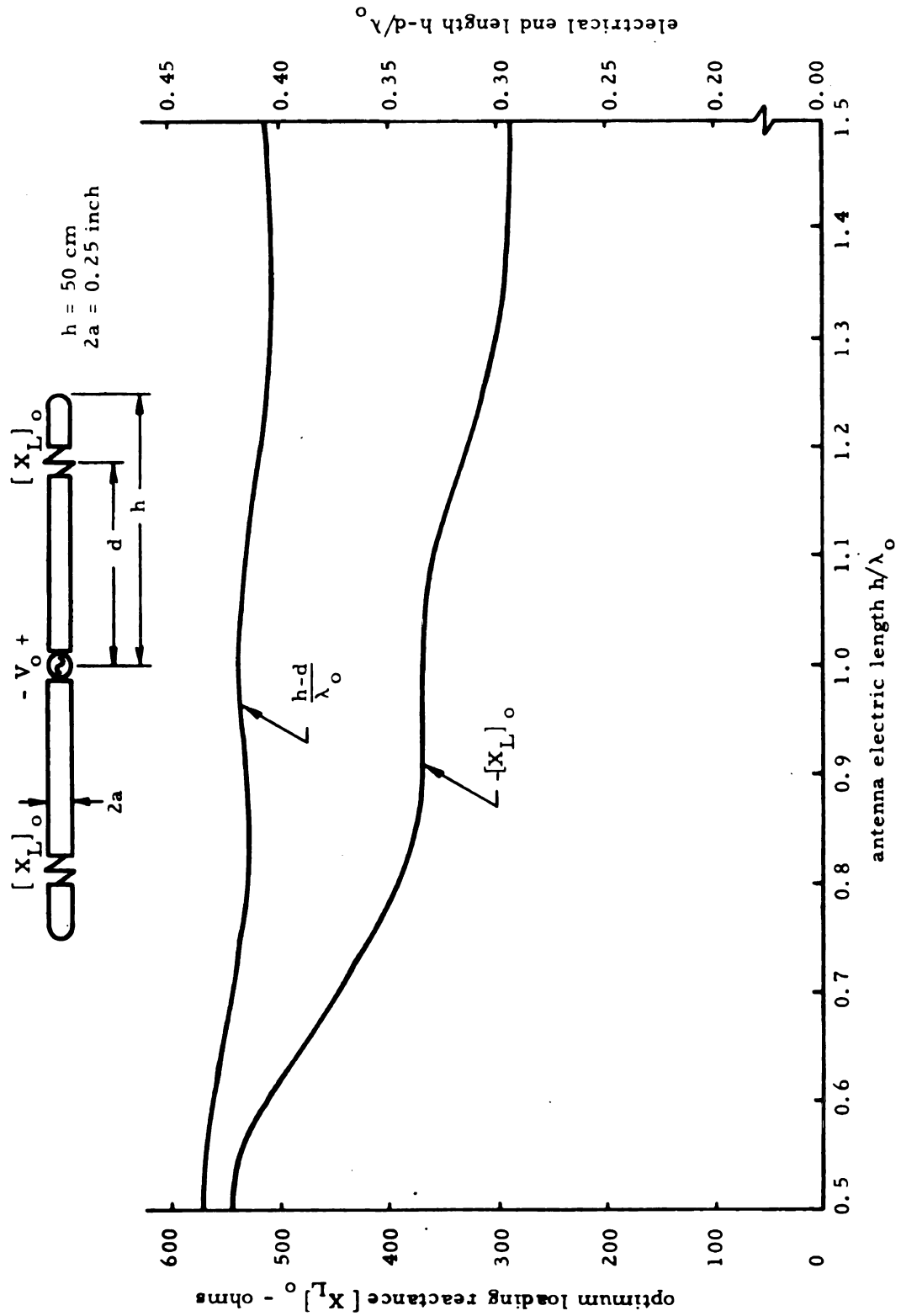


Figure 3.3. Reactance and Position of Optimum Non-Dissipative Loading as a Function of the Antenna Electrical Length ($h = 50$ cm $= \lambda_o$ at 600 mhz).



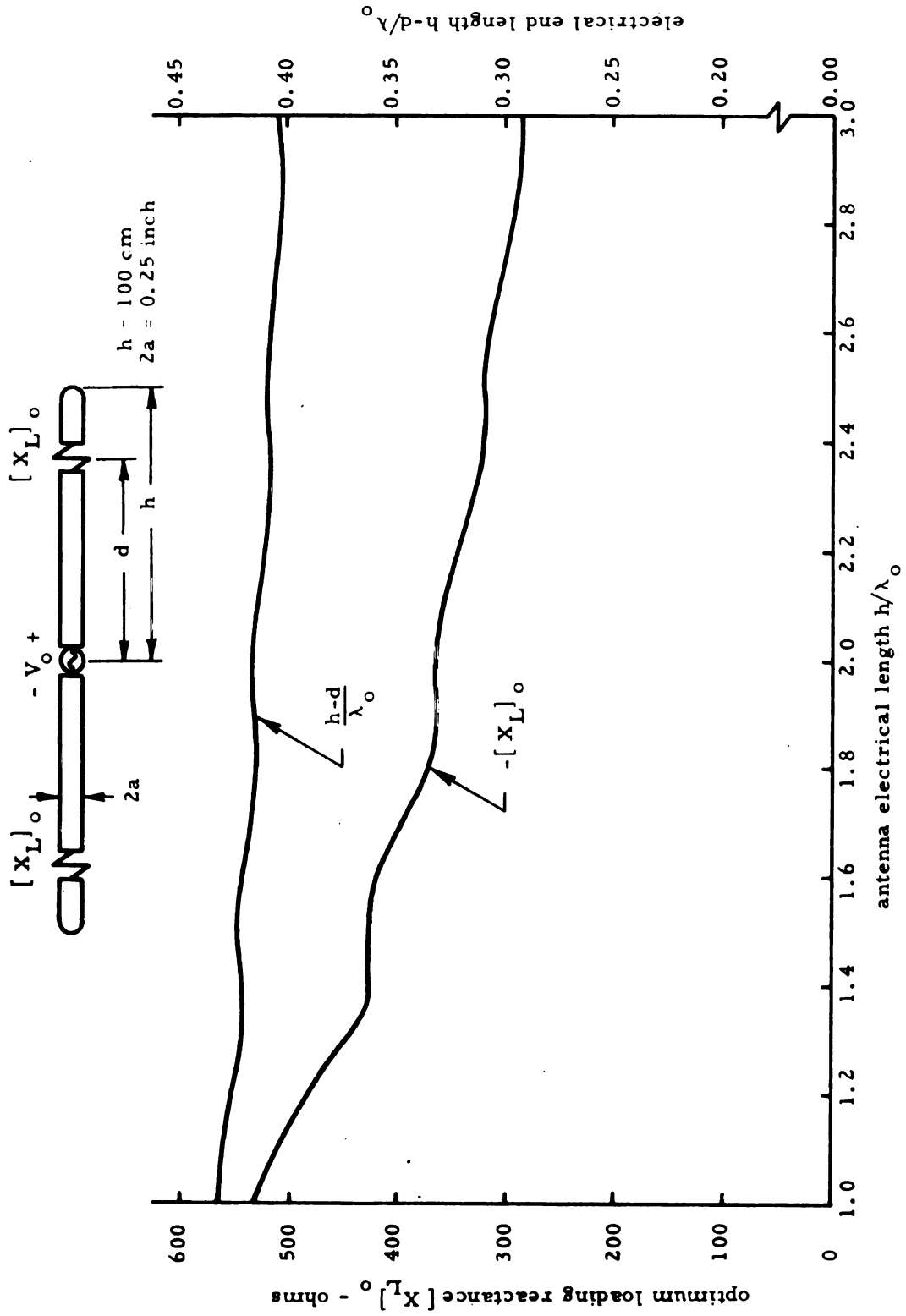


Figure 3.4. Reactance and Position of Optimum Non-Dissipative Loading as a Function of the Antenna Electrical Length ($h = 100$ cm $= 2\lambda_o$ at 600 mhz).

numeric

frequency

its neces

even thou

In particu

optimum

(1)

(2)

This resul

section 3.6

dent of the

of a wavele

the cylinder

function of

It ha

the necessa

dependent up

practical ar

that the pos

With this re

be realized

impedance

given frequ

resistive an

A comparison of Figures 3.3 and 3.4 indicates that these numerical results are nearly identical for antennas (1) and (2). The frequency dependence of the optimum loading reactance $[X_L]_0$ and its necessary position $(h-d)/\lambda_0$ are almost the same in either case, even though the half-length of one antenna is twice that of the other. In particular, at a frequency of 600 mhz the parameters of an optimum non-dissipative loading for these two antennas are

$$(1) \quad h = \lambda_0; [X_L]_0 = -366 \text{ ohms}, (h-d) = 0.418 \lambda_0.$$

$$(2) \quad h = 2\lambda_0; [X_L]_0 = -363 \text{ ohms}, (h-d) = 0.417 \lambda_0.$$

This result is a consequence of the fact (as will be discussed in section 3.6) that the expansion parameter Ψ is essentially independent of the antenna half-length whenever this dimension is of the order of a wavelength or greater. A similar situation is not observed when the cylinder diameter $2a$ is varied, however, since Ψ is a strong function of the cylinder diameter for all values of its half-length h .

It has been indicated that, for a given set of cylinder dimensions, the necessary position of an optimum non-dissipative loading is strongly dependent upon the frequency of excitation. Physically, however, a practical arrangement of such a doubly loaded linear antenna requires that the position of the loading be fixed at some point along the cylinder. With this restriction, an optimum purely reactive loading may therefore be realized only at a single frequency. If the location of such an optimum impedance loading is so chosen that it becomes purely reactive at a given frequency, then at any other frequency it must consist of both resistive and reactive components.

interest

whose 1

reactive

numeric

again be

equation

come pur

specific a

(1)

(2)

The

indicated a

and 3.6 for

(1) and (2) a

reactive at

from the ge

fixed at the

resistive c

frequency w

any other fr

resistive a

wave distrib

Since the position of the impedance must be fixed, it is of interest to consider the frequency dependence of an optimum loading whose location is so chosen that its impedance becomes purely reactive at a given frequency. In order to obtain some specific numerical results, the two antennas considered previously will again be utilized. The loading positions are chosen according to equation (3.12) such that the corresponding optimum impedances become purely reactive at a frequency of 600 mhz ($\lambda_o = 50$ cm). The specific antenna dimensions and loading locations are then as follows:

(1) $h = 50$ cm, $2a = 0.25$ inch, $d = 29.1$ cm; at 600 mhz:

$$h = \lambda_o, (h-d) = 0.418 \lambda_o, [X_L]_0 = -366 \text{ ohms.}$$

(2) $h = 100$ cm, $2a = 0.25$ inch, $d = 79.2$ cm; at 600 mhz:

$$h = 2\lambda_o, (h-d) = 0.417 \lambda_o, [X_L]_0 = -363 \text{ ohms.}$$

The optimum impedance of a loading with fixed position is indicated as a function of the antenna electrical length in Figures 3.5 and 3.6 for the configurations corresponding, respectively, to antennas (1) and (2) above. Since the optimum impedance is no longer purely reactive at every excitation frequency, these results were obtained from the general expression (3.5), with the dimensions h and d fixed at the appropriate values. It is noted that in either case the resistive component of the optimum impedance vanishes only at the frequency where $h = \lambda_o$ or $h = 2\lambda_o$, respectively (600 mhz). At any other frequency, an optimum loading impedance must have a resistive as well as a reactive component in order to yield a traveling wave distribution of antenna current.

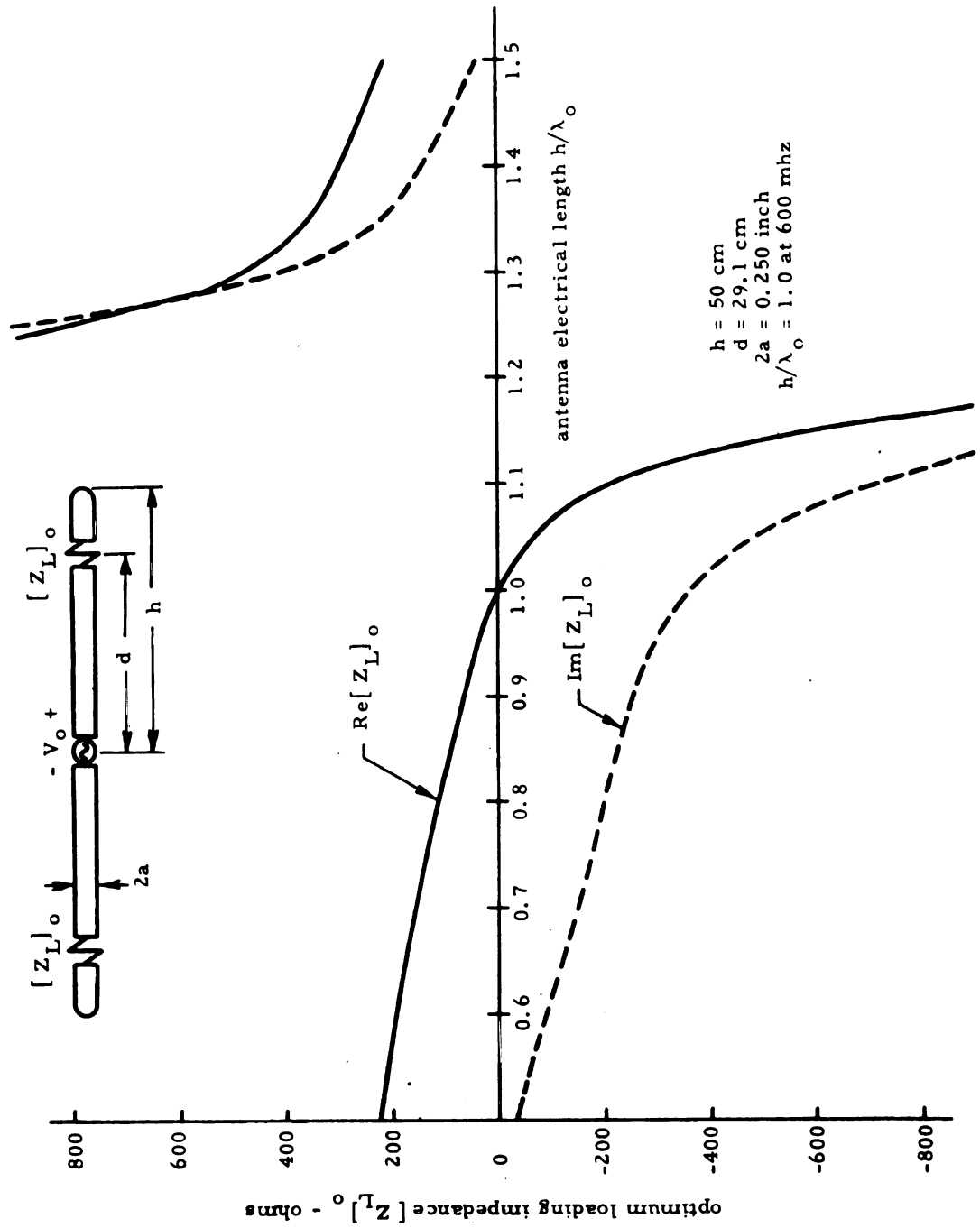


Figure 3.5. Optimum Impedance (purely reactive at 600 mhz) of Loading with Fixed Position as a Function of the Antenna Electrical Length ($h = 50$ cm).

1871

+

12.1.0

7008

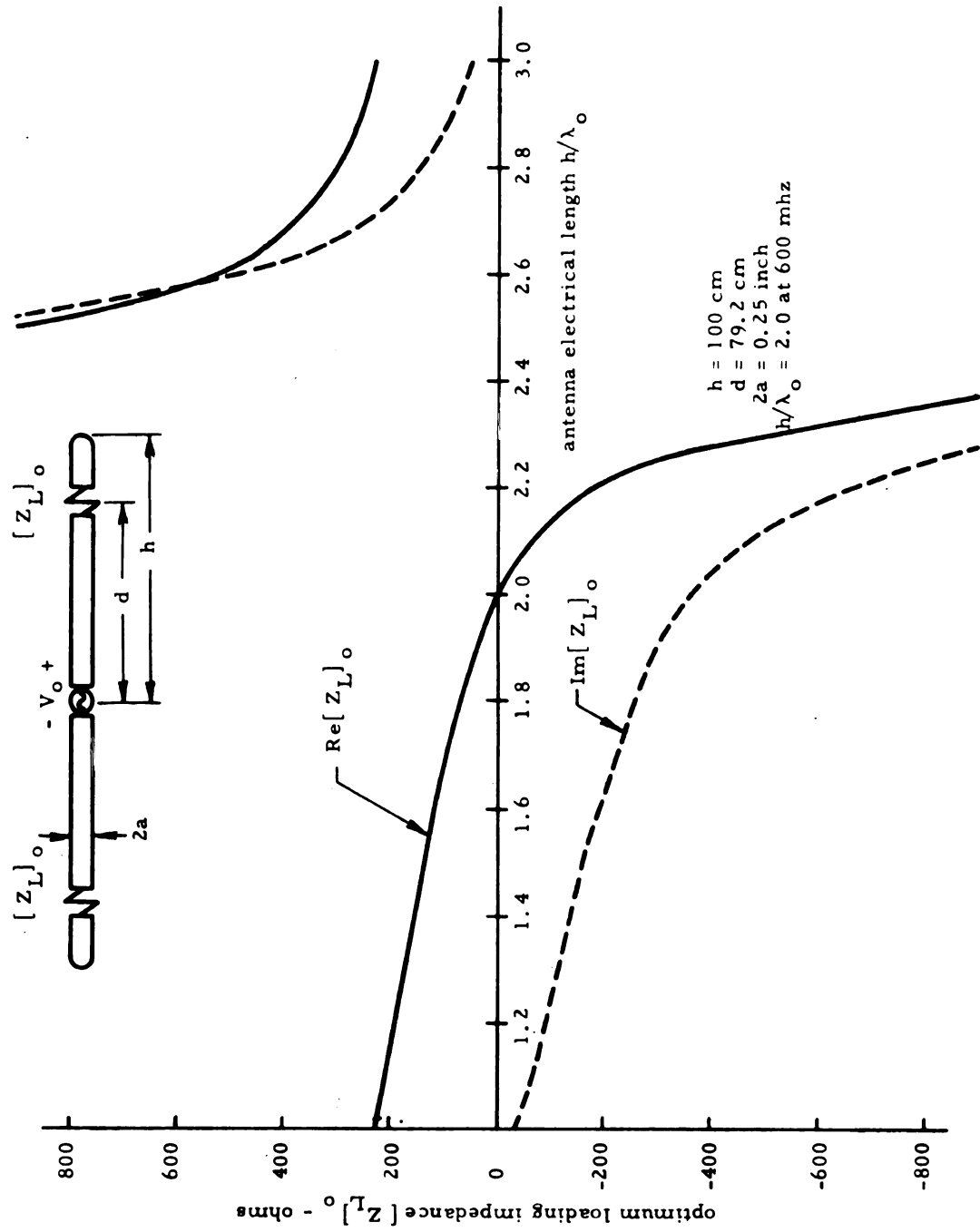


Figure 3.6. Optimum Impedance (purely reactive at 600 mhz) of Loading with Fixed Position as a Function of the Antenna Electrical Length ($h = 100$ cm).

Th

Figures 3

fixed posit

(i)

(ii)

(iii)

(iv)

It is there

to yield a

every freq

be utilized

no practice

a frequency

Since

The following important characteristics are observed from Figures 3.5 and 3.6 for the case of an optimum impedance loading of fixed position:

- (i) In general, an optimum loading impedance requires both resistive and reactive components. The resistive component vanishes only at a single frequency.
- (ii) Both the resistive and reactive components of the optimum impedance are strong functions of frequency. There is a frequency just above that where the resistive impedance component vanishes at which both impedance components tend to infinity.
- (iii) The sign of both impedance components changes within a relatively narrow frequency range. An optimum impedance thus requires a negative resistance component (active element) at certain frequencies, and its reactive component varies from capacitive to inductive as the frequency is increased.
- (iv) The reactive component of the optimum impedance has a negative slope as a function of frequency.

It is therefore evident that synthesis of an exact optimum impedance, to yield a purely outward traveling wave distribution of current at every frequency, is out of the question. Although an Esaki diode might be utilized to obtain a given negative resistance component, there is no practical means of realizing a variable negative resistance having a frequency dependence of the type indicated.

Since the high efficiency associated with a non-dissipative

loading is
dealing with
reactive co
dissipative
its effective
from this v
 $0 \leq z \leq d$
excitation f
will gradua
frequency

For

the current
will remain
since, refe
variations
small comp
in the frequ
component
and the eff
necessarily

An

therefore b
frequencies
position.
must match
of fixed pos

loading is of fundamental interest, one is led to consider, when dealing with a loading of fixed position, a loading consisting of the reactive component of the optimum impedance. Such a purely non-dissipative loading is optimum only at a single given frequency, and its effectiveness diminishes as the frequency of excitation is varied from this value. That is, the distribution of cylinder current on $0 \leq z \leq d$ will consist of a purely outward traveling wave at an excitation frequency corresponding to the given center frequency, but will gradually revert back to an essentially standing wave as the frequency of excitation deviates from this value.

For reasonably small excursions about the center frequency, the current distribution corresponding to such a non-dissipative loading will remain an essentially outward traveling wave. This is evident since, referring to Figures 3.5 and 3.6, for such small frequency variations the resistive component of the optimum impedance is small compared with its reactive component. For large deviations in the frequency of excitation, however, the magnitude of the resistance component becomes comparable with that of the reactive component, and the effectiveness of a purely non-dissipative loading will be necessarily reduced.

An approximately traveling wave distribution of current may therefore be maintained on a linear antenna over a band of excitation frequencies through the use of a non-dissipative loading of fixed position. The frequency dependence of this purely reactive loading must match that of the reactive component of the optimum impedance of fixed position. The circuit and radiation characteristics of an

antenna w

those for

In

it is neces

way as the

position, a

is to reali

Due to the

the use of

A similar

line section

is thus not

difficult sy

beyond the

In o

experiment

dissipative

demonstra

be excited

optimum p

Ex

an optimum

significant

its excitati

leading to

readily cal

antenna with such a non-dissipative loading will thus be typical of those for an ideal traveling wave antenna over this range of frequencies.

In order to realize an effective purely non-dissipative loading, it is necessary that its reactance depend upon frequency in the same way as the reactive component of the optimum impedance of fixed position, as indicated in Figures 3.5 and 3.6. The problem therefore is to realize such a frequency dependent reactance characteristic. Due to the negative slope of this reactance as a function of frequency, the use of an ordinary lumped capacitance would be relatively ineffective. A similar difficulty is encountered with a short circuited transmission line section, or a coaxial cavity. Such a frequency dependent reactance is thus not realizable with simple circuit elements, and presents a difficult synthesis problem. The consideration of this problem is beyond the scope of the present research.

In order to verify the preceding theoretical results, an experimental investigation of a linear antenna having a purely non-dissipative loading is made in Chapter 5. In particular, it is demonstrated that a traveling wave distribution of current may indeed be excited on a linear antenna through the use of a properly positioned optimum purely reactive loading.

Expressions (3.12) and (3.13) for the position and reactance of an optimum non-dissipative double loading are perhaps the most significant results of this research. Given the antenna dimensions and its excitation frequency, the parameters of an optimum non-dissipative loading to yield a traveling wave distribution of cylinder current are readily calculated from these simple expressions. Through the use of

such a load:

retains the

worthy of no

Alshuler³

in this case

open circuit

regardless

analog between

transmission

3.5. The D
to an

A ge

weld a trav

was determi

by this expr

reactive op

having both

(3.3) holds

The distrib

from equat

such a loading, a traveling wave linear antenna may be realized which retains the high efficiency of a conventional unloaded dipole. It is worthy of note that the simple transmission line analogy utilized by Altshuler³ in the study of a resistance loaded dipole fails completely in this case. A lossless transmission line section terminated in an open circuit cannot be matched with a purely reactive series loading regardless of its position. It is thus indicated that there is no real analogy between a linear antenna and an open circuited section of transmission line.

3.5. The Distribution of Current and Input Impedance Corresponding to an Optimum Loading

A general expression for the optimum loading impedance to yield a traveling wave distribution of cylinder current on $0 \leq z \leq d$ was determined as equation (3.5). Whenever the impedance is given by this expression, whether it consists of a purely resistive or reactive optimum loading of proper position or one of arbitrary position having both resistive and reactive impedance components, then condition (3.3) holds, i. e.,

$$\frac{D_1}{D_2} - \frac{Z_L}{30T} e^{-j\beta_o d} \left(\frac{D_1}{D_2} \cos \beta_o d + e^{-j\beta_o d} \right) = 0 \quad (3.3)$$

The distribution of cylinder current on $0 \leq z \leq d$ therefore becomes from equation (3.1)

$$I_z(z) = \frac{2 V_o \pi}{\zeta_o \Psi} e^{-j\beta_o z} \quad (3.14)$$

while by r

$I_z(\theta)$

These exp

current wa

wave which

It i

clearly the

be written

where A a

dimensions

and B is v

the cylinde

must be sa

The result

while by result (3.2) that on $d \leq z \leq h$ is given by

$$I_z(z) = \frac{V_o \pi}{\zeta_o \Psi} \left\{ \left[2 - \frac{Z_L}{30T} \left(\frac{D_1}{D_2} \cos \beta_o d + e^{-j\beta_o d} \right) \right] e^{-j\beta_o z} + \left[\frac{D_1}{D_2} \right] e^{j\beta_o z} \right\} \quad (3.15)$$

These expressions represent, respectively, the outward traveling current wave which has been realized on $0 \leq z \leq d$ and the standing wave which remains on $d \leq z \leq h$.

It is desired to simplify result (3.15) in order to indicate more clearly the distribution of current on $d \leq z \leq h$. This equation may be written in the general form

$$I_z(z) = \frac{2 V_o \pi}{\zeta_o \Psi} \left[A e^{-j\beta_o z} + B e^{j\beta_o z} \right] \quad (3.16)$$

where A and B are complex constants depending upon the antenna dimensions and the loading parameters. The direct evaluation of A and B is very tedious, so an alternate method will be used. Since the cylinder current is continuous at $z = d$, then the condition

$$I_z(z=d^-) = I_z(z=d^+) \quad (3.17)$$

must be satisfied, along with the obvious requirement that

$$I_z(z=h) = 0 \quad (3.18)$$

The result of equation (3.14) may be utilized to obtain

$$I_z(z=d^-) = \frac{2 V_o \pi}{\zeta_o \Psi} e^{-j\beta_o d} \quad (3.19)$$

Applying

(3.16) in

evaluate

If expres

substitute

$d \leq z \leq h$

I_z

It is

$d \leq z \leq h$

impedance

$0 \leq z \leq d$,

wave. This

zeroth-ord

antenna.

Since

point, then

cylinder can

be express

Applying the two boundary conditions (3.17) and (3.18) to expression (3.16) in conjunction with result (3.19), the constants A and B are evaluated in a straightforward manner as

$$A = \frac{1}{1 - e^{-j2\beta_o(h-d)}} \quad (3.20)$$

$$B = \frac{-e^{-j2\beta_o h}}{1 - e^{-j2\beta_o(h-d)}} \quad (3.21)$$

If expressions (3.20) and (3.21) for A and B , respectively, are substituted into equation (3.16), the distribution of current on $d \leq z \leq h$ is obtained as

$$I_z(z) = \frac{j4V_o\pi}{\zeta_o\Psi} \frac{e^{-j\beta_o h}}{1 - e^{-j2\beta_o(h-d)}} \sin \beta_o(h-z) \quad (3.22)$$

It is observed from result (3.22) that the cylinder current on $d \leq z \leq h$ has a sinusoidal distribution. Thus although an optimum impedance loading yields an outward traveling wave of current on $0 \leq z \leq d$, the distribution on $d \leq z \leq h$ remains a purely standing wave. This standing wave distribution is in fact identical with the zeroth-order distribution of current on a conventional unloaded linear antenna.

Since the antenna current is symmetric about its excitation point, then $I_z(-z) = I_z(z)$. In summary then, the distribution of cylinder current corresponding to an optimum impedance loading may be expressed on $-h \leq z \leq h$ as

$$I_z(z) = \frac{V_o}{60\Psi} e^{-j\beta_o|z|} \quad -d \leq z \leq d \quad (3.23)$$

loading v
purely re
previous
dimension

(1)

(2)

In
of current
(1) and (2),
It is noted
is constant
of current
indicate a
of the star.
In Figure
length (h-
region wh
the optimum

$$I_z(z) = \frac{jV_o}{30\Psi} \frac{e^{-j\beta_o h}}{1 - e^{-j2\beta_o(h-d)}} \sin \beta_o(h-|z|) \quad (3.24)$$

$$-h \leq z \leq -d, \quad d \leq z \leq h$$

The distribution of current corresponding to an optimum impedance loading will be illustrated by considering a pair of antennas having the purely resistive and purely reactive optimum loadings discussed previously in sections 3.3 and 3.4. Specifically, the antenna dimensions and optimum loading parameters are taken as:

- (1) $h = 31.25$ cm, $2a = 0.25$ inch, $d = 22.9$ cm, $[R_L]_0 = 220$ ohms;
purely resistive optimum loading at 600 mhz where:
 $h = 0.625 \lambda_o$, $(h-d) = 0.17 \lambda_o$.
- (2) $h = 100$ cm, $2a = 0.25$ inch, $d = 79.2$ cm, $[X_L]_0 = -363$ ohms;
purely reactive optimum loading at 600 mhz where :
 $h = 2\lambda_o$, $(h-d) = 0.417 \lambda_o$.

In Figures 3.7 and 3.8 are indicated the amplitude and phase of current (obtained from expressions (3.23) and (3.24)) for antennas (1) and (2), respectively, as a function of position along the cylinder. It is noted that in either case the amplitude of the current on $0 \leq z \leq d$ is constant while its phase is linear, corresponding to a traveling wave of current along that region. On $d \leq z \leq h$, however, both figures indicate a sinusoidal standing wave with constant phase. The appearance of the standing wave on this region is quite different for the two cases. In Figure 3.7, corresponding to the optimum resistive loading, the length $(h-d)$ is only $0.17 \lambda_o$ so the standing wave exists only on a region whose length is less than a quarter free space wavelength. For the optimum reactive loading of Figure 3.8, however, $(h-d) = 0.417 \lambda_o$



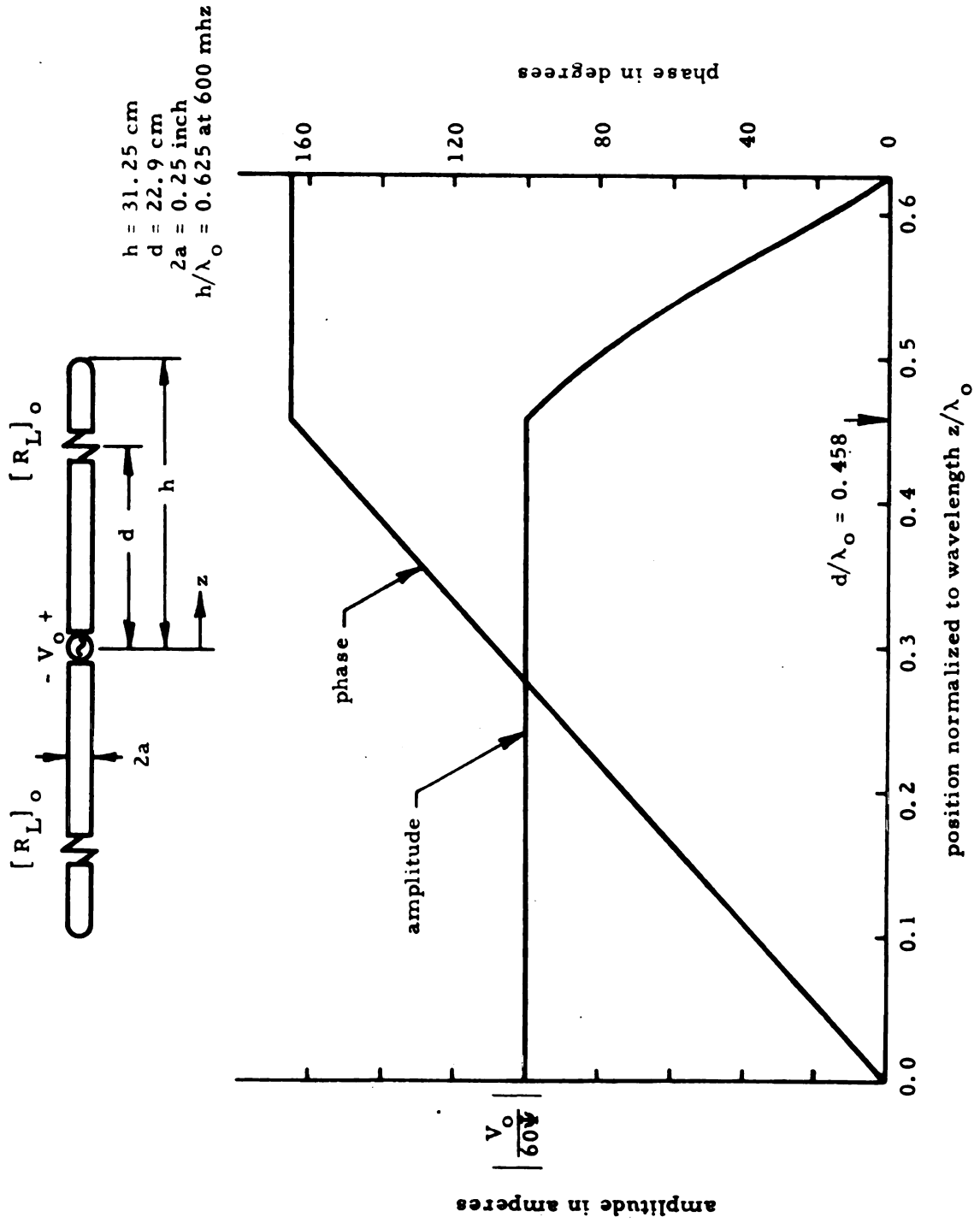


Figure 3.7. Amplitude and Phase of Antenna Current Corresponding to an Optimum Resistance Loading $[R_L]_o$ as a Function of Position Along Antenna.

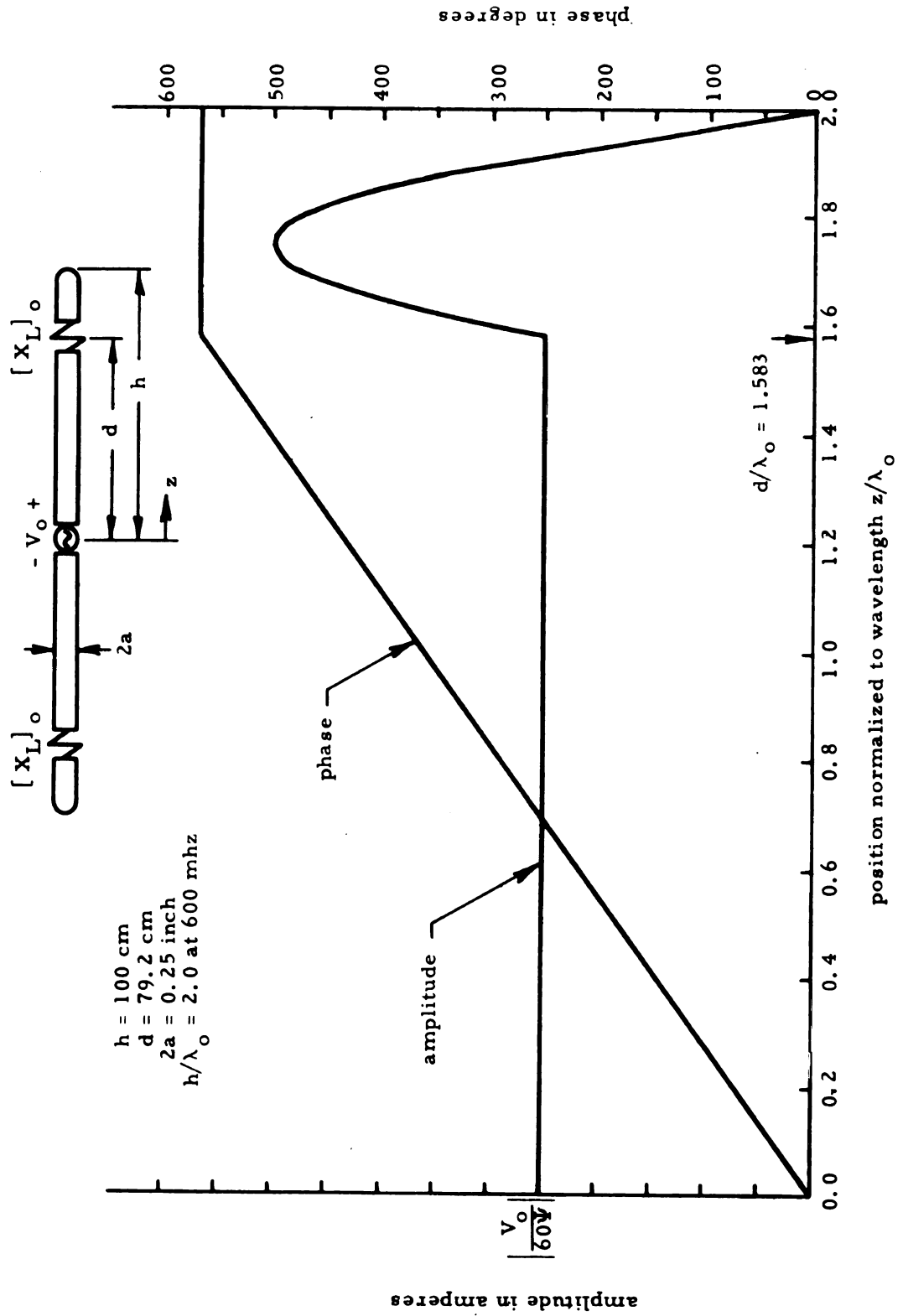


Figure 3.8: Amplitude and Phase of Antenna Current Corresponding to an Optimum Non-Dissipative Loading as a Function of Position Along Antenna.

and nearly a f

The in

obtained from

It is to be note

and position of

equation (3. 5)

Z_L is not $[Z$

must be utiliz

$$Z_{in} = 6$$

This general r

impedance is

In orde

a linear antenn

having purely

considered. Z

optimum at ev

position given

antenna dimen

(1) h

as

and nearly a full half wavelength of the standing wave is present.

The input impedance to a traveling wave linear antenna is obtained from equation (3.23) as

$$\begin{aligned} Z_{in} &= \frac{V_o}{I_z(z=0)} \\ &= 60 \Psi \end{aligned} \quad (3.25)$$

It is to be noted that this expression is valid only when the impedance and position of the double loading are chosen to be optimum, i. e., equation (3.5) is satisfied. Under any other circumstances, when Z_L is not $[Z_L]_0$, the general input impedance expression (2.33) must be utilized as

$$Z_{in} = 60 \Psi \left[1 + \frac{D_1}{D_2} - \frac{Z_L}{30T} e^{-j\beta_o d} \left(\frac{D_1}{D_2} \cos \beta_o d + d^{-j\beta_o d} \right) \right]^{-1} \quad (2.33)$$

This general result reduces to equation (3.25) when the loading impedance is optimum.

In order to demonstrate the input impedance characteristic of a linear antenna having an optimum impedance loading, the two dipoles having purely resistive and purely reactive loadings will again be considered. In this instance, however, the loadings are taken to be optimum at every frequency, that is, to have the impedance and position given by Figures 3.1 and 3.4, respectively. The specific antenna dimensions and loadings are thus:

- (1) $h = 31.25$ cm, $2a = 0.25$ inch; optimum resistance loading as in Figure 3.1.

(2) h

as

An indication

these two con

3.10. These

(3.25) using t

section 3.6.

which support

essentially in

approximate t

an input imped

with the well k

antenna.

It was

or purely reac

single frequen

of either the r

with their loca

a given frequ

a purely outwa

single frequen

input impedanc

In Figu

was indicated

having dimens

loading positio

- (2) $h = 100$ cm, $2a = 0.25$ inch; optimum reactance loading as in Figure 3.4.

An indication of the frequency dependence of the input impedance for these two configurations is given, respectively, in Figures 3.9 and 3.10. These numerical results were calculated from expression (3.25) using the approximate value of Ψ given by equation (3.37) of section 3.6. It is noted that the input impedance of a linear antenna which supports a traveling wave of current at every frequency is essentially independent of the frequency of excitation. The approximate theory developed in this research therefore predicts an input impedance characteristic which is in general agreement with the well known circuit properties of a traveling wave linear antenna.

It was indicated in sections 3.3 and 3.4 that a purely resistive or purely reactive loading of fixed position can be optimum only at a single frequency. Consideration was thus directed to loadings consisting of either the resistive or reactive components of the optimum impedance, with their locations selected in such a way that they became optimum at a given frequency. Since such loadings are optimum, and hence yield a purely outward traveling current wave on $0 \leq z \leq d$, only at a single frequency, then the frequency dependence of the corresponding input impedance must be calculated from expression (2.33).

In Figure 3.2 of section 3.3, the optimum loading impedance was indicated as a function of antenna electrical length for a dipole having dimensions $h = 31.25$ cm, $2a = 0.25$ inch, and for which the loading position was fixed at $d = 22.9$ cm. The reactive component

$[R_L]_o$

z_{in}
 $-V_o^+$

$[R_L]_o$

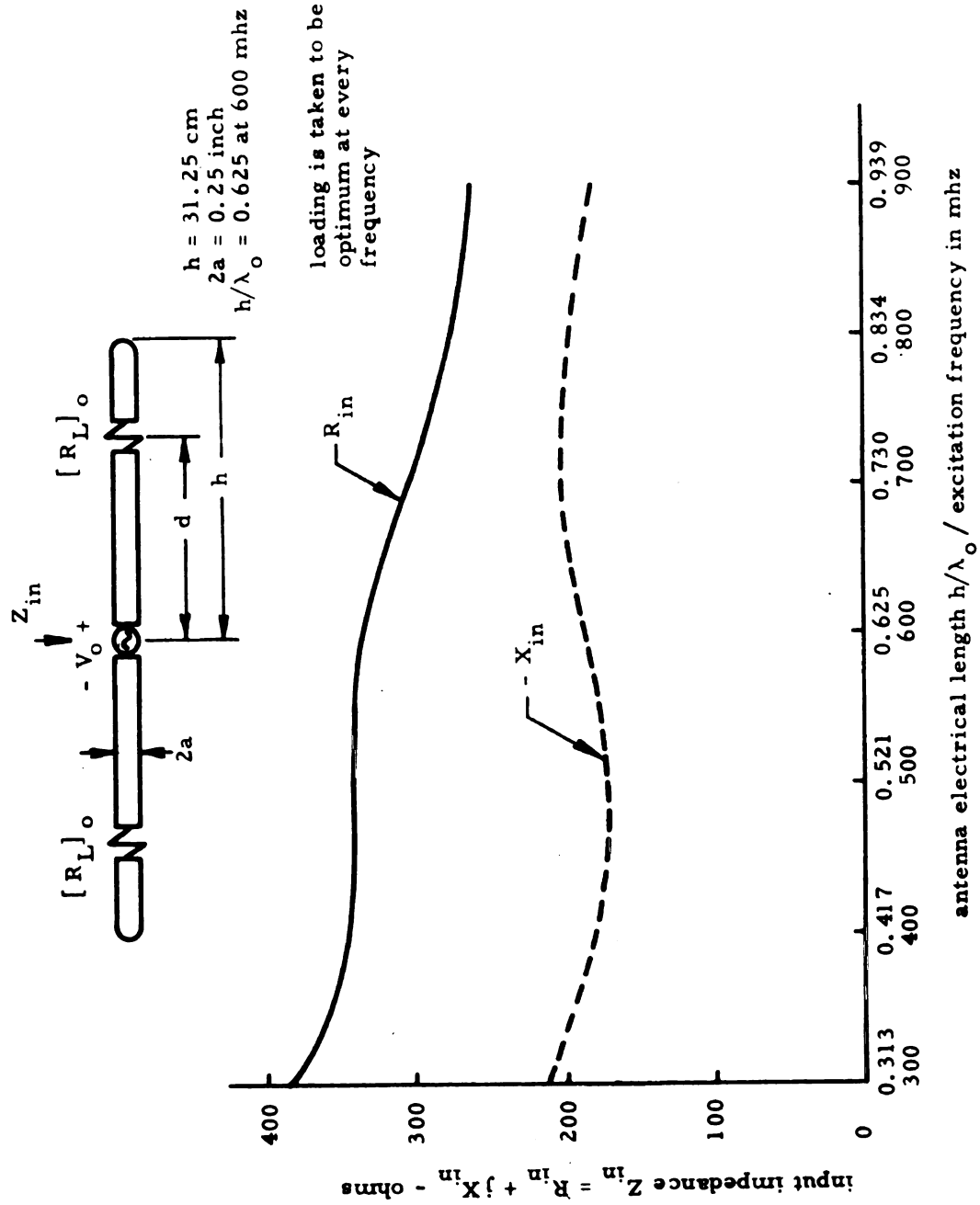


Figure 3.9. Input Impedance of Antenna with Optimum Resistance Loading as a Function of its Electrical Length ($h = 31.25 \text{ cm}$).

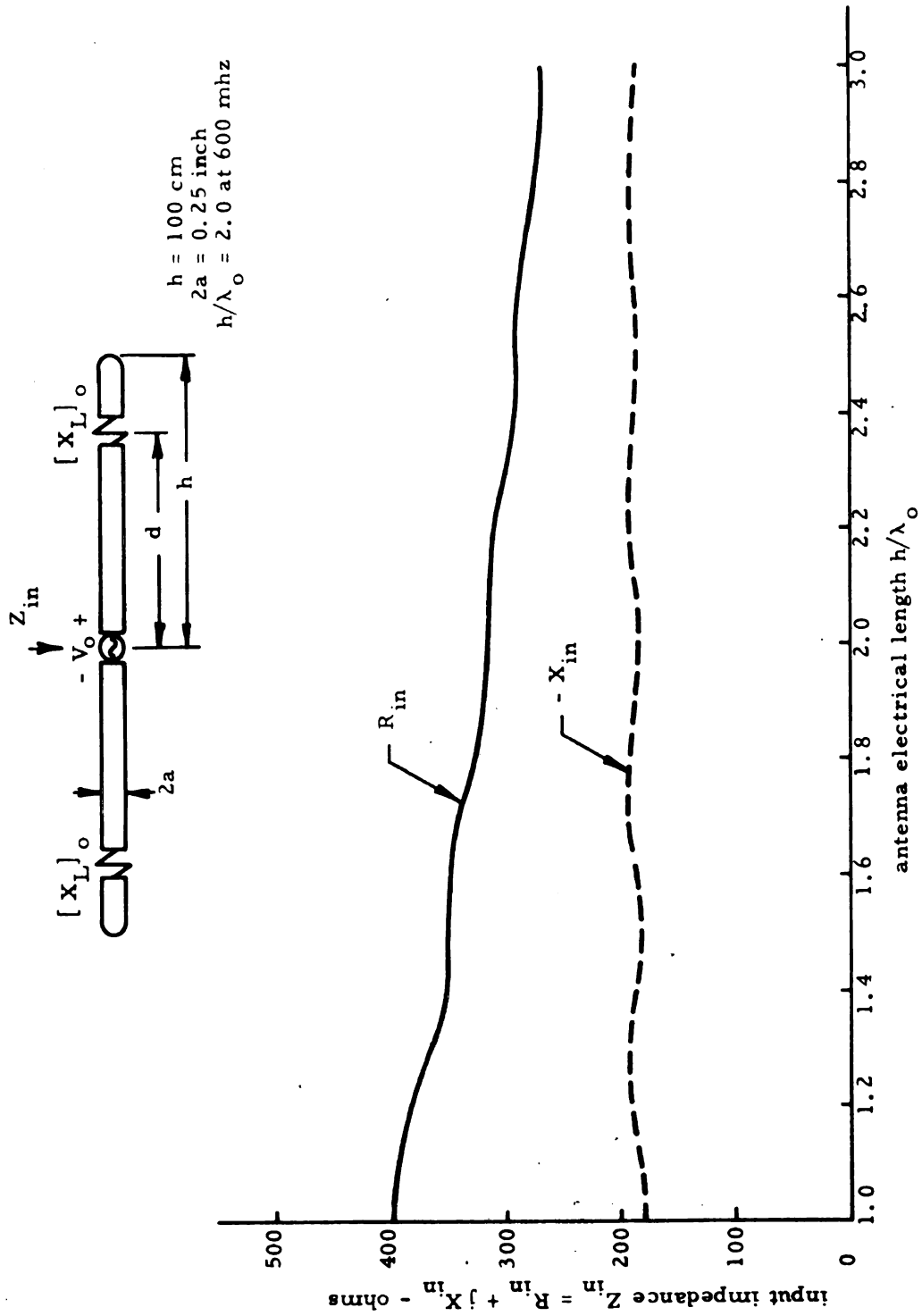


Figure 3.10. Input Impedance of Antenna with Optimum Reactance Loading as a Function of its Electrical Length ($h = 100$ cm).

of the o

where h

$[R_L]_0 =$

correspo

positione

is optimu

a range o

is therefo

where h

Th

resistance

electrical

from expre

presented.

relatively c

$h = 0.625 \lambda$

frequency de

dipole, whic

It is r

values for the

agreement.

correspondin

display basic

from one and

sources for t

of the optimum impedance was found to vanish at a frequency of 600 mhz, where $h = 0.625 \lambda_0$ and $(h-d) = 0.17 \lambda_0$. A resistance loading of $[R_L]_0 = 220$ ohms is optimum at that frequency. The input impedance corresponding to a constant resistance loading of $R_L = 220$ ohms positioned at $d = 22.9$ cm is now to be considered. Since the loading is optimum for $h = 0.625 \lambda_0$, then it is approximately optimum for a range of frequencies centered about this point. The input impedance is therefore expected to be relatively broadband about the frequency where $h = 0.625 \lambda_0$.

The input impedance to a linear antenna having such a constant resistance loading of fixed position is indicated as a function of its electrical length in Figure 3.11. Both the theoretical result calculated from expression (2.33) and Altshuler's experimental result³ are presented. It is observed that in either case the input impedance is relatively constant for a range of frequencies about that where $h = 0.625 \lambda_0$. This broadband character is quite in contrast to the frequency dependent impedance of a conventional unloaded linear dipole, which is a very strong function of the frequency of excitation.

It is noted from the figure that the theoretical and experimental values for the resistive component of input impedance are in close agreement. There is, however, considerable error present for the corresponding reactive components. While the two reactance curves display basically the same functional dependence, they are displaced from one another along the impedance axis. There are several probable sources for this error as follows:

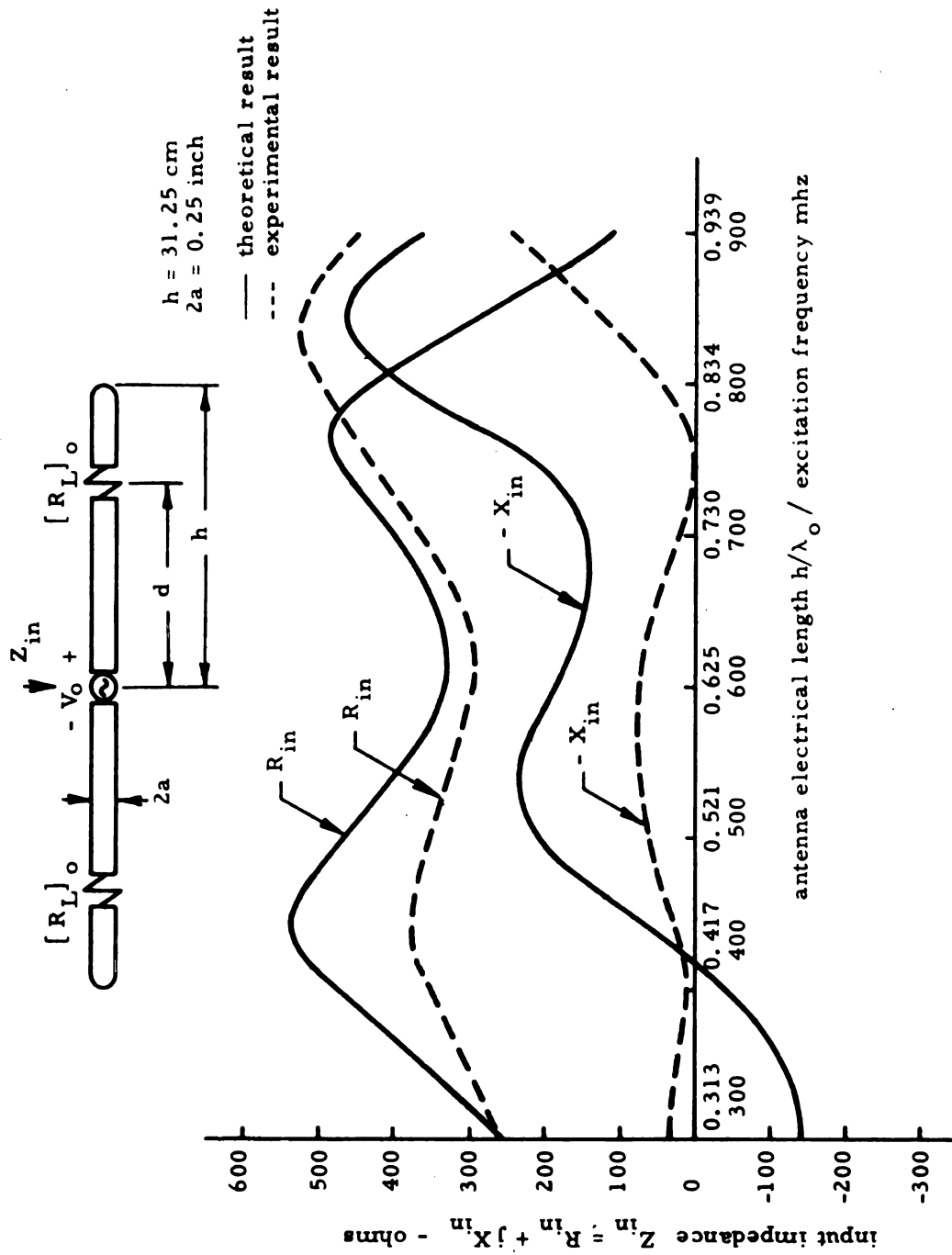


Figure 3.11. Input Impedance as a Function of Antenna Electrical Length for Constant Resistance Loading of Fixed Position (optimum at 600 mhz).

(i)

(ii)

(iii)

It is felt that
above. As v
expression u
long antenna
which the tra
the length (h
present case
of the approx
This particul
with the dime

An ant
with a loading
in section 3.4
indicated in F
With this par
impedance be
 $h = 2\lambda_0$ and
with similar
of the reactiv
be considered

- (i) The approximate technique utilized to obtain the distribution of current on the doubly loaded cylinder.
- (ii) The approximate nature of the expression utilized for the expansion parameter Ψ (to be discussed in section 3.6).
- (iii) There is some question as to whether end-effect correction factors were applied to the experimental results.

It is felt that the major contribution to the error is due to point (ii) above. As will be indicated in the following section, the approximate expression utilized to calculate Ψ is accurate only for the case of a long antenna. It is necessary that the length d of the cylinder on which the traveling wave of current exists be considerably greater than the length $(h-d)$ which supports a standing wave distribution. In the present case, the antenna length is relatively short, and the accuracy of the approximate expression for Ψ is consequently questionable. This particular cylinder length was chosen initially only to correspond with the dimensions used by Altshuler in his experimental investigation.

An antenna having the dimensions $h = 100$ cm and $2a = 0.25$ inch, with a loading impedance fixed at the position $d = 79.2$ cm was considered in section 3.4. The corresponding optimum loading impedance was indicated in Figure 3.6 as a function of the antenna electrical length. With this particular choice of the loading position, the optimum impedance becomes purely reactive at a frequency of 600 mhz where $h = 2\lambda_0$ and $(h-d) = 0.417 \lambda_0$. The input impedance of an antenna with similar dimensions having a non-dissipative loading consisting of the reactive component of the above optimum impedance is now to be considered. Since this loading is optimum for $h = 2\lambda_0$, then the

distribu

travelin

corresp

broadban

In

antenna h

function o

calculated

is noted th

of frequen

is optimum

as for the c

loading is r

indicated by

From

doubly react

the values o

a half-length

wavelength in

over the situ

where the an

electrical le

properties o

the use of a

loading meth

same high le

distribution of cylinder current on $0 \leq z \leq d$ will approximate a traveling wave for a range of frequencies about this point. The corresponding input impedance is therefore expected to be relatively broadband about the frequency where $h = 2\lambda_0$.

In Figure 3.12 is indicated the input impedance of a linear antenna having such a non-dissipative loading of fixed position, as a function of its electrical length. This theoretical result was calculated from the general input impedance expression (2.33). It is noted that the input impedance is relatively constant for a range of frequencies about that where $h = 2\lambda_0$, at which point the loading is optimum. This broadbanding effect is not as pronounced, however, as for the case of a purely resistive loading. Since a purely resistive loading is more nearly optimum over a band of frequencies, as indicated by Figures 3.2 and 3.6, such a difference is to be expected.

From Figure 3.12 it is observed that the input impedance of the doubly reactance loaded dipole is reasonably constant for h/λ_0 between the values of 1.75 and 2.25. Thus a broadbanding effect is evident for a half-length variation of 0.5 wavelengths, or for a variation of a full wavelength in the total antenna length. This is a notable improvement over the situation which exists with a conventional unloaded dipole, where the antenna input impedance is a much stronger function of its electrical length. It is evident therefore that the desirable circuit properties of a traveling wave linear antenna may be realized through the use of a purely non-dissipative loading. In contrast to the resistance loading method, this technique maintains the antenna efficiency at the same high level as that of a conventional linear dipole.



o

700

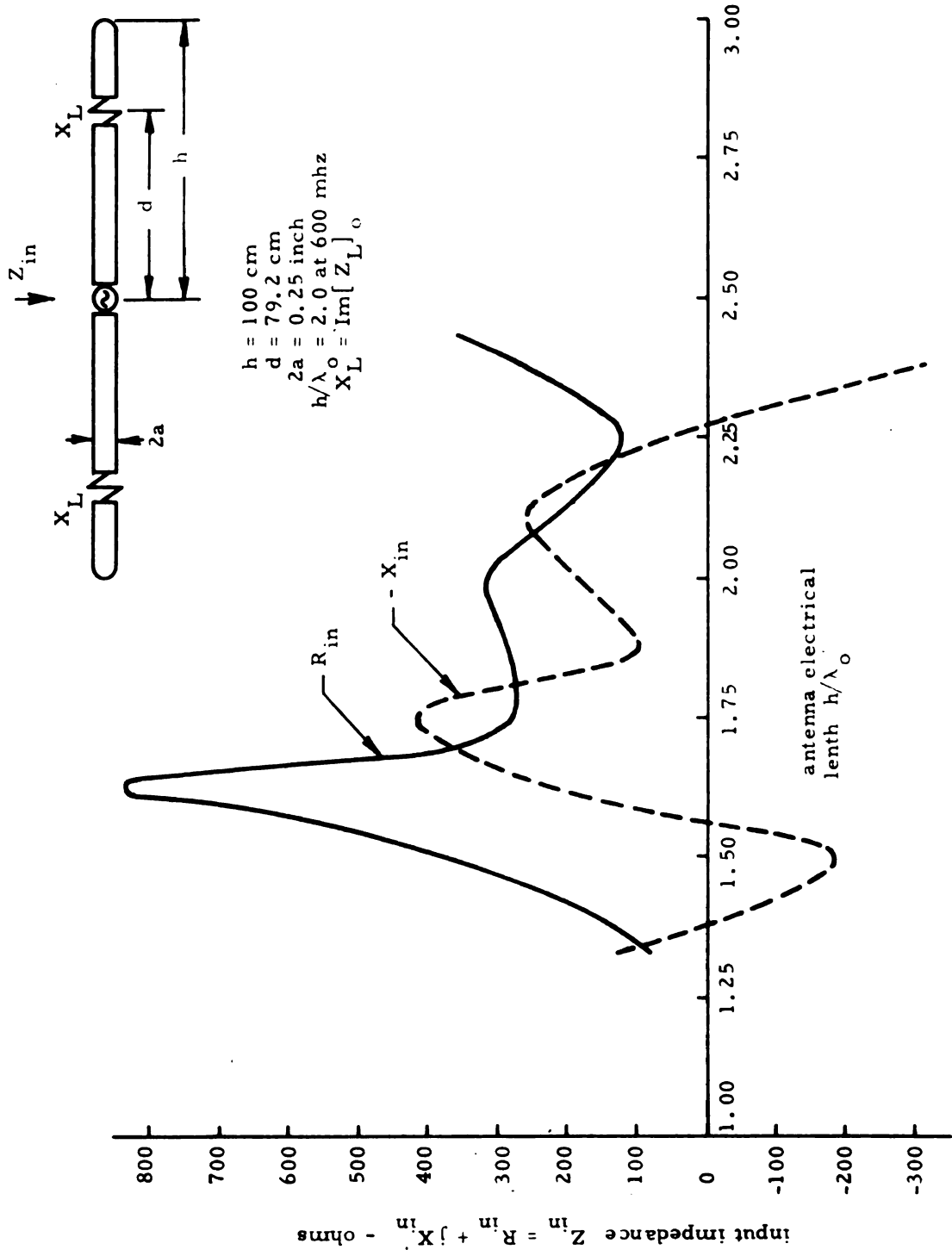


Figure 3.12. Input Impedance as a Function of Frequency for Antenna with Loading Consisting of Reactive Component of Optimum Impedance.

position

consider

evident

non-dis

is allow

is indica

3.6. Ca

by equati

where A_z

and $I_z(z)$

that this ve

where $K(z, z)$

Using result

It should be remarked that if a non-dissipative loading of fixed position is desired, then the reactive component of $[Z_L]_0$, as considered above, is not the optimum reactance. Although it is not evident from the present theory, there may exist a more suitable non-dissipative loading for the purpose. Further, if some dissipation is allowed, a more effective broadbanding of the input impedance than is indicated in Figure 3.12 should be obtainable.

3.6. Calculation of the Expansion Parameter $\Psi(z)$

The expansion parameter $\Psi(z)$ has been defined in Chapter 2 by equation (2.25), and may be written in the form

$$\Psi(z) = \frac{4\pi}{\mu_0} \frac{A_z(z)}{I_z(z)} \quad -h \leq z \leq h \quad (3.26)$$

where $A_z(z)$ is the vector potential at a point on the antenna surface and $I_z(z)$ is the corresponding cylinder current. It has been indicated that this vector potential may be expressed as

$$A_z(z) = \frac{\mu_0}{4\pi} \int_{-h}^h I_z(z') K(z, z') dz' \quad (2.20)$$

where $K(z, z')$ is the Green's function

$$K(z, z') = \frac{e^{-j\beta_0 \sqrt{(z-z')^2 + a^2}}}{\sqrt{(z-z')^2 + a^2}} \quad (2.21)$$

Using result (2.20) in equation (3.26), the expansion parameter becomes

$$\Psi(z) = \frac{1}{I_z(z)} \int_{-h}^h I_z(z') K(z, z') dz' \quad (3.27)$$

traveling

it is this

parameter

independence

primarily

by using the

distribution

actually de

is not $[Z_L]$

In the

cylinder cu

loading may

where the co

and (3.21), r

expansion pa

in the integr

the current e

$I_2(z)$, then f

current may

Since the current distribution of fundamental interest is the traveling wave corresponding to an optimum impedance loading, then it is this distribution which will be used to evaluate the expansion parameter. It has been indicated by King³ that $\Psi(z)$ is relatively independent of the distribution of cylinder current, and depends primarily upon its dimensions. Hence no great error will be made by using the value of $\Psi(z)$ corresponding to a traveling wave distribution when carrying out calculations where the cylinder current actually departs moderately from a traveling wave, i.e., when Z_L is not $[Z_L]_0$.

In the preceding section, it was found that the distribution of cylinder current on $0 \leq z \leq h$ corresponding to an optimum impedance loading may be expressed as

$$I_z(z) = \frac{2 V_o \pi}{\zeta_o \Psi} e^{-j\beta_o z} \quad 0 \leq z \leq d \quad (3.14)$$

$$I_z(z) = \frac{2 V_o \pi}{\zeta_o \Psi} [A e^{-j\beta_o z} + B e^{j\beta_o z}] \quad d \leq z \leq h \quad (3.16)$$

where the complex constants A and B are given by equations (3.20) and (3.21), respectively. It is clear from equation (3.27) for the expansion parameter, that, since the cylinder current appears both in the integrand and in the denominator, the constant multipliers of the current expression may be dropped. Furthermore, since $I_z(-z) = I_z(z)$, then for the calculation of $\Psi(z)$ the distribution of cylinder current may be taken as

obtained

$$\int_{-h}^h I_z(z')$$

which may

$$\int_{-h}^h I_z(z') K$$

Result (3.30)

$$\int_{-h}^h I_z(z') K(z$$

where $G_a(h,$

$$\begin{aligned}
I_z(z) &= e^{-j\beta_o |z|} & -d \leq z \leq d \\
I_z(z) &= A e^{-j\beta_o |z|} + B e^{j\beta_o |z|} & -h \leq z \leq -d, \\
& & d \leq z \leq h
\end{aligned} \tag{3.28}$$

With the current distribution of equations (3.28), there is obtained the result

$$\begin{aligned}
\int_{-h}^h I_z(z') K(z, z') dz' &= \int_{-h}^{-d} [A e^{-j\beta_o |z'|} + B e^{j\beta_o |z'|}] K(z, z') dz' \\
&+ \int_{-d}^d e^{-j\beta_o |z'|} K(z, z') dz' \\
&+ \int_d^h [A e^{-j\beta_o |z'|} + B e^{j\beta_o |z'|}] K(z, z') dz'
\end{aligned} \tag{3.29}$$

which may be written as

$$\begin{aligned}
\int_{-h}^h I_z(z') K(z, z') dz' &= \int_{-h}^h [A e^{-j\beta_o |z'|} + B e^{j\beta_o |z'|}] K(z, z') dz' \\
&+ \int_{-d}^d e^{-j\beta_o |z'|} K(z, z') dz' \\
&- \int_{-d}^d [A e^{-j\beta_o |z'|} + B e^{j\beta_o |z'|}] K(z, z') dz'
\end{aligned} \tag{3.30}$$

Result (3.30) may finally be expressed in the form

$$\begin{aligned}
\int_{-h}^h I_z(z') K(z, z') dz' &= (A+B) Ca(h, z) - j(A-B) Sa(h, z) \\
&+ (1-A-B) Ca(d, z) - j(1+B-A) Sa(d, z)
\end{aligned} \tag{3.31}$$

where $Ca(h, z)$ and $Sa(h, z)$ represent the integrals

These in
were num
expansion

If
then $\Psi(z)$

$$\Psi(z) = \frac{(z^2 - 1)}{(z^2 + 1)}$$

$$\Psi(z) = \frac{(A - Bz^2)}{(z^2 + 1)}$$

It is noted fr
upon the pos
antenna dimen
loading posit
is found to d
loading. Fur
 $\Psi(z) = \Psi$ w
indicate that
Some further
demonstrate

$$Ca(h, z) = \int_{-h}^h \cos \beta_o z' K(z, z') dz' \quad (3.32)$$

$$Sa(h, z) = \int_{-h}^h \sin \beta_o |z'| K(z, z') dz'$$

These integrals occur frequently in the theory of linear antennas, and were numerically machine calculated to facilitate evaluation of the expansion parameter $\Psi(z)$.

If equations (3.28) and (3.31) are used in expression (3.27), then $\Psi(z)$ is immediately obtained as

$$\Psi(z) = \frac{(A+B) Ca(h, z) - j(A-B) Sa(h, z) + (1-A-B) Ca(d, z) - j(1+B-A) Sa(d, z)}{e^{-j\beta_o z}} \quad 0 \leq z \leq d \quad (3.33)$$

$$\Psi(z) = \frac{(A+B) Ca(h, z) - j(A-B) Sa(h, z) + (1-A-B) Ca(d, z) - j(1+B-A) Sa(d, z)}{A e^{-j\beta_o z} + B e^{j\beta_o z}} \quad d \leq z \leq h \quad (3.34)$$

It is noted from these results that the expansion parameter depends upon the position d of the optimum impedance loading as well as the antenna dimensions h and a . This poses a new problem, since the loading position was previously determined in terms of Ψ , but now Ψ is found to depend in a complicated way upon the location d of the loading. Furthermore, it was postulated that the expansion parameter $\Psi(z) = \Psi$ was indeed a constant, while expressions (3.33) and (3.34) indicate that $\Psi(z)$ is generally a function of position along the antenna. Some further approximations are evidently in order, and it must be demonstrated that $\Psi(z)$ is essentially independent of z .

It is a
expansion pa
distribution
having an op
cylinder sup
with that on
be made in c
current to ex
compared wi
in result (3.
expression

In this appro
dimensions
here be appl
loading.

An in
obtained. T
and a diamet
that an optim
that a travel
This configu
loading disc
preceding se

It is a well known result in linear antenna theory that the expansion parameter $\Psi(z)$ is a relatively weak function of the distribution of cylinder current.² In the present case of an antenna having an optimum impedance loading therefore, if the portion of the cylinder supporting a standing wave of current is short compared with that on which a traveling wave exists, then no great error will be made in calculating $\Psi(z)$ by assuming the traveling wave of current to exist over the entire cylinder. That is, if $(h-d)$ is small compared with d , then it should be a valid approximation to let $d = h$ in result (3.33). Making this substitution yields the greatly simplified expression

$$\Psi(z) \doteq \frac{Ca(h, z) - jSa(h, z)}{e^{-j\beta_0 z}} \quad 0 \leq z \leq h \quad (3.35)$$

In this approximate result, $\Psi(z)$ depends only upon the antenna dimensions h and a . The methods of sections 3.3 and 3.4 may therefore be applied to directly evaluate the necessary position of an optimum loading.

An indication of the error in approximation (3.35) is now to be obtained. The special case of an antenna having a half-length of $h = 100$ cm and a diameter of $2a = 0.25$ inch will be considered. It is assumed that an optimum impedance loading is positioned at $d = 79.2$ cm such that a traveling wave distribution of current exists on $0 \leq z \leq d$. This configuration corresponds to the antenna with non-dissipative loading discussed in conjunction with Figures 3.8 and 3.12 in the preceding section. In Figure 3.13 a comparison is indicated between

Figure 3.13. Comparison of Approximate and Exact Values of Expansions Parameters $\Psi(z)$ as a Function of Electrical Position Along Antenna.

the exact

(3.35). T

parts of

It i

correspon

for both its

results is

would be ex

beyond whi

of the appro

justified pr

(i)

t

(ii) T

A sec

the expansion

the cylinder.

of section 2.

Since $\Psi(z)$

$z = 0$, and si

defined, then

$\Psi = \Psi(0)$

become from

the exact result of expression (3.33) and the approximate one of equation (3.35). The figure indicates the dependence of the real and imaginary parts of $\Psi(z)$ upon position along the cylinder for $0 \leq z \leq d$.

It is observed from Figure 3.13 that there is a very close correspondence between the approximate and exact values of $\Psi(z)$ for both its real and imaginary parts. The deviation between the two results is small near $z = 0$ and becomes progressively larger (as would be expected by physical reasoning) as the position of the loading, beyond which a standing wave of current exists, is approached. Use of the approximate expression (3.35) for $\Psi(z)$ is therefore quite well justified provided that:

- (i) The ratio $d/(h-d)$ is relatively large (in the preceding case this ratio had the value 3.81).
- (ii) The expression is not applied for values of z close to d .

A second very important observation from Figure 3.13 is that the expansion parameter is indeed nearly independent of position along the cylinder. This fact justifies the original approximating assumption of section 2.4, in which $\Psi(z)$ was taken to be a constant of value Ψ . Since $\Psi(z)$ is well represented by its value at the excitation point $z = 0$, and since this is the point at which the input impedance is defined, then it will be taken that the constant value of Ψ is given by $\Psi = \Psi(0)$. The exact and approximate expressions for Ψ then become from equations (3.33) and (3.35), respectively,

Again

(h-d) i

given b

Figure

$h = 100$

mate va

of the cy

position

each freq

section 3.

was obtain

deviation b

negligible f

part in the

In a

obtained fro

in this appr

the order of

sufficiently

preceding s

a wavelength

$$\begin{aligned}\Psi = & (A+B) Ca(h, 0) - j(A-B) Sa(h, 0) \\ & + (1-A-B) Ca(d, 0) - j(1+B-A) Sa(d, 0)\end{aligned}\quad (3.36)$$

$$\Psi \doteq Ca(h, 0) - j Sa(h, 0) \quad (3.37)$$

Again, result (3.37) will be a satisfactory approximation whenever $(h-d)$ is small compared with d .

A comparison between the exact and approximate values of Ψ given by expressions (3.36) and (3.37), respectively, is indicated in Figure 3.14. The antenna is again taken to have a half-length of $h = 100$ cm and a diameter of $2a = 0.25$ inch. A plot of the approximate value of Ψ given by equation (3.37) is presented as a function of the cylinder's electrical length. From this value of Ψ , the position d of a purely reactive optimum loading was calculated for each frequency (see Figure 3.4) according to the method indicated in section 3.4. Using these results for d , a corrected result for Ψ was obtained from expression (3.36), as indicated in the figure. The deviation between the approximate and corrected values of Ψ is negligible for its real part, but becomes appreciable for the imaginary part in the case of a short antenna.

In all of the preceding numerical calculations, the value of Ψ was obtained from the approximate expression (3.37). The error inherent in this approximation is small whenever the antenna half-length is of the order of a wavelength or greater, and the ratio of d to $(h-d)$ is sufficiently large. In the case of the resistance loaded antenna of the preceding section, the half-length was relatively short (always less than a wavelength), and the accuracy of equation (3.37) is accordingly doubtful.

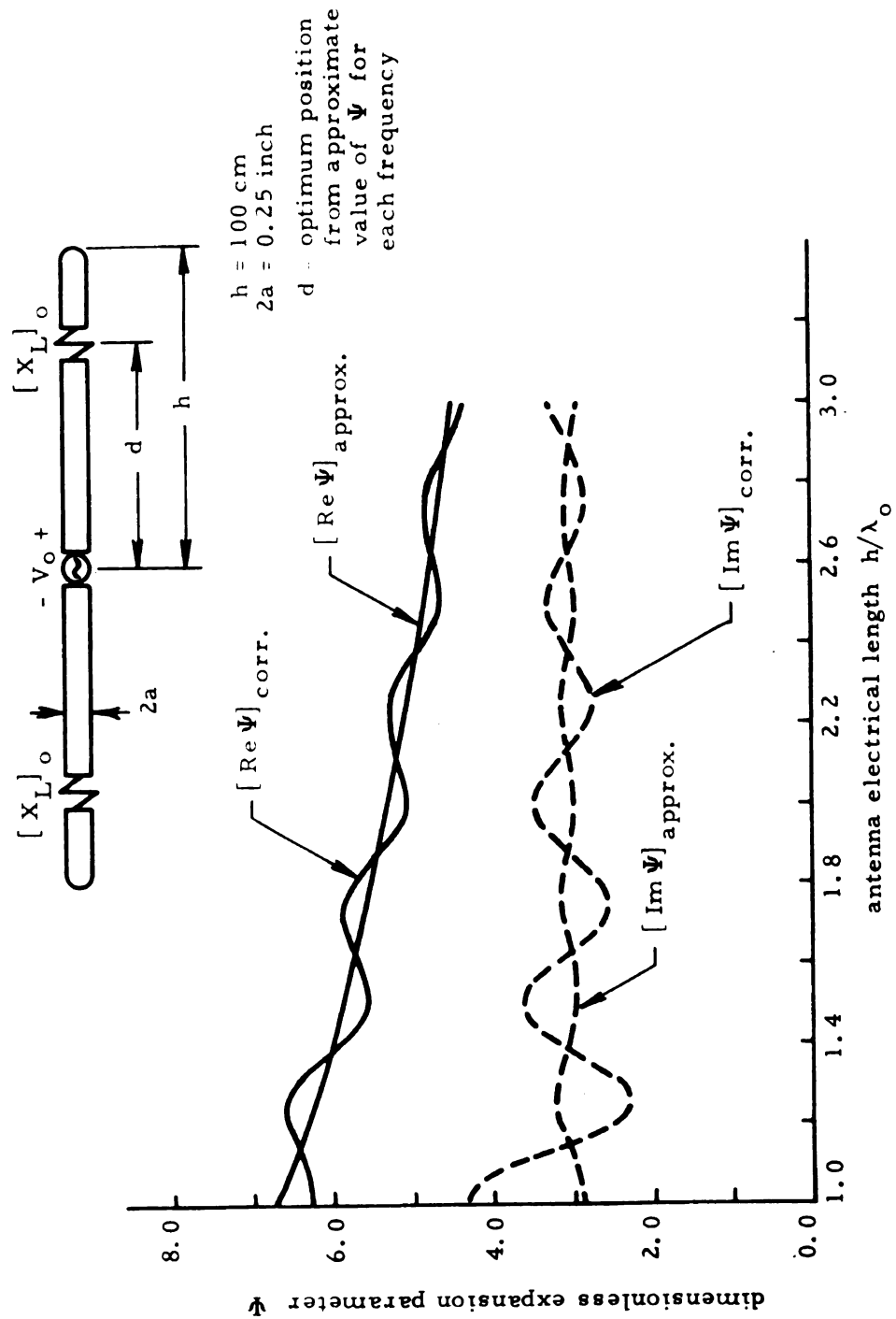


Figure 3.14. Comparison of Approximate and Corrected Values of Expansion Parameter Ψ as a Function of Antenna Electrical Length.

As was note
approximati
felt that this
deviation be
reactive con
connection v

As was noted in connection with Figure 3.14, the error due to the approximation occurs primarily in the imaginary part of Ψ . It is felt that this inaccuracy in Ψ is primarily responsible for the deviation between theoretical and experimental values for the reactive component of input impedance which was observed in connection with Figure 3.11.

4.1. Dist
Rad

It v

teristics c

distributio

the doubly

that corres

in Chapter

the travelin

are to be c

condition p

element on

Figure 4.1.

the observa

by many wa

fields, the

ctpimum in

particular,

distribution

In s

on the doub

loading was

CHAPTER 4

RADIATION CHARACTERISTICS OF A TRAVELING WAVE LINEAR ANTENNA

4.1. Distribution of Cylinder Current for Calculation of Radiation Fields

It was indicated in the introduction that the radiation characteristics of a linear antenna are completely characterized by its distribution of current. The approximate current distribution on the doubly loaded cylinder was determined in Chapter 2, while that corresponding to an optimum impedance loading was established in Chapter 3. In the present chapter, the electromagnetic fields of the traveling wave linear antenna at the radiation zone (or far zone) are to be calculated. These radiation fields are defined by the condition $\beta_0 R \gg 1$, where R is the distance from a current element on the cylinder to an observation point P as indicated in Figure 4.1. This condition is equivalent to the requirement that the observation point P be separated from every point of the dipole by many wavelengths. In order to determine these electromagnetic fields, the distribution of cylinder current corresponding to an optimum impedance loading will be utilized. Since it is, in particular, the radiation fields which are to be determined, this distribution will be further approximated to simplify the calculations.

In section 3.5 of the preceding chapter, the current distribution on the doubly loaded cylinder corresponding to an optimum impedance loading was found as

I_z

[

Figure

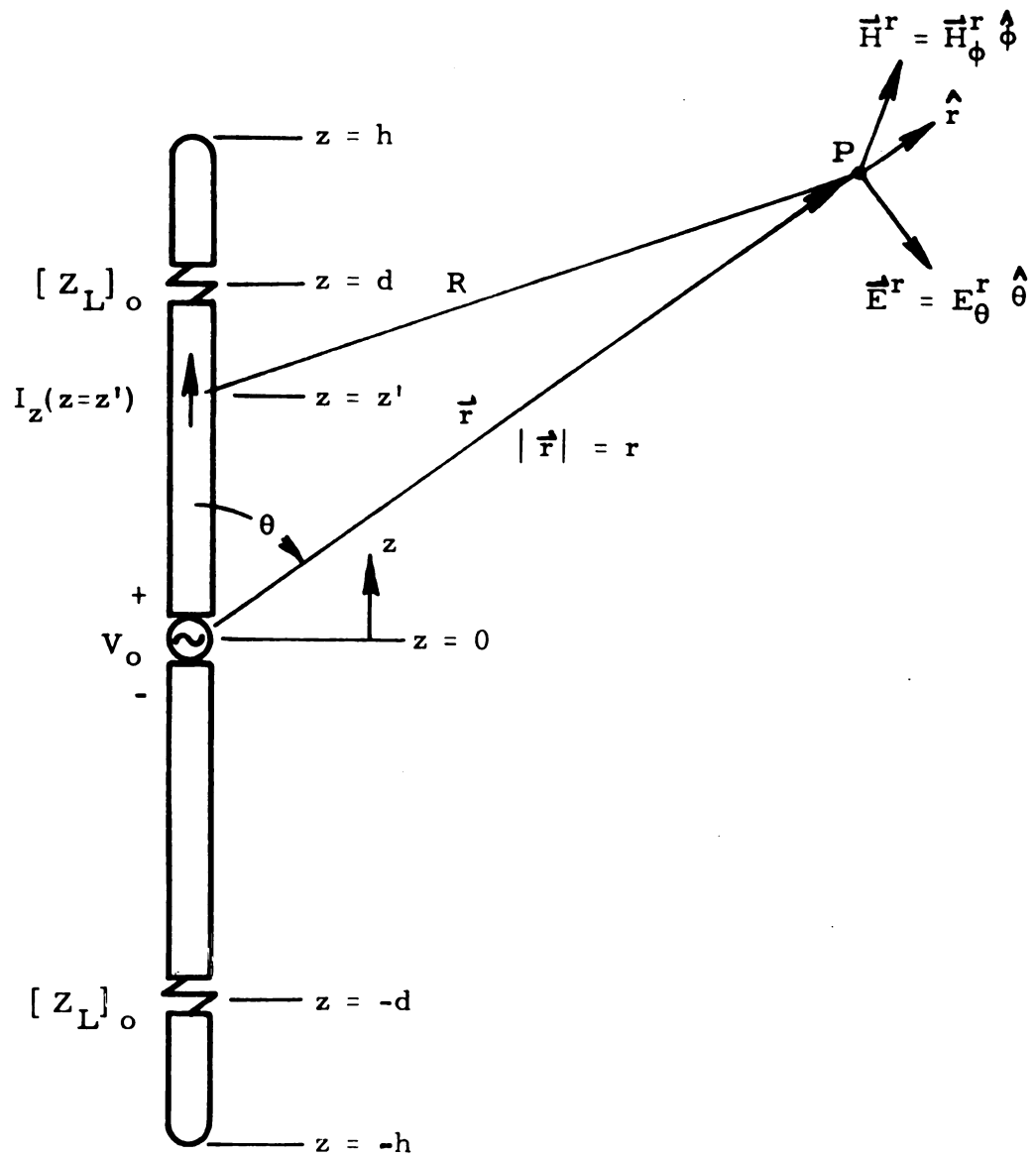


Figure 4.1. Geometry for Calculation of Radiation Zone Electromagnetic Fields of a Traveling Wave Linear Antenna.

These exp

current ov

$-h \leq z \leq -$

of a linear

current. ²,

of current

exists, the

traveling w

is reasonab

made in cal

equation (3.

From

lengths for w

Consider an

the dimension

from that fi

the half-len

or greater.

considered i

2.0 or great

length. Her

$$I_z(z) = \frac{V_o}{60\psi} e^{-j\beta_o |z|} \quad -d \leq z \leq d \quad (3.23)$$

$$I_z(z) = \frac{jV_o}{30\psi} \frac{e^{-j\beta_o h}}{1 - e^{-j2\beta_o(h-d)}} \sin \beta_o(h - |z|) \quad (3.24)$$

$$-h \leq z \leq -d, \quad d \leq z \leq h$$

These expressions represent, respectively, a traveling wave of cylinder current over the region $-d \leq z \leq d$ and a standing wave on the regions $-h \leq z \leq -d$ and $d \leq z \leq h$. It is well known that the radiation fields of a linear antenna are not a strong function of its distribution of current.^{2, 5} If the regions of the dipole supporting a standing wave of current are short compared with the one on which a traveling wave exists, then it is a reasonable approximation to assume that the traveling wave is present over the entire cylinder. That is, if $(h-d)$ is reasonably small compared with d , then no great error will be made in calculating the radiation zone electromagnetic fields if equation (3.23) is assumed to be valid for $-h \leq z \leq h$.

From the results of sections 3.3 and 3.4, the range of antenna lengths for which the above approximation is applicable may be deduced. Consider an antenna with a purely resistive optimum loading having the dimensions utilized in conjunction with Figure 3.1. It is observed from that figure that the ratio $d/(h-d)$ is greater than 2.0 whenever the half-length h of the cylinder is of the order of 0.5 wavelengths or greater. Similarly, for the antenna with the non-dissipative loading considered in Figure 3.4, it is found that $d/(h-d)$ is of the order of 2.0 or greater whenever the half-length h is greater than a wavelength. Hence, for either type of loading, there exists a range of

cylinder

is a reas

will be u

linear an

4.2. Ra

T

time har

(see Appe

o, respe

In the par

are given

integrals

where, a

antenna a

cylinder a

is the dis

$I_z(z)$ the

cylinder lengths for which the distribution of current

$$I_z(z) = \frac{V_o}{60\Psi} e^{-j\beta_o|z|} \quad -h \leq z \leq h \quad (4.1)$$

is a reasonable approximation. It is this current distribution which will be utilized to calculate the radiation fields of a traveling wave linear antenna.

4.2. Radiation Fields of the Traveling Wave Linear Antenna

The electric and magnetic fields at a point in space due to a time harmonic current-charge distribution are given quite generally (see Appendix A) in terms of the vector and scalar potentials \vec{A} and ϕ , respectively, as

$$\begin{aligned} \vec{E} &= -\nabla\phi - j\omega\vec{A} \\ \vec{B} &= \nabla \times \vec{A} \end{aligned} \quad (4.2)$$

In the particular case of a linear antenna, the electromagnetic potentials are given in terms of the charge-current distribution by the Helmholtz integrals

$$\vec{A} = \frac{\mu_o}{4\pi} \int_{-h}^h \hat{z} I_z(z') \frac{e^{-j\beta_o R}}{R} dz' \quad (4.3)$$

$$\phi = \frac{1}{4\pi\epsilon_o} \int_{-h}^h q(z') \frac{e^{-j\beta_o R}}{R} dz' \quad (4.4)$$

where, as indicated in Figure 4.1, \hat{z} is a unit vector parallel to the antenna axis and R is the distance between a source point on the cylinder at $z = z'$ and the point of observation at P . Further, $q(z)$ is the distribution of charge per unit length along the cylinder and $I_z(z)$ the corresponding distribution of current. Actually the charge

distribution

through the

By

(4.3) and (

(4.2), the

determine

The gener

observatio

It has been

antenna m

where \vec{E}

respective

to equation

\vec{r} which l

of the ant

Let

(r, θ, ϕ)

by equation

distribution is not independent, but is related to the cylinder current through the equation of continuity as

$$q(z) = \frac{-1}{j\omega} \frac{\partial}{\partial z} I_z(z) \quad (4.5)$$

By substituting the electromagnetic potentials given by equations (4.3) and (4.4), in conjunction with relation (4.5), into expressions (4.2), the electromagnetic fields \vec{E} and \vec{B} at any point in space are determined in terms of the distribution of cylinder current $I_z(z)$. The general expressions for these fields are quite complex, but for observation points in the radiation zone they are greatly simplified. It has been indicated by King⁵ that the radiation fields of a linear antenna may be expressed as

$$\vec{B}^r(\vec{r}) = -j\beta_0 [\hat{r} \times \vec{A}^r(\vec{r})] \quad (4.6)$$

$$\vec{E}^r(\vec{r}) = v_0 [\vec{B}^r(\vec{r}) \times \hat{r}] \quad (4.7)$$

where $\vec{E}^r(\vec{r})$ and $\vec{B}^r(\vec{r})$ are the radiation electric and magnetic fields, respectively, $\vec{A}^r(\vec{r})$ is the radiation zone vector potential corresponding to equation (4.3), and \hat{r} is a unit vector in the direction of the vector \vec{r} which locates the observation point P with respect to the center of the antenna.

Let the point P be specified by the spherical coordinates (r, θ, ϕ) as indicated in Figure 4.1. The electromagnetic fields given by equations (4.6) and (4.7) then become

$$\begin{aligned} \vec{B}^r(\vec{r}) &= -j\beta_0 [\hat{r} \times \hat{z} A_z^r(\vec{r})] = j\beta_0 A_z^r(\vec{r}) \sin \theta \hat{\phi} \\ &= -j\beta_0 A_\theta^r(\vec{r}) \hat{\phi} \end{aligned} \quad (4.8)$$

Thus the ra
another as
may finally

where

In
it is neces
the integr
be expres

Since in t
be droppe
expansion

The value

$$\begin{aligned}
\vec{E}^r(\vec{r}) &= -j\beta_o v_o A_\theta^r(\vec{r}) (\hat{\phi} \times \hat{r}) \\
&= -j\omega A_\theta^r(\vec{r}) \hat{\theta}
\end{aligned} \tag{4.9}$$

Thus the radiation electric and magnetic fields are transverse to one another as well as to the direction \hat{r} of propagation. These fields may finally be expressed in the form

$$E_\theta^r(\vec{r}) = -j\omega A_\theta^r(\vec{r}) \tag{4.10}$$

$$B_\phi^r(\vec{r}) = -\frac{1}{v_o} E_\theta^r(\vec{r}) \tag{4.11}$$

where

$$\begin{aligned}
A_\theta^r(\vec{r}) &= -A_z^r(\vec{r}) \sin \theta \\
&= -\sin \theta \frac{\mu_o}{4\pi} \int_{-h}^h I_z(z') \frac{e^{-j\beta_o R}}{R} dz'
\end{aligned} \tag{4.12}$$

In order to carry out the integration indicated in equation (4.12), it is necessary to obtain an expression for the distance R in terms of the integration variable z' . With reference to Figure 4.1, R may be expressed by the law of cosines as

$$\begin{aligned}
R &= [r^2 + z'^2 - 2rz' \cos \theta]^{1/2} \\
&= r[1 - 2(z'/r) \cos \theta + (z'/r)^2]^{1/2}
\end{aligned}$$

Since in the radiation zone $z' \ll r$, then the term in $(z'/r)^2$ may be dropped. Retaining only the two leading terms of a binomial expansion then gives

$$R \doteq r - z' \cos \theta \tag{4.13}$$

The value for R in expression (4.12) will thus be taken approximately

as

and making

A_{θ}^r

This result

are essential

are modified

which depends

In

of the travel

it is only

the approximation

Making this

potential

A_{θ}^r

The integral

$$\int_{-h}^h e^{-}$$

and a straight

as

$$\begin{aligned} R &\doteq r && \text{..... amplitude term} \\ R &\doteq r - z' \cos \theta && \text{..... phase term} \end{aligned} \quad (4.14)$$

and making this substitution gives

$$A_{\theta}^r(\vec{r}) = -\frac{\mu_o}{4\pi} \frac{e^{-j\beta_o r}}{r} \sin \theta \int_{-h}^h I_z(z') e^{j\beta_o z' \cos \theta} dz' \quad (4.15)$$

This result indicates that the radiation zone electromagnetic fields are essentially outward traveling spherically diverging waves which are modified by a function of the polar angle θ , the exact form of which depends upon the distribution of cylinder current.

In order to determine the radiation zone electromagnetic fields of the traveling wave linear antenna with optimum impedance loading, it is only necessary to evaluate the integral in equation (4.15) using the approximate distribution of cylinder current given by equation (4.1). Making this substitution, the θ -component of radiation zone vector potential becomes

$$A_{\theta}^r(\vec{r}) = \frac{\mu_o V_o}{240\pi \Psi} \frac{e^{-j\beta_o r}}{r} \sin \theta \int_{-h}^h e^{-j\beta_o |z'|} e^{j\beta_o z' \cos \theta} dz' \quad (4.16)$$

The integral in this expression may be rewritten in the form

$$\int_{-h}^h e^{-j\beta_o |z'|} e^{j\beta_o z' \cos \theta} dz' = 2 \int_0^h e^{-j\beta_o z'} \cos(\beta_o z' \cos \theta) dz' \quad (4.17)$$

and a straightforward integration yields the result

$$\int_{-h}^h e^{\dots}$$

It is conv

$$G(\beta_0 h)$$

in terms of

If

and (4.11)

of the trav

These exp
antenna as
of an obse
with the c
symmetri
the variat
hence des

$$\begin{aligned}
& \int_{-h}^h e^{-j\beta_o |z'|} e^{j\beta_o z' \cos \theta} dz' = \\
& = \frac{2}{\beta_o \sin^2 \theta} \{ e^{-j\beta_o h} [j \cos(\beta_o h \cos \theta) - \cos \theta \sin(\beta_o h \cos \theta)] - j \}
\end{aligned}
\tag{4.18}$$

It is convenient to define a quantity $G(\beta_o h, \theta)$ as

$$G(\beta_o h, \theta) = \frac{1}{\sin \theta} \{ e^{-j\beta_o h} [j \cos(\beta_o h \cos \theta) - \cos \theta \sin(\beta_o h \cos \theta)] - j \}
\tag{4.19}$$

in terms of which the vector potential of equation (4.16) becomes

$$A_{\theta}^r(\vec{r}) = - \frac{\mu_o V_o}{\zeta_o \Psi} \frac{e^{-j\beta_o r}}{\beta_o r} G(\beta_o h, \theta)
\tag{4.20}$$

If the last result is used in conjunction with expressions (4.10) and (4.11), the radiation electric and magnetic fields, respectively, of the traveling wave linear antenna are obtained as

$$E_{\theta}^r(\vec{r}) = \frac{j V_o}{\Psi} \frac{e^{-j\beta_o r}}{r} G(\beta_o h, \theta)
\tag{4.21}$$

$$B_{\phi}^r(\vec{r}) = \frac{j V_o}{v_o \Psi} \frac{e^{-j\beta_o r}}{r} G(\beta_o h, \theta)
\tag{4.22}$$

These expressions give the electromagnetic fields of the traveling wave antenna as a function of its electrical length and the coordinates (r, θ) of an observation point P in the radiation zone. There is no variation with the ϕ -coordinate since the fields of a linear antenna are azimuthally symmetric. For fixed values of $\beta_o h$, the function $G(\beta_o h, \theta)$ describes the variation of the radiation fields with the polar angle θ , and is hence designated as the "polar pattern factor."

It is noted that $G(\beta_0 h, \theta)$ is a complex number, and the radiation fields therefore vary in phase as well as amplitude with the polar angle θ . Physically however, it is the amplitude of the fields at each point in the radiation zone which is of primary interest. Consideration will henceforth be restricted, therefore, to the modulus of the polar pattern factor. After considerable calculation, $|G(\beta_0 h, \theta)|$ is obtained as

$$\begin{aligned}
 |G(\beta_0 h, \theta)| = \frac{1}{\sin \theta} [& \cos^2(\beta_0 h \cos \theta) + \cos^2 \theta \sin^2(\beta_0 h \cos \theta) \\
 & - 2 \cos \beta_0 h \cos(\beta_0 h \cos \theta) + 1 \\
 & - 2 \sin \beta_0 h \cos \theta \sin(\beta_0 h \cos \theta)]^{1/2}
 \end{aligned}
 \tag{4.23}$$

This expression gives the relative amplitude of the radiation zone electromagnetic fields as a function of the polar angle θ and the electrical length of the traveling wave antenna.

Considering the complexity of expression (4.23), it is clear why the approximation discussed in the preceding section was necessary. If, instead of approximating the distribution of cylinder current as a traveling wave over its entire length $-h \leq z \leq h$, account were taken of the standing wave on the regions $-h \leq z \leq -d$ and $d \leq z \leq h$, then the position d of the loading impedance would appear in the expression for the polar pattern. The result would be a further complication of this expression, to the extent that it would become quite intractable for calculating even specific radiation patterns. On the other hand, the error associated with the approximate expression

(4.23) will be small, and its relative simplicity renders it useful for making practical calculations.

4.3. Comparison of Radiation Patterns for Traveling Wave and Standing Wave Linear Antennas

As was mentioned earlier, it is quite well known that the radiation characteristics of traveling wave and standing wave linear antennas differ considerably. The radiation patterns of a conventional dipole and a traveling wave dipole utilizing an optimum lumped resistance loading were measured experimentally and compared in the research reported by Altshuler.³ Further, Wu and King⁴ determined theoretically the polar pattern of a traveling wave antenna having a distributed resistance loading. These investigations have disclosed that the radiation patterns of traveling wave antennas are in general characterized by a wider major lobe beamwidth and an absence of minor lobes, as compared with an ordinary standing wave dipole. It is to be expected, therefore, that the radiation patterns resulting from the present theory should display essentially the same character.

The approximate expression (4.23) may be utilized to evaluate numerically the radiation patterns of traveling wave linear antennas having various electrical lengths. These polar patterns are obtained by plotting $|G(\beta_0 h, \theta)|$ as a function of θ in polar coordinates, with the appropriate constant values of $\beta_0 h$ as parameter. Typical patterns are indicated in Figures 4.2, 4.3, and 4.4 for $\beta_0 h$ values of 2π , $7\pi/2$, and 4π , respectively. The corresponding respective half-lengths are $h = \lambda_0$, $h = 1.75 \lambda_0$, and $h = 2\lambda_0$. In each case, the radiation patterns of the corresponding standing wave dipoles, given by $|F(\beta_0 h, \theta)|$ are included for comparison.²

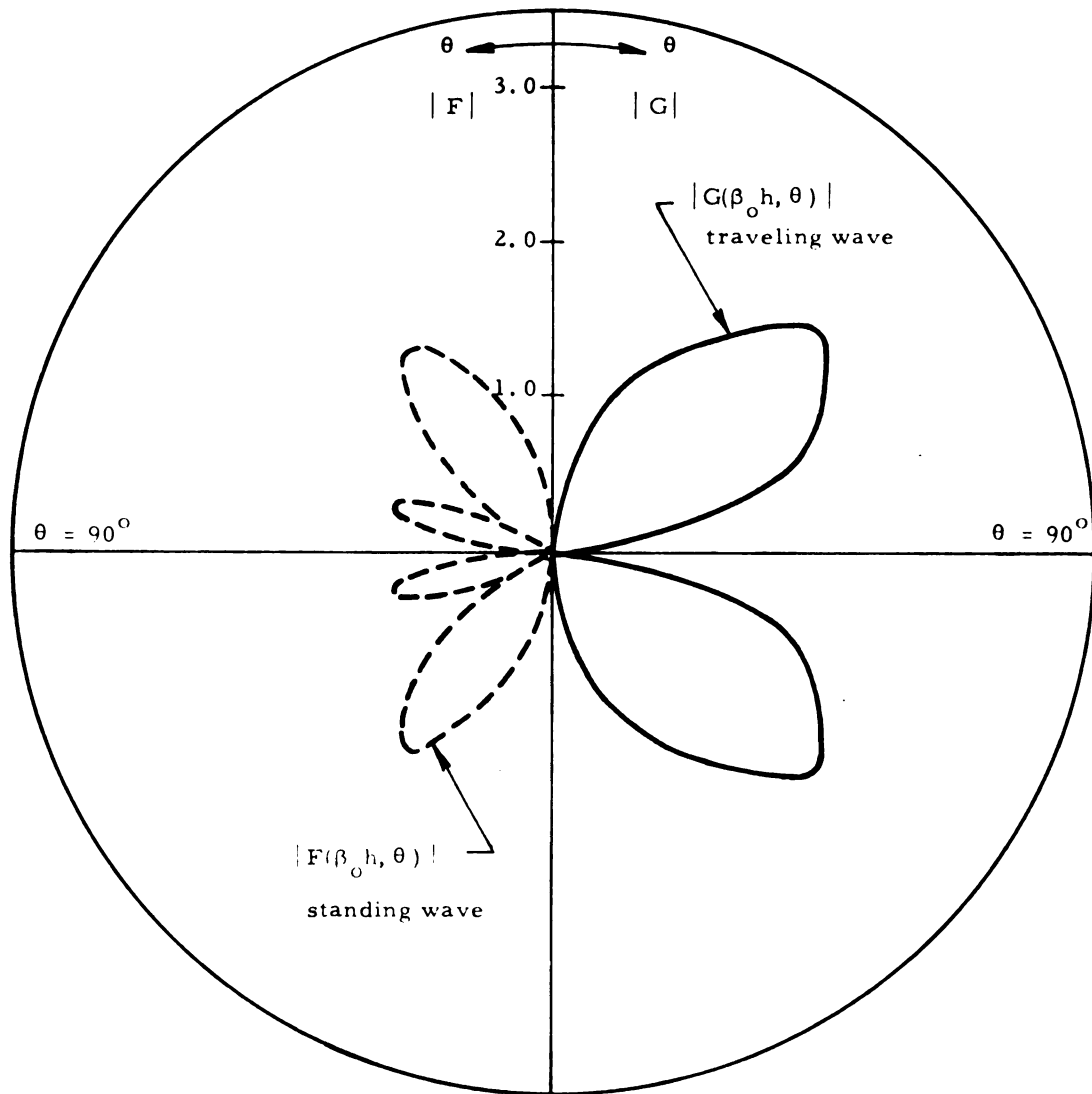


Figure 4.2. Radiation Patterns of Traveling and Standing Wave Antennas with $\beta_0 h = 2\pi$.

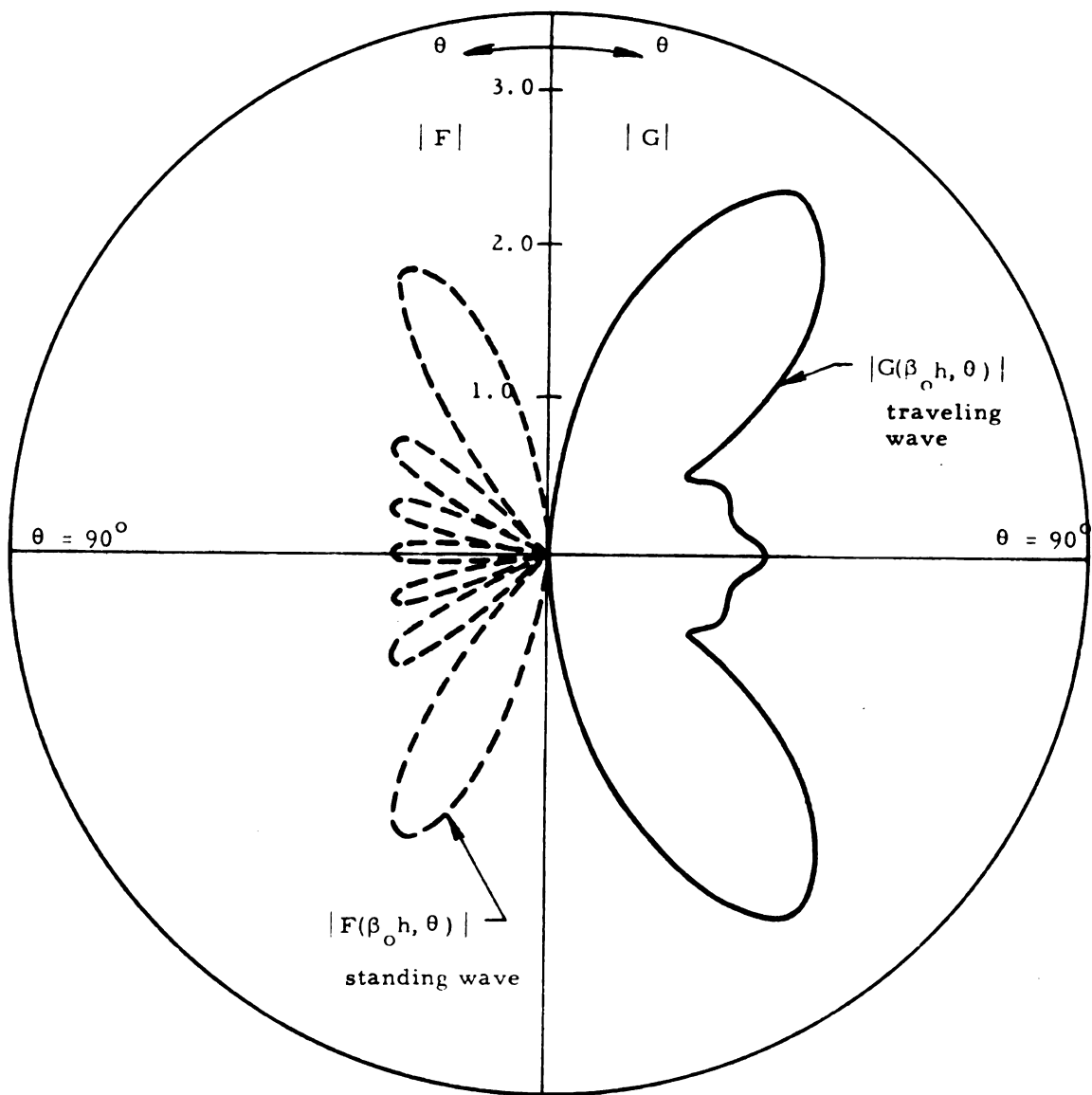


Figure 4.3. Radiation Patterns of Traveling and Standing Wave Antennas with $\beta_0 h = 7\pi/2$.

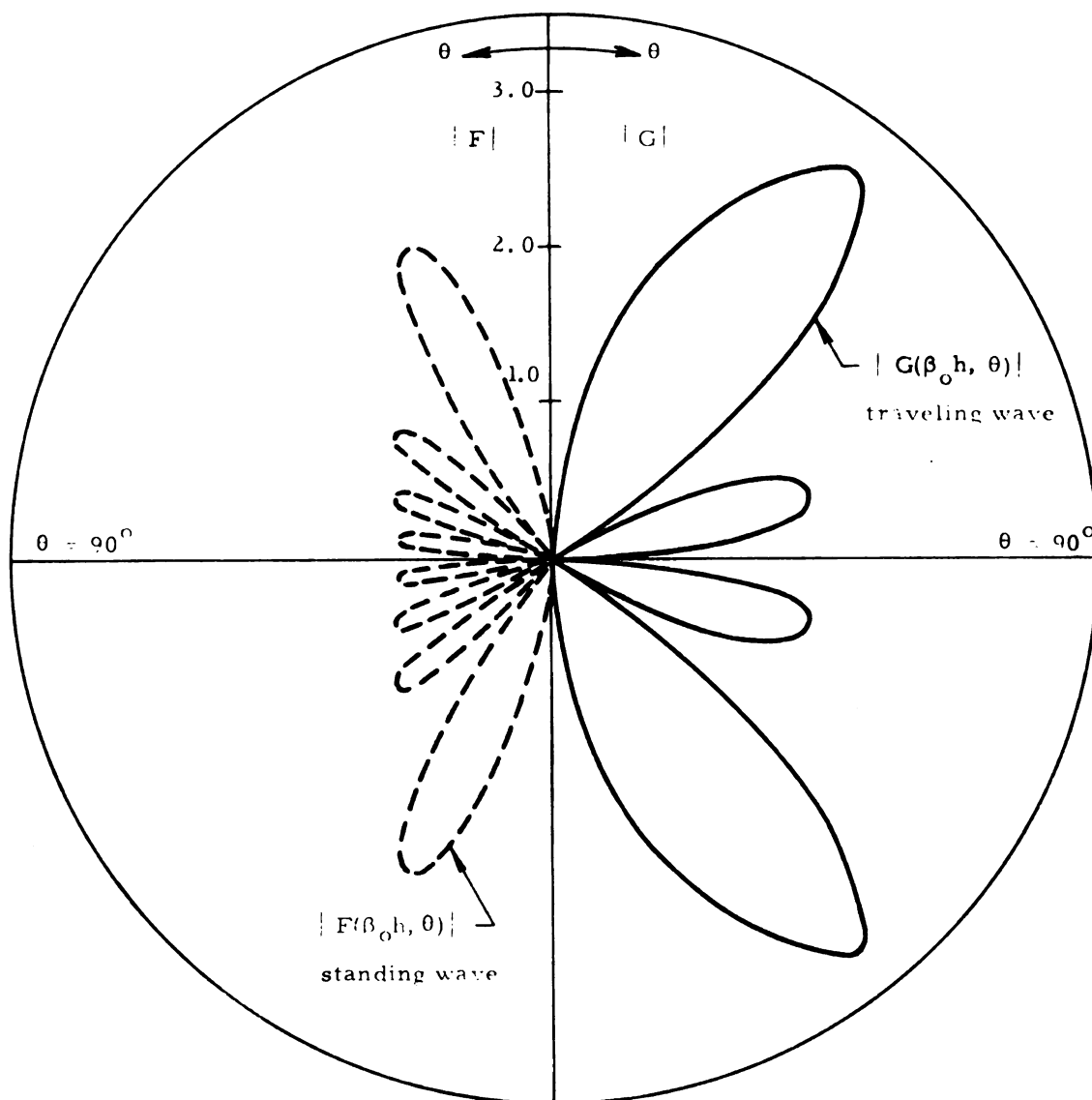


Figure 4.4. Radiation Patterns of Traveling and Standing Wave Antennas with $\beta_0 h = 4\pi$.

An inspection of the figures reveals that a traveling wave linear antenna possesses the following radiation characteristics:

- (i) The polar pattern of a traveling wave antenna has a major lobe beamwidth which is wider than the one of its standing wave counterpart.
- (ii) A minor lobe does not appear in the pattern of a traveling wave antenna until its length is much greater than that of the corresponding standing wave dipole. In particular, the first appearance of a minor lobe in the traveling wave antenna pattern occurs for a half-length of $h = 2\lambda_0$. The first minor lobe occurs for $h = 0.75 \lambda_0$ in the case of a standing wave dipole.
- (iii) The radiation pattern of a traveling wave antenna is much less dependent upon the cylinder's electrical length (frequency of excitation) than is the one of a standing wave antenna.

In these figures, the radiation patterns of the traveling wave and standing wave antennas are not normalized to the same absolute values of field intensity, but are merely independent relative field strength patterns. Thus while it appears from the figures that the traveling wave antenna radiates more power than its standing wave counterpart, this is only apparent. Actually, in the case of a traveling wave antenna with non-dissipative loading, the efficiencies of the two antennas are equal (essentially 100%) and the power radiated by each will be the same.

From the above remarks, it is noted that the radiation patterns calculated from the approximate theoretical expression (4.23) display

the characteristics generally associated with those of traveling wave antennas. Whether or not these characteristics represent any particular advantage will depend, of course, upon the intended application of the antenna. The relatively wide beamwidth associated with a short traveling wave antenna, and the absence of minor lobes in the radiation pattern of a long antenna should be useful in certain applications.

It should be emphasized that the radiation characteristics calculated in section 4.2 correspond to the traveling wave distribution of antenna current associated with an optimum impedance loading. As the loading deviates from its optimum value, the traveling wave of current gradually reverts back to an essentially standing wave. Under these circumstances, the corresponding radiation patterns would again be characterized by the narrower beamwidth and presence of multiple minor lobes associated with a conventional unloaded dipole.

CHAPTER 5

EXPERIMENTAL STUDY OF TRAVELING WAVE ANTENNA WITH NON-DISSIPATIVE LOADING

5.1. Object of the Experimental Investigation

An approximate expression for the distribution of current on a linear antenna consisting of a doubly impedance loaded cylinder was obtained theoretically in Chapter 2. This result gave the current distribution on the cylinder as a function of its dimensions, the excitation frequency, and the impedance and position of the double loading. In Chapter 3 the optimum loading impedance to yield a traveling wave of current over most of the antenna was determined from its current distribution. This optimum impedance was expressed in terms of the cylinder dimensions, the frequency of excitation, and the position of the loading. It was found that a pure resistance or a pure reactance could constitute an optimum impedance loading if their locations were properly selected. The results of this theory indicate therefore, that a traveling wave distribution of current may be excited on a linear antenna having either a purely resistive or a purely non-dissipative loading of proper position.

As was indicated earlier, the observation that a traveling wave linear antenna may be realized through the use of a properly located lumped resistance loading is not original with the present research. An experimental study of such a resistance loaded dipole was made by Altshuler.³ In order to determine the necessary position of the resistance loading, he relied upon a transmission line analogy.

It is well known that an analogy exists between a linear antenna and a section of lossless transmission line terminated in an open circuit, since: (1) the current at the end of either is zero; and (2) both support an essentially standing wave distribution of current. The section of transmission line may be matched by placing a series resistance equal to the characteristic resistance of the line a quarter wavelength from its open-circuited end. A traveling wave of current will then exist on all but the end quarter wavelength of the line.

Through this analogy, Altshuler proposed that a traveling wave linear antenna might be realized by placing an optimum resistance loading a quarter wavelength from the cylinder ends. He verified experimentally that this was indeed possible, and determined the optimum value of the loading resistance. The distribution of current on the antenna with optimum resistance loading was found experimentally to consist of a traveling wave between the excitation point and the position of the loading, and a standing wave between the loading and the cylinder ends.

The theoretical prediction that a traveling wave current distribution may be obtained on a linear antenna through the use of a purely resistive loading is thus found to be in agreement with Altshuler's experimental results. Specific numerical comparisons between the theoretical and experimental values for the parameters of an optimum loading were made in section 3.3 of the preceding chapter. The close correspondence between these results gives an indication of the validity of the approximate theory presented in Chapter 2.

Although it has been predicted theoretically that a traveling wave distribution of current may be excited on a linear antenna through the use of a properly located lumped non-dissipative loading, there are no existing experimental results to verify this assertion. In fact the transmission line analogy just considered appears to indicate that such a technique must fail to yield a traveling wave of current, since an open-circuited section of lossless transmission line cannot be matched with a purely reactive loading regardless of its position. The need for an experimental study of such a linear antenna utilizing a non-dissipative loading is thus apparent. In particular, the experiment should verify that a traveling wave antenna may indeed be realized through the use of a lumped purely reactive loading.

In accordance with the above remarks, an experimental investigation of a linear antenna utilizing a purely non-dissipative loading was conducted. The object of the experiment was threefold: (1) verify that a traveling wave of current may be excited on a dipole having a purely reactive loading; (2) study the effect of variations in the loading parameters and excitation frequency upon the distribution of antenna current; (3) determine the frequency dependence of the input impedance to a traveling wave antenna utilizing a particular reactance loading which is optimum only at a single frequency.

In order to facilitate comparison of these experimental results with the theory presented in Chapter 3, the dimensions of the model antennas were taken to be the same as those considered in the numerical results of section 3.4. The theoretical and experimental values for the

position of an optimum non-dissipative loading and the input impedance to the corresponding traveling wave antennas may therefore be directly compared.

5.2. Description of the Experimental Arrangement

The experimental arrangement is indicated in Figure 5.1. An anechoic chamber was constructed with an aluminum image plane on one wall and with R. F. absorber covering the remaining walls. The monopole antenna consisted of an extension of the movable centerwire of the exciting coaxial line, and emerged from the center of the image plane. A purely reactive loading impedance was obtained through the use of an adjustable coaxial cavity structure in the end section of the antenna, as indicated in Figure 5.2. The length (h-d) of the end section was made adjustable so that the effective position as well as the reactance of the loading could be varied. A movable current probe of the type indicated in Figure 5.3 was employed to sense the amplitude of the antenna current. A slotted section in the exciting transmission line was provided to facilitate measurement of the antenna input impedance.

The anechoic chamber consisted of a cubical wooden structure having dimensions of 6.0 feet on each side. Since an excitation frequency of 600 mhz ($\lambda_o = 50$ cm) was used in the experiment, the chamber dimensions were of the order of 4.0 wavelengths. An aluminum ground plane having a thickness of 0.125 inches completely covered the chamber wall through which the antenna projected. The remaining walls of the chamber were covered with radio frequency absorbing material, which was effective, at the frequency utilized, in reducing

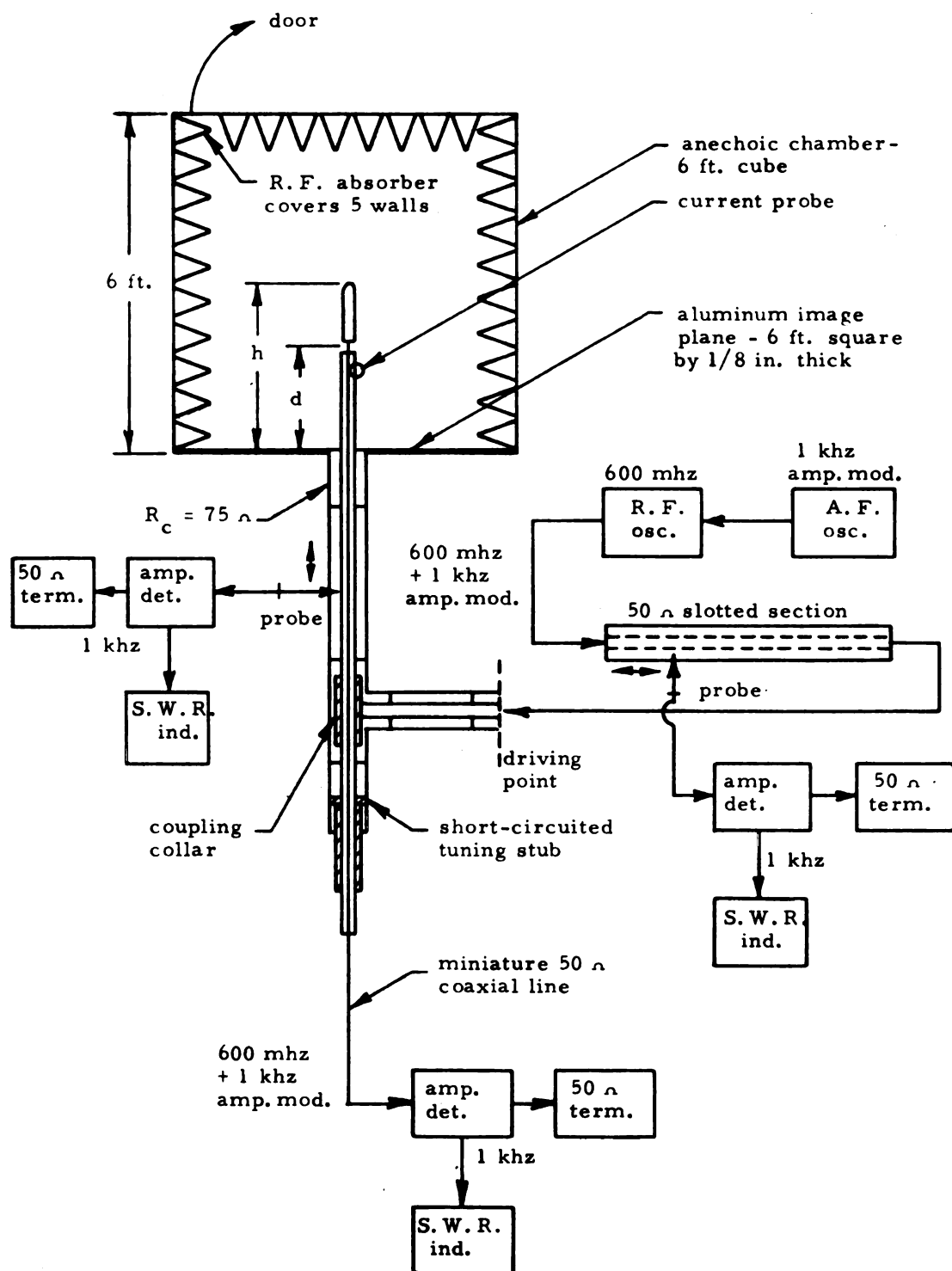


Figure 5.1. Experimental Arrangement.

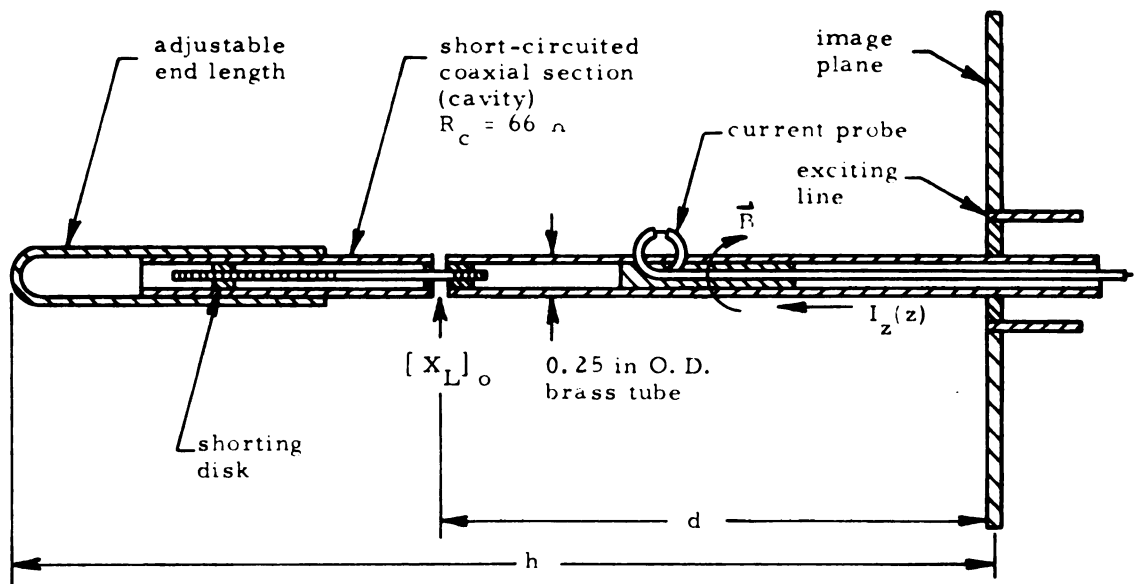


Figure 5.2. Structure of Model Monopole Antenna.

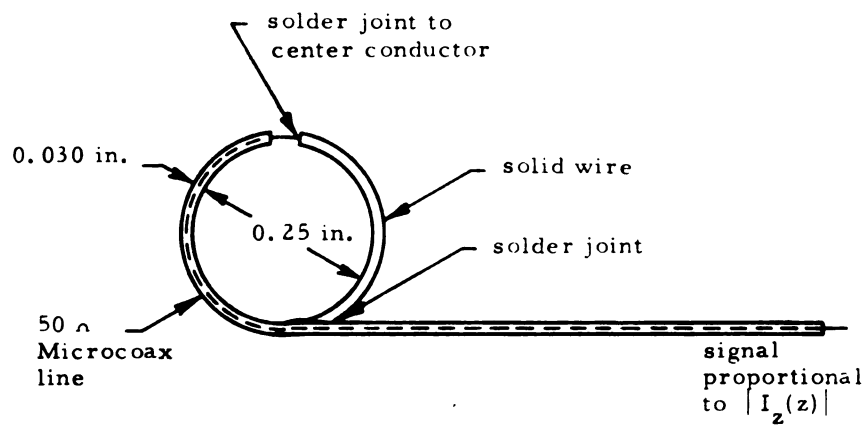


Figure 5.3. Structure of Loop Type Current Probe.

the reflected power by at least 20 db. It is felt that any interaction of the reflected fields with the radiating antenna was entirely negligible. Access was provided to the chamber through a door opposite the ground plane, this being the region of minimum radiation. Only the antenna itself was interior to the chamber, with all excitation and monitoring equipment situated on the outside.

A coaxial transmission line was used to excite the antenna, and its outer conductor terminated in an electrical contact with the aluminum ground plane at its center. The outer conductor of this line consisted of a brass tube with an outside diameter of 1.0 inches and an inside diameter of 0.875 inches, while the inner conductor was a brass tube having an outside diameter of 0.25 inches. Several thin dielectric wafers were used to support the centerwire and maintain it concentric with the outer tube, except for which the coaxial line was air filled. The corresponding characteristic resistance of the line was therefore calculated as $R_c = 75$ ohms.

At the end of the coaxial line opposite the ground plane, and approximately 1.5 wavelengths ($\lambda_0 = 50$ cm at 600 mhz) from it, an adjustable short-circuit was provided between the inner and outer conductors. The coaxial line was fed through a tee-section located about 0.5 wavelengths from its short-circuited end. At the tee-section, the joint between the two center conductors was effected through the use of a coupling collar about the centerwire of the line exciting the antenna. This arrangement allowed the centerwire of the exciting line, which becomes the antenna after emerging through the ground plane, to remain freely movable. The short-circuited tuning stub

was utilized to tune out the reactive component of the input impedance to the coaxial exciting system, as viewed from its driving point at the tee-section. This arrangement allowed a reasonably good impedance match to be realized between the coaxial exciting system and the transmission line driving it at the tee-section.

In the region between the ground plane and the tee-section, the outer conductor of the coaxial line was slotted axially to allow the insertion of a charge probe. A movable carriage was constructed to support a conventional probe in the slot, and thus facilitate monitoring the \vec{E} -field of the line at each point along its length. This arrangement was utilized to make the standing wave ratio measurements necessary in the experimental evaluation of the antenna input impedance.

The monopole antenna itself consisted of an extension of the center conductor from the exciting coaxial line, and projected into the anechoic chamber through the center of the ground plane. Since this monopole was imaged into the highly conducting aluminum ground plane, its distribution of current was exactly that of a corresponding dipole. The monopole is therefore equivalent to its dipole counterpart, except that it is driven by an effective voltage of $V_0/2$, where V_0 is the excitation potential of the corresponding dipole. Measured values of the monopole input impedance thus correspond to one half those of the equivalent dipole.

A detailed drawing of the impedance loaded monopole antenna is given in Figure 5.2. The section of the monopole for $0 \leq z \leq d$ consisted of the extended centerwire from the coaxial line, while that for $d \leq z \leq h$ was a separately constructed segment. Since

the center conductor of the coaxial line was free to move along its axis, then the total length of the antenna was readily adjustable. The portion of the monopole for $0 \leq z \leq d$, i. e., the center conductor of the coaxial line, was constructed of a brass tube having an outside diameter of 0.25 inches. This section of tubing was slotted axially to allow a small current probe to project through its surface. The current probe consisted of a small loop, and was supported in the slot by a plastic guide which prevented it from making contact with the antenna. With this arrangement, it was possible to measure the relative amplitude of axial current at each point $0 \leq z \leq d$ along the monopole.

Figure 5.3 indicates the detailed construction of the current probe. The probe consisted of a loop having a diameter of approximately 0.25 inches, and was fabricated from a section of Microcoax coaxial line. This coaxial cable had a solid copper outer sheath with a diameter of 0.030 inches, and its characteristic resistance was 50 ohms. At its end, this section of Microcoax line was bent into a semicircle to form half of the current loop. The second half of the loop was formed from a semi-circular arc of solid wire having the same diameter as the Microcoax, and was soldered to the coaxial section at the base of the loop. At the point where the two halves of the loop met a small gap was left, and the center conductor of the Microcoax line was soldered to the solid wire loop segment.

The circumferential magnetic field near the antenna surface links the open surface subtended by the plane loop and induces an e. m. f. around its circumference. Since the loop is essentially perfectly

conducting except at the small gap, then this induced voltage appears across the gap and excites a wave on the Microcoax line. At each point along the surface of the monopole, the magnetic \vec{B} -field is essentially proportional to the axial current at the same point. The amplitude of the voltage wave excited on the Microcoax line by the loop probe is therefore proportional to the amplitude of the axial monopole current.

A length of thin flexible 50 ohm coaxial line was joined to the Microcoax comprising the loop, and was passed through the center of the tube forming the monopole, as well as the center conductor of its exciting line, to the monitoring instruments outside the chamber. Since the loop was free to move in the axial slot of the monopole, its position could be varied over $0 \leq z \leq d$ by simply feeding this line in or out of the center conductor of the coaxial line driving the antenna. Dimensional calibrations were placed on the flexible line such that the position of the loop along the monopole could be determined accurately. With this arrangement, it was possible to measure the amplitude of the current distribution on the monopole by operations completely exterior to the chamber.

A pair of concentric telescoping brass tubes comprised the end section of the monopole having length $(h-d)$, as indicated in Figure 5.2. The inner tube had an outside diameter of 0.25 inches and an inside diameter of 0.188 inches, while the outer tube made a tight electrical contact with the inner one, had a wall thickness of 0.015 inches, and was fitted with a hemispherical end cap. This telescoping arrangement allowed the end length $(h-d)$ of the monopole to be adjusted to any desired value.

Within the inside tube of the concentric end section was constructed a short-circuited section of coaxial transmission line. The details are again indicated in Figure 5.2. A center conductor having a diameter of 0.063 inches was used for this coaxial section and, since the line was air filled, its characteristic resistance was calculated as $R_c = 66$ ohms. A short-circuiting disk terminated the coaxial section, while a dielectric wafer supported its center-wire at the excited end. The center conductor and shorting disk were threaded to facilitate adjusting the length ℓ of the short-circuited section.

The input impedance to the short-circuited coaxial line section is given by the well known expression

$$Z_{in} = j R_c \tan \beta_o \ell \quad (5.1)$$

where R_c is its characteristic resistance and β_o the free space wave number. It is clear from Figure 5.2 that this input impedance is exactly the impedance which loads the monopole antenna at $z = d$. Hence, in accordance with the definitions made in Chapter 2, the loading impedance appearing at $z = d$ is

$$Z_L = j R_c \tan \beta_o \ell \quad (5.2)$$

This impedance is purely reactive, and may be made to have any value between plus and minus infinity by proper adjustment of the length ℓ of the short-circuited coaxial section.

The experimental arrangement just described provided the means for realizing a monopole antenna having a purely non-dissipative loading. With this apparatus, the total length h of the monopole, the

effective position d of the impedance loading, and its reactance X_L were all readily adjustable. Further, means were available for monitoring the distribution of current along $0 \leq z \leq d$ on the monopole, and for measurement of its input impedance.

Excitation of the entire experimental setup was provided at the input arm of the tee-section in the coaxial line driving the antenna. A 50 ohm coaxial transmission system was used to deliver energy from the R. F. oscillator (General Radio 1209-B) through a 50 ohm slotted section (General Radio 874-LBA) to the input of the tee-section. The antenna tuning stub was then adjusted to minimize the S.W.R. measured on this slotted section, and consequently result in maximum power being transferred to the monopole.

In order to avoid the necessity for complicated measuring apparatus, the 600 mhz signal from the R. F. oscillator was amplitude modulated at 1 khz by a sinusoidal signal from an audio oscillator (General Radio 200-C), as indicated in Figure 5.1. The R. F. signals from the current probe and the charge probes of the two slotted sections were then amplitude detected by coaxial detectors (General Radio 874-VQL) terminated in the 50 ohm characteristic resistance common to all three transmission systems. Bolometer detectors (Narda N-610B) were utilized to assure accurate square law detection. These detector outputs were coupled to standard S.W.R. indicators (General Radio 415-B), which provided the necessary bolometer bias currents and which were calibrated for square law detection. The desired values of standing wave ratio or relative amplitude of monopole current could then be read directly from the meter scales.

5.3. Traveling Wave Distribution of Current on Monopole with Purely Non-Dissipative Loading

It was the primary object of the experimental study to verify the theoretical prediction that a traveling wave of current could be excited on a linear monopole antenna through the use of a properly positioned non-dissipative loading. The experimental arrangement described in the preceding section was ideally suited to this purpose since:

- (i) It provided an impedance loaded monopole whose total length h was freely variable.
- (ii) The loading impedance was purely non-dissipative, and its reactance could be varied to obtain any desired value from $-\infty$ to $+\infty$ ohms.
- (iii) The position of the loading d and the length $(h-d)$ of the end section of the monopole were readily adjustable.
- (iv) Means were provided to measure the distribution of monopole current on $0 \leq z \leq d$ for each combination of antenna length and loading parameters.

For this portion of the experiment, the antenna was excited at a constant frequency of 600 mhz corresponding to a wavelength of $\lambda_0 = 50$ cm.

Two different monopole antennas, having lengths of $h = \lambda_0 = 50$ cm and $h = 2\lambda_0 = 100$ cm, were studied experimentally. These monopoles correspond to the dipoles considered in section 3.4, where the reactance and position of an optimum non-dissipative loading were given in Figures 3.3 and 3.4, respectively, as a function of the antenna electrical length. In either case, the end length $(h-d)$ was

first set to its theoretically optimum value. The optimum loading reactance was then determined by observing the distribution of current on the monopole as the length ℓ of the coaxial cavity was varied. Through this technique, it was possible to determine the cavity setting which minimized the current standing wave ratio on the monopole. Similarly, the end length (h-d) was slightly readjusted until a traveling wave of current was realized over the region $0 \leq z \leq d$ of the monopole.

The experimentally measured distributions of monopole current are indicated in Figures 5.4 and 5.5. In these figures, the traveling wave of current obtained with the purely non-dissipative loading is compared with the standing wave which exists on a conventional unloaded monopole. It is noted that, in either case, a decaying traveling wave of current was obtained over the region $0 \leq z \leq d$ through the use of a properly located purely reactive loading. The current over the region $d \leq z \leq h$ of the monopole with optimum loading remains a standing wave. On this region the current was not measured, but represents the theoretical sinusoidal standing wave distribution. These results provide direct experimental verification of the theory presented in Chapter 3.

A comparison is made between the theoretically and experimentally determined values of the optimum monopole end length (h-d) in Table 5.1. It is noted that the agreement between these two sets of results is quite close, in that the experimental values are only of the order of 9% smaller than the theoretical ones. Further, the theoretical prediction that the optimum end length should be essentially

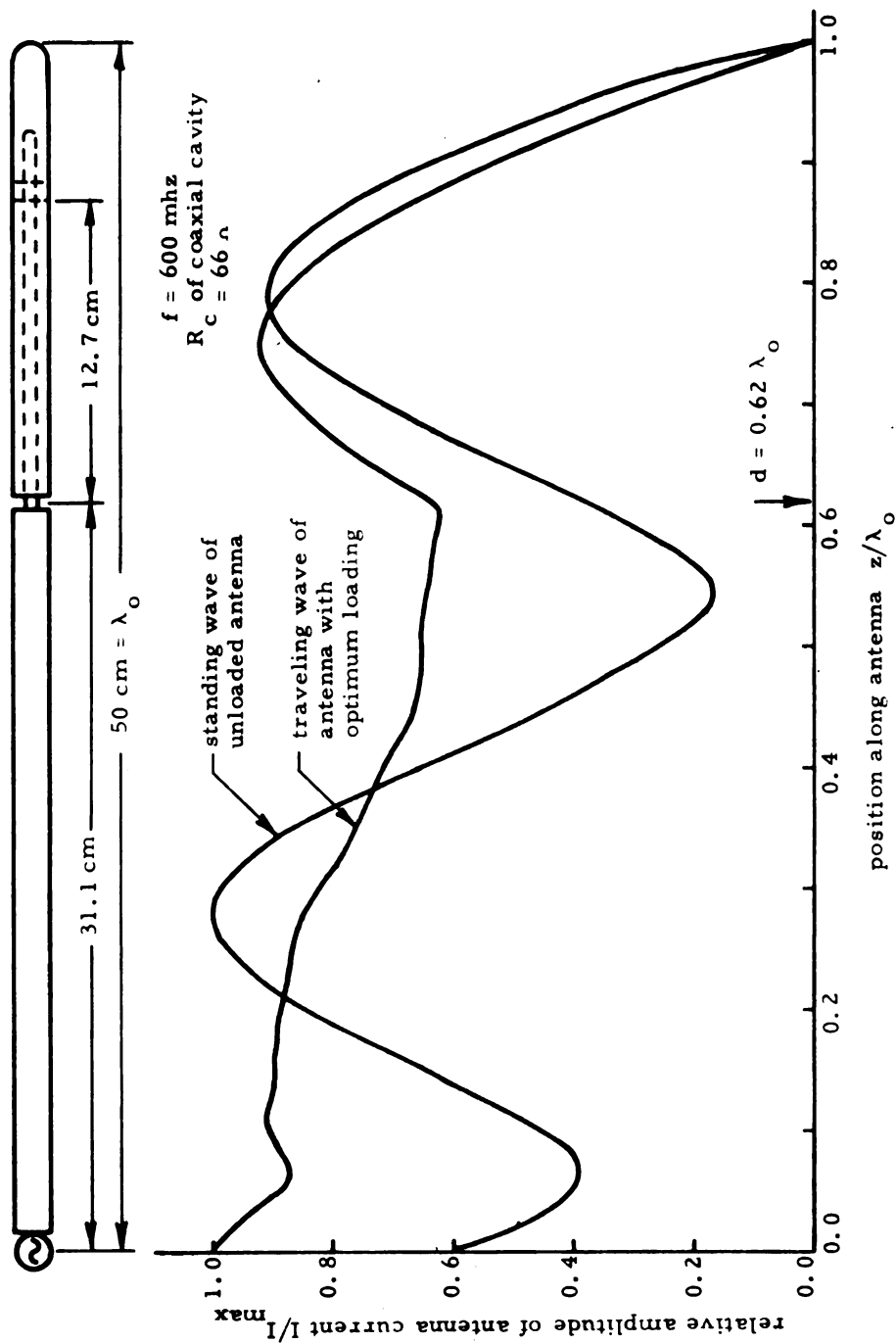


Figure 5.4. Experimental Current Distribution of Antenna with $h = \lambda_0$; Unloaded and with Optimum Reactance Loading.

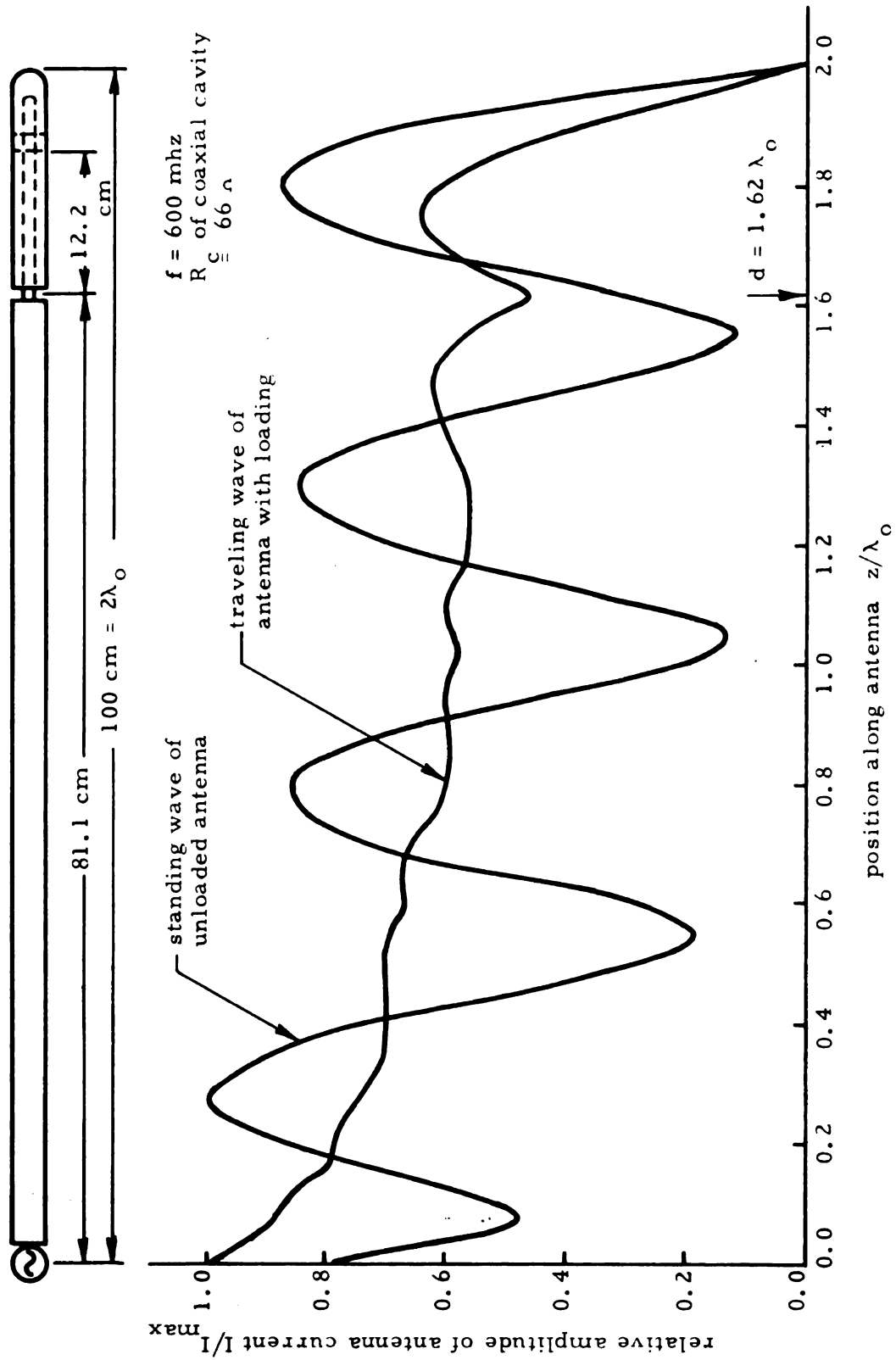


Figure 5.5. Experimental Current Distribution of Antenna with $h = 2\lambda_0$; Unloaded and with Optimum Reactance Loading.

independent of the total antenna length is found to be fully verified by the experimental measurements.

Table 5.1. Comparison of Optimum Monopole End Lengths

total length h of monopole	optimum monopole end length $(h-d)$	
	theoretical	experimental
$h = \lambda_o = 50 \text{ cm}$	$(h-d) = 0.418\lambda_o = 20.9 \text{ cm}$	$(h-d) = 0.378\lambda_o = 18.9 \text{ cm}$
$h = 2\lambda_o = 100 \text{ cm}$	$(h-d) = 0.417\lambda_o = 20.8 \text{ cm}$	$(h-d) = 0.378\lambda_o = 18.9 \text{ cm}$

No attempt was made to measure the loading reactance provided by the coaxial cavity, since it would be virtually impossible to account for the stray capacitances which would necessarily influence the cavity adjustment. At the frequency of 600 mhz utilized in the experiment, the theoretically optimum loading reactance of approximately - 365 ohms corresponds to a capacitance of less than one picofarad. It therefore becomes evident that any stray capacitances, which are effectively paralleled with the input to the cavity across the antenna gap at $z = d$, would have a definite but unpredictable effect upon the necessary optimum length l of the coaxial cavity.

5.4. Effects of Variations in Loading Parameters and Frequency Upon the Traveling Wave Distribution of Current

In the preceding section, the parameters of an optimum non-dissipative loading to yield a decaying traveling wave distribution of current on a linear monopole antenna were determined experimentally. It was found in particular that, for a monopole having a length of $2\lambda_o = 100 \text{ cm}$ at an excitation frequency of 600 mhz, the optimum

reactance corresponded to a cavity length of $\ell = 12.2$ cm while its necessary position was $d = 81.1$ cm. The sensitivity of the traveling wave distribution of monopole current on $0 \leq z \leq d$ to variations in these loading parameters and the frequency of excitation is to be evaluated experimentally in the present section.

The first effect to be considered was that due to variations in the loading position d , or equivalently the end length $(h-d)$ of the monopole. An optimum non-dissipative loading requires an end length of $(h-d) = 18.9$ cm. Figure 5.6 indicates a comparison between the traveling wave of current obtained with this loading position and the distribution of current which was measured corresponding to end lengths of $(h-d) = 17.9$ cm and $(h-d) = 19.9$ cm. It is noted that due to the 1.0 cm variation from the optimum end length (about 5%) the traveling wave distribution of monopole current is altered substantially, and begins to revert back to a standing current wave. This indicates that the current distribution on the monopole is a strong function of the loading position, in accordance with the theoretical observations of Chapter 3.

An optimum loading reactance corresponding to a coaxial cavity length of $\ell = 12.2$ cm was determined experimentally for the monopole having a total length of $h = 2\lambda_0 = 100$ cm. If the cavity length is changed, then the position but not the reactance of the non-dissipative loading is optimum, and the current distribution will deviate from the traveling wave corresponding to an optimum loading. In Figure 5.7 a comparison is indicated between the traveling wave of monopole current associated with an optimum loading and the measured

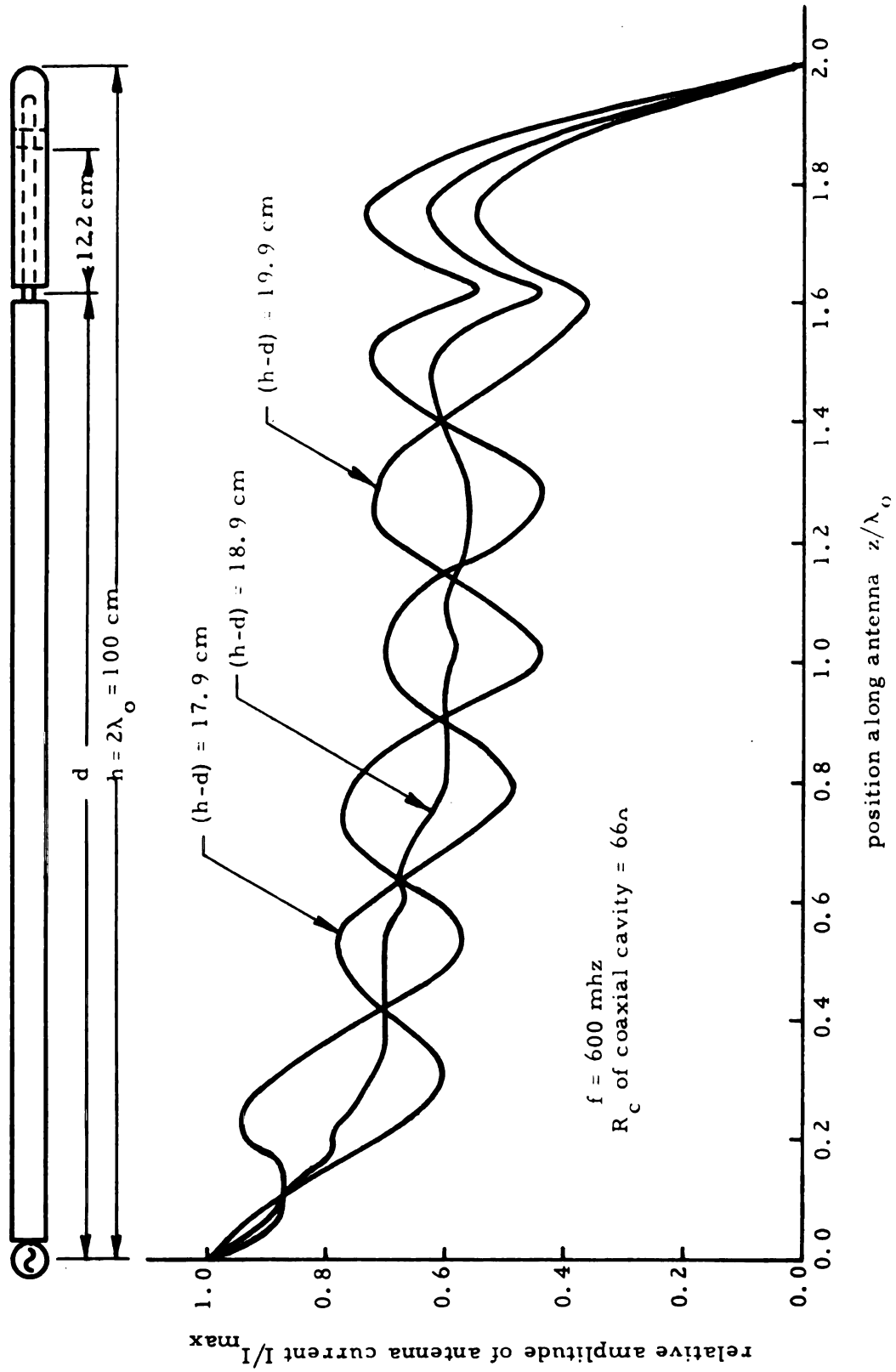


Figure 5.6. Effect (experimental) of Variations in Monopole End Length $(h-d)$ upon its Traveling Wave Distribution of Current.

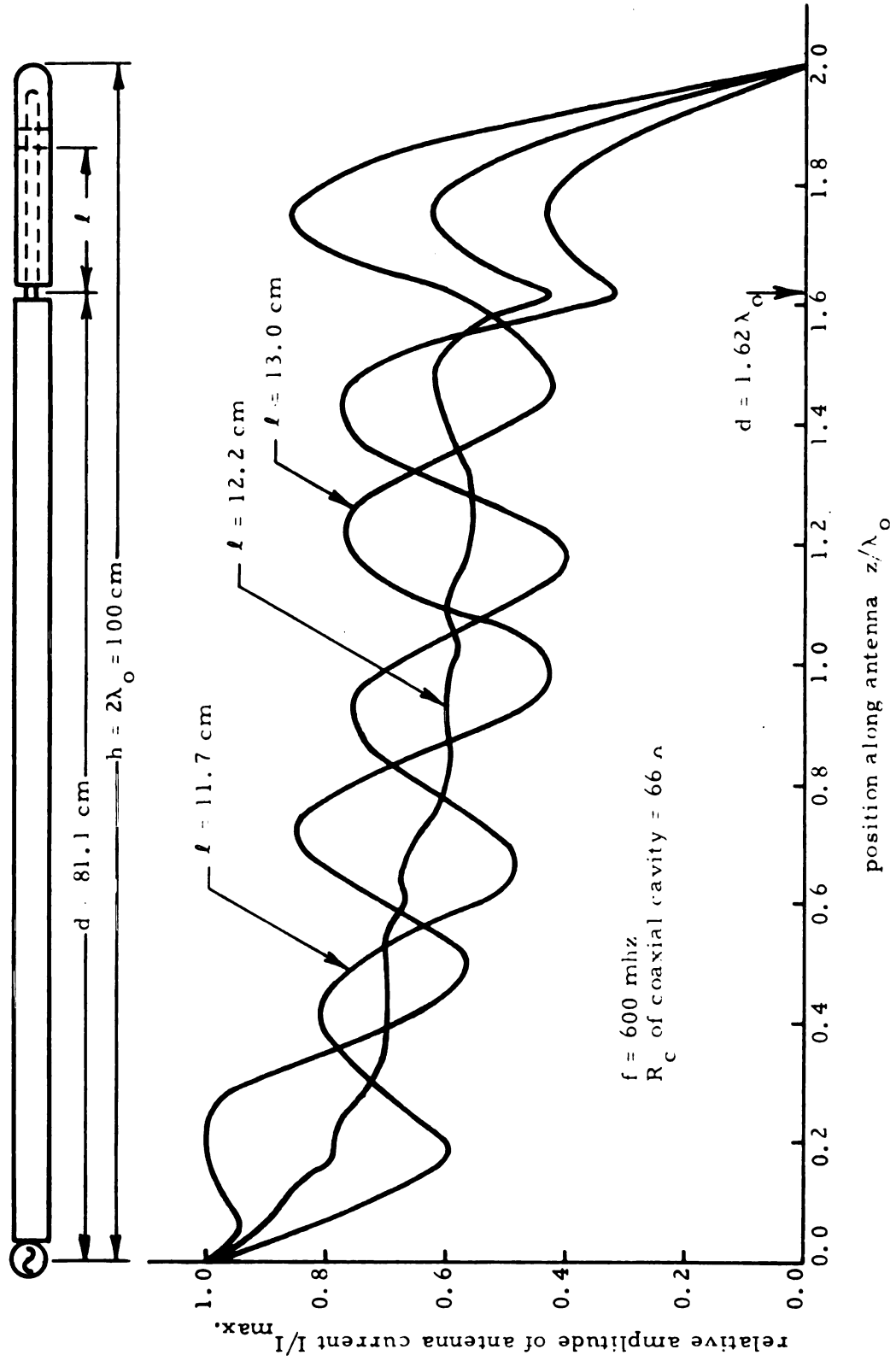


Figure 5.7. Effect (experimental) of Variation in Loading Reactance on the Traveling Wave Distribution of Monopole Current.

distribution of current obtained when the coaxial cavity length was set to values of $\ell = 11.7$ cm and $\ell = 13.0$ cm. It is again noted that the traveling wave distribution of monopole current is substantially altered by such variations, and that it deviates toward the standing wave distribution characteristic of a conventional dipole. The dependence of the monopole current distribution upon the reactance of the non-dissipative loading is thus observed to be very pronounced.

It has been indicated, both in theory and by experiment, that a purely reactive loading of fixed position may be optimum only at a single frequency. At any other frequency, an optimum loading impedance must have a resistive component as well as a reactive one. In section 3.4, consideration was given to a purely non-dissipative loading consisting at each frequency of the reactive component of the corresponding optimum impedance. It was observed that, with such a loading, an approximately traveling wave distribution of current could be maintained for a band of frequencies about the one where the loading became optimum.

The monopole antenna having a length of $h = 2\lambda_0 = 100$ cm at an excitation frequency of 600 mhz was found experimentally to require the optimum loading parameters: $d = 81.1$ cm, $\ell = 12.2$ cm. A decaying traveling wave of current was measured on $0 \leq z \leq d$ for an antenna having such a loading. Figure 5.8 indicates a comparison between this traveling wave of current and the distribution of monopole current measured when the excitation frequency was varied to 560 mhz and 640 mhz, with the loading parameters fixed at the above indicated values. Evidently the

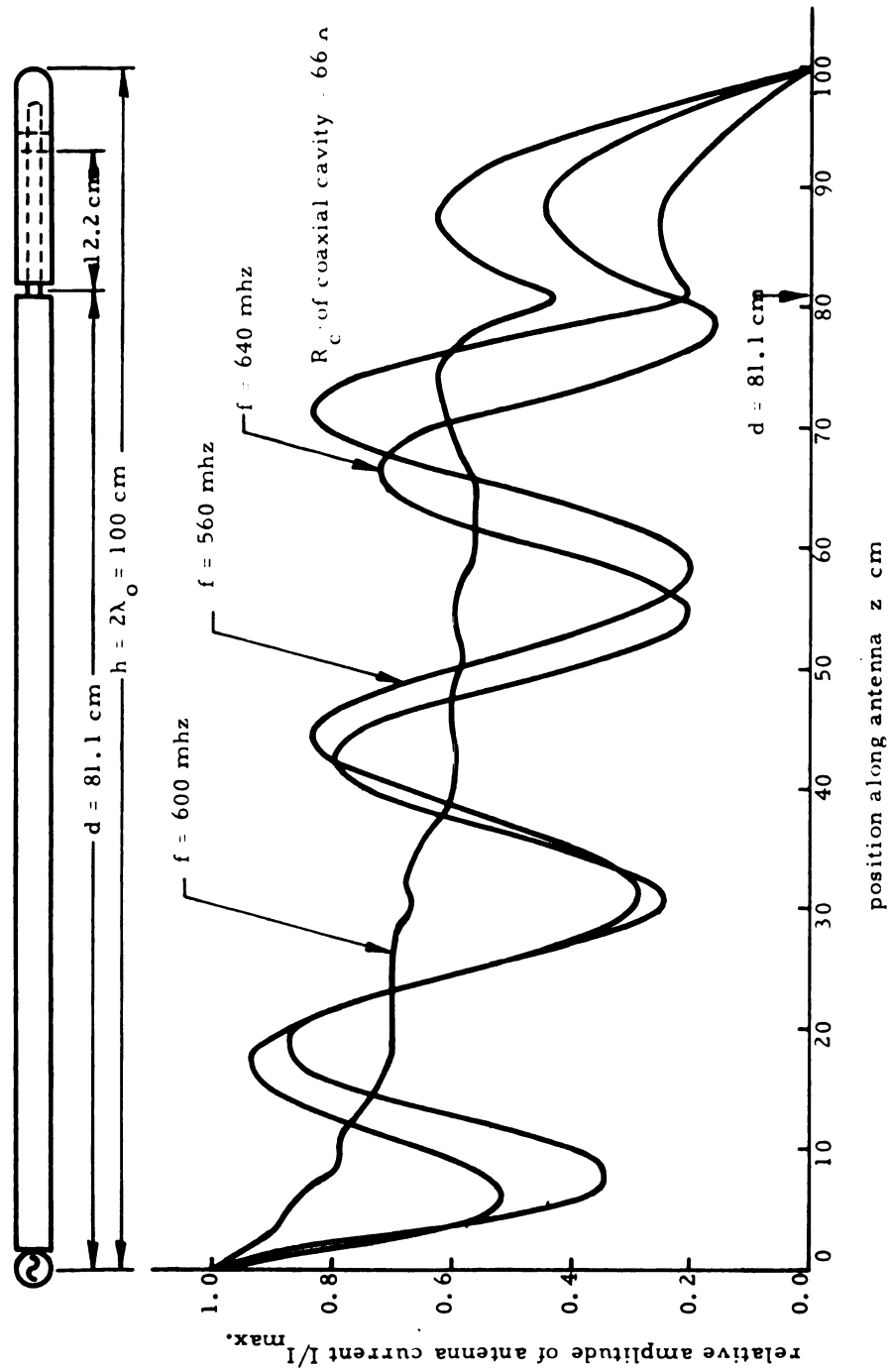


Figure 5.8. Effect (experimental) of Variations in Excitation Frequency on the Traveling Wave Distribution of Monopole Current.

frequency dependence of the antenna current distribution is quite strong. There are two reasons for this result: (1) there was no resistive impedance component present in the loading; (2) the frequency dependence of the coaxial cavity reactance does not at all match that of the reactive component of an optimum impedance loading. The distribution of monopole current therefore reverts rather rapidly back to an essentially standing wave as the excitation frequency deviates from 600 mhz. This situation could be greatly improved upon if a more appropriate optimum loading reactance were realized.

5.5. Input Impedance of a Traveling Wave Linear Antenna with Non-Dissipative Loading

It is of particular interest to consider the frequency dependence of the input impedance to a traveling wave linear antenna utilizing a purely non-dissipative optimum loading. According to the theory of section 3.5, this input impedance should be relatively broadband about the frequency at which the purely reactive loading becomes optimum. The extent of this broadbanding will depend, of course, upon just how well the frequency dependence of the loading reactance matches that of the reactive component of an optimum loading impedance.

The monopole having a length of $h = 2\lambda_0 = 100$ cm at an excitation frequency of 600 mhz was again utilized for this part of the experimental study. A purely reactive coaxial cavity loading having the parameters $d = 81.1$ cm, $\ell = 12.2$ cm was utilized. Such a loading is optimum at a frequency of 600 mhz. With the loading parameters held constant at the indicated values, the input impedance

to the monopole was measured for excitation frequencies between 480 and 720 mhz. Since the input impedance of the monopole antenna is effectively the impedance which terminates its exciting coaxial line, then this impedance was readily determined by conventional S.W.R. measurements⁸ on the slotted section of that line.

The experimentally measured input impedance to the reactance loaded dipole is indicated as a function of frequency in Figure 5.9, where it is compared with that of an unloaded antenna of the same dimensions. Since the input impedance to a monopole antenna is one half that of its dipole counterpart, the values given in the figure are just twice the experimentally measured ones. It is noted that the input impedance of the reactance loaded antenna is somewhat broadband about the frequency of 600 mhz, where the loading becomes optimum, as compared with the impedance of the conventional dipole. It must be emphasized that the frequency dependence of the coaxial cavity reactance does not at all match that of the reactive component of an optimum loading impedance. If a more appropriate non-dissipative loading could be realized, the above indicated broadbanding would be greatly increased.

A direct comparison may be made between the experimentally measured value of input impedance to a traveling wave antenna and the one calculated from the theory of section 3.5. At an excitation frequency of 600 mhz where the purely reactive loading becomes optimum, i. e., yields a traveling wave distribution of antenna current, the corresponding values of input impedance are: (1) theoretical,

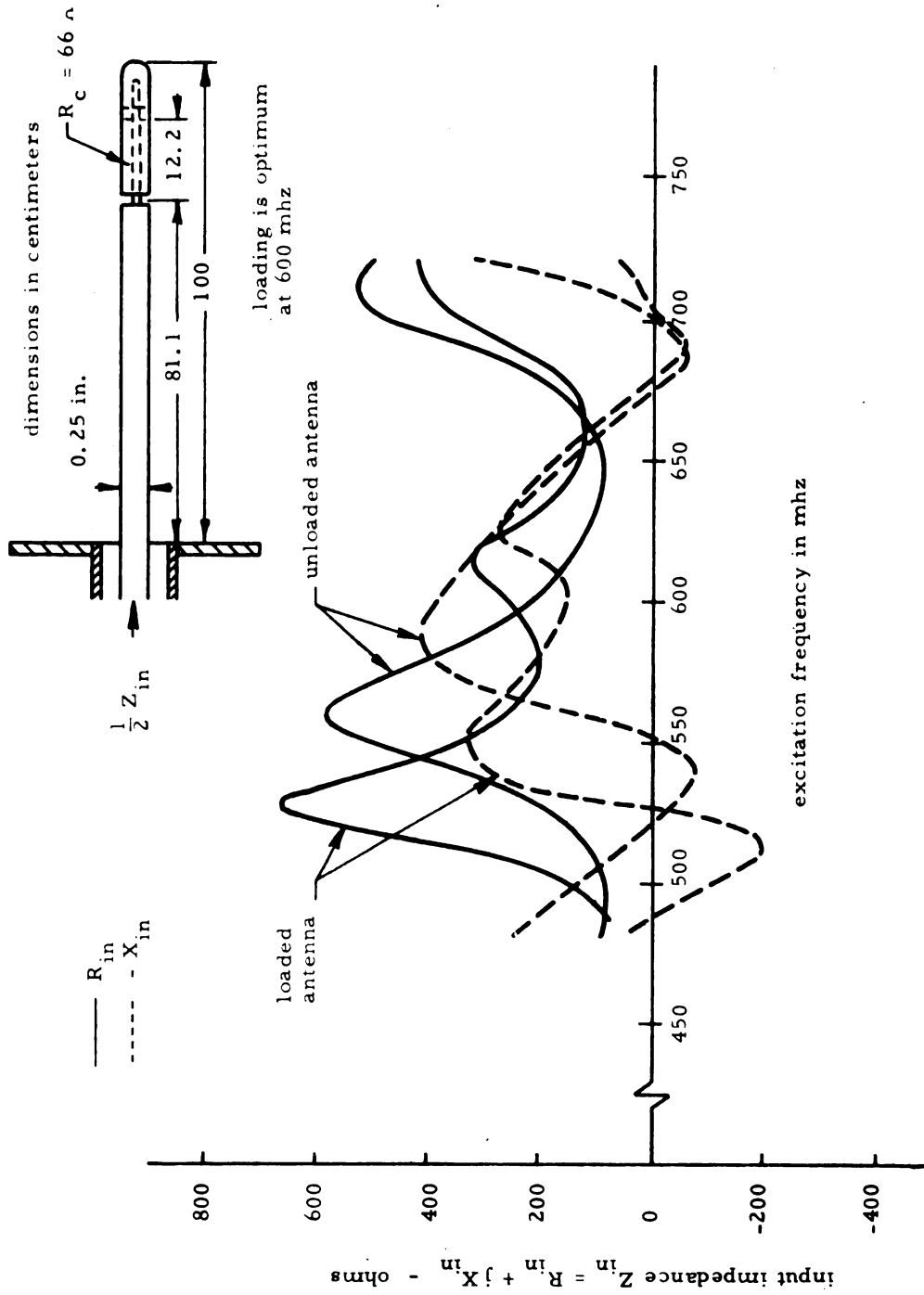


Figure 5.9. Experimental Input Impedance as a Function of Frequency for Loaded and Unloaded Monopole Antennas.

$Z_{in} = 316 - j184$ ohms; (2) experimental, $Z_{in} = 264 - j156$ ohms. The error in the theoretical result is approximately 15%, which is well within the range to be expected for such an approximate theory. It is felt that the major contribution to this error is due to the approximate nature of expression (3.37), which was used to evaluate the expansion parameter Ψ .

PART II

TRAVELING WAVE LOOP ANTENNA
WITH OPTIMUM IMPEDANCE LOADING

CHAPTER 6

INTRODUCTION

6.1. Introduction

In the second part of this research, attention is to be directed to the realization of a traveling wave loop antenna and to the evaluation of its corresponding circuit and radiation characteristics. An impedance loading technique is utilized whereby the circular loop antenna is doubly loaded with a pair of identical lumped impedances. A theoretical study of this configuration is made to determine approximately the distribution of current on the loop as a function of its dimensions, the excitation frequency, and the impedance and position of the double loading. From this result the optimum loading impedance to yield a traveling wave of current over the major extent of the loop circumference is determined. In particular, the possibility of utilizing a purely non-dissipative optimum loading is thoroughly investigated. Finally, the input impedance and radiation fields of a traveling wave loop antenna having a non-dissipative optimum loading are evaluated as a function of its dimensions and the frequency of excitation.

6.2. Definition of a Traveling Wave Loop Antenna

A traveling wave loop antenna will henceforth be considered as a circular loop antenna which supports a traveling wave distribution of current. The traveling wave of current is excited by a voltage generator at a point on the loop, and advances outward along its circumference toward a point 180 degrees removed from the point of excitation. While the phase of the current is essentially a linear

function of position along the loop circumference, the amplitude of the traveling wave decays as it advances outward from the excitation point, since it constantly radiates energy into space. A restriction to the class of thin-wire loop antennas is made in this research, such that an expedient one-dimensional theory will be approximately valid. In this one-dimensional approximation, the distribution of loop current is assumed to flow parallel to the axis of the thin wire constituting the loop.

The theory of circular loop antennas remains relatively undeveloped when compared with the extensive research which has been reported concerning the linear antenna. A mathematical theory describing the circuit properties of a circular loop antenna was first developed by Hallen,¹ at the same time at which he formulated the corresponding theory for a linear antenna. The result of this theory was an integral equation for the distribution of loop current. Hallen solved this integral equation through a Fourier series technique, but pointed out that the series did not converge when the loop diameter became an appreciable fraction of the wavelength. Some eighteen years later, Storer⁹ found that, by a more careful evaluation of the Fourier coefficients, the Fourier series for the distribution of loop current could be made to converge. This modified theory yielded numerical results which were in good agreement with corresponding experimental measurements of the loop current, and indicated that the current distribution on a loop antenna consists of an essentially standing wave.

Since it is well known that a conventional loop antenna supports an essentially standing wave of current, then evidently some modification of its structure is necessary in order that it might support a traveling wave current distribution. In the present research, an impedance loading technique is utilized to obtain the desired traveling current wave on the circular loop. This method consists of doubly loading the loop with a pair of identical lumped impedances placed symmetrically with respect to its excitation point. When the loading is optimum, that is, when its impedance and position are properly selected, a traveling wave distribution of current may be excited on the loop over most of its circumference.

A loop antenna is completely characterized by its distribution of current. The loop is fully described by its circuit and radiation characteristics, which are readily determined in terms of the current distribution. If the current at its excitation point is known, then the input impedance to the circular loop may be immediately calculated. Furthermore the radiation pattern of the loop is determined in a straightforward manner in terms of its distribution of current. Since the circuit and radiation characteristics of a loop antenna are determined by its current distribution, then it might be expected that these characteristics should differ greatly for distributions corresponding, respectively, to the standing and traveling current waves.

6.3. Important Characteristics of a Traveling Wave Loop Antenna

A conventional circular loop antenna is very frequency sensitive, that is, its input impedance depends strongly upon the excitation frequency. This frequency dependence is a direct consequence of the standing wave

distribution of antenna current. As the frequency of excitation is varied, the maxima and minima of the standing wave of current shift in position along the circumference of the loop. With the excitation potential fixed therefore, the current at the driving point of the loop, and hence its input impedance, varies strongly with changes in the frequency of excitation. As a result of this frequency sensitivity, a conventional loop antenna is ordinarily used only at a single frequency or over a very narrow band of frequencies.

A traveling wave antenna, in contrast to its standing wave counterpart, has an input impedance which is relatively frequency independent. This broadband character is a consequence of the traveling wave distribution of current. Since the amplitude of the traveling wave of current is essentially constant along the circumference of the loop, except for the smooth decay due to radiation, a variation in the excitation frequency does not result in a rapid change in the current at the driving point. The input impedance of a traveling wave loop antenna is therefore a relatively weak function of frequency. It is this broadband character which is the most important property of a traveling wave loop antenna.

The radiation pattern in the plane of a relatively small conventional loop antenna consists of two broad lobes separated in space by 180 degrees. As the diameter of this standing wave loop is increased, both the shape and the spatial orientation of the pair of lobes in its radiation pattern undergo radical variations, although they remain oppositely directed in space. Finally, as the loop circumference is further increased, the pair of lobes split to form several narrower lobes of equal but smaller amplitude.

On the other hand, the radiation pattern of a traveling wave loop antenna of small dimensions is essentially unidirectional, having a very broad major lobe in one spatial direction and a narrow minor lobe of relatively small amplitude in the opposite direction. As the electrical diameter of the traveling wave loop is increased, the narrow lobe grows in amplitude while the broad lobe shifts in its spacial orientation, decreases in amplitude, and finally splits to form a minor lobe structure of relatively small amplitude. An electrically large traveling wave loop antenna is thus characterized by a single narrow major lobe which is accompanied by a relatively low minor lobe structure. The major lobe of this pattern is spatially oriented in a direction 180 degrees removed from the excitation point of the loop, i. e., in the direction of the traveling wave of current.

It is indicated therefore that the radiation characteristics of a traveling wave loop antenna in no way resemble those of its standing wave counterpart. The modified radiation pattern characteristic of the traveling wave loop may be desirable for certain purposes. In particular, the broad unidirectional pattern of a small loop or the directive pattern of an electrically large loop may be useful for certain applications.

6.4. Previous Research on the Traveling Wave Loop Antenna

It was mentioned earlier that little research has been directed to the study of circular loop antennas, and that the theory of such antennas remains relatively undeveloped. A formulation for the distribution of current and circuit characteristics of such a loop was presented by Storer.⁹ This theory expresses the current distribution

on the loop antenna in the form of a Fourier series, a result which is very intractable for practical calculations. No theory has been developed which yields a closed form solution for the distribution of loop current in terms of simple functions. Further, no complete formulation for the radiation field of a circular loop antenna in terms of its distribution of current is available. Only the special case of an electrically small loop, on which the current is assumed to be constant along its circumference, has been considered in any detail. It is therefore perhaps not surprising that no specific consideration has been given to the realization of a traveling wave circular loop antenna.

A circular loop antenna multiloading with lumped resistors has been considered by Iizuka.¹⁰ In this theory, use was made of Storer's technique and the principle of linear superposition to obtain a Fourier series solution for the distribution of current on the multiloading loop. It was noted that, when the loop was loaded with a single positive resistance of approximately 100 ohms at a point 180 degrees removed from the excitation point, its input impedance became relatively broadband as a function of frequency. A study of the corresponding amplitude and phase of the current distribution on the loop, which was presented by Iizuka, indicates that it approximates a traveling wave distribution. Thus, while Iizuka's research was not directed toward realizing a traveling wave loop antenna, his results appear to indicate that such a traveling wave of current may be obtained through the use of a lumped impedance loading technique, and that the corresponding input impedance will exhibit a broadband character.

It will be demonstrated in Chapter 7, through a formulation similar to Iizuka's, that the Fourier series solution for the distribution of loop current cannot yield an explicit expression for the optimum loading impedance to excite a traveling wave of current. A more approximate closed form solution in terms of simple functions must be resorted to in order to determine the optimum impedance in terms of the dimensions of the loop and its frequency of excitation.

6.5. Object of the Present Research

It is the object of the present research to realize a traveling wave loop antenna through the use of a lumped impedance loading technique. In this investigation, the loop antenna is assumed to consist of a thin perfectly conducting circular cylinder bent into the form of a circular loop. The loop is excited at an origin point and doubly loaded with a pair of identical impedances which are placed symmetrically along its circumference with respect to the origin. With such a configuration, there are two degrees of freedom in choosing a loading; its impedance and position. The optimum loading to yield a traveling wave distribution of current on the loop is to be determined. In particular, the possibility of utilizing a properly located purely reactive optimum loading is to be investigated.

Through the use of such a reactance loading technique, the desirable circuit and radiation characteristics associated with a traveling wave distribution of current may be obtained while avoiding the introduction of dissipative elements. A traveling wave loop antenna is therefore realized while maintaining the high efficiency of a conventional standing wave loop.

6.6. Outline for Theoretical Investigation of a Traveling Wave Loop Antenna with Optimum Impedance Loading

The present research concerning a traveling wave circular loop antenna with optimum impedance loading is restricted to a theoretical investigation. It will be the primary goal of this theory to determine the parameters of an optimum loading to yield a purely outward traveling wave of current over the circumference of the loop. No experimental investigation will be conducted in conjunction with this portion of the research, since the theoretical results will be found to be very similar to those obtained for the case of an impedance loaded linear antenna, which were thoroughly verified by an experimental study.

It is the purpose of the theoretical analysis to: (1) determine approximately the distribution of current on the doubly loaded loop as a function of its dimensions, the excitation frequency, and the impedance and position of the loading; (2) obtain from this result (in terms of the loop dimensions and its frequency of excitation) the parameters of an optimum double loading to yield a traveling wave distribution of current along the circumference of the loop; (3) investigate the possibility of utilizing a purely non-dissipative optimum loading; (4) calculate the circuit and radiation characteristics of a circular loop antenna utilizing such an optimum impedance loading.

CHAPTER 7

DISTRIBUTION OF CURRENT ON A DOUBLY LOADED CIRCULAR LOOP ANTENNA

7.1. Geometry of the Doubly Loaded Circular Loop Antenna

The geometry of the doubly impedance loaded circular loop antenna is taken to be as indicated in Figure 7.1. A thin perfectly conducting circular cylinder of diameter $2a$ is bent into the form of a circular loop having an outside diameter of $2b$. A system of polar coordinates (r, θ) is established with its origin at the center of the plane loop. The loop antenna is excited at $\theta = 0$ by a harmonic voltage source of frequency ω and potential V_0 , and is symmetrically loaded at $\theta = \pm\theta_0$ with a pair of identical lumped impedances Z_L . With such a configuration, there are two degrees of freedom in choosing a loading; its impedance and position.

In this research, both the source of excitation and the loading impedances are idealized to be point elements. The gap in the loop at its excitation point $\theta = 0$ is assumed to be centered about that point and to have a length of $2b\delta\theta$. Similarly, the gaps at the loading impedances at $\theta = \pm\theta_0$ are taken to have a length of $2b\delta\theta$ and to be centered about those points. The point element assumption then corresponds to letting $\delta\theta$ tend to zero as a limit. This mathematical approximation corresponds to the physical requirement that the linear dimensions of the excitation and loading elements be negligibly small compared with the circumference of the loop itself.

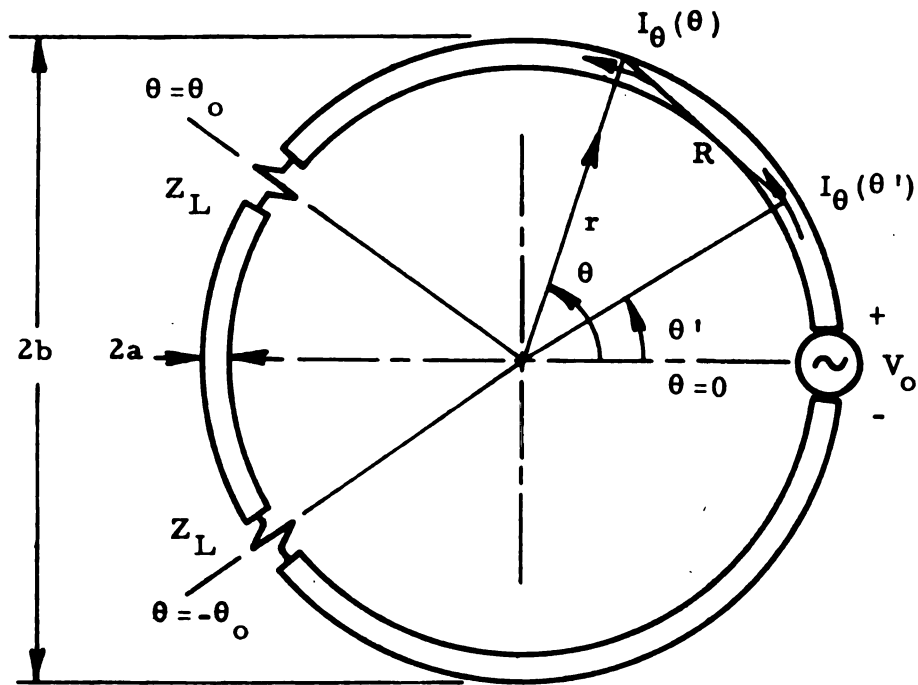


Figure 7.1. Geometry of the Doubly Impedance Loaded Loop Antenna.

7.2. Dimensions of Interest for a One-Dimensional Theory

It is assumed that the circular loop antenna consists of a very thin cylinder, whose radius is much smaller than the loop diameter and at the same time is a small fraction of the wavelength. Under these circumstances, it may be assumed that a one-dimensional distribution of current is excited on the thin loop by its source at $\theta = 0$. That is, the current is taken to have only a θ -component $I_\theta(\theta)$ which flows parallel to the cylinder axis at each point along the circumference of the loop. The dimensional restrictions which validate this one-dimensional theory are thus

$$\begin{aligned} a &<< b \\ \beta_o a &<< 1 \end{aligned} \tag{7.1}$$

where $\beta_o = 2\pi/\lambda_o$ is the free space wave number corresponding to the free space wavelength λ_o .

Conditions (7.1) are also sufficient to validate the usual approximation technique utilized in the study of thin-wire antennas. With this technique, the vector potential at the antenna surface is calculated as a contour integral over the total antenna current, which is assumed to be confined to flow along the axis of the thin wire. In reality, the current flows throughout the cross section of the wire, and is actually most concentrated at its surface due to the skin effect phenomenon. The vector potential at the antenna surface should in general, therefore, be calculated as a volume integral over the current density on the thin wire. It has been indicated by Hallen,¹ however, that when conditions (7.1) are satisfied the error introduced

by the above mentioned approximation is negligible. This approximation facilitates the solution for the distribution of current on the thin wire loop antenna, which would otherwise be very much more difficult.

7.3. A Rigorous Fourier Series Solution for the Distribution of Current on a Doubly Loaded Loop; Its Failure to Yield the Parameters of an Optimum Loading

The boundary condition on the electric field at the surface of the loop is given by

$$(\hat{n} \times \vec{E}) = 0 \quad (7.2)$$

where \hat{n} is a unit outward normal vector at a point on the surface and \vec{E} the electric field at the same point. This condition requires that the tangential component of electric field be continuous across the surface of the cylinder forming the circular loop. Since conditions (7.1) are assumed to be satisfied, the distribution of loop current may be taken to be one-dimensional, i. e., to have only a θ -component $I_\theta(\theta)$. Under these circumstances, the electric field at the loop surface will have only a θ -component and an r -component. The tangential component of electric field at the surface of the loop is therefore $E_\theta(\theta)$, and condition (7.2) becomes

$$E_\theta^a(\theta) = E_\theta^i(\theta) \quad (7.3)$$

where $E_\theta^a(\theta)$ is the field just within the loop surface and $E_\theta^i(\theta)$ is that just outside its surface.

Since the cylinder comprising the loop is taken to be perfectly conducting, then the applied field $E_\theta^a(\theta)$ may be non-vanishing only in the gaps at $\theta = 0, \pm\theta_0$. Thus $E_\theta^a(\theta)$ may be expressed as

$$E_{\theta}^a(\theta) = \begin{cases} \frac{Z_L I_{\theta}(\theta_o)}{2b\delta\theta} & \text{for } -\theta_o - \delta\theta < \theta < -\theta_o + \delta\theta \\ -\frac{V_o}{2b\delta\theta} & \text{for } -\delta\theta < \theta < \delta\theta \\ \frac{Z_L I_{\theta}(\theta_o)}{2b\delta\theta} & \text{for } \theta_o - \delta\theta < \theta < \theta_o + \delta\theta \end{cases} \quad (7.4)$$

$$E_{\theta}^a(\theta) = 0 \quad \text{for} \quad \begin{cases} \delta \leq \theta \leq \theta_o - \delta\theta \\ \theta_o + \delta\theta \leq \theta \leq -\theta_o - \delta\theta \\ -\theta_o + \delta\theta \leq \theta \leq -\delta\theta \end{cases} \quad (7.5)$$

where $I_{\theta}(\theta_o)$ is the current flowing at the loading impedances and $2\delta\theta$ tends to zero in accordance with point element assumption. In result (7.4), the symmetry of the distribution of current has been utilized as

$$I_{\theta}(-\theta) = I_{\theta}(\theta) \quad (7.6)$$

The total voltage drop along the circumference of the loop must be given by

$$-\int_{-\pi}^{\pi} E_{\theta}^a(\theta) b d\theta = V_o - 2 Z_L I_{\theta}(\theta_o) \quad (7.7)$$

A result consistent with equations (7.6) and (7.7) is

$$E_{\theta}^a(\theta) = \frac{1}{b} \{ -V_o \delta(\theta) + Z_L I_{\theta}(\theta_o) [\delta(\theta - \theta_o) + \delta(\theta + \theta_o)] \} \quad (7.8)$$

where $\delta(\theta)$ is the Dirac delta function.

The induced electric field $E_{\theta}^i(\theta)$ just outside the surface of the loop, due to the current and charge on the loop, may be calculated from the vector and scalar potentials⁵ (see Appendix A) \vec{A} , ϕ as

$$E_{\theta}^i(\theta) = -(\nabla \phi)_{\theta} - \left(\frac{\partial \vec{A}}{\partial t} \right)_{\theta} \quad (7.9)$$

Since the time variation is assumed to be harmonic of the form $e^{j\omega t}$, it is possible to make the replacement $\frac{\partial}{\partial t} \rightarrow j\omega$, where the potentials and fields are then understood to be complex valued. There is then obtained

$$E_{\theta}^i(\theta) = -(\nabla \phi)_{\theta} - j\omega A_{\theta} \quad (7.10)$$

where A_{θ} and ϕ are the potentials at the surface of the loop.

The vector and scalar potentials at the surface of the loop may be expressed in terms of its distribution of current and charge by the Helmholtz integral (see Figure 7.1) as

$$A_{\theta}(\theta) = \frac{\mu_0}{4\pi} \int_{-\pi}^{\pi} I_{\theta}(\theta') \cos(\theta - \theta') \frac{e^{-j\beta_0 R}}{R} b d\theta' \quad (7.11)$$

$$\phi(\theta) = \frac{1}{4\pi\epsilon_0} \int_{-\pi}^{\pi} q(\theta') \frac{e^{-j\beta_0 R}}{R} b d\theta' \quad (7.12)$$

In these expressions, μ_0 and ϵ_0 are the permeability and permittivity of free space, respectively, $q(\theta)$ is the charge per unit length distribution along the loop, and R is the Euclidean distance between an observation point on the loop surface at θ and a source point on its axis at θ' . The distribution of charge on the loop is related to its current distribution by the equation of continuity as

$$\nabla \cdot \vec{I}(\theta) + j\omega q(\theta) = 0 \quad (7.13)$$

and since the current is one-dimensional this becomes

$$\begin{aligned} q(\theta) &= \left. \frac{j}{\omega} \frac{1}{r} \frac{\partial}{\partial \theta} I_{\theta}(\theta) \right|_{r=b} \\ &= \frac{j}{\omega b} \frac{\partial}{\partial \theta} I_{\theta}(\theta) \end{aligned} \quad (7.14)$$

With this result, the scalar potential may be expressed as

$$\phi(\theta) = \frac{j}{4\pi\epsilon_0\omega} \int_{-\pi}^{\pi} \frac{\partial}{\partial \theta'} I_{\theta}(\theta') \frac{e^{-j\beta_0 R}}{R} d\theta' \quad (7.15)$$

Referring to Figure 7.1, the Euclidean distance R may be calculated from the law of cosines to give

$$\begin{aligned} R &= [b^2 + (b-a)^2 - 2b(b-a) \cos(\theta - \theta')]^{1/2} \\ &= b[4(1-a/b) \sin^2(\frac{\theta - \theta'}{2}) + a^2/b^2]^{1/2} \end{aligned} \quad (7.16)$$

In the thin wire approximation a/b may be dropped, but a^2/b^2 must be retained since $\sin^2(\frac{\theta - \theta'}{2})$ may also be very small. An approximate expression for R which is valid for $a \ll b$ is thus

$$R \doteq b[4 \sin^2(\frac{\theta - \theta'}{2}) + a^2/b^2]^{1/2} \quad (7.17)$$

Equation (7.15) for the scalar potential $\phi(\theta)$ may be integrated by parts to obtain

$$\begin{aligned} \phi(\theta) &= \frac{j}{4\pi\epsilon_0\omega} \left\{ \left[I_{\theta}(\theta') \frac{e^{-j\beta_0 R}}{R} \right]_{\theta'=-\pi}^{\theta'=\pi} \right. \\ &\quad \left. - \int_{-\pi}^{\pi} I_{\theta}(\theta') \frac{\partial}{\partial \theta'} \frac{e^{-j\beta_0 R}}{R} d\theta' \right\} \end{aligned} \quad (7.18)$$

The integrated term vanishes since, by equations (7.5) and (7.16), respectively, it is found that $I_{\theta}(-\pi) = I_{\theta}(\pi)$ and $R(\theta'=\pi) = R(\theta'=-\pi)$.

Further, it is noted from expression (7.17) that

$$\frac{\partial R}{\partial \theta'} = - \frac{\partial R}{\partial \theta}$$

and equation (7.18) therefore becomes

$$\phi(\theta) = \frac{j}{4\pi\epsilon_o\omega} \int_{-\pi}^{\pi} I_{\theta}(\theta') \frac{\partial}{\partial \theta} \frac{e^{-j\beta_o R}}{R} d\theta' \quad (7.19)$$

Relations (7.11) and (7.19) may be substituted into expression (7.10) to obtain the induced electric field just outside the surface of the loop as

$$\begin{aligned} E_{\theta}^i(\theta) = & - \frac{1}{b} \frac{\partial}{\partial \theta} \left[\frac{j}{4\pi\epsilon_o\omega} \int_{-\pi}^{\pi} I_{\theta}(\theta') \frac{\partial}{\partial \theta} \frac{e^{-j\beta_o R}}{R} d\theta' \right] \\ & - \frac{j\omega\mu_o b}{4\pi} \int_{-\pi}^{\pi} I_{\theta}(\theta') \cos(\theta - \theta') \frac{e^{-j\beta_o R}}{R} d\theta' \end{aligned} \quad (7.20)$$

Upon combining terms and rearranging slightly, equation (7.20) may be expressed in the form

$$E_{\theta}^i(\theta) = - \frac{j\zeta_o}{4\pi b} \int_{-\pi}^{\pi} I_{\theta}(\theta') K(\theta, \theta') d\theta' \quad (7.21)$$

In this result, $\zeta_o = \sqrt{\mu_o/\epsilon_o}$ is the intrinsic impedance of free space and the kernel $K(\theta, \theta')$ is defined by

$$K(\theta, \theta') = \left[\beta_o b \cos(\theta - \theta') + \frac{1}{\beta_o b} \frac{\partial^2}{\partial \theta^2} \right] \frac{e^{-j\beta_o R_1}}{R_1} \quad (7.22)$$

where

$$R_1 = \frac{R}{b} = \left[4 \sin^2 \left(\frac{\theta - \theta'}{2} \right) + a^2/b^2 \right]^{1/2} \quad (7.23)$$

If expressions (7.8) and (7.21) for $E_{\theta}^a(\theta)$ and $E_{\theta}^i(\theta)$, respectively, are used in equation (7.3), an integral equation for the distribution of loop current is obtained as

$$\begin{aligned} \frac{j\zeta_o}{4\pi} \int_{-\pi}^{\pi} I_{\theta}(\theta') K(\theta, \theta') d\theta' &= V_o \delta(\theta) \\ &- Z_L I_{\theta}(\theta_o) [\delta(\theta - \theta_o) + \delta(\theta + \theta_o)] \end{aligned} \quad (7.24)$$

The unknown distribution of loop current $I_{\theta}(\theta)$ appears in the integrand on the left side of this integral equation, while its value $I_{\theta}(\theta_o)$ at the location of the loading impedances appears on the right hand side in a term analogous to the excitation function $V_o \delta(\theta)$. This equation is parameterized by the loop dimensions a, b which occur in the kernel $K(\theta, \theta')$ and by the impedance and position Z_L, θ_o of the double loading. In the special case where $Z_L = 0$, result (7.24) reduces to the integral equation obtained by Storer⁹ for the current on a conventional circular loop antenna.

A rigorous Fourier series solution has been obtained by Storer⁹ for the distribution of current on a conventional loop antenna. Integral equation (7.24) for the current distribution on a doubly impedance loaded loop is very similar to the one obtained by Storer for an ordinary loop, the only difference being the additional shifted Dirac delta function terms on its right hand side. It is a consequence of this similarity that Storer's Fourier series technique may be applied, almost without modification, to obtain a rigorous solution to integral equation (7.24). The application of this method to obtain an exact solution for the distribution of loop current will be sketched in the development to follow.

It is noted that $R_1(\theta, \theta') = R_1(\theta - \theta')$ is continuously differentiable and that $R_1(\theta - \theta') > 0$ for $-\pi \leq (\theta - \theta') \leq \pi$. The function

$$f(\theta - \theta') = \frac{e^{-j\beta_o b R_1(\theta - \theta')}}{R_1(\theta - \theta')} \quad (7.25)$$

is therefore bounded and continuous with a continuous first derivative for $-\pi \leq (\theta - \theta') < \pi$, and is periodic with $f(-\pi) = f(\pi)$. This function may thus be expanded in a Fourier series as

$$\frac{e^{-j\beta_o b R_1(\theta - \theta')}}{R_1(\theta - \theta')} = \sum_{n=-\infty}^{\infty} k_n e^{jn(\theta - \theta')} \quad (7.26)$$

which converges uniformly to $f(\theta - \theta')$ on $-\pi \leq (\theta - \theta') \leq \pi$. The Fourier coefficients of this expansion are given by

$$k_n = \frac{1}{2\pi} \int_{-\pi}^{\pi} \frac{e^{-j\beta_o b R_1(\phi)}}{R_1(\phi)} e^{-jn\phi} d\phi \quad (7.27)$$

Expansion (7.26) may be substituted into equation (7.22) to obtain a new expression for the kernel $K(\theta, \theta')$. The Fourier series (7.26) may be differentiated term by term, and $K(\theta, \theta')$ becomes after some straightforward manipulation

$$K(\theta, \theta') = \sum_{n=-\infty}^{\infty} a_n e^{jn(\theta - \theta')} \quad (7.28)$$

where

$$a_n = \beta_o b \left[\frac{k_{n+1} - k_{n-1}}{2} \right] - \frac{n^2 k_n}{\beta_o b} \quad (7.29)$$

Equation (7.28) expresses the Fourier series expansion of $K(\theta - \theta')$ on $-\pi \leq (\theta - \theta') \leq \pi$ with coefficients specified by relation (7.29). The Fourier series of an absolutely integrable function may be integrated term by term, thus substituting expansion (7.28) for $K(\theta, \theta')$ into

the left hand side of integral equation (7.24) and interchanging the order of summation and integration gives

$$\begin{aligned} \frac{j\zeta_o}{4\pi} \sum_{n=-\infty}^{\infty} a_n \int_{-\pi}^{\pi} I_{\theta}(\theta') e^{jn(\theta - \theta')} d\theta' &= \\ &= V_o \delta(\theta) - Z_L I_{\theta}(\theta_o) [\delta(\theta - \theta_o) + \delta(\theta + \theta_o)] \end{aligned} \quad (7.30)$$

Since the loop current is bounded and continuously differentiable (by physical necessity) with $I_{\theta}(-\pi) = I_{\theta}(\pi)$, then it may be expanded in a Fourier series as

$$I_{\theta}(\theta) = \sum_{n=-\infty}^{\infty} I_n e^{jn\theta} \quad (7.31)$$

which converges uniformly to $I_{\theta}(\theta)$ on $-\pi \leq \theta \leq \pi$. If expansion (7.31) is substituted into equation (7.30) and the order of summation and integration interchanged (by the uniform convergence), there is obtained

$$\begin{aligned} \frac{j\zeta_o}{4\pi} \sum_{n=-\infty}^{\infty} a_n \sum_{p=-\infty}^{\infty} I_p \int_{-\pi}^{\pi} e^{jn(\theta - \theta')} e^{jp\theta'} d\theta' &= \\ &= V_o \delta(\theta) - Z_L I_{\theta}(\theta_o) [\delta(\theta - \theta_o) + \delta(\theta + \theta_o)] \end{aligned} \quad (7.32)$$

However, by the orthogonality of the set $\{e^{jn\theta}\}$

$$\int_{-\pi}^{\pi} e^{jn\theta} e^{j(p-n)\theta'} d\theta' = 2\pi e^{jn\theta} \delta_n^p \quad (7.33)$$

where δ_n^p is the Kroneker δ -function, and result (7.32) becomes

$$\frac{j\zeta_o}{2} \sum_{n=-\infty}^{\infty} a_n I_n e^{jn\theta} = V_o \delta(\theta) - Z_L I_{\theta}(\theta_o) [\delta(\theta - \theta_o) + \delta(\theta + \theta_o)] \quad (7.34)$$

If equation (7.34) is first multiplied by $e^{-jm\theta}$ and then integrated with respect to θ on $-\pi \leq \theta \leq \pi$ there is obtained, after interchanging the order of summation and integration on the left hand side

$$\begin{aligned} \frac{j\zeta_o}{2} \sum_{n=-\infty}^{\infty} a_n I_n \int_{-\pi}^{\pi} e^{jn\theta} e^{-jm\theta} d\theta &= \\ &= \int_{-\pi}^{\pi} \{ V_o \delta(\theta) - Z_L I_{\theta}(\theta_o) [\delta(\theta - \theta_o) + \delta(\theta + \theta_o)] \} e^{-jm\theta} d\theta \end{aligned} \quad (7.35)$$

Making use of the orthogonality of the set $\{e^{jn\theta}\}$ and carrying out the straightforward integration on the right of expression (7.35) results in

$$j\zeta_o \pi \sum_{n=-\infty}^{\infty} a_n I_n \delta_n^m = V_o - 2 Z_L I_{\theta}(\theta_o) \cos(m\theta_o) \quad (7.36)$$

From equation (7.36), a relation between the Fourier coefficients I_n and the coefficients a_n is immediately obtained as

$$I_n = \frac{1}{j\pi \zeta_o a_n} [V_o - 2 Z_L I_{\theta}(\theta_o) \cos(n\theta_o)] \quad (7.37)$$

It is a simple matter to complete the solution for the distribution of loop current by writing out the Fourier series for $I_{\theta}(\theta)$, with coefficients given by result (7.37), as

$$I_{\theta}(\theta) = \frac{1}{j\pi \zeta_o} \sum_{n=-\infty}^{\infty} \frac{V_o - 2 Z_L I_{\theta}(\theta_o) \cos(n\theta_o)}{a_n} e^{jn\theta} \quad (7.38)$$

The coefficients a_n are given by equation (7.29), and have been evaluated in detail by Storer.⁹ Expression (7.38) indicates that the distribution of loop current depends upon the impedance and position Z_L and θ_o , respectively, of the double loading as well as upon the

loop dimensions (which are implicit in a_n). In the special case where $Z_L = 0$, this solution becomes identical with the one obtained by Storer.

The constant $I_\theta(\theta_o)$ in solution (7.38) for the distribution of loop current remains as yet undetermined. Since the loop current is continuous, however, the condition

$$I_\theta(\theta = \theta_o) = I_\theta(\theta_o) \quad (7.39)$$

must be satisfied. With this condition, equation (7.38) may be solved for $I_\theta(\theta_o)$ in terms of the loop dimensions and the impedance and position of the loading as

$$I_\theta(\theta_o) = \frac{V_o}{j\pi\zeta_o} \left[1 + \frac{2Z_L}{j\pi\zeta_o} \sum_{n=-\infty}^{\infty} \frac{e^{jn\theta_o} \cos(n\theta_o)}{a_n} \right]^{-1} \sum_{n=-\infty}^{\infty} \frac{e^{jn\theta_o}}{a_n} \quad (7.40)$$

If $H(Z_L, \theta_o)$ is defined as

$$H(Z_L, \theta_o) = \frac{2Z_L}{j\pi\zeta_o} \left[1 + \frac{2Z_L}{j\pi\zeta_o} \sum_{n=-\infty}^{\infty} \frac{e^{jn\theta_o} \cos(n\theta_o)}{a_n} \right]^{-1} \sum_{n=-\infty}^{\infty} \frac{e^{jn\theta_o}}{a_n} \quad (7.41)$$

then the final solution for the distribution of loop current becomes

$$I_\theta(\theta) = \frac{V_o}{j\pi\zeta_o} \sum_{n=-\infty}^{\infty} \frac{1 - H(Z_L, \theta_o) \cos(n\theta_o)}{a_n} e^{jn\theta} \quad (7.42)$$

It is observed from solution (7.42) that the coefficients of the Fourier series for the distribution of loop current depend in a very complicated way upon the impedance and position of the double loading. Furthermore, it has been indicated by Storer⁹ that this is a slowly

converging Fourier series. The possibility of obtaining an approximate solution by truncating the series and retaining only a few of the leading terms is thus precluded.

Expression (7.42) does, however, represent a formal solution for the distribution of loop current. For a given set of loop dimensions, excitation frequency, and loading parameters, the series could be machine summed using Storer's values for the coefficients a_n . It is evident, however, that there is no way of determining from this solution an explicit expression for the parameters of an optimum loading to yield a traveling wave distribution of loop current. A trial and error process would therefore be required and, since there are two degrees of freedom in choosing a loading for each set of loop dimensions and each excitation frequency, this process would appear to be highly impractical.

The failure of the formal Fourier series solution to provide an explicit expression for the optimum loading impedance severely limits its practical usefulness. A more approximate technique is therefore required to obtain a simple closed form solution for the loop current, from which an expression for the parameters of an optimum loading may be determined. Such an approximate theory is the subject of the following section, where explicit expressions for the impedance and position of an optimum loading are obtained.

7.4. Approximate Distribution of Current on a Doubly Loaded Loop Antenna

In this section, an approximate theory for the distribution of current on a doubly impedance loaded loop antenna is presented. Quite in contrast to the rigorous Fourier series solution obtained in the preceding section, a closed form result is obtained in

terms of simple functions. From this approximate solution, explicit expressions may be obtained for the parameters of an optimum loading to yield a traveling wave distribution of current.

It was found in the preceding section that the electric field at the surface of the loop must satisfy the boundary condition

$$E_{\theta}^a(\theta) = E_{\theta}^i(\theta) \quad (7.3)$$

where $E_{\theta}^a(\theta)$ is the field just within the loop surface and $E_{\theta}^i(\theta)$ is that just outside its surface. An expression for the applied field $E_{\theta}^a(\theta)$ was determined as

$$E_{\theta}^a(\theta) = \frac{1}{b} \{ -V_o \delta(\theta) + Z_L I_{\theta}(\theta_o) [\delta(\theta - \theta_o) + \delta(\theta + \theta_o)] \} \quad (7.8)$$

where $\delta(\theta)$ is the Dirac δ -function. The induced electric field $E_{\theta}^i(\theta)$ at the surface of the antenna, due to the current and charge on the loop, was written as

$$E_{\theta}^i(\theta) = -(\nabla \phi)_{\theta} - j\omega A_{\theta} \quad (7.10)$$

where $A_{\theta}(\theta)$ and $\phi(\theta)$ are the time harmonic vector and scalar potentials, respectively, at the antenna surface.

The vector and scalar potentials at the surface of the loop may be expressed in terms of its distributions of current and charge by the Helmholtz integrals⁵ (see Appendix A) as

$$A_{\theta}(\theta) = \frac{\mu_o}{4\pi} \int_{-\pi}^{\pi} I_{\theta}(\theta') \cos(\theta - \theta') K(\theta, \theta') b d\theta' \quad (7.43)$$

$$\phi(\theta) = \frac{1}{4\pi\epsilon_o} \int_{-\pi}^{\pi} q(\theta') K(\theta, \theta') b d\theta' \quad (7.44)$$

where $K(\theta, \theta')$ is the Green's function

$$K(\theta, \theta') = \frac{e^{-j\beta_0 R(\theta, \theta')}}{R(\theta, \theta')} \quad (7.45)$$

In the above expressions, $I_\theta(\theta)$ is the distribution of total loop current, $q(\theta)$ is its charge per unit length distribution, and $R(\theta, \theta')$ is the Euclidean distance between a source element on the axis of the loop at θ' and an observation point on its surface at θ . An approximate expression for $R(\theta, \theta')$ was developed in the preceding section as

$$R(\theta, \theta') = b \left[4 \sin^2 \left(\frac{\theta - \theta'}{2} \right) + a^2/b^2 \right]^{1/2} \quad (7.17)$$

which is valid in the thin-wire approximation where $a \ll b$.

The peaking property of the kernel $K(\theta, \theta')$ is exploited to formulate an approximate theory for the impedance loaded loop antenna. Since $(a/b)^2 \ll 1$ by the thin-wire assumption, then $K(\theta, \theta')$ has a very sharp peak at $\theta' = \theta$ when considered as a function of θ' on $-\pi \leq \theta' \leq \pi$. The contribution to the vector and scalar potentials $A_\theta(\theta)$ and $\phi(\theta)$, respectively, at each point on $-\pi \leq \theta \leq \pi$, as calculated from equations (7.43) and (7.44), is therefore due primarily to source elements in a small neighborhood about the point $\theta' = \theta$. Because the source distributions are continuous, then the current and charge $I_\theta(\theta')$ and $q(\theta')$, respectively, for $\theta' = \theta$ make the major contributions to the vector and scalar potentials at a point θ on the loop surface. It is therefore expected from this argument that the ratios $A_\theta(\theta)/I_\theta(\theta)$ and $\phi(\theta)/q(\theta)$ should be essentially constant at each point along the loop circumference, or for $-\pi \leq \theta \leq \pi$.

A pair of essentially constant dimensionless quantities are defined by

$$\Psi_i(\theta) = \frac{4\pi}{\mu_o} \frac{A_\theta(\theta)}{I_\theta(\theta)} \quad -\pi \leq \theta \leq \pi \quad (7.46)$$

$$\Psi_q(\theta) = 4\pi\epsilon_o \frac{\phi(\theta)}{q(\theta)} \quad -\pi \leq \theta \leq \pi \quad (7.47)$$

and are designated as the "current expansion parameter" and "charge expansion parameter," respectively. In accordance with the foregoing argument, the functions $\Psi_i(\theta)$ and $\Psi_q(\theta)$ should be essentially independent of θ , and be determined primarily by the loop dimensions. Furthermore, these functions will not depend strongly upon the source distributions $I_\theta(\theta)$ and $q(\theta)$. It is therefore asserted that $\Psi_i(\theta) = \Psi_i$ and $\Psi_q(\theta) = \Psi_q$ are indeed constants depending only upon the loop dimensions. The validity of this assumption will be discussed more fully in section 8.5 of the next chapter.

According to the approximations described in the last paragraph, the vector and scalar potentials at the loop surface are related to the corresponding current and charge distributions as

$$A_\theta(\theta) = \frac{\mu_o \Psi_i}{4\pi} I_\theta(\theta) \quad (7.48)$$

$$\phi(\theta) = \frac{\Psi_q}{4\pi\epsilon_o} q(\theta) \quad (7.49)$$

The distribution of charge is, however, not independent, but related to the current distribution through the equation of continuity as

$$\begin{aligned}
 q(\theta) &= \frac{j}{\omega} \nabla \cdot \vec{I} \Big|_{r=b} \\
 &= \frac{j}{\omega b} \frac{\partial}{\partial \theta} I_{\theta}(\theta)
 \end{aligned} \tag{7.50}$$

With this last result, expression (7.49) becomes

$$\phi(\theta) = \frac{j\Psi_q}{4\pi\epsilon_o\omega b} \frac{\partial}{\partial \theta} I_{\theta}(\theta) \tag{7.51}$$

From equation (7.10), the induced electric field $E_{\theta}^i(\theta)$ at the surface $r = b$ of the loop may be expressed as

$$\begin{aligned}
 E_{\theta}^i(\theta) &= -(\nabla \phi)_{\theta} - j\omega A_{\theta} \\
 &= -\frac{1}{b} \frac{\partial \phi}{\partial \theta} - j\omega A_{\theta}
 \end{aligned} \tag{7.52}$$

If expressions (7.48) and (7.51) are used for $A_{\theta}(\theta)$ and $\phi(\theta)$, respectively, result (7.52) becomes

$$E_{\theta}^i(\theta) = \frac{-j\Psi_q}{4\pi\epsilon_o\omega b^2} \left[\frac{\partial^2}{\partial \theta^2} + \beta_o^2 b^2 \frac{\Psi_i}{\Psi_q} \right] I_{\theta}(\theta) \tag{7.53}$$

where the definition $\beta_o^2 = \omega^2 \mu_o \epsilon_o$ has been used. A complex wave number β is defined as

$$\beta = \beta_o \sqrt{\frac{\Psi_i}{\Psi_q}} \tag{7.54}$$

in terms of which equation (7.53) may be expressed as

$$E_{\theta}^i(\theta) = \frac{-j\Psi_q}{4\pi\epsilon_o\omega b^2} \left[\frac{\partial^2}{\partial \theta^2} + \beta^2 b^2 \right] I_{\theta}(\theta) \tag{7.55}$$

If results (7.8) and (7.55) are substituted into equation (7.3), in order to satisfy the boundary condition on the electric field at the surface of the loop, a second order inhomogeneous differential equation for the distribution of loop current on $-\pi \leq \theta \leq \pi$ is obtained as

$$\left[\frac{\partial^2}{\partial \theta^2} + \beta^2 b^2 \right] I_\theta(\theta) = \frac{j4\pi b \beta^2}{\omega \mu_o \Psi_i} \{ -V_o \delta(\theta) + Z_L I_\theta(\theta) [\delta(\theta - \theta_o) + \delta(\theta + \theta_o)] \} \quad (7.56)$$

A complementary solution to this equation is well known to be

$$I_\theta^c(\theta) = c_1 e^{j\beta b \theta} + c_2 e^{-j\beta b \theta} \quad -\pi \leq \theta \leq \pi \quad (7.57)$$

where c_1 and c_2 are arbitrary complex constants. The particular solution is determined as

$$I_\theta^p(\theta) = \frac{2\pi V_o}{\zeta_o \Psi} e^{-j\beta b |\theta|} - \frac{2\pi}{\zeta_o \Psi} Z_L I_\theta(\theta_o) [e^{-j\beta b |\theta - \theta_o|} + e^{-j\beta b |\theta + \theta_o|}] \quad -\pi \leq \theta \leq \pi \quad (7.58)$$

which is readily verified by direct substitution into differential equation (7.56). In this last result, $\zeta_o = \sqrt{\mu_o / \epsilon_o}$ is the intrinsic impedance of free space, and the "expansion parameter" Ψ has been defined as

$$\Psi = \sqrt{\Psi_i \Psi_q} \quad (7.59)$$

The complete solution for the distribution of loop current is obtained by superposition of results (7.57) and (7.58) as

$$\begin{aligned}
I_{\theta}(\theta) = & c_1 e^{j\beta b\theta} + c_2 e^{-j\beta b\theta} + \frac{2\pi V_o}{\zeta_o \Psi} e^{-j\beta b|\theta|} \\
& - \frac{2\pi}{\zeta_o \Psi} Z_L I_{\theta}(\theta_o) [e^{-j\beta b|\theta-\theta_o|} + e^{-j\beta b|\theta+\theta_o|}] \\
& -\pi \leq \theta \leq \pi
\end{aligned}
\tag{7.60}$$

It should be noted that a solution in terms of complex exponentials has been obtained since a traveling wave distribution of current having such a functional dependence is to be sought eventually.

Solution (7.60) contains the three as yet undetermined constants c_1 , c_2 , and $I_{\theta}(\theta_o)$. There are three physical boundary conditions which facilitate the evaluation of these constants. Due to the symmetry of the loop, its distribution of current must be symmetric and its charge distribution antisymmetric about the point of excitation at $\theta = 0$. These conditions may be expressed mathematically as

$$I_{\theta}(-\theta) = I_{\theta}(\theta) \tag{7.61}$$

$$q(-\theta) = -q(\theta) \tag{7.62}$$

Since the distribution of charge must be continuous at $\theta = \pi$, then condition (7.62) may be satisfied at that point only if $q(\pi) = 0$. However, $q(\theta)$ is related to $I_{\theta}(\theta)$ through the equation of continuity as

$$q(\theta) = \frac{j}{\omega b} \frac{\partial}{\partial \theta} I_{\theta}(\theta) \tag{7.50}$$

The condition $q(\pi) = 0$ thus implies that

$$\left. \frac{\partial}{\partial \theta} I_{\theta}(\theta) \right|_{\theta=\pi} = 0 \tag{7.63}$$

A third condition is obtained from the continuity of the distribution of current at $\theta = \theta_o$ as

$$I_{\theta}(\theta = \theta_o) = I_{\theta}(\theta_o) \quad (7.64)$$

Solution (7.60) is consequently subject to the set of three boundary conditions

$$\begin{aligned} I_{\theta}(-\theta) &= I_{\theta}(\theta) \\ \left. \frac{\partial}{\partial \theta} I_{\theta}(\theta) \right|_{\theta = \pi} &= 0 \\ I_{\theta}(\theta = \theta_o) &= I_{\theta}(\theta_o) \end{aligned} \quad (7.65)$$

The first of conditions (7.65) may be satisfied by the distribution of loop current (7.60) only if $c_2 = c_1$, which yields the simplified result

$$\begin{aligned} I_{\theta}(\theta) &= c_1 e^{j\beta b \theta} + c_1 e^{-j\beta b \theta} + \frac{2\pi V_o}{\zeta_o \Psi} e^{-j\beta b |\theta|} \\ &\quad - \frac{2\pi}{\zeta_o \Psi} Z_L I_{\theta}(\theta_o) [e^{-j\beta b |\theta - \theta_o|} + e^{-j\beta b |\theta + \theta_o|}] \\ &\quad - \pi \leq \theta \leq \pi \end{aligned} \quad (7.66)$$

A straightforward but tedious application of the last two of boundary conditions (7.65) to result (7.66) yields finally the approximate distribution of current on the loop as

$$\begin{aligned} I_{\theta}(\theta) &= \frac{V_o \pi}{\zeta_o \Psi} \left[\frac{P_1}{P_2} e^{j\beta b \theta} + \frac{P_1}{P_2} e^{-j\beta b \theta} + 2 e^{-j\beta b |\theta|} \right. \\ &\quad - \frac{Z_L}{30T} \left(\frac{P_1}{P_2} \cos \beta b \theta_o + e^{-j\beta b \theta_o} \right) \left(e^{-j\beta b |\theta - \theta_o|} \right. \\ &\quad \left. \left. + e^{-j\beta b |\theta + \theta_o|} \right) \right] \quad - \pi \leq \theta \leq \pi \end{aligned} \quad (7.67)$$

In this result, the factors T , P_1 , and P_2 are constants depending upon the excitation frequency, the loop dimensions, and the impedance and position of the double loading as

$$T = \Psi + \frac{Z_L}{60} (1 + e^{-j2\beta b\theta_o}) \quad (7.68)$$

$$P_1 = 1 - \frac{Z_L}{30T} e^{-j\beta b\theta_o} \cos \beta b\theta_o \quad (7.69)$$

$$P_2 = j e^{j\beta b\pi} \sin \beta b\pi + \frac{Z_L}{30T} \cos^2 \beta b\theta_o \quad (7.70)$$

An approximate expression for the distribution of current on the doubly loaded loop antenna has been obtained in equation (7.67). This distribution completely characterizes the loop antenna, and is given in terms of its dimensions, the excitation frequency, the impedance and position of the double loading, and the as yet undetermined expansion parameter. The optimum loading to yield a traveling wave distribution of current on the loop will be obtained from this result in the next chapter. This traveling wave current distribution will then be used to calculate the value of the expansion parameter Ψ .

The similarity between the distribution of current (7.67) on an impedance loaded loop antenna and the expression (2.28) for that on a doubly loaded linear antenna is quite apparent. If the constants β_o , D_1 , and D_2 in the result for the linear antenna are replaced by βb , P_1 , and P_2 , the corresponding expression for the loop antenna is obtained. In the case of a loop antenna, however, β is a complex number, and the expression for P_2 is quite different from its counterpart D_2 . The functional dependence of the current upon position along the antenna is otherwise identical in either case.

7.5. Input Impedance of a Doubly Loaded Loop Antenna

The input impedance to the loop antenna is defined by

$$Z_{in} = \frac{V_o}{I_o(\theta=0)} \quad (7.71)$$

This impedance is readily evaluated by using result (7.67) for the approximate distribution of current on the doubly loaded loop, and is found to be

$$Z_{in} = 60 \Psi \left[1 + \frac{P_1}{P_2} - \frac{Z_L}{30T} e^{-j\beta b \theta_o} \left(\frac{P_1}{P_2} \cos \beta b \theta_o + e^{-j\beta b \theta_o} \right) \right]^{-1} \quad (7.72)$$

An approximate relation for the input impedance of a doubly impedance loaded loop antenna is thus obtained in terms of its dimensions, the frequency of excitation, and the impedance and position of the loading. Again the similarity between this result and the corresponding expression (2.33) for a linear antenna is immediately apparent.

CHAPTER 8

OPTIMUM LOADING FOR A TRAVELING WAVE DISTRIBUTION OF LOOP CURRENT

8.1. Physical Interpretation of the Distribution of Current on a Doubly Loaded Loop Antenna

An approximate expression for the distribution of current on a doubly impedance loaded loop antenna has been developed as equation (7.67). This solution is valid on $-\pi \leq \theta \leq \pi$, but since $I_\theta(-\theta) = I_\theta(\theta)$ it is sufficient to consider only the current on $0 \leq \theta \leq \pi$. If attention is restricted to the regions $0 \leq \theta \leq \theta_o$ and $\theta_o \leq \theta \leq \pi$, then the various terms in expression (7.67) may be combined to yield a pair of results which are more physically meaningful.

The distribution of loop current on $0 \leq \theta \leq \theta_o$ is obtained from the general result (7.67) as

$$I_\theta(\theta) = \frac{V_o \pi}{\zeta_o \Psi} \left\{ \left[2 + \frac{P_1}{P_2} - \frac{Z_L}{30T} e^{-j\beta b \theta_o} \left(\frac{P_1}{P_2} \cos \beta b \theta_o + e^{-j\beta b \theta_o} \right) \right] e^{-j\beta b \theta} + \left[\frac{P_1}{P_2} - \frac{Z_L}{30T} e^{-j\beta b \theta_o} \left(\frac{P_1}{P_2} \cos \beta b \theta_o + e^{-j\beta b \theta_o} \right) \right] e^{j\beta b \theta} \right\} \quad (8.1)$$

while that on $\theta_o \leq \theta \leq \pi$ becomes

$$I_\theta(\theta) = \frac{V_o \pi}{\zeta_o \Psi} \left\{ \left[2 + \frac{P_1}{P_2} - \frac{Z_L}{15T} \cos \beta b \theta_o \left(\frac{P_1}{P_2} \cos \beta b \theta_o + e^{-j\beta b \theta_o} \right) \right] e^{-j\beta b \theta} + \left[\frac{P_1}{P_2} \right] e^{j\beta b \theta} \right\} \quad (8.2)$$

A physical interpretation of the current distribution is readily obtained from expressions (8.1) and (8.2).

It is noted from equation (8.1) that the total loop current on $0 \leq \theta \leq \theta_0$ may be considered as a superposition of a pair of outward and inward traveling current waves. The first term in this expression represents an outward traveling wave of current which is excited by the source at $\theta = 0$. At $\theta = \theta_0$ this current wave is partially reflected and partially transmitted. The second term of equation (8.1) represents an inward traveling wave of current which results from the reflection of the outward traveling wave by the impedance discontinuity at $\theta = \theta_0$.

Similarly, equation (8.2) indicates that the distribution of loop current on $\theta_0 \leq \theta \leq \pi$ is composed of a pair of oppositely directed traveling current waves. The first term of this expression represents an outward traveling wave of current which is excited by the potential difference at $\theta = \theta_0$. The second term of equation (8.2) represents the inward traveling wave of current which results from the reflection by Z_L at $\theta = -\theta_0$.

It is indicated by the above results therefore, that in general both outward and inward traveling waves of current are supported on each of the two antenna regions $0 \leq \theta \leq \theta_0$ and $\theta_0 \leq \theta \leq \pi$. The superposition of these oppositely directed traveling waves results in a standing wave distribution of current along either region. Thus in the usual case a standing wave of current is supported along the entire circumference of the loop.

8.2. Optimum loading Impedance for a Traveling Wave Distribution of Loop Current

It was indicated in the preceding section that the doubly loaded loop generally supports a standing wave distribution of current over

its entire circumference. The possibility that this distribution might be modified, through the selection of an optimum impedance loading, to yield a purely outward traveling wave of current over most of the loop is now to be investigated.

It is evident physically that no choice of the loading will give a purely outward traveling current wave on $\theta_o \leq \theta \leq \pi$, since the current should be maximum at $\theta = \pi$ subject to the boundary condition at that point. However, it is reasonable to suspect that if the loading is properly chosen the inward traveling wave on $0 \leq \theta \leq \theta_o$ might be eliminated, leaving only the desired outward traveling wave of current over that region. Since this inward traveling wave is actually reflected from the impedance discontinuity at $\theta = \theta_o$, it is expected that such an optimum loading should exist.

The optimum loading impedance to yield a purely outward traveling wave of loop current on $0 \leq \theta \leq \theta_o$ may be obtained from expression (8.1). This condition evidently requires that the inward traveling current wave on that region should vanish. Realization of this condition is accomplished by equating the coefficient of the second term in equation (8.1), which represents the amplitude of the inward traveling wave, to zero as

$$\frac{P_1}{P_2} - \frac{Z_L}{30T} e^{-j\beta b\theta_o} \left(\frac{P_1}{P_2} \cos \beta b\theta_o + e^{-j\beta b\theta_o} \right) = 0 \quad (8.3)$$

Using the defining relations (7.68), (7.69), and (7.70) for T , P_1 , and P_2 , respectively, this equation may be solved for the optimum loading impedance, designated as $[Z_L]_o$, to yield

$$[Z_L]_o = 30\Psi \frac{e^{j\beta b\theta_o}}{\cos \beta b\theta_o + je^{j\beta b(\pi - \theta_o)} \sin \beta b\pi} \quad (8.4)$$

After some lengthy but straightforward manipulation, result (8.4) may be put into the simpler form

$$[Z_L]_o = 30\Psi[1 - j \tan \beta b(\pi - \theta_o)] \quad (8.5)$$

When the loading impedance is given by this relation, the loop current on $0 \leq \theta \leq \theta_o$ becomes the desired purely outward traveling wave, while that on $\theta_o \leq \theta \leq \pi$ remains the usual standing wave

Expression (8.5) gives the optimum loading impedance in terms of the excitation frequency, the loop dimensions, and the position of the loading. For a given set of antenna dimensions a and b , this optimum impedance is a function only of the frequency ω and its position θ_o . At this point the loading location is completely arbitrary, and may be freely specified in order that the corresponding impedance may satisfy certain prescribed conditions.

8.3. Purely Reactive Optimum Loading

A purely non-dissipative optimum loading is of particular interest, since such a loading would permit the realization of a high efficiency traveling wave loop antenna. It has been indicated that the optimum loading impedance $[Z_L]_o$ depends only upon its position θ_o and the excitation frequency ω once the loop dimensions a and b have been specified. This leads one to suspect that, at least at a single frequency, it should be possible to choose an optimum position for the loading such that $[Z_L]_o$ will become purely reactive.

Since Ψ and β are in general complex numbers, then the

following designations will be established

$$\Psi = M + jN \quad (8.6)$$

$$\beta b(\pi - \theta_o) = x + jy \quad (8.7)$$

$$\tan \beta b(\pi - \theta_o) = u + jv \quad (8.8)$$

With these definitions, expression (8.5) for the optimum loading impedance becomes

$$\begin{aligned} [Z_L]_o &= 30 (M + jN) [1 - j(u + jv)] \\ &= 30 \{ [M(1+v) + Nu] + j[N(1+v) - Mu] \} \end{aligned} \quad (8.9)$$

The condition for a non-dissipative loading is obtained by equating the real part of equation (8.9) to zero, which gives

$$\frac{u}{1+v} = -\frac{M}{N} \quad (8.10)$$

With this result, the corresponding optimum loading reactance becomes

$$[X_L]_o = 30(1+v) \left(N + \frac{M^2}{N} \right) \quad (8.11)$$

It is indicated therefore that a loop antenna which is doubly loaded with an optimum non-dissipative impedance, whose reactance $[X_L]_o$ is given by expression (8.11) and whose position θ_o is so selected that equation (8.10) is satisfied, will support an outward traveling wave of current on $0 \leq \theta \leq \theta_o$.

The necessary position of an optimum non-dissipative loading may be obtained from relation (8.10). It is first necessary to express u, v in equation (8.8) in terms of x, y from definitions (8.7) as

$$\begin{aligned} u &= \frac{\sin(2x)}{\cos(2x) + \cosh(2y)} \\ v &= \frac{\sinh(2y)}{\cos(2x) + \cosh(2y)} \end{aligned} \quad (8.12)$$

In terms of these results, condition (8.10) for a purely reactive optimum loading becomes

$$\frac{\sin(2x)}{\cos(2x) + \cosh(2y) + \sinh(2y)} = -\frac{M}{N} \quad (8.13)$$

From this expression, it is desired to determine $(\pi - \theta_o)$ where by definition $\beta b(\pi - \theta_o) = x + jy$, and M/N and βb are known quantities. Evidently some approximations are in order to facilitate the solution of this transcendental equation.

According to definition (7.54) for β , it is possible to express β/β_o as

$$\frac{\beta}{\beta_o} = \sqrt{\frac{\Psi_i}{\Psi_q}} \quad (8.14)$$

The current and charge expansion parameters Ψ_i and Ψ_q , respectively, corresponding to a traveling wave distribution of current, will be evaluated in section 8.5. These results may be utilized to calculate the ratio β/β_o , as expressed by equation (8.14). Figure 8.1 indicates a plot of β/β_o as a function of the electrical loop circumference $\beta_o b$ for a loop having dimensions specified by $a/b = 0.0423$ or $\alpha = 2 \ln(2\pi b/a) = 10$. It is noted that the real part of β/β_o is always of the order of unity, while its imaginary part is always less than approximately 0.05 in absolute value.

In accordance with the remarks of the last paragraph, it would appear that for a zeroth-order approximation the imaginary part of β may be dropped entirely and the value of β taken as $\beta = \beta_o$. Under these circumstances, the position of an optimum pure reactive loading is determined immediately by equating the real part of equation (8.5)

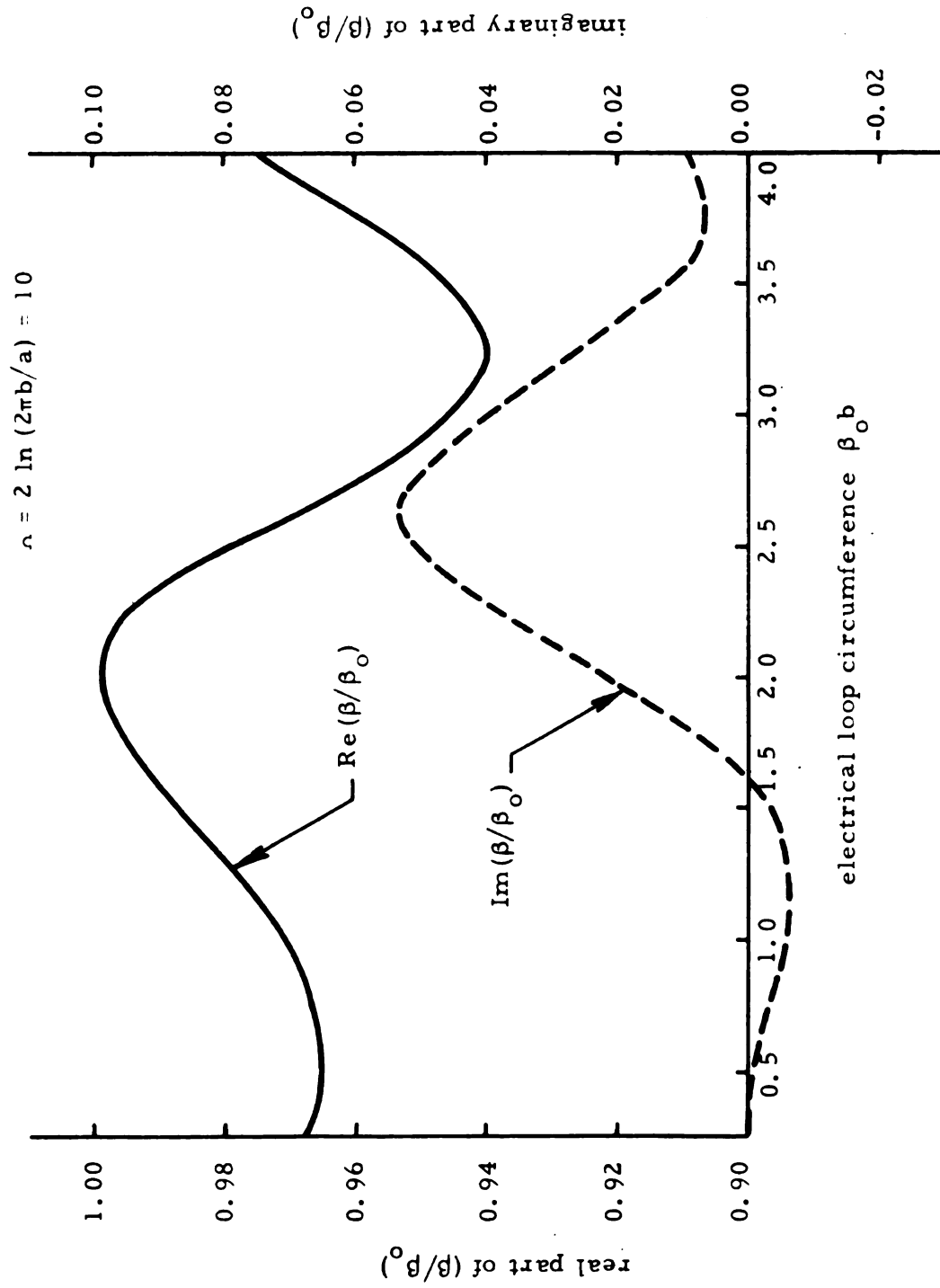


Figure 8.1. Real and Imaginary Parts of the Normalized Complex Wave Number as a Function of the Electrical Loop Circumference.

to zero as

$$\beta_o b(\pi - \theta_o) = \tan^{-1} \left(-\frac{M}{N} \right) \quad (8.15)$$

The ratio M/N is always negative and greater than 3.0 in absolute value for a loop with $\Lambda = 10$ and for $0.25 \leq \beta_o b \leq 4.0$. Thus $\beta_o b(\pi - \theta_o)$ is always of the order of $\pi/2$ for a loop of such dimensions.

Using the result $\beta_o b(\pi - \theta_o) \doteq \pi/2$ of the zeroth-order approximate solution, a more accurate formulation may be obtained from equation (8.13). Since the maximum value of $\text{Im}(\beta/\beta_o)$ is of the order of 0.05, then

$$[y]_{\max} = [\text{Im } \beta b(\pi - \theta_o)]_{\max} \doteq (0.05) \frac{\pi}{2} = 0.08$$

and the maximum value of $2y$ is of the order of 0.16. The hyperbolic functions in expression (8.13) have the power series expansions

$$\cosh(2y) = 1 + \frac{(2y)^2}{2!} + \dots$$

$$\sinh(2y) = (2y) + \frac{(2y)^3}{3!} + \dots$$

and since it has been found that $2y < 0.16$, then a very good approximation is obtained by retaining only the leading term in each expansion. With this approximation, condition (8.13) becomes

$$\frac{\sin(2x)}{1 + \cos(2x) + 2y} = -\frac{M}{N}$$

which may be written in the form

$$\frac{\sin x \cos x}{\cos^2 x + y} = -\frac{M}{N} \quad (8.16)$$

Result (8.16) may be further approximated by noting that

$$x = \operatorname{Re}[\beta b(\pi - \theta_o)] \doteq \beta_o b(\pi - \theta_o) \doteq \pi/2$$

Power series expansions of $\sin x$ and $\cos x$ are then made as

$$\sin x = \cos(\pi/2 - x) = 1 - \frac{1}{2}(\pi/2 - x)^2 + \dots \quad (8.17)$$

$$\cos x = \sin(\pi/2 - x) = (\pi/2 - x) - \frac{1}{6}(\pi/2 - x)^3 + \dots \quad (8.18)$$

and since $x \doteq \pi/2$ only the first few terms of each expansion need be retained. Substituting expansions (8.17) and (8.18) into equation (8.16), and dropping all terms in $(\pi/2 - x)^3$ and higher powers gives

$$\frac{(\pi/2 - x)}{(\pi/2 - x)^2 + y} = -\frac{M}{N} \quad (8.19)$$

If the constants β_1 , β_2 , ϕ , and Q are defined as

$$\begin{aligned} \beta_1 &= \operatorname{Re}(\beta b) \\ \beta_2 &= \operatorname{Im}(\beta b) \\ \phi &= (\pi - \theta_o) \\ Q &= -M/N \end{aligned} \quad (8.20)$$

then

$$\begin{aligned} x &= \operatorname{Re}[\beta b(\pi - \theta_o)] = \beta_1 \phi \\ y &= \operatorname{Im}[\beta b(\pi - \theta_o)] = \beta_2 \phi \end{aligned} \quad (8.21)$$

and condition (8.19) becomes

$$\phi^2 + \left[\frac{\beta_2}{\beta_1^2} + \frac{1}{Q\beta_1} - \frac{\pi}{\beta_1} \right] \phi + \frac{\pi}{2\beta_1^2} \left[\frac{\pi}{2} - \frac{1}{Q} \right] = 0 \quad (8.22)$$

Since β_1 , β_2 , and Q are known constants, then quadratic equation (8.22) may be solved directly for $\phi = (\pi - \theta_0)$ to obtain the necessary position of an optimum non-dissipative loading.

In order to verify the accuracy of result (8.22), it was solved to obtain $\phi = (\pi - \theta_0)$ for several values of the electrical loop circumference $\beta_0 b$. The values of x and y were then calculated according to equations (8.21). These results were then substituted back into equation (8.13), which was found to be satisfied identically. Hence the approximate solution (8.22) was verified to be essentially 100% accurate. It should be noted that only the smaller of the two roots to equation (8.22) was considered, since it is desired to minimize the length of the region $\theta_0 \leq \theta \leq \pi$ on which a standing current wave exists.

To summarize, the position $\phi = (\pi - \theta_0)$ of an optimum purely non-dissipative loading may be calculated from equation (8.22) in terms of the loop dimensions and its frequency of excitation if $\beta_0 b (\pi - \theta_0) \approx \pi/2$. The corresponding optimum reactance of the loading is then given by expression (8.11), which may be written approximately as

$$[X_L]_0 = 30 \left(1 + \frac{y}{\cos^2 x} \right) \left(N + \frac{M^2}{N} \right) \quad (8.23)$$

When a non-dissipative loading having these parameters is utilized, then the corresponding distribution of loop current on $0 \leq \theta \leq \theta_0$ becomes a purely outward traveling wave.

In order to obtain some specific numerical results, a loop antenna specified by the dimensions $a/b = 0.0423$, or $\alpha = 2 \ln(2\pi b/a) = 10$

will be considered. The position $(\pi - \theta_o)$ and reactance $[X_L]_o$ of an optimum non-dissipative loading for such a loop are indicated in Figures 8.2 and 8.3, respectively, as a function of the electrical loop circumference $\beta_o b$, as $\beta_o b$ varies from 0.25 to 4.0. These results were calculated from expressions (8.22) and (8.23) using the relations for Ψ_i , Ψ_q , and Ψ which will be presented in section 8.5. Since $\beta_o = \omega/v_o$ where v_o is the velocity of propagation in free space, then $\beta_o b = \omega b/v_o$ is a linear function of the angular frequency ω of excitation. It is noted from Figure 8.2 that $(\pi - \theta_o)$ is a strong function of frequency, and that in fact $\beta_o b(\pi - \theta_o)$ is essentially frequency independent. Further, the nearly constant value of $\beta_o b(\pi - \theta_o)$ is of the order of $\pi/2$, which justifies the approximations leading to solution (8.22). Figure 8.3 indicates that the optimum loading reactance $[X_L]_o$ is a strong function of frequency for relatively small loops, but settles down to a value of approximately - 500 ohms when $\beta_o b$ is greater than 1.5.

Expressions (8.22) and (8.23) for the position and reactance of an optimum non-dissipative double loading are perhaps the most significant results of the present research. Given the loop dimensions and its excitation frequency, the parameters of an optimum non-dissipative loading are readily calculated from these simple expressions. By utilizing such a loading, a traveling wave antenna may be realized which retains the high efficiency of a conventional loop. Since the theory leading to results (8.22) and (8.23) is very similar to that of the linear antenna of Part I, which was successfully verified

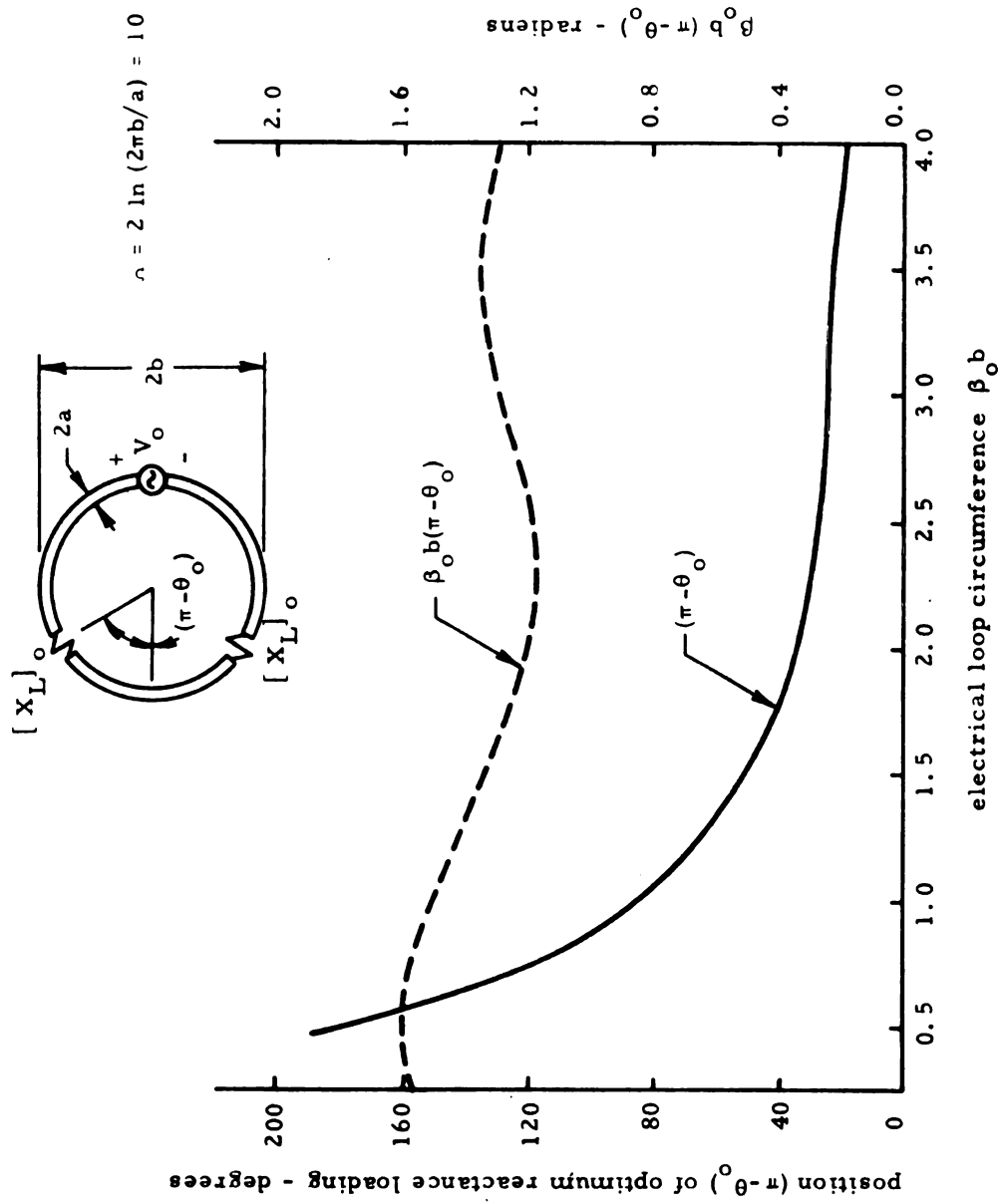


Figure 8.2. Position of Optimum Non-Dissipative Loading as a Function of the Electrical Loop Circumference.

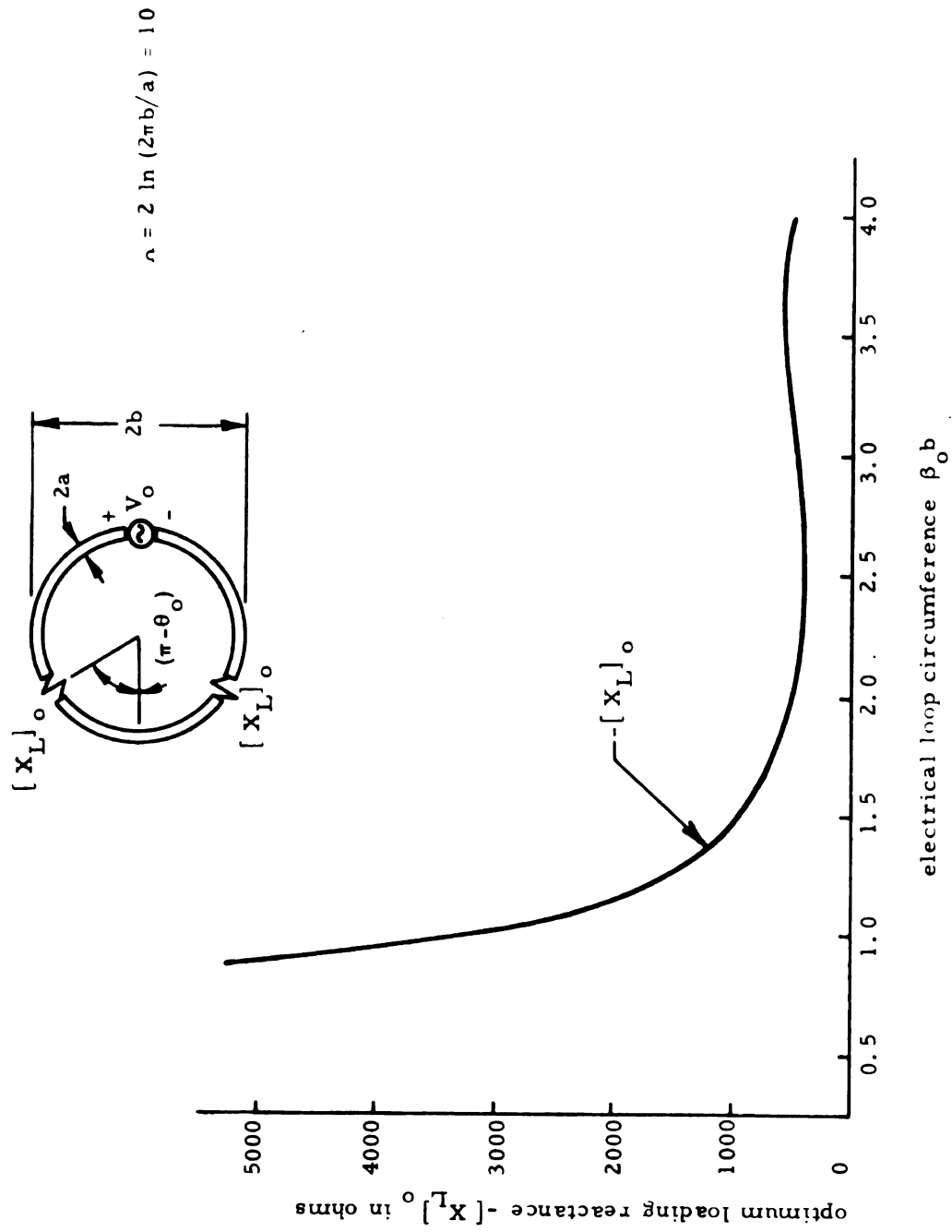


Figure 8.3. Reactance of Optimum Non-Dissipative Loading as a Function of the Electrical Loop Circumference.

experimentally, it was felt that no experimental study of the reactance loaded loop antenna was warranted.

It has been indicated that, for a given set of loop dimensions, the necessary position of an optimum non-dissipative loading is strongly dependent upon the excitation frequency. Physically, however, a practical arrangement of such a doubly loaded loop requires that the position of the loading be fixed at some point along its circumference. With this restriction, an optimum purely reactive loading may therefore be realized only at a single frequency. If the position of such an optimum impedance loading is so chosen that it becomes purely reactive at a given frequency, then at any other frequency it must have both resistive and reactive components.

Since the position of the impedance must be fixed, it is of interest to consider the frequency dependence of an optimum loading whose location is so chosen that its impedance becomes purely reactive at a predetermined frequency. In order to obtain specific numerical results, the loop specified by $\alpha = 10$ will again be considered. A loading position of $(\pi - \theta_o) = 27.1^\circ$ is chosen so that the optimum impedance becomes purely reactive when $\beta_o b = 2.5$ (see Figure 8.2). Figure 8.4 indicates the optimum impedance of such a fixed loading as a function of the antenna's electrical circumference $\beta_o b$. These results were calculated from expression (8.9) for $[Z_L]_o$, with the values of u, v taken from equations (8.12). It is noted from the figure that the resistive component of the optimum impedance vanishes only for $\beta_o b = 2.5$. At any other frequency, an optimum loading must consist of both resistive and reactive components in order

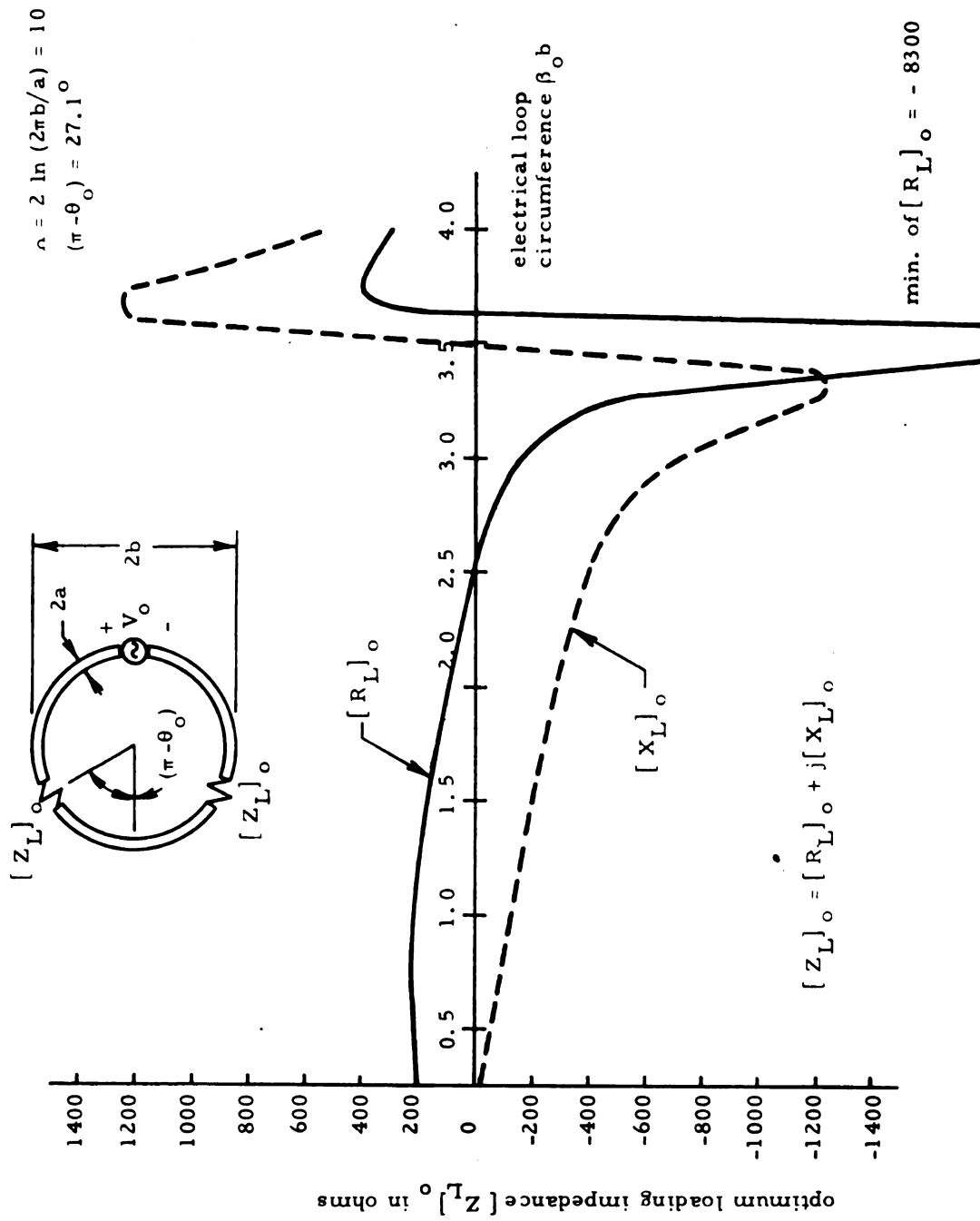


Figure 8.4. Impedance of Optimum Loading (purely reactive for $\beta_o b = 2.5$) with Fixed Position as a Function of Electrical Loop Circumference $\beta_o b$.

to yield a traveling wave distribution of loop current.

From Figure 8.4 the following important characteristics are observed for the case of an optimum impedance loading of fixed position:

- (i) In general an optimum loading impedance requires both resistive and reactive components.
- (ii) Both the resistive and reactive components of the optimum impedance are strong functions of frequency. There is a particular frequency where the resistive component takes on a very large negative value.
- (iii) The sign of both impedance components changes within a relatively narrow frequency range. An optimum impedance thus requires a negative resistance component (active element) at certain frequencies, and its reactive component changes from capacitive to inductive as the frequency is increased.
- (iv) The reactive component of the optimum impedance has a negative slope as a function of frequency.

It is thus evident that synthesis of an exact optimum loading impedance, to yield a purely outward traveling wave distribution of loop current at every frequency, is out of the question. Although an Esaki diode might be utilized to yield a given negative resistance component, there is no practical means of realizing a frequency variable negative resistance characteristic of the type indicated.

Since the high efficiency associated with a non-dissipative loading is of fundamental interest, one is led to consider, when dealing

with a loading of fixed position, one consisting of the reactive component of the optimum impedance. Such a purely non-dissipative loading is optimum only at a given center frequency, and its effectiveness diminishes as the frequency of excitation is varied from this value. That is, the distribution of loop current on $0 \leq \theta \leq \theta_0$ will be an outward traveling wave at an excitation frequency corresponding to the chosen optimum center frequency, but will gradually revert back to an essentially standing wave as the frequency of excitation deviates from this value.

For relatively small excursions about the center frequency, the current distribution corresponding to such a non-dissipative loading will remain an essentially outward traveling wave. Referring back to Figure 8.4, this is evident since for such small frequency variations the resistive component of the optimum impedance is small compared with its reactive component. For large deviations in the frequency of excitation, however, the magnitude of the resistive component becomes comparable with that of the reactive component, and the effectiveness of a purely non-dissipative loading will be necessarily reduced.

An approximately traveling wave distribution of loop current may therefore be maintained over a band of excitation frequencies through the use of a purely reactive loading of fixed position, provided that its reactance is a proper function of frequency. The circuit and radiation characteristics of a loop with such a non-dissipative loading will thus be typical of those of an ideal traveling wave loop over this range of frequencies.

In order to obtain an effective non-dissipative loading therefore, it is necessary that the frequency dependence of its reactance match that of the reactive component of the optimum impedance, as indicated in Figure 8.4. The consideration of this synthesis problem is beyond the scope of the present research.

8.4. The Distribution of Current and Input Impedance Corresponding to an Optimum Loading

A general expression for the optimum loading impedance to yield a traveling wave distribution of loop current on $0 \leq \theta \leq \theta_o$ was determined as expression (8.5). Whenever the impedance is given by this equation, then condition (8.3) holds, i. e.,

$$\frac{P_1}{P_2} - \frac{Z_L}{30T} e^{-j\beta b\theta_o} \left(\frac{P_1}{P_2} \cos \beta b\theta_o + e^{-j\beta b\theta_o} \right) = 0 \quad (8.3)$$

Hence the distribution of current on $0 \leq \theta \leq \theta_o$ becomes from equation (8.1)

$$I_\theta(\theta) = \frac{2 V_o \pi}{\zeta_o \Psi} e^{-j\beta b\theta} \quad (8.24)$$

while by result (8.2) that on $\theta_o \leq \theta \leq \pi$ may be expressed as

$$I_\theta(\theta) = \frac{V_o \pi}{\zeta_o \Psi} \left\{ \left[2 - \frac{Z_L}{30T} e^{j\beta b\theta_o} \left(\frac{P_1}{P_2} \cos \beta b\theta_o + e^{-j\beta b\theta_o} \right) \right] e^{-j\beta b\theta} + \left[\frac{P_1}{P_2} \right] e^{j\beta b\theta} \right\} \quad (8.25)$$

These expressions represent, respectively, the outward traveling wave which has been realized on $0 \leq \theta \leq \theta_o$ and the standing wave which remains on $\theta_o \leq \theta \leq \pi$.

It is desired to simplify result (8.25) in order to indicate more clearly the distribution of loop current on $\theta_o \leq \theta \leq \pi$. This equation may be written in the general form

$$I_{\theta}(\theta) = \frac{2 V_o \pi}{\zeta_o \Psi} [A e^{-j\beta b \theta} + B e^{j\beta b \theta}] \quad (8.26)$$

where A and B are complex constants depending upon the antenna dimensions and the loading parameters. The direct evaluation of A and B is very tedious, so an alternate method will be utilized. Since the loop current is continuous at $\theta = \theta_o$, then the condition

$$I_{\theta}(\theta = \theta_o^-) = I_{\theta}(\theta = \theta_o^+) \quad (8.27)$$

must be satisfied. Further, it was found in the preceding chapter that the antisymmetry of the distribution of charge implies that

$$\left. \frac{\partial}{\partial \theta} I_{\theta}(\theta) \right|_{\theta = \pi} = 0 \quad (8.28)$$

The result of equation (8.24) may be utilized to obtain

$$I_{\theta}(\theta = \theta_o^-) = \frac{2 V_o \pi}{\zeta_o \Psi} e^{-j\beta b \theta} \quad (8.29)$$

Applying the two boundary conditions (8.27) and (8.28) in conjunction with result (8.29) to expression (8.26), the constants A and B are evaluated in a straightforward manner as

$$A = \frac{1}{1 + e^{-j2\beta b(\pi - \theta_o)}} \quad (8.30)$$

$$B = \frac{e^{-j2\beta b\pi}}{1 + e^{-j2\beta b(\pi - \theta_o)}} \quad (8.31)$$

If expression (8.30) and (8.31) for A and B, respectively, are substituted into equation (8.26), the distribution of loop current on $\theta_0 \leq \theta \leq \pi$ is obtained as

$$I_{\theta}(\theta) = \frac{4 V_o \pi}{\zeta_o \Psi} \frac{e^{-j\beta b \pi}}{1 + e^{-j2\beta b(\pi - \theta_0)}} \cos \beta b(\pi - \theta) \quad (8.32)$$

It is observed from result (8.32) that the loop current on $\theta_0 \leq \theta \leq \pi$ has a cosinusoidal distribution. Thus although the optimum impedance loading yields an outward traveling wave of current on $0 \leq \theta \leq \theta_0$, the distribution on $\theta_0 \leq \theta \leq \pi$ remains a pure standing wave. This standing wave distribution is in fact identical with the zeroth-order distribution of current on a conventional loop antenna.

Since the loop current is symmetric about the excitation point, then $I_{\theta}(-\theta) = I_{\theta}(\theta)$. In summary then, the distribution of loop current corresponding to an optimum impedance loading may be expressed on $-\pi \leq \theta \leq \pi$ as

$$I_{\theta}(\theta) = \frac{V_o}{60\Psi} e^{-j\beta b |\theta|} \quad -\theta_0 \leq \theta \leq \theta_0 \quad (8.33)$$

$$I_{\theta}(\theta) = \frac{V_o}{30\Psi} \frac{e^{-j\beta b \pi}}{1 + e^{-j2\beta b(\pi - \theta_0)}} \cos \beta b(\pi - |\theta|) \quad (8.34)$$

$$-\pi \leq \theta \leq -\theta_0, \theta_0 \leq \theta \leq \pi$$

In order to illustrate the distribution of loop current corresponding to an optimum impedance loading, as given by expressions (8.33) and (8.34), the loop having dimensions specified by $\alpha = 10$ will again be considered. If it is taken that $\beta_o b = 2.5$, then the parameters of an

optimum non-dissipative loading are found from Figures 8.2 and 8.3 to be: $(\pi - \theta_o) = 27.1^\circ$, $[X_L]_o = -421$ ohms. Figure 8.5 indicates the amplitude and phase of the distribution of loop current corresponding to such a loading, as a function of the angular position θ along the circumference of the loop. These results were obtained from equations (8.33) and (8.34), where the very small imaginary part of β was neglected. It is noted that the amplitude of the current on $0 \leq \theta \leq \theta_o$ is constant while its phase is linear, corresponding to a traveling wave along that region. On $\theta_o \leq \theta \leq \pi$, however, the current is represented by a sinusoidal standing wave of constant phase.

The input impedance to the traveling wave loop antenna is obtained from equation (8.33) as

$$\begin{aligned} Z_{in} &= \frac{V_o}{I_\theta(\theta=0)} \\ &= 60 \Psi \end{aligned} \quad (8.35)$$

It is to be noted that this expression is valid only when the position and impedance of the double loading are chosen to be optimum, i.e., equation (8.5) is satisfied. Under any other circumstances, when Z_L is not $[Z_L]_o$, the general input impedance expression (7.72) must be utilized as

$$Z_{in} = 60 \Psi \left[1 + \frac{P_1}{P_2} - \frac{Z_L}{30T} e^{-j\beta b \theta_o} \left(\frac{P_1}{P_2} \cos \beta b \theta_o + e^{-j\beta b \theta_o} \right) \right]^{-1} \quad (7.72)$$

This result reduces to equation (8.35) when the loading is optimum.

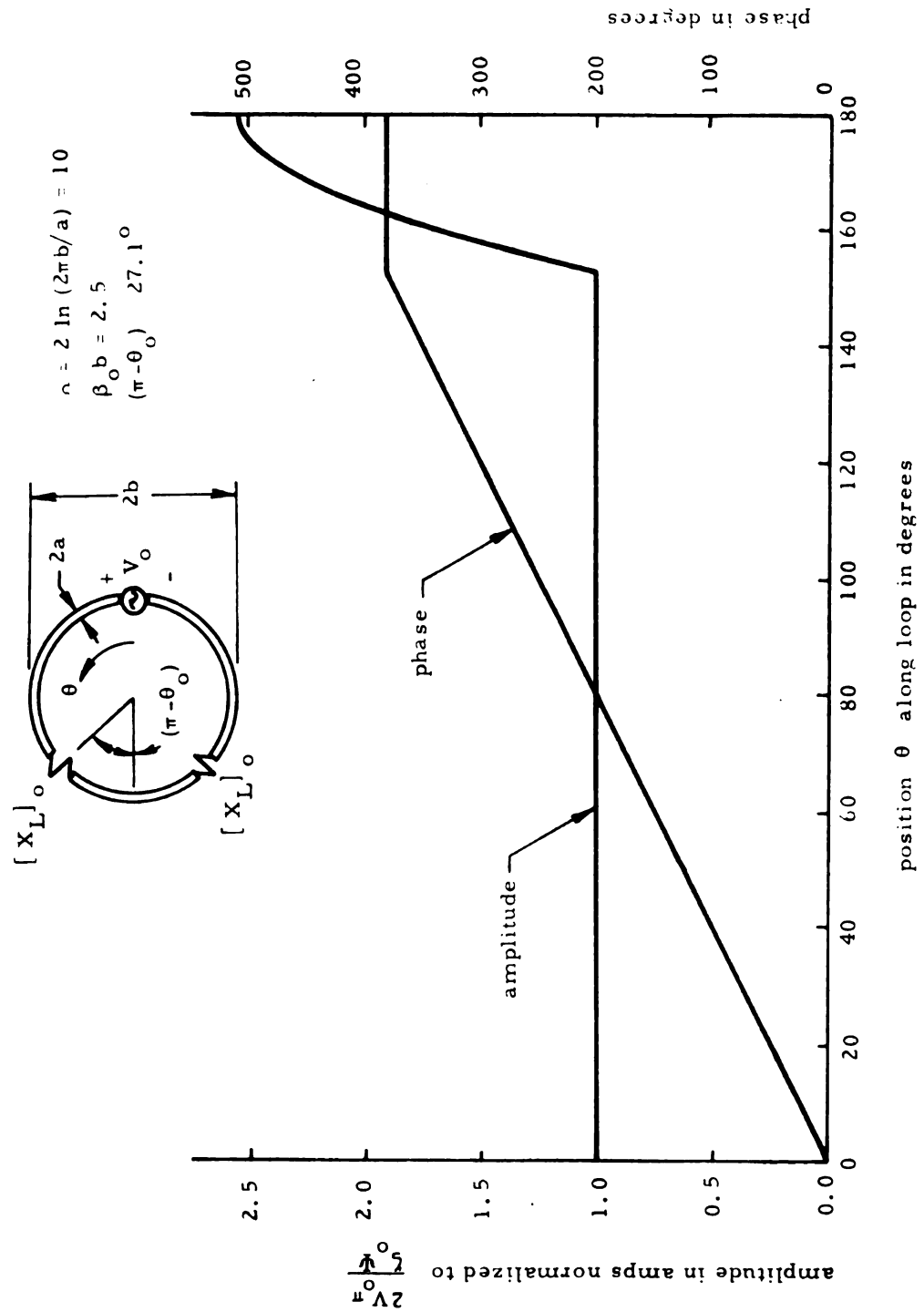


Figure 8.5. Amplitude and Phase of Current Along Loop Corresponding to an Optimum Non-Dissipative Loading.

Figure 8.6 indicates the input impedance of a loop antenna with $\alpha = 10$ as a function of its electrical circumference $\beta_0 b$. These results were obtained from expression (8.35), and it is assumed that the loading is optimum at every frequency. It is noted from the figure that the input impedance of a loop antenna which supports a traveling wave of current at each frequency is essentially independent of the excitation frequency.

In section 8.3 it was indicated that a non-dissipative loading of fixed position can be optimum only at a single frequency. Special consideration was thus given to a loading consisting of the reactive component of the optimum impedance. The position of the loading was selected in such a way that it became optimum at a given frequency. Since such a loading is optimum, and hence yields a purely outward traveling wave of loop current on $0 \leq \theta \leq \theta_0$, only at a single frequency, then the frequency dependence of the corresponding input impedance must be calculated from expression (7.72). As indicated in Figure 8.4, for a loop with $\alpha = 10$, an optimum impedance loading located such that $(\pi - \theta_0) = 27.1^\circ$ becomes purely reactive when $\beta_0 b = 2.5$. The input impedance to a loop antenna having a loading consisting of the reactive component of the optimum impedance given in Figure 8.4 must therefore be calculated from expression (7.72) for all frequencies except that where $\beta_0 b = 2.5$.

In the corresponding case for a linear antenna, similar calculations were made from expression (2.33) and the results presented in Figure 3.12. Since the input impedance expressions (2.33) and (7.72)

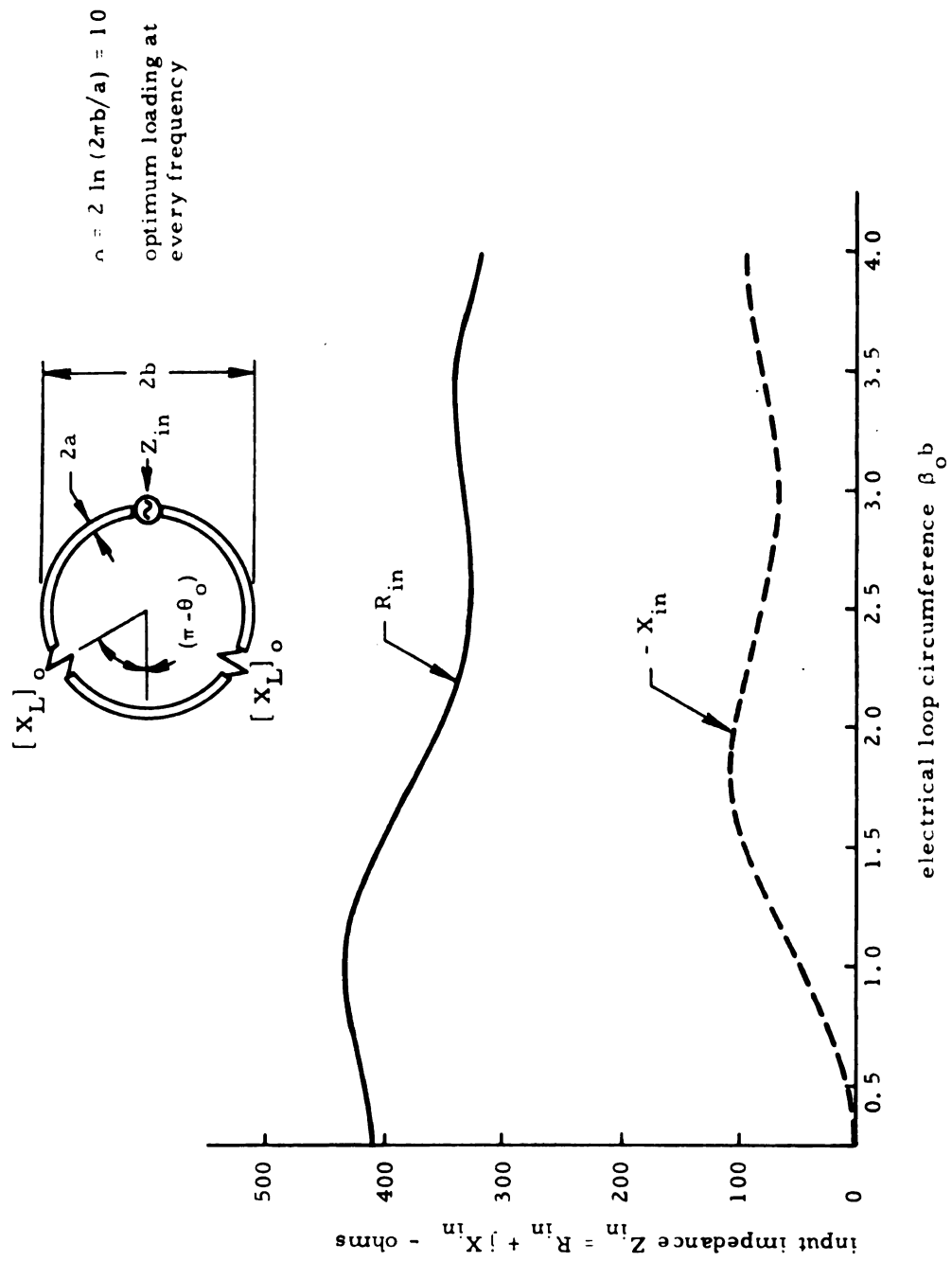


Figure 8.6. Input Impedance of Loop with Optimum Loading as a Function of the Electrical Loop Circumference.

are essentially identical, and resulted from similar approximate theories for the distribution of current on linear and loop antennas, respectively, then the input impedance of the two antenna types will exhibit a very similar frequency dependence. Thus the calculations outlined in the preceding paragraph will not be carried out for the case of a loop antenna. By analogy to Figure 3.12, however, the frequency dependence of the input impedance to a loop antenna having such a purely reactive loading, which becomes optimum for $\beta_o b = 2.5$, will be relatively broadband about the frequency where $\beta_o b = 2.5$.

8.5. Calculation of the Expansion Parameters $\Psi_i(\theta)$, $\Psi_q(\theta)$, and $\Psi(\theta)$

The expansion parameters $\Psi_i(\theta)$, $\Psi_q(\theta)$, and $\Psi(\theta)$ were defined in section 7.4 as

$$\Psi_i(\theta) = \frac{4\pi}{\mu_o} \frac{A_\theta(\theta)}{I_\theta(\theta)} \quad (7.46)$$

$$\Psi_q(\theta) = 4\pi \epsilon_o \frac{\phi(\theta)}{q(\theta)} \quad (7.47)$$

$$\Psi(\theta) = \sqrt{\Psi_i(\theta) \Psi_q(\theta)} \quad (7.59)$$

where $A_\theta(\theta)$ and $\phi(\theta)$ are the vector and scalar potentials at the surface of the loop, and $I_\theta(\theta)$ and $q(\theta)$ are the corresponding distributions of current and charge. It has been indicated that the potentials may be expressed as

$$A_\theta(\theta) = \frac{\mu_o}{4\pi} \int_{-\pi}^{\pi} I_\theta(\theta') \cos(\theta - \theta') K(\theta, \theta') b d\theta' \quad (7.43)$$

$$\phi(\theta) = \frac{1}{4\pi \epsilon_o} \int_{-\pi}^{\pi} q(\theta') K(\theta, \theta') b d\theta' \quad (7.44)$$

where $K(\theta, \theta')$ is the Green's function

$$K(\theta, \theta') = \frac{e^{-j\beta_0 R(\theta, \theta')}}{R(\theta, \theta')} \quad (7.45)$$

and the Euclidean distance $R(\theta, \theta')$ is given approximately by

$$R(\theta, \theta') = b \left[4 \sin^2 \left(\frac{\theta - \theta'}{2} \right) + a^2/b^2 \right]^{1/2} \quad (7.17)$$

Using expressions (7.43) and (7.44) for the potentials, the current and charge expansion parameters $\Psi_i(\theta)$ and $\Psi_q(\theta)$, respectively, are obtained from their definitions (7.46) and (7.47) as

$$\Psi_i(\theta) = \frac{1}{I_\theta(\theta)} \int_{-\pi}^{\pi} I_\theta(\theta') \cos(\theta - \theta') K(\theta, \theta') b d\theta' \quad (8.36)$$

$$\Psi_q(\theta) = \frac{1}{q(\theta)} \int_{-\pi}^{\pi} q(\theta') K(\theta, \theta') b d\theta' \quad (8.37)$$

Since the current distribution of fundamental interest is the traveling wave corresponding to an optimum impedance loading, then it is this distribution which will be used to evaluate the expansion parameters. By analogy to the linear antenna, it is expected that $\Psi_i(\theta)$ and $\Psi_q(\theta)$ will be relatively independent of the distribution of loop current, and depend primarily upon its dimensions. Hence no great error will be made by using the values of $\Psi_i(\theta)$ and $\Psi_q(\theta)$ corresponding to a traveling wave distribution when the loop current actually departs moderately from a traveling wave, i.e., when Z_L is not $[Z_L]_0$.

In the preceding section, it was found that the distribution of loop current on $-\pi \leq \theta \leq \pi$ corresponding to an optimum loading

may be expressed as

$$I_{\theta}(\theta) = \frac{V_o}{60\Psi} e^{-j\beta b|\theta|} \quad -\theta_o \leq \theta \leq \theta_o \quad (8.33)$$

$$I_{\theta}(\theta) = \frac{V_o}{30\Psi} \frac{e^{-j\beta b\pi}}{1 + e^{-j2\beta b(\pi - \theta_o)}} \cos \beta b (\pi - |\theta|) \quad (8.34)$$

$$-\pi \leq \theta \leq -\theta_o, \quad \theta_o \leq \theta \leq \pi$$

It is necessary to know the position θ_o of the loading impedance before results (8.33) and (8.34) may be utilized for the calculation of $\Psi_i(\theta)$ and $\Psi_q(\theta)$. This presents some difficulty, since the loading position was previously determined in terms of $\Psi = \sqrt{\Psi_i \Psi_q}$ and $\beta = \beta_o \sqrt{\Psi_i / \Psi_q}$, but now it is found necessary to know the location θ_o of the loading in order to evaluate $\Psi_i(\theta)$ and $\Psi_q(\theta)$. Some further approximations are consequently in order to allow the explicit evaluation of the expansion parameters.

It is a well known result in linear antenna theory that the expansion parameter $\Psi(z)$ associated with such an antenna is a weak function of the distribution of cylinder current.² This fact was demonstrated in section 3.5 and was indicated by Figure 3.13. It was found that no great error was introduced by neglecting the standing wave of current on $d \leq z \leq h$ and assuming a traveling wave to exist on $0 \leq z \leq h$ when calculating $\Psi(z)$. Such an approximation was found to yield reasonably accurate results whenever the length d of the antenna supporting a traveling wave of current was sufficiently greater than the length $(h-d)$ which supports a standing wave distribution. It was indicated that, whenever the ratio $d/(h-d)$ is of the order of three or greater, sufficiently accurate results may be obtained

through this approximation technique.

A close analogy may be drawn between thin-wire traveling wave linear and loop antennas. Not only are the current distributions corresponding to an optimum impedance loading essentially identical for the two antenna types, but a very close correspondence between the theoretical developments of Chapters 2 and 7 exists as well. It is thus to be expected that an approximation technique analogous to the one described in the preceding paragraph will be valid for the calculation of the loop expansion parameters $\Psi_i(\theta)$ and $\Psi_q(\theta)$.

According to the above arguments, if $(\pi - \theta_0)$ is reasonably small compared with θ_0 , no great error will be made in the calculation of $\Psi_i(\theta)$ and $\Psi_q(\theta)$ if the traveling wave distribution of current is assumed to exist over the entire loop, i. e., for $-\pi \leq \theta \leq \pi$. As indicated in Figure 8.2, the necessary position $(\pi - \theta_0)$ of an optimum non-dissipative loading is always less than 50° when $\beta_0 b$ is greater than 1.5. Thus, for a loop with $n = 10$, the above indicated approximation should be valid whenever the electrical loop circumference is of the order $\beta_0 b = 1.5$ or greater. It was indicated in Figure 8.1 that the imaginary part of the complex wave number β is always very small, while its real part is essentially equal to β_0 . The further approximating assumption that β is real and has the value $\beta = \beta_0$ will thus be made to facilitate the calculation of $\Psi_i(\theta)$ and $\Psi_q(\theta)$.

In accordance with the approximations outlined in the preceding paragraph, the distribution of loop current to be utilized in calculating the expansion parameters will be taken as

$$I_{\theta}(\theta) = \frac{V_o}{60\Psi} e^{-j\beta_o b|\theta|} \quad -\pi \leq \theta \leq \pi \quad (8.38)$$

The corresponding approximate distribution of charge is related to the loop current through the equation of continuity as

$$q(\theta) = \frac{j}{\omega b} \frac{\partial}{\partial \theta} I_{\theta}(\theta) \quad (7.50)$$

$$= \frac{2\pi \epsilon_o V_o}{\Psi_q} e^{-j\beta_o b|\theta|} \text{sgn}(\theta) \quad -\pi \leq \theta \leq \pi \quad (8.39)$$

where the signum function $\text{sgn}(\theta)$ is defined by

$$\text{sgn}(\theta) = \begin{cases} 1 & \text{for } \theta > 0 \\ 0 & \text{for } \theta = 0 \\ -1 & \text{for } \theta < 0 \end{cases} \quad (8.40)$$

Using the distributions of loop current and charge given by results (8.38) and (8.39), the expansion parameters $\Psi_i(\theta)$ and $\Psi_q(\theta)$ are obtained from expressions (8.36) and (8.37), respectively, as

$$\Psi_i(\theta) = e^{j\beta_o b\theta} \int_{-\pi}^{\pi} e^{-j\beta_o b|\theta'|} \cos(\theta - \theta') K(\theta, \theta') b d\theta' \quad (8.41)$$

$$0 \leq \theta \leq \pi$$

$$\Psi_q(\theta) = e^{j\beta_o b\theta} \int_{-\pi}^{\pi} e^{-j\beta_o b|\theta'|} \text{sgn}(\theta') K(\theta, \theta') b d\theta' \quad (8.42)$$

$$0 \leq \theta \leq \pi$$

The results may be written in the form

$$\Psi_i(\theta) = e^{j\beta_o b\theta} [C_{a,b}^i(\beta_o b, \theta) - j S_{a,b}^i(\beta_o b, \theta)] \quad 0 \leq \theta \leq \pi \quad (8.43)$$

$$\Psi_q(\theta) = e^{j\beta_o b\theta} [C_{a,b}^q(\beta_o b, \theta) - j S_{a,b}^q(\beta_o b, \theta)] \quad 0 \leq \theta \leq \pi \quad (8.44)$$

where the quantities $C_{a,b}^i(\beta_o b, \theta)$, $S_{a,b}^i(\beta_o b, \theta)$, $C_{a,b}^q(\beta_o b, \theta)$, and $S_{a,b}^q(\beta_o b, \theta)$ are defined by

$$C_{a,b}^i(\beta_o b, \theta) = \int_{-\pi}^{\pi} \cos \beta_o b \theta' \cos(\theta - \theta') K(\theta, \theta') b d\theta' \quad (8.45)$$

$$S_{a,b}^i(\beta_o b, \theta) = \int_{-\pi}^{\pi} \sin \beta_o b |\theta'| \cos(\theta - \theta') K(\theta, \theta') b d\theta' \quad (8.46)$$

$$C_{a,b}^q(\beta_o b, \theta) = \int_{-\pi}^{\pi} \text{sgn}(\theta') \cos \beta_o b \theta' K(\theta, \theta') b d\theta' \quad (8.47)$$

$$S_{a,b}^q(\beta_o b, \theta) = \int_{-\pi}^{\pi} \text{sgn}(\theta') \sin \beta_o b |\theta'| K(\theta, \theta') b d\theta' \quad (8.48)$$

The Green's function $K(\theta, \theta')$ is given by equation (7.45). Integrals (8.45) through (8.48) were numerically machine calculated for the following values of the parameters a/b , $\beta_o b$, and θ :

$$a/b = 0.0423, \text{ or } n = 2 \ln(2\pi b/a) = 10$$

$$\beta_o b = 0.25 \text{ through } 4.0$$

$$\theta = 0^\circ \text{ through } 180^\circ \text{ for each } \beta_o b$$

With these numerical results, the values of $\Psi_i(\theta)$ and $\Psi_q(\theta)$ are readily calculated from expressions (8.43) and (8.44), respectively.

The dependence of $\Psi_i(\theta)$ and $\Psi_q(\theta)$ upon the angular position θ along the loop circumference is indicated in Figures 8.7 and 8.8, respectively, for the case of $\beta_o b = 2$. These results were calculated from expressions (8.43) and (8.44), and correspond to a loop having $n = 10$ and an electrical circumference of $\beta_o b = 2.0$. It will be recalled that in the approximate theory of Chapter 7 it was asserted that $\Psi_i(\theta)$ and $\Psi_q(\theta)$ were indeed essentially constant. A study of Figure 8.7 reveals that $\Psi_i(\theta)$ is relatively independent of θ for

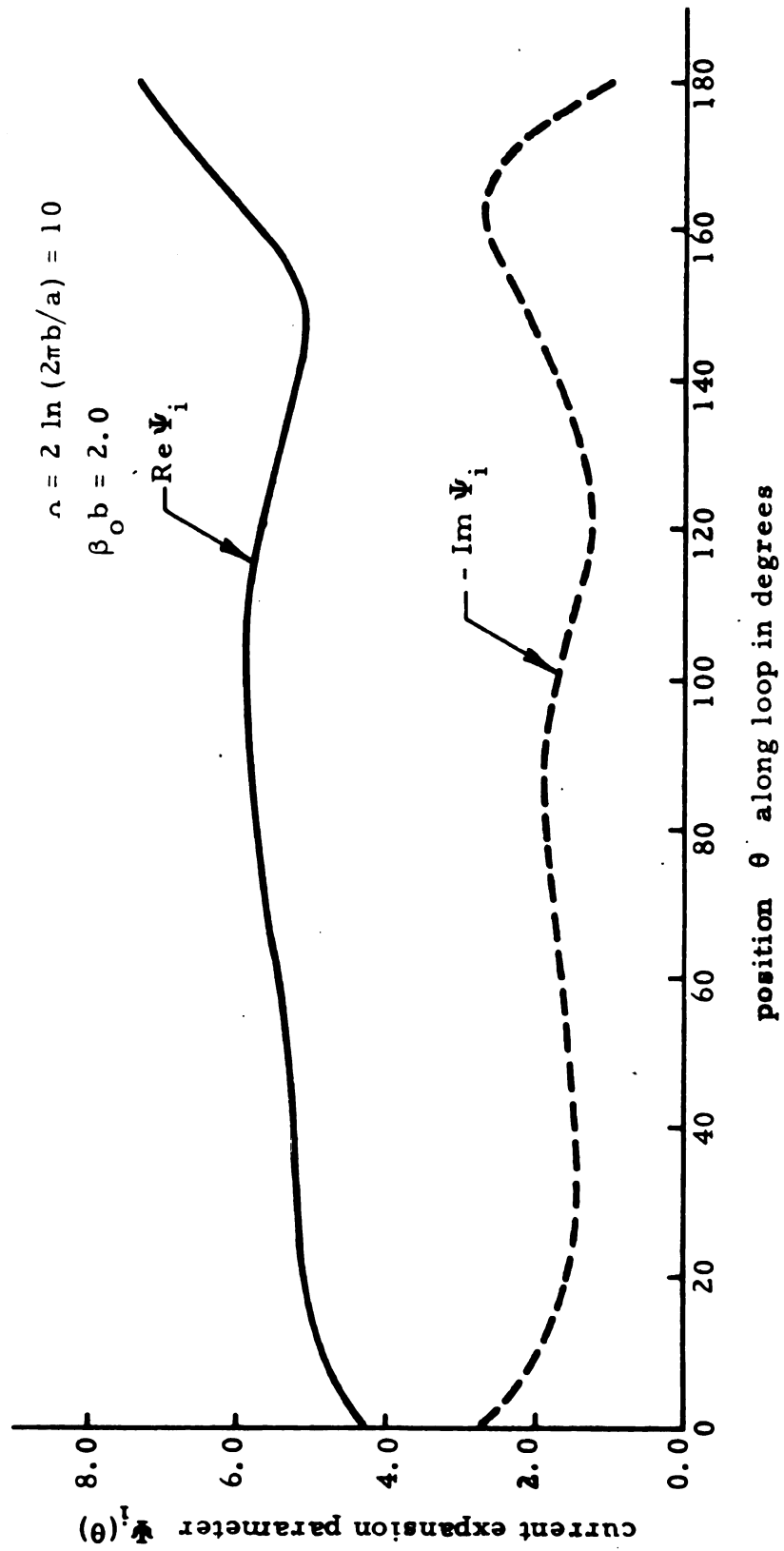


Figure 8.7. Current Expansion Parameter $\Psi_i(\theta)$ as a Function of Position Along the Loop.

$$\alpha = 2 \ln (2\pi b/a) = 10$$

$$\beta_0 b = 2.0$$

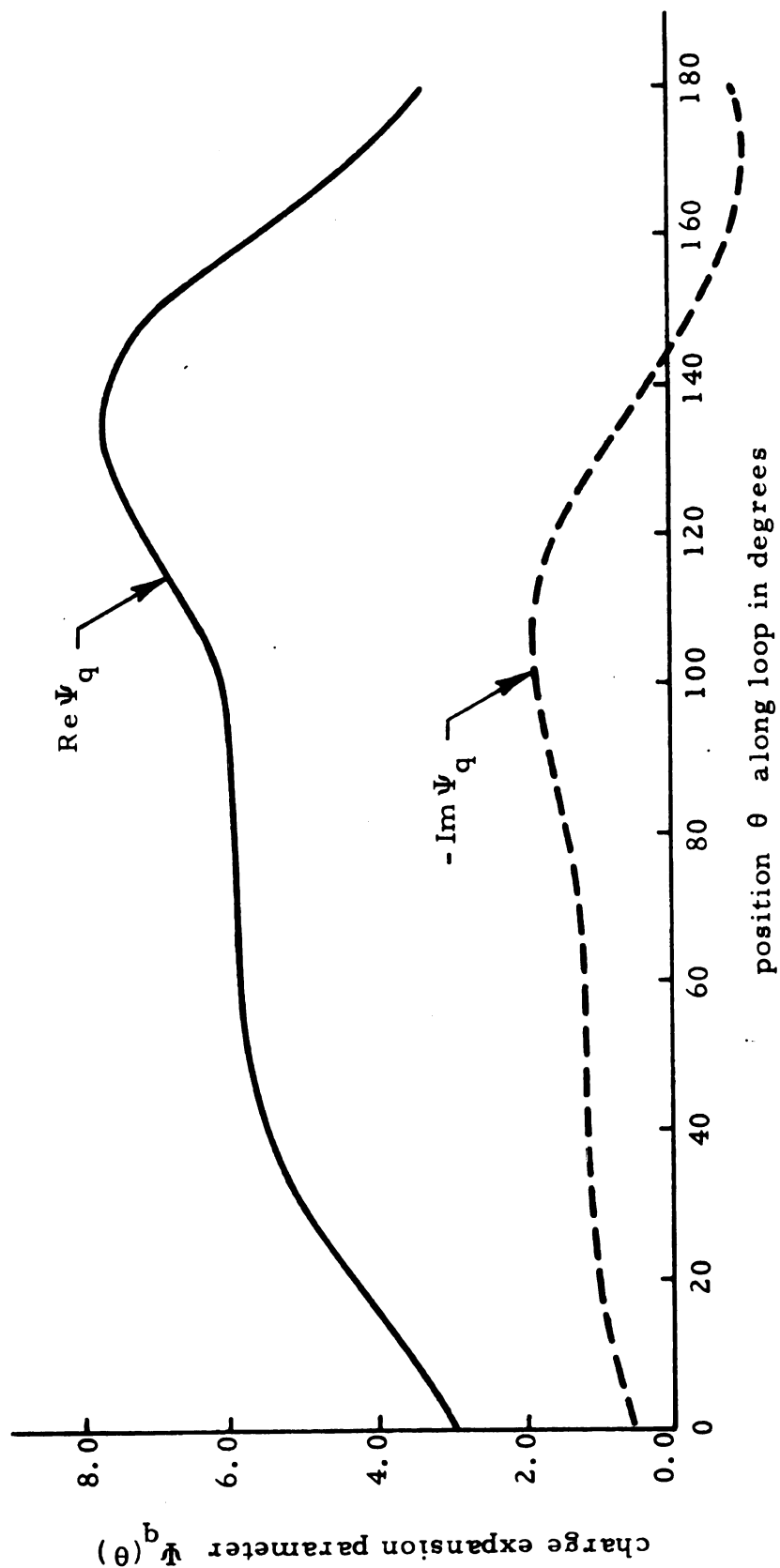


Figure 8.8. Charge Expansion Parameter $\Psi_q(\theta)$ as a Function of Position Along the Loop.

$0^\circ \leq \theta \leq 160^\circ$. The variation of $\Psi_q(\theta)$ as depicted by Figure 8.8 is more pronounced, but its value is relatively constant for $30^\circ \leq \theta \leq 130^\circ$. In either case, the rapid variation for large values of θ (near 180°) is very likely due to the approximate nature of expressions (8.43) and (8.44), where the standing wave of current on $145^\circ \leq \theta \leq 180^\circ$ was neglected. The strong variation in $\Psi_q(\theta)$ for small arguments may be attributed to the discontinuity in both the scalar potential $\phi(\theta)$ and the charge distribution $q(\theta)$ at the excitation point $\theta = 0$.

It has been indicated by King² that in the case of a linear antenna the greatest accuracy is obtained by evaluating the expansion parameter $\Psi(z)$ at a point of maximum antenna current. By the analogy discussed previously, this criterion should also be valid for a loop antenna. Thus Ψ_i should be evaluated at a point of maximum loop current and Ψ_q at a point of maximum charge. Due to the traveling wave of current on $0 \leq \theta \leq \theta_o$, the amplitudes of both $I_\theta(\theta)$ and $q(\theta)$ are constant for $0 \leq \theta \leq \theta_o$, while $q(\theta)$ is discontinuous with $q(0) = 0$ at $\theta = 0$. It would thus appear that $\Psi_i(\theta)$ and $\Psi_q(\theta)$ might be evaluated at any point where the traveling wave exists, except near the discontinuity at $\theta = 0$ or the standing wave at $\theta = \theta_o$, to yield the constant values Ψ_i and Ψ_q . Since both $\Psi_i(\theta)$ and $\Psi_q(\theta)$ are well represented by their values at $\theta = \pi/2$, it is taken that

$$\begin{aligned}\Psi_i &= \Psi_i(\theta = \pi/2) \\ \Psi_q &= \Psi_q(\theta = \pi/2)\end{aligned}\tag{8.50}$$

These values of Ψ_i and Ψ_q were utilized to obtain all the preceding numerical results of this chapter.

Figures 8.9, 8.10, and 8.11 indicate the variation of Ψ_i , Ψ_q , and $\Psi = \sqrt{\Psi_i \Psi_q}$, respectively, as a function of the electrical loop circumference $\beta_o b$. These results were obtained from expressions (8.43) and (8.44) in conjunction with conditions (8.50) for a loop with $n = 10$. The numerical values given by these figures may be used in conjunction with the theory of sections 8.3 and 8.4 to determine the parameters of an optimum non-dissipative loading and the corresponding input impedance to the traveling wave loop antenna.

$$\alpha = 2 \ln (2\pi b/a) = 10$$

$$\theta = 90^\circ$$

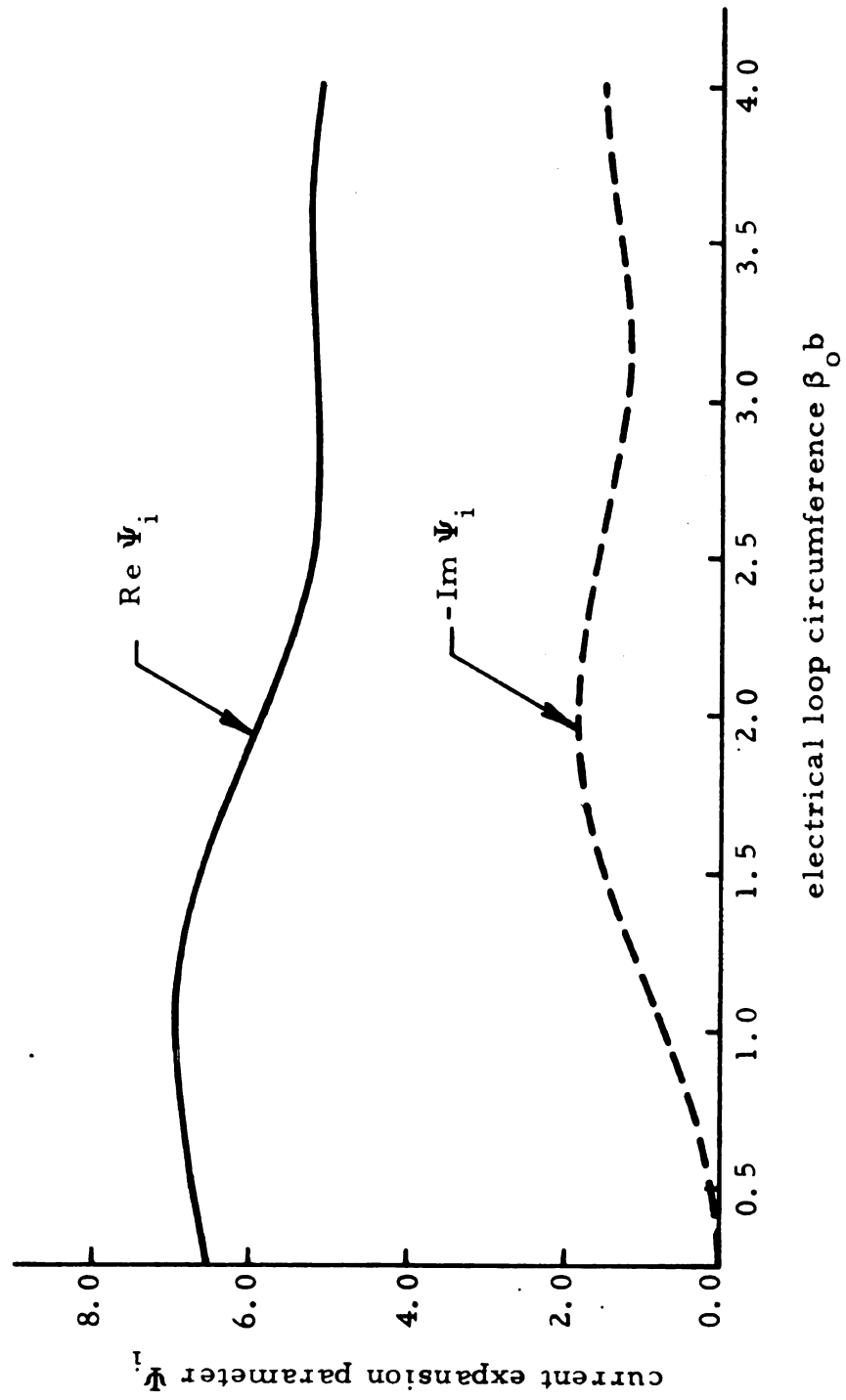


Figure 8.9. Current Expansion Parameter Ψ_i as a Function of the Electrical Loop Circumference.

$$\kappa = 2 \ln (2\pi b/a) = 10$$

$$\theta = 90^\circ$$

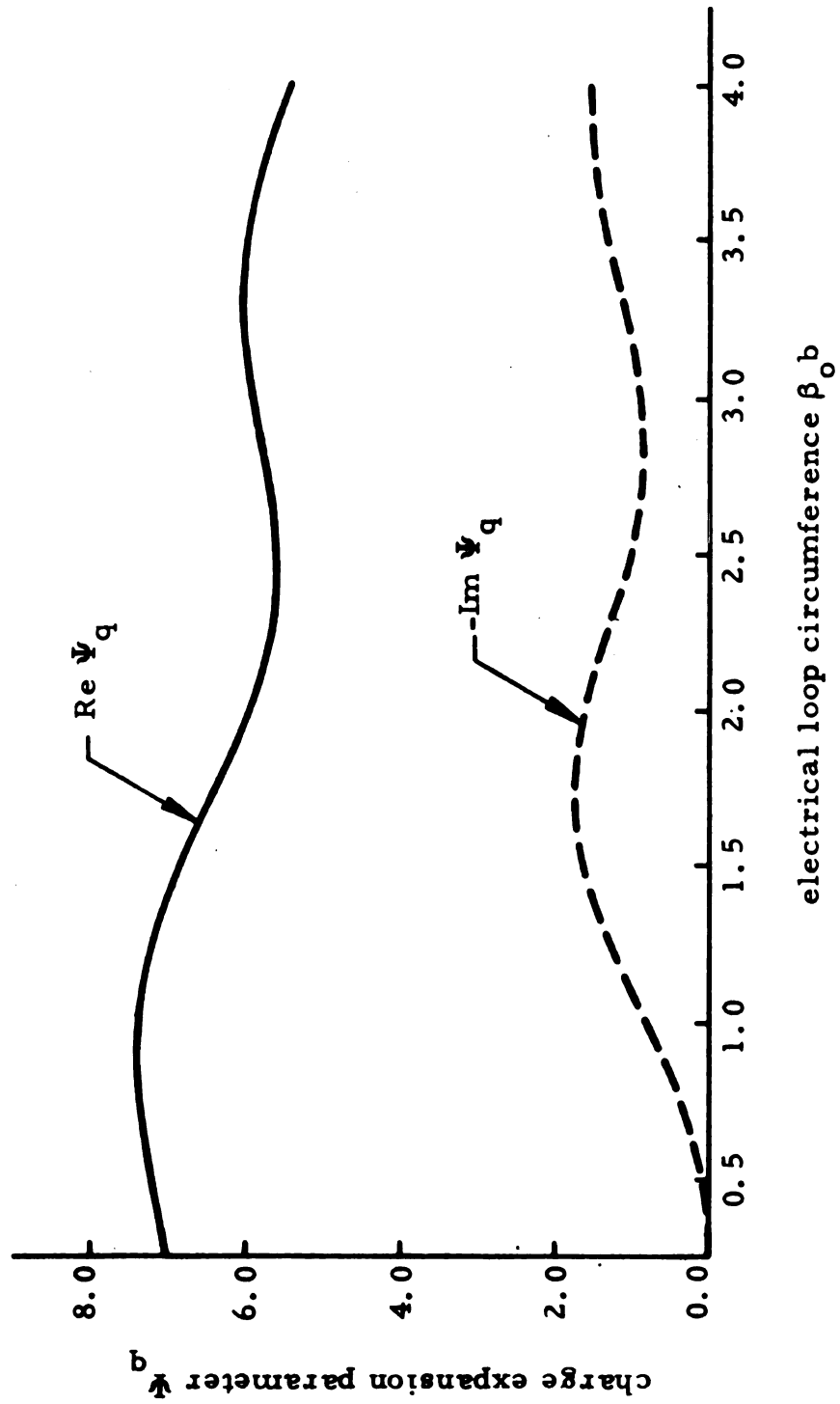


Figure 8.10. Charge Expansion Parameter Ψ_q as a Function of the Electrical Loop Circumference.

$$\kappa = 2 \ln (2\pi b/a) = 10$$

$$\theta = 90^\circ$$

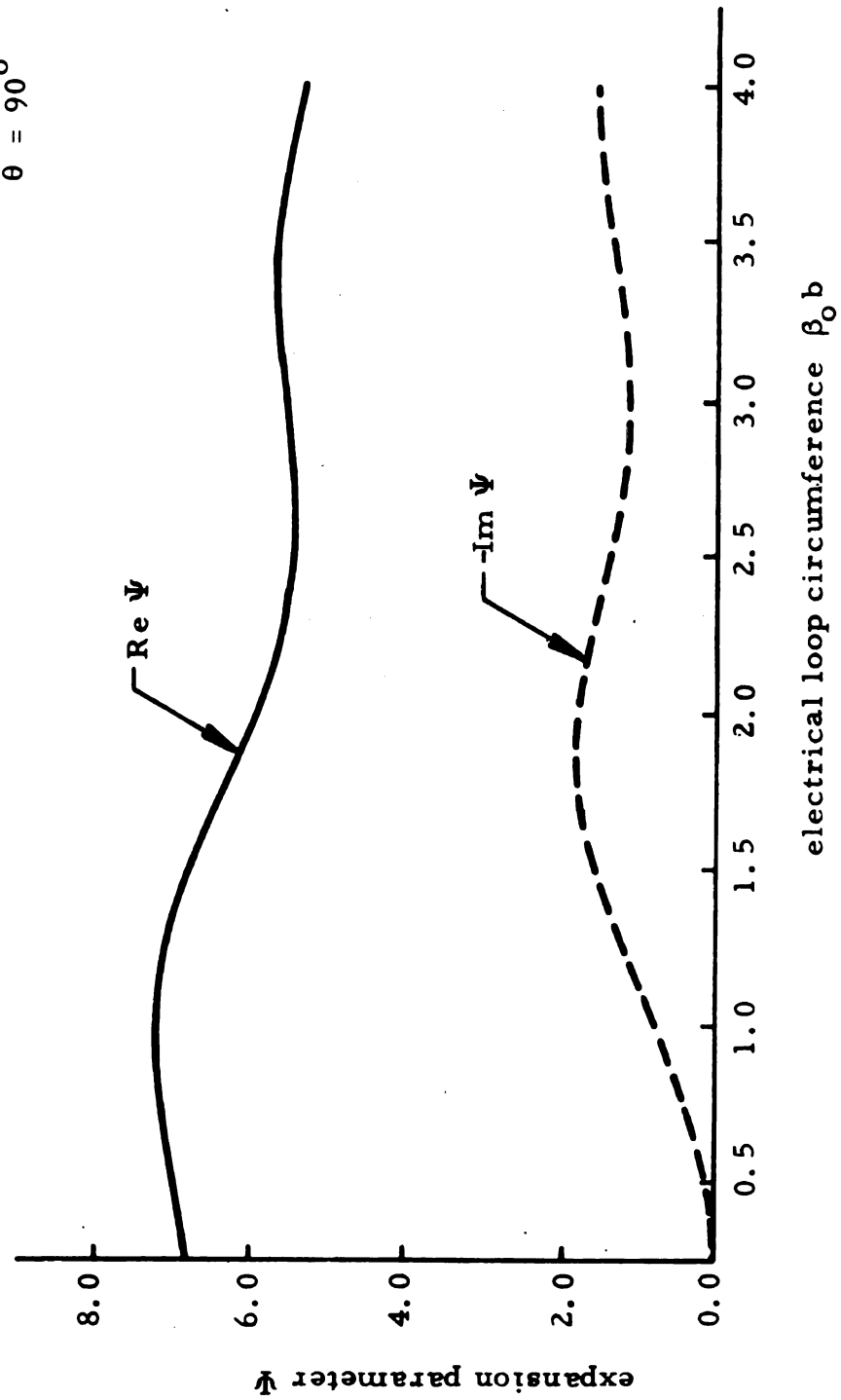


Figure 8.11. Expansion Parameter Ψ as a Function of the Electrical Loop Circumference.

CHAPTER 9

RADIATION CHARACTERISTICS OF A TRAVELING WAVE LOOP ANTENNA

9.1. Distribution of Loop Current for Calculation of Radiation Fields

It was indicated in the introduction that the radiation characteristics of a loop antenna are completely characterized by its distribution of current. The approximate current distribution on the doubly loaded loop was determined in Chapter 7, and that corresponding to an optimum impedance loading was established in Chapter 8. In the present chapter, the radiation zone fields of the traveling wave loop antenna are to be calculated. These fields are defined by the condition $\beta_o R \gg 1$, where R is the distance from a current element on the loop to an observation point P . This condition is equivalent to the requirement that the point of observation P should be separated from every point of the loop by many wavelengths. To determine these fields, the distribution of current corresponding to an optimum loading will be utilized. Since it is, in particular, the radiation zone fields which are to be determined, this distribution will be further approximated to simplify the calculations.

In section 8.4 of the preceding chapter, the current distribution on the doubly loaded loop corresponding to an optimum impedance loading was found as

$$I_\theta(\theta) = \frac{V_o}{60\Psi} e^{-j\beta b|\theta|} \quad -\theta_o \leq \theta \leq \theta_o \quad (8.33)$$

$$I_{\theta}(\theta) = \frac{V_o}{30\Psi} \frac{e^{-j\beta b\pi}}{1 + e^{-j2\beta b(\pi-\theta_o)}} \cos(\pi - |\theta|) \quad (8.34)$$

$$-\pi \leq \theta \leq -\theta_o, \quad \theta_o \leq \theta \leq \pi$$

These expressions represent a traveling wave of loop current over the region $-\theta_o \leq \theta \leq \theta_o$ and a standing wave on the regions $-\pi \leq \theta \leq -\theta_o$ and $\theta_o \leq \theta \leq \pi$. It is well known that the radiation zone fields of an antenna are not a strong function of its distribution of current. If the regions of the loop supporting a standing wave of current are short compared with the one on which a traveling wave exists, it is reasonable to assume that the traveling wave is supported over the entire loop. That is, if $(\pi - \theta_o)$ is reasonably small compared with θ_o , then no great error will be made by assuming equation (8.33) to hold on $-\pi \leq \theta \leq \pi$ when calculating the radiation fields of the loop.

From the results of section 8.3, the range of loop sizes for which the above outlined approximation is applicable may be deduced. Consider a loop with $n = 10$ and having a purely non-dissipative optimum loading. It is noted from Figure 8.2 that the ratio $\theta_o/(\pi - \theta_o)$ is greater than 2.0 whenever the electrical loop circumference is of the order of $\beta_o b = 1.25$ or greater. Further, it was indicated in Figure 8.1 that the complex wave number β is essentially equal to the free space wave number β_o . It is therefore a valid approximation to take $\beta = \beta_o$ in calculating the radiation fields. Hence there exists a range of loop sizes for which the distribution of current

$$I_{\theta}(\theta) = \frac{V_o}{60\Psi} e^{-j\beta_o b |\theta|} \quad -\pi \leq \theta \leq \pi \quad (9.1)$$

is a reasonable approximation. It is this current distribution which will be utilized to calculate the radiation fields of a traveling wave loop antenna.

9.2. Radiation Fields of the Traveling Wave Loop Antenna

It was found that a general formulation for the radiation zone fields of a circular loop antenna is not available in the existing literature. The case which is invariably treated is that of an electrically small loop for which the distribution of current is assumed constant along its circumference. No theory could be found which formulated the radiation fields of a circular loop in terms of a general current distribution. This is a rather surprising fact in view of the relative popularity of loop type antennas. It is first necessary therefore, to calculate the radiation zone fields of a loop of arbitrary size in terms of a general distribution of current. The fields corresponding to standing and traveling waves of current may then be obtained from this general result.

The electric and magnetic fields at a point in space due to some localized time harmonic current-charge distribution are given quite generally in terms of the vector and scalar potentials \vec{A} and ϕ , respectively, as

$$\begin{aligned}\vec{E} &= -\nabla\phi - j\omega\vec{A} \\ \vec{B} &= \nabla \times \vec{A}\end{aligned}\tag{9.2}$$

It is possible to express the potentials in terms of the Helmholtz integrals over the volume density of current $\vec{J}(\vec{r})$ and the volume density of charge $\rho(\vec{r})$ as

$$\begin{aligned}\vec{A}(\vec{r}) &= \frac{\mu_o}{4\pi} \int_v \vec{J}(\vec{r}') \frac{e^{-j\beta_o R}}{R} dv' \\ \phi(\vec{r}) &= \frac{1}{4\pi\epsilon_o} \int_v \rho(\vec{r}') \frac{e^{-j\beta_o R}}{R} dv'\end{aligned}\quad (9.3)$$

where $R = |\vec{r} - \vec{r}'|$ is the distance between a source point located by \vec{r}' and an observation point at \vec{r} , and v the region of non-vanishing source densities. By substituting the potentials (9.3) into expressions (9.2), it has been shown by King⁵ that the radiation zone electromagnetic fields become

$$\vec{E}^r(\vec{r}) = \frac{j\beta_o}{4\pi\epsilon_o} \int_v \left[\hat{R} \rho(\vec{r}') - \frac{\vec{J}(\vec{r}')}{v_o} \right] \frac{e^{-j\beta_o R}}{R} dv' \quad (9.4)$$

$$\vec{B}^r(\vec{r}) = -\frac{j\beta_o\mu_o}{4\pi} \int_v \hat{R} \times \vec{J}(\vec{r}') \frac{e^{-j\beta_o R}}{R} dv' \quad (9.5)$$

where

$$R = |\vec{r} - \vec{r}'|, \quad \hat{R} = \frac{\vec{r} - \vec{r}'}{|\vec{r} - \vec{r}'|}$$

and v_o is the velocity of propagation in free space, with β_o the free space wave number.

Figure 9.1 illustrates the geometry of interest for calculating the radiation fields of a circular loop antenna. The loop is taken to lie in the x-y plane of a system of rectangular coordinates (x, y, z) and to be centered about the origin 0 at (0, 0, 0). A position vector \vec{r} locates the observation point $P(r, \theta, \phi)$, having the spherical coordinates (r, θ, ϕ) , with respect to the origin 0. The vector \vec{r}' locates a source element along the loop having the spherical coordinates $(b, \pi/2, \phi')$. The loop current $\vec{I}(\vec{r}')$ thus has only a

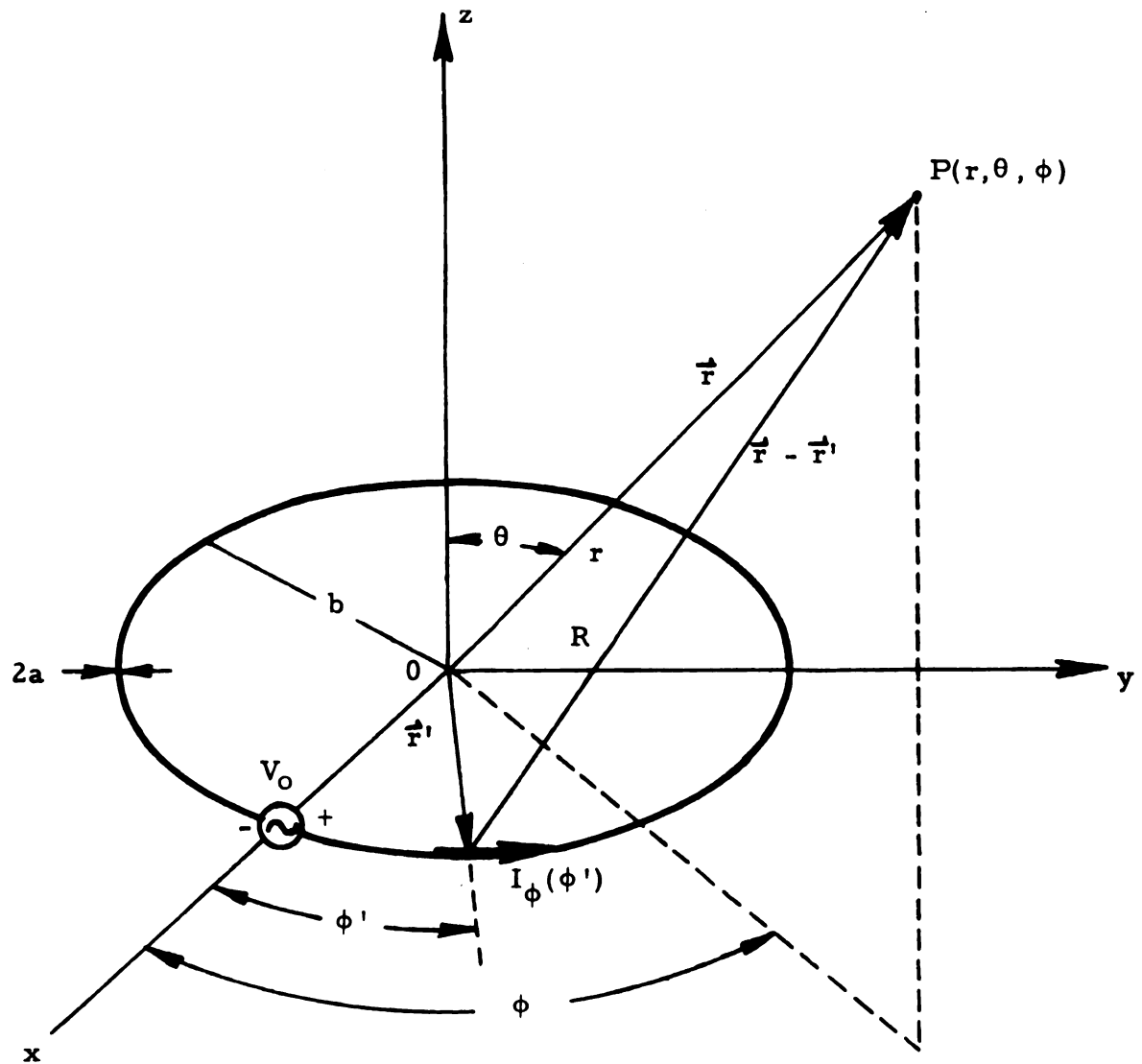


Figure 9.1. Loop Geometry for Calculation of Radiation Zone Fields.

ϕ -component and is a function of ϕ' , with the result that

$$\vec{I}(\vec{r}') = \hat{\phi}' I_{\phi}(\phi') \quad (9.6)$$

It is assumed that the loop is excited at the point $\phi' = 0$.

Due to the assumption of a thin-wire loop where $\beta_o a \ll 1$, it may be taken that

$$\vec{J}(\vec{r}') dv' = \vec{I}(\vec{r}') b d\phi' = \hat{\phi}' I_{\phi}(\phi') b d\phi' \quad (9.7)$$

$$\rho(\vec{r}') dv' = q(\vec{r}') b d\phi' = q(\phi') b d\phi' \quad (9.8)$$

where $I_{\phi}(\phi)$ and $q(\phi)$ are the current and charge per unit length, respectively, along the loop. Further, $q(\phi)$ is related to $I_{\phi}(\phi)$ through the equation of continuity as

$$q(\phi) = \frac{j}{\omega b} \frac{\partial}{\partial \phi} I_{\phi}(\phi) \quad (9.9)$$

so that finally

$$\vec{J}(\vec{r}') dv' = \hat{\phi}' I_{\phi}(\phi') b d\phi' \quad (9.10a)$$

$$\rho(\vec{r}') dv' = \frac{j}{\omega} \frac{\partial}{\partial \phi'} I_{\phi}(\phi') d\phi' \quad (9.10b)$$

If results (9.10) are substituted into expressions (9.4) and (9.5), the radiation zone electromagnetic fields become

$$\begin{aligned} \vec{E}^r(\vec{r}) &= \frac{j\beta_o}{4\pi\epsilon_o} \int_{-\pi}^{\pi} \hat{R} \frac{j}{\omega} \frac{\partial}{\partial \phi'} I_{\phi}(\phi') \frac{e^{-j\beta_o R}}{R} d\phi' \\ &\quad - \frac{j\beta_o}{4\pi\epsilon_o} \int_{-\pi}^{\pi} \hat{\phi}' \frac{I_{\phi}(\phi')}{v_o} \frac{e^{-j\beta_o R}}{R} b d\phi' \end{aligned} \quad (9.11)$$

$$\vec{B}^r(\vec{r}) = - \frac{j\beta_o \mu_o}{4\pi} \int_{-\pi}^{\pi} \hat{R} \times \hat{\phi}' I_{\phi}(\phi') \frac{e^{-j\beta_o R}}{R} b d\phi' \quad (9.12)$$

Before proceeding further, it is necessary to evaluate the Euclidean distance R between a source element at \vec{r}' and the observation point P at \vec{r} . With reference to Figure 9.1, an application of the law of cosines gives

$$\begin{aligned} R^2 &= r^2 + b^2 - 2rb \sin \theta \cos (\phi - \phi') \\ &= r^2 [1 + (b/r)^2 - 2(b/r) \sin \theta \cos (\phi - \phi')] \end{aligned} \quad (9.13)$$

Since the radiation zone is characterized by $r \gg b$, the term in $(b/r)^2$ may be dropped, leaving

$$R \doteq r [1 - 2(b/r) \sin \theta \cos (\phi - \phi')]^{1/2} \quad (9.14)$$

Using the two leading terms of a binomial series expansion gives finally

$$R \doteq r - b \sin \theta \cos (\phi - \phi') \quad (9.15)$$

It will thus be taken that, for observation points P in the radiation zone, the distance R is given approximately by

$$R \doteq \begin{cases} r & \dots \dots \dots \text{amplitude terms} \\ r - b \sin \theta \cos (\phi - \phi') & \dots \text{phase terms} \end{cases} \quad (9.16)$$

Further, the unit vector \hat{R} may be approximated in the radiation zone as

$$\hat{R} \doteq \hat{r} \quad (9.17)$$

If approximations (9.16) and (9.17) are substituted into equations (9.11) and (9.12), the radiation fields may be expressed as

1

$$\begin{aligned}\vec{E}^r(\vec{r}) &= \frac{j\beta_o}{4\pi\epsilon_o} \frac{e^{-j\beta_o r}}{r} \int_{-\pi}^{\pi} \hat{r} \frac{j}{\omega} \frac{\partial}{\partial \phi'} I_{\phi}(\phi') e^{j\beta_o b \sin\theta \cos(\phi - \phi')} d\phi' \\ &- \frac{j\beta_o}{4\pi\epsilon_o} \frac{e^{-j\beta_o r}}{r} \int_{-\pi}^{\pi} \frac{I_{\phi}(\phi')}{v_o} \hat{\phi}' e^{j\beta_o b \sin\theta \cos(\phi - \phi')} b d\phi'\end{aligned}\quad (9.18)$$

$$\vec{B}^r(\vec{r}) = -\frac{j\beta_o \mu_o}{4\pi} \frac{e^{-j\beta_o r}}{r} \int_{-\pi}^{\pi} I_{\phi}(\phi') (\hat{r} \times \hat{\phi}') e^{j\beta_o b \sin\theta \cos(\phi - \phi')} b d\phi' \quad (9.19)$$

The integration in the first term of result (9.18) may be carried out by parts, and the integrated term is found to vanish. Making use of the fact that

$$\sin\theta \sin(\phi - \phi') = \hat{r} \cdot \hat{\phi}' \quad (9.20)$$

the remaining term may be combined with the second integral in equation (9.18) to give

$$\begin{aligned}\vec{E}^r(\vec{r}) &= \frac{j\beta_o b}{4\pi\epsilon_o v_o} \frac{e^{-j\beta_o r}}{r} \int_{-\pi}^{\pi} [\hat{r}(\hat{r} \cdot \hat{\phi}') - \hat{\phi}'] I_{\phi}(\phi') \\ &\quad e^{j\beta_o b \sin\theta \cos(\phi - \phi')} d\phi'\end{aligned}\quad (9.21)$$

If the vector identity

$$\hat{r} \times (\hat{r} \times \hat{\phi}') = (\hat{r} \cdot \hat{\phi}') \hat{r} - \hat{\phi}' \quad (9.22)$$

is utilized, then result (9.21) may be rewritten, and the radiation zone fields become

$$\begin{aligned}\vec{E}^r(\vec{r}) &= j\omega \hat{r} \times \frac{e^{-j\beta_o r}}{r} \frac{\mu_o b}{4\pi} \int_{-\pi}^{\pi} (\hat{r} \times \hat{\phi}') I_{\phi}(\phi') \\ &\quad e^{j\beta_o b \sin\theta \cos(\phi - \phi')} d\phi'\end{aligned}\quad (9.23)$$

$$\vec{B}^r(\vec{r}) = -j\beta_o \frac{e^{-j\beta_o r}}{r} \frac{\mu_o b}{4\pi} \int_{-\pi}^{\pi} (\hat{r} \times \hat{\phi}') I_{\phi}(\phi') e^{j\beta_o b \sin \theta \cos(\phi - \phi')} d\phi' \quad (9.24)$$

From these expressions, it is observed that

$$\vec{E}^r(\vec{r}) = v_o [\vec{B}^r(\vec{r}) \times \hat{r}] \quad (9.25)$$

and $\vec{E}^r(\vec{r})$ and $\vec{B}^r(\vec{r})$ are orthogonal to one another as well as to the direction of propagation \hat{r} , as is typical of radiation fields.

Since the unit vector $\hat{\phi}'$ may be expressed as

$$\hat{\phi}' = \sin \theta \sin(\phi - \phi') \hat{r} + \cos \theta \sin(\phi - \phi') \hat{\theta} + \cos(\phi - \phi') \hat{\phi} \quad (9.26)$$

then

$$\hat{r} \times \hat{\phi}' = -\cos(\phi - \phi') \hat{\theta} + \cos \theta \sin(\phi - \phi') \hat{\phi} \quad (9.27)$$

The radiation zone vector potential $\vec{A}^r(\vec{r})$ is given by

$$\begin{aligned} \vec{A}^r(\vec{r}) &= \frac{\mu_o}{4\pi} \frac{e^{-j\beta_o r}}{r} \int_{-\pi}^{\pi} \hat{\phi}' I_{\phi}(\phi') e^{j\beta_o b \sin \theta \cos(\phi - \phi')} b d\phi' \\ &= \frac{\mu_o b}{4\pi} \frac{e^{-j\beta_o r}}{r} \int_{-\pi}^{\pi} [\sin \theta \sin(\phi - \phi') \hat{r} + \cos \theta \sin(\phi - \phi') \hat{\theta} \\ &\quad + \cos(\phi - \phi') \hat{\phi}] I_{\phi}(\phi') e^{j\beta_o b \sin \theta \cos(\phi - \phi')} d\phi' \end{aligned} \quad (9.28)$$

Using result (9.27) in expressions (9.23) and (9.24) and comparing with equation (9.28) shows immediately that

$$\vec{E}^r(\vec{r}) = j\omega \hat{r} \times [-A_\phi^r(\vec{r}) \hat{\theta} + A_\theta^r(\vec{r}) \hat{\phi}] \quad (9.29)$$

$$\vec{B}^r(\vec{r}) = j\beta_o [A_\phi^r(\vec{r}) \hat{\theta} - A_\theta^r(\vec{r}) \hat{\phi}] \quad (9.30)$$

If the cross product in result (9.29) is expanded, the radiation fields may finally be expressed as

$$\begin{aligned} \vec{E}^r(\vec{r}) &= -j\omega [A_\phi^r(\vec{r}) \hat{\phi} + A_\theta^r(\vec{r}) \hat{\theta}] \\ \vec{B}^r(\vec{r}) &= -j\beta_o [A_\theta^r(\vec{r}) \hat{\phi} - A_\phi^r(\vec{r}) \hat{\theta}] \end{aligned} \quad (9.31)$$

The components of vector potential are obtained from equation (9.28) as

$$A_\phi^r(\vec{r}) = \frac{\mu_o b}{4\pi} \frac{e^{-j\beta_o r}}{r} \int_{-\pi}^{\pi} I_\phi(\phi') \cos(\phi - \phi') e^{j\beta_o b \sin \theta \cos(\phi - \phi')} d\phi' \quad (9.32)$$

$$A_\theta^r(\vec{r}) = \frac{\mu_o b}{4\pi} \frac{e^{-j\beta_o r}}{r} \cos \theta \int_{-\pi}^{\pi} I_\phi(\phi') \sin(\phi - \phi') e^{j\beta_o b \sin \theta \cos(\phi - \phi')} d\phi' \quad (9.33)$$

Expressions (9.31) give the radiation fields $\vec{E}^r(\vec{r})$ and $\vec{B}^r(\vec{r})$ of a loop antenna, at an observation point $P(\vec{r})$ in the radiation zone, in terms of its distribution of current. These fields depend in general upon each of the spherical coordinates (r, θ, ϕ) of the point $P(\vec{r})$. A special case which is commonly considered is that of the radiation fields in the plane of the loop, specified by $\theta = \pi/2$. For this case, $A_\theta^r(\vec{r}) = 0$ by equation (9.33) while $A_\phi^r(\vec{r})$ becomes

$$A_{\phi}^r(\vec{r}) = \frac{\mu_o b}{4\pi} \frac{e^{-j\beta_o r}}{r} \int_{-\pi}^{\pi} I_{\phi}(\phi') \cos(\phi - \phi') e^{j\beta_o b \cos(\phi - \phi')} d\phi' \quad (9.34)$$

The radiation fields in the plane of the loop are therefore given by

$$\begin{aligned} \vec{E}^r(\vec{r}) &= -j\omega A_{\phi}^r(\vec{r}) \hat{\phi} \\ \vec{B}^r(\vec{r}) &= j\beta_o A_{\phi}^r(\vec{r}) \hat{\theta} \end{aligned} \quad (9.35)$$

It was indicated in section (9.1) that the traveling wave distribution of current corresponding to an optimum impedance loading may be approximated as

$$I_{\phi}(\phi) = \frac{V_o}{60\Psi} e^{-j\beta_o b |\phi|} \quad -\pi \leq \phi \leq \pi \quad (9.36)$$

Further, the zeroth-order standing wave current distribution on a conventional loop antenna may be written as

$$I_{\phi}(\phi) = I_m \cos \beta_o b (\pi - |\phi|) \quad -\pi \leq \phi \leq \pi \quad (9.37)$$

Using distributions (9.36) and (9.37) in equation (9.34), the vector potential in the plane of the loop, corresponding to the traveling and standing waves of current, respectively, becomes

$$[A_{\phi}^r(\vec{r})]_T = \frac{V_o b \mu_o}{240\pi \Psi} \frac{e^{-j\beta_o r}}{r} G_T(\beta_o b, \phi) \quad (9.38)$$

$$[A_{\phi}^r(\vec{r})]_S = \frac{I_m b \mu_o}{4\pi} \frac{e^{-j\beta_o r}}{r} G_S(\beta_o b, \phi) \quad (9.39)$$

where

$$G_T(\beta_o b, \phi) = \int_{-\pi}^{\pi} \cos(\phi - \phi') e^{j\beta_o b [\cos(\phi - \phi') - |\phi'|]} d\phi' \quad (9.40)$$

$$G_S(\beta_o b, \phi) = \int_{-\pi}^{\pi} \cos \beta_o b (\pi - |\phi'|) \cos(\phi - \phi') e^{j\beta_o b \cos(\phi - \phi')} d\phi' \quad (9.41)$$

With result (9.38), the electric field in the plane of the traveling wave loop may be obtained from expression (9.35) as

$$[E_{\phi}^r(\vec{r})]_T = - \frac{jV_o \beta_o b}{2\eta} \frac{e^{-j\beta_o r}}{r} G_T(\beta_o b, \phi) \quad (9.42)$$

while that corresponding to the standing wave of current is determined from equations (9.35) and (9.39) as

$$[E_{\phi}^r(\vec{r})]_S = - \frac{jI_m \omega \mu_o b}{4\pi} \frac{e^{-j\beta_o r}}{r} G_S(\beta_o b, \phi) \quad (9.43)$$

The functions $G_T(\beta_o b, \phi)$ and $G_S(\beta_o b, \phi)$ are defined as the polar pattern factors of the traveling wave and standing wave loop antennas, respectively. These expressions describe the variation of the amplitude and phase of the radiation fields as a function of the electrical loop circumference $\beta_o b$ and the azimuth angle ϕ of spherical coordinates. For fixed values of $\beta_o b$, these factors become functions of ϕ alone, and describe the radiation patterns of the fields in the plane of the loop.

It is noted that $G_T(\beta_o b, \phi)$ and $G_S(\beta_o b, \phi)$ are in general complex numbers. Hence the radiation fields vary in phase as well as amplitude with the angle ϕ . Physically, however, it is the amplitude of the fields at each point in the radiation zone which is of primary interest. Consideration will henceforth be restricted, therefore, to the modulus $|G_T(\beta_o b, \phi)|$ and $|G_S(\beta_o b, \phi)|$ of the polar pattern factors. These expressions give the relative amplitudes

of the radiation fields as a function of the angle ϕ and the electrical circumference of the traveling or standing wave loop antennas.

9.3. Comparison of Radiation Patterns for Traveling Wave and Standing Wave Loop Antennas

The functions $G_T(\beta_0 b, \phi)$ and $G_S(\beta_0 b, \phi)$, which describe the radiation patterns of traveling and standing wave loop antennas, respectively, were determined in the preceding section as

$$G_T(\beta_0 b, \phi) = \int_{-\pi}^{\pi} \cos(\phi - \phi') e^{j\beta_0 b [\cos(\phi - \phi') - |\phi'|]} d\phi' \quad (9.40)$$

$$G_S(\beta_0 b, \phi) = \int_{-\pi}^{\pi} \cos \beta_0 b (\pi - |\phi'|) \cos(\phi - \phi') e^{j\beta_0 b \cos(\phi - \phi')} d\phi' \quad (9.41)$$

These integrals cannot be evaluated in closed form to yield a result in terms of simple functions. It was therefore necessary to determine the values of $G_T(\beta_0 b, \phi)$ and $G_S(\beta_0 b, \phi)$ by numerical machine calculation. Specific numerical results were obtained for values of $\beta_0 b$ between 0.25 and 4.0. For each value of $\beta_0 b$, the angle ϕ was allowed to take values of 0 - 180 degrees.

The radiation patterns corresponding to the above numerical results are obtained by plotting $|G_T(\beta_0 b, \phi)|$ and $|G_S(\beta_0 b, \phi)|$ as a function of ϕ in polar coordinates, with the appropriate values of $\beta_0 b$ as parameter. Typical patterns are indicated in Figures 9.2 through 9.5 for $\beta_0 b$ values of 1.0, 1.5, 2.5, and 4.0, respectively. In each case, the traveling wave and standing wave patterns are plotted in the same figure to facilitate comparison. Each pattern is actually symmetric about the $\phi = 0$ axis, but only half of every pattern is shown to avoid obscuring the figures.

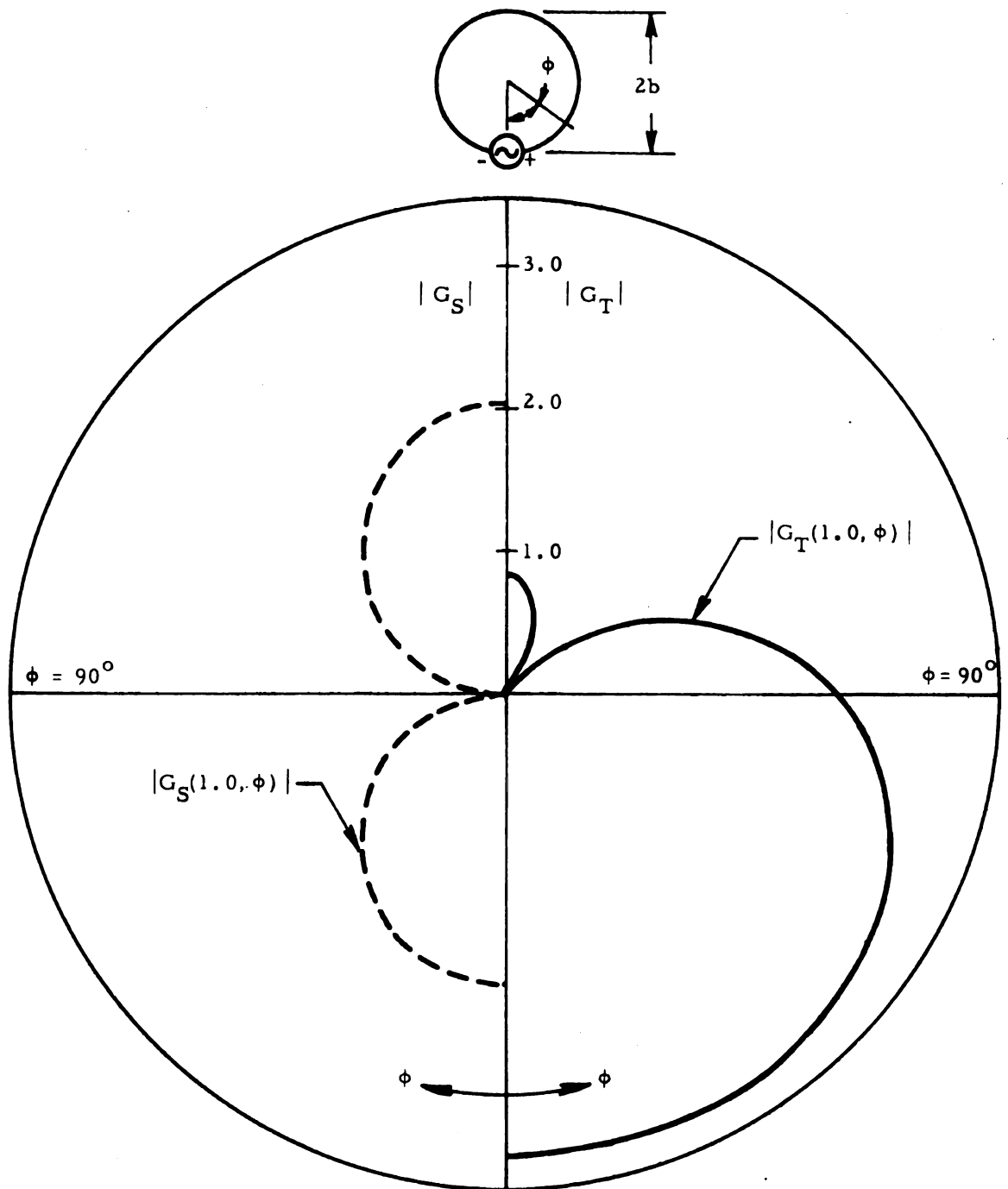


Figure 9.2. Radiation Pattern in Plane of Loop ($\theta = 90^\circ$) as a Function of ϕ for $\beta_0 b = 1$.

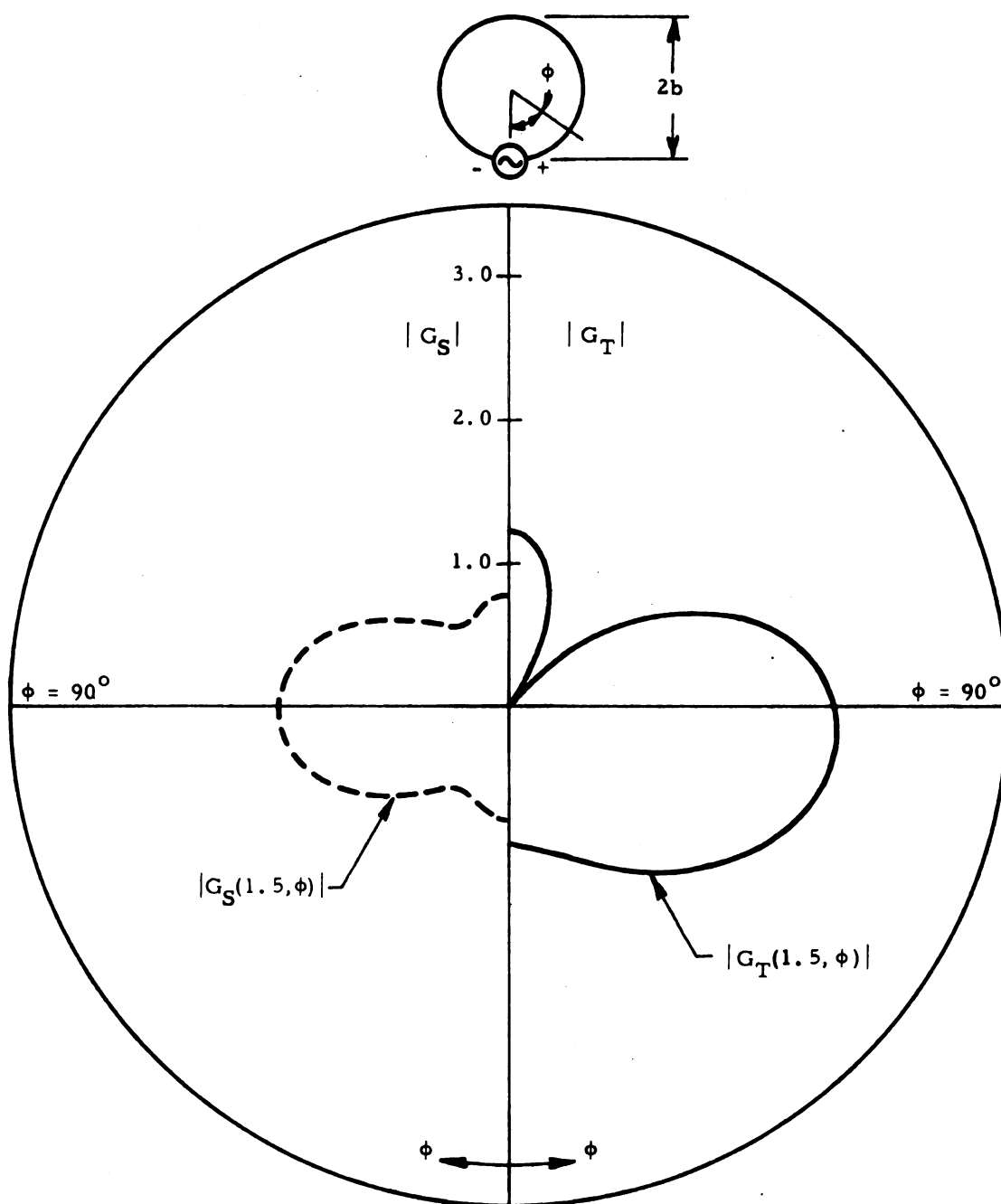


Figure 9.3. Radiation Pattern in Plane of Loop ($\theta = 90^\circ$) as a Function of ϕ for $\beta_0 b = 1.5$.

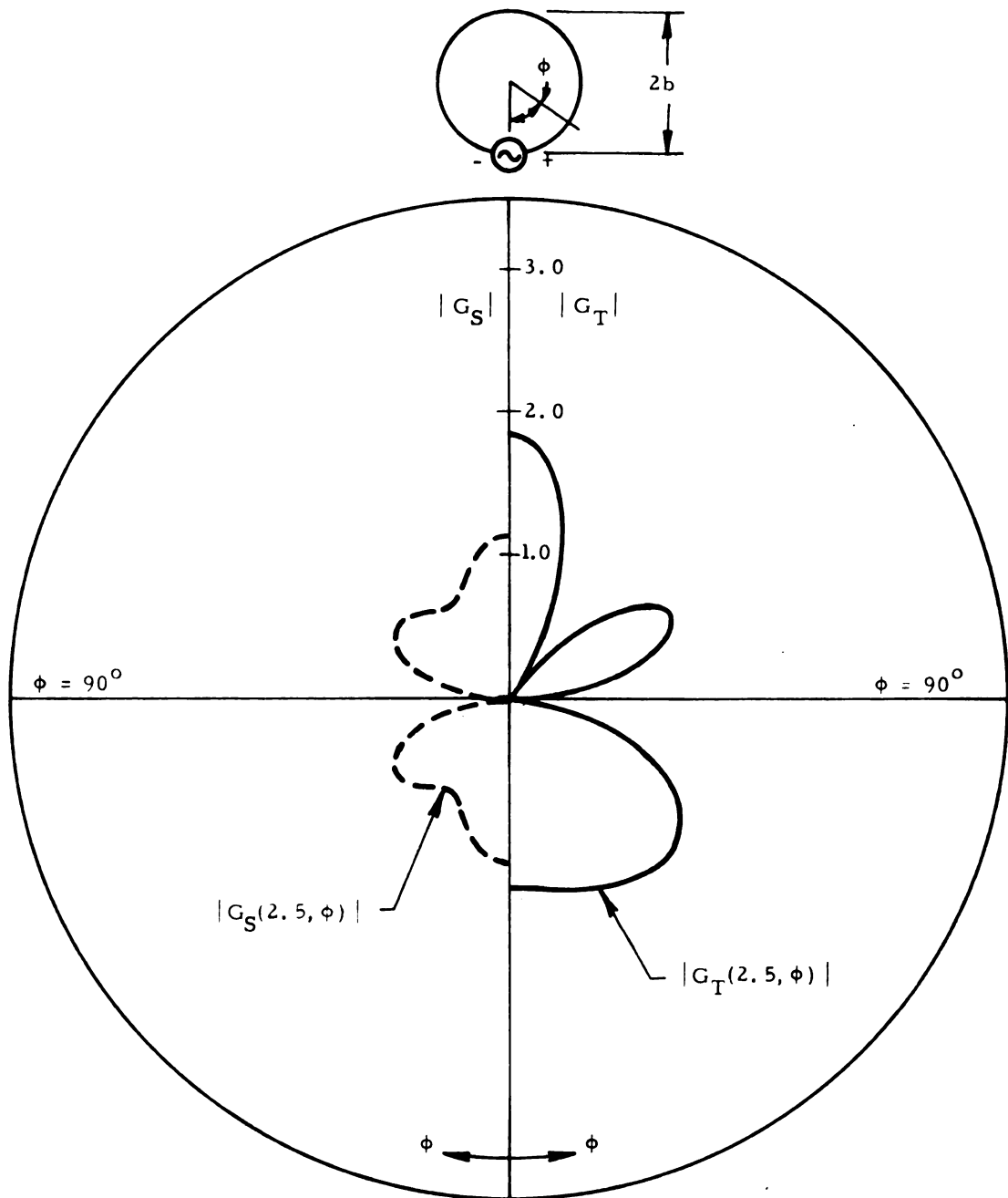


Figure 9.4. Radiation Pattern in Plane of Loop ($\theta = 90^\circ$) as a Function of ϕ for $\beta_0 b = 2.5$.

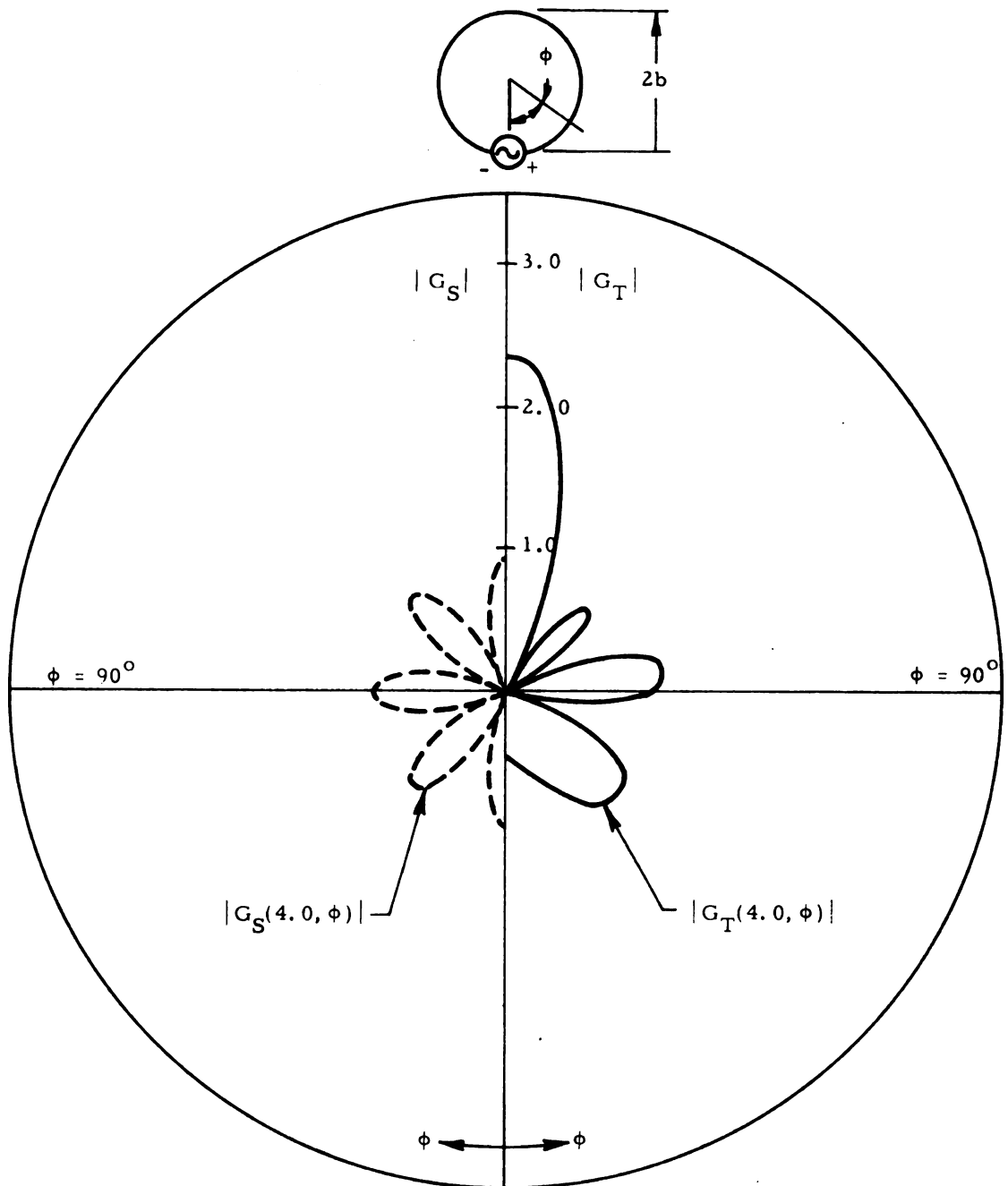


Figure 9.5. Radiation Pattern in Plane of Loop ($\theta = 90^\circ$) as a Function of ϕ for $\beta_0 b = 4.0$.

An inspection of Figures 9.2 through 9.5 reveals the following radiation characteristics for traveling and standing wave loop antennas:

- (i) The radiation pattern in the plane of a conventional loop antenna consists of two broad lobes separated in space by 180° . On the other hand, the pattern of a small traveling wave loop is essentially unidirectional, having a very broad major lobe in one spatial direction and a narrow minor lobe of relatively small amplitude in the opposite direction.
- (ii) As the diameter of the standing wave loop is increased, both the shape and the spatial orientation of the pair of lobes in its radiation pattern undergo radical variations, although they remain oppositely directed in space. Finally, as the loop size is further increased, the pair of lobes split to form several narrower lobes of smaller but equal amplitude. As the electrical diameter of the traveling wave loop is increased, the narrow minor lobe grows in amplitude while the broad major lobe shifts in its spatial orientation, decreases in amplitude, and finally splits to form a minor lobe structure of relatively small amplitude.
- (iii) An electrically large traveling wave loop antenna is characterized by a single narrow major lobe accompanied by a minor lobe structure. As the diameter of the loop increases, the amplitude of the major lobe steadily increases with respect to that of the minor lobe structure. The major lobe of this pattern is spatially oriented in a direction 180° removed from the excitation point of the loop, i. e., in the direction of the traveling wave of current.

It is indicated by the above remarks that the radiation characteristics of a traveling wave loop antenna in no way resemble those of its standing wave counterpart.

Whether or not the radiation characteristics of a traveling wave loop offer any particular advantage will depend of course upon the intended application of the antenna. The modified radiation pattern which characterizes the traveling wave loop may, however, be desirable for some purposes. In particular, the broad unidirectional pattern of a small loop or the narrow directive pattern of an electrically large loop should be useful for certain applications.

It should be emphasized that the radiation characteristics determined in the preceding section correspond to the traveling wave distribution of current associated with an optimum impedance loading. As the loading deviates from its optimum value, the traveling wave of current gradually reverts back to an essentially standing wave. Under these circumstances, the corresponding radiation patterns would again become similar to those characteristic of a conventional loop antenna.

REFERENCES

1. Hallen, E., "Theoretical Investigations into the Transmitting and Receiving Qualities of Antennae," *Nova Acta Regiae Societatis Scientiarum Upsaliensis*, Uppsala, Sweden, Series IV, Vol. II, No. 4, Nov. 1938, pp. 1-44.
2. King, R. W. P., The Theory of Linear Antennas, Harvard University Press, Cambridge, Massachusetts, 1956.
3. Altshuler, E. E., "The Traveling Wave Linear Antenna," *IRE Trans. on Antennas and Propagation*, July, 1961, pp. 324-329.
4. Wu, T. T. and R. W. P. King, "The Cylindrical Antenna with Nonreflecting Resistive Loading," *IEEE Trans. on Antennas and Propagation*, Vol. AP-13, No. 3, May, 1965, pp. 369-373.
5. King, R. W. P., Fundamental Electromagnetic Theory, Second Edition, Dover, New York, 1963.
6. Chen, K. M., "Minimization of Back Scattering of a Cylinder by Double Loading," *IEEE Trans. on Antennas and Propagation*, Vol. AP-13, No. 2, March, 1965, pp. 262-270.
7. Chen, K. M., "Minimization of End-Fire Radar Echo of a Long Thin Body by Impedance Loading," *IEEE Trans. on Antennas and Propagation*, Vol. AP-14, No. 2, May, 1966, pp. 318-323.
8. Stewart, J. L., Circuit Analysis of Transmission Lines, John Wiley and Sons, New York, 1958.
9. Storer, J. E., "Impedance of Thin-Wire Loop Antennas," *Trans. AIEE*, Vol. 75 (Communications and Electronics), Nov., 1956, pp. 606-619.

10. Iizuka, K., "The Circular Loop Antenna Multiloaded with Positive and Negative Resistors," IEEE Trans. on Antennas and Propagation, Vol. AP-13, No. 1, Jan., 1965, pp. 7-20.
11. Jackson, J. D., Classical Electrodynamics, John Wiley and Sons, New York, 1962.

APPENDIX A

ELECTROMAGNETIC POTENTIALS IN ANTENNA THEORY

It is convenient to formulate the theory of thin-wire antennas in terms of the electromagnetic scalar and vector potentials. Such a formulation is expedient since the distributions of antenna current and charge are more closely related to these potential functions than to the electric and magnetic fields themselves. A brief survey of the set of electromagnetic potentials useful in the study of thin-wire antennas is presented here.

It will be assumed that the antenna is immersed in an infinite free space region characterized by a permittivity ϵ_0 and a permeability μ_0 . Maxwell's equations for such a free space region may be expressed as¹¹

$$\nabla \cdot \vec{E} = \frac{\rho}{\epsilon_0} \quad (\text{A. 1})$$

$$\nabla \times \vec{E} = - \frac{\partial \vec{B}}{\partial t} \quad (\text{A. 2})$$

$$\nabla \times \vec{B} = \mu_0 \vec{J} + \mu_0 \epsilon_0 \frac{\partial \vec{E}}{\partial t} \quad (\text{A. 3})$$

$$\nabla \cdot \vec{B} = 0 \quad (\text{A. 4})$$

where \vec{E} is the electric field, \vec{B} the magnetic field, and \vec{J} and ρ are the volume densities of current and charge, respectively. The basic problem in the theory of thin-wire antennas is to determine the distributions of antenna current and charge as solutions to equations (A.1) through (A.4). Such a solution is greatly facilitated by the introduction of a set of electromagnetic potentials.

Equation (A.4) implies that

$$\vec{B} = \nabla \times \vec{A} \quad (\text{A.5})$$

where \vec{A} is the vector potential. If expression (A.5) is used in equation (A.2), there is obtained

$$\nabla \times \left(\vec{E} + \frac{\partial \vec{A}}{\partial t} \right) = 0$$

which implies

$$\vec{E} + \frac{\partial \vec{A}}{\partial t} = -\nabla \phi$$

where ϕ is the scalar potential. The electromagnetic fields may therefore be expressed in terms of the vector and scalar potentials as

$$\begin{aligned} \vec{E} &= -\nabla \phi - \frac{\partial \vec{A}}{\partial t} \\ \vec{B} &= \nabla \times \vec{A} \end{aligned} \quad (\text{A.6})$$

If equations (A.6) are substituted into equations (A.1) and (A.3), a pair of equations for the potentials are obtained as

$$\begin{aligned} \nabla^2 \phi + \frac{\partial}{\partial t} \nabla \cdot \vec{A} &= -\frac{\rho}{\epsilon_0} \\ \nabla^2 \vec{A} - \mu_0 \epsilon_0 \frac{\partial^2 \vec{A}}{\partial t^2} - \nabla \left(\nabla \cdot \vec{A} + \mu_0 \epsilon_0 \frac{\partial \phi}{\partial t} \right) &= -\mu_0 \vec{J} \end{aligned}$$

Since $\nabla \cdot \vec{A}$ is as yet unspecified, it may be taken that

$$\nabla \cdot \vec{A} + \mu_0 \epsilon_0 \frac{\partial \phi}{\partial t} = 0 \quad (\text{A.7})$$

.... Lorentz condition

and the differential equations for ϕ and \vec{A} become

$$\begin{aligned}\nabla^2 \phi - \mu_o \epsilon_o \frac{\partial^2 \phi}{\partial t^2} &= - \frac{\rho}{\epsilon_o} \\ \nabla^2 \vec{A} - \mu_o \epsilon_o \frac{\partial^2 \vec{A}}{\partial t^2} &= - \mu_o \vec{J}\end{aligned}\tag{A. 8}$$

In the special case where the sources are time harmonic of the form

$$\begin{aligned}\rho(\vec{r}, t) &= \rho(\vec{r}) e^{j\omega t} \\ \vec{J}(\vec{r}, t) &= \vec{J}(\vec{r}) e^{j\omega t}\end{aligned}$$

the results of the preceding paragraph become

$$\begin{aligned}\vec{E} &= -\nabla \phi - j\omega \vec{A} \\ \vec{B} &= \nabla \times \vec{A}\end{aligned}\tag{A. 9}$$

$$\nabla^2 \phi + \beta_o^2 \phi = -\rho / \epsilon_o \tag{A. 10}$$

$$\nabla^2 \vec{A} + \beta_o^2 \vec{A} = -\mu_o \vec{J}$$

$$\nabla \cdot \vec{A} + \frac{j\beta_o^2}{\omega} \phi = 0 \tag{A. 11}$$

.... Lorentz condition

The time factor $e^{j\omega t}$ is implied in these results, and the fields and potentials are understood to be complex valued. Further, the free space wave number has been defined by $\beta_o^2 = \omega^2 \mu_o \epsilon_o$. It is possible to integrate the inhomogeneous wave equations (A. 8) through the use of a Green's function technique¹¹ to obtain

$$\phi(\vec{r}) = \frac{1}{4\pi\epsilon_o} \int_V \rho(\vec{r}') \frac{e^{-j\beta_o R}}{R} dv' \tag{A. 12}$$

$$\vec{A}(\vec{r}) = \frac{\mu_o}{4\pi} \int_v J(\vec{r}') \frac{e^{-j\beta_o R}}{R} dv' \quad (\text{A.13})$$

where $R = |\vec{r} - \vec{r}'|$ is the distance between an observation point located by \vec{r} and a source point at \vec{r}' .

For the case of a thin-wire antenna, solutions (A.12) and (A.13) may be integrated over the cross section of the wire to obtain

$$\phi(\vec{r}) = \frac{1}{4\pi\epsilon_o} \int_c q(\vec{r}') \frac{e^{-j\beta_o R}}{R} d\ell'$$

$$\vec{A}(\vec{r}) = \frac{\mu_o}{4\pi} \int_c \vec{I}(\vec{r}') \frac{e^{-j\beta_o R}}{R} d\ell'$$

where $q(\vec{r})$ is the charge per unit length and $\vec{I}(\vec{r})$ the total current on the wire forming the contour c . It has been indicated by Hallen¹ and King^{2, 5} that the potentials at the surface of a thin-wire antenna may be calculated by assuming $q(\vec{r})$ and $\vec{I}(\vec{r})$ to be concentrated along the axis of the wire. In such a case, $R = |\vec{r} - \vec{r}'|$ is the distance between an observation point on the wire surface at \vec{r} and a source point on its axis at \vec{r}' .